CHARLES UNIVERSITY IN PRAGUE

Faculty of Science

Ph.D. study program: Immunology

Multiple regulatory roles of the transmembrane adaptor protein NTAL in gene transcription and mast cell physiology

Iva Polakovičová

Ph.D. Dissertation in Immunology

Supervised by RNDr. Petr Dráber, DrSc.

Institute of Molecular Genetics

Academy of Sciences of the Czech Republic

Prague, 2014

This thesis was prepared at the Institute of Molecular Genetics, Academy of Sciences of the Czech Republic, Laboratory of Signal Transduction. Experimental data were compiled into three original articles and one review. One of the articles is submitted for publication in Molecular and Cellular Biology.

I hereby declare, that I have elaborated this thesis independently, and all the resources are employed as well as co-authors are indicated. I further declare that I did not submit this thesis, or an essential part of it, to obtain other, or the same university degree.

Prague, September 2014 Iva Polakovičová

I would like to thank my supervisor Petr Dráber for his guidance and exceptional help during my Ph.D. study and also for giving me the opportunity of a 5 moth internship at Massachusetts General Hospital and Harvard Medical School in Boston.

Many sincere thanks also belong to my colleagues for their help, support, useful discussions and advices and for creating friendly atmosphere in the laboratory, namely (in alphabetical order) Monika Bambousková, Romana Budovičová, Viktor Bugajev, Lubica Dráberová, Jiří Eitler, Filip Franko, Ivana Hálová, Petr Heneberg, Lukáš Kocanda, Anna Koffer, Martin Machyna, Hana Mrázová, Anna Koffer, Dana Lorenčíková, Tomáš Paulenda, Gouse Mohidin Shaik, Daniel Smrž, Lucie Potůčková, Magda Tůmová, Michal Šimíček and Pavol Utekal. I also would like to thank to Petr Šimeček and Michal Kolář for introducing me to the world of microarray analysis. I also very much appreciated the collaboration with Ramnik Xavier and colleagues from Massachusetts General Hospital, especially Agnes Gardet for her excellent teaching skills and critical thinking and Behfar Ardehali for stimulating discussions and support.

I would like to express my sincere gratitude to my family, especially my mother who has been always very supportive, and many thanks go also to my friends for their patience and understanding.

INDEX

ABSTRACT (EN)

This thesis focuses mainly on understanding of the regulatory roles of the transmembrane adaptor proteins, non-T cell activation linker (NTAL) and phosphoprotein associated with glycosphingolipid-enriched microdomains (PAG), in murine mast cell signaling. There are conflicting reports on the role of NTAL in the high affinity immunoglobulin E receptor (FcεRI) activation pathways in mast cells. Studies carried out on mast cells prepared from NTAL knock-out mice have indicated that NTAL is a negative regulator of FcεRI signaling, whereas experiments performed on human mast cells and rat basophilic leukemia cells with silenced NTAL expression have suggested its positive regulatory role. To thoroughly examine the involvement of NTAL in FcεRI-mediated signaling events in mouse mast cells and to determine whether different methodologies of NTAL ablation have different physiological consequences, we utilized a broad range of assays. Using bone marrow-derived mast cells (BMMCs) as a model, we obtained cells from NTAL wild type and knock-out cells and using lentiviral delivery approach we transduced part of the wild type cells, with vector bearing NTAL shRNA or empty vector to generate NTAL knock-down cells and control cells, respectively. Comparison of all four groups of generated cells in our assays revealed that both types of NTAL-deficient BMMCs exhibited enhanced degranulation, calcium mobilization, chemotaxis, tyrosine phosphorylation of linker for activation of T cells (LAT) and ERK and depolymerization of filamentous actin. These data provide evidence that NTAL is a negative regulator of FcεRI activation events in murine BMMCs, independently of possible compensatory developmental alterations.

To gain further insight into the downstream signaling activity of NTAL, we examined the resting and antigen-activated transcriptome profiles of all four types of generated BMMCs. Through this analysis we identified several genes that were differentially regulated in nonactivated and antigen-activated control and NTAL-deficient cells. Interestingly, a subset of these genes was involved in regulation of cholesterol-dependent events in antigen-mediated chemotaxis. The combined data indicate multiple regulatory roles of NTAL in gene expression and mast cell physiology.

We have also shown that another transmembrane adaptor protein, PAG, has both positive and negative role in mast cell FcεRI-mediated activation depending on the signaling pathway involved.

Since both studies demanded numerous quantitative real-time PCR examinations, part of the focus was also dedicated to development of new PCR master mixes suitable for amplification of difficult-to-amplify DNA fragments. We found excellent performance of a PCR mix supplemented with 1 M 1,2-propanediol and 0.2 M trehalose. This master mix is now also commercially available.

Lastly, we have reviewed recent approaches towards inhibiting mast cell mediated events in diseases or with mast cell related pathology, with the main focus being on recently developed inhibitors of intracellular signaling pathways and their relevance to clinical trials.

ABSTRACT (CZ)

Tato dizertační práce se zaměřuje především na pochopení regulačních úloh transmembránových adaptorových proteinů NTAL („non-T cell activation linker“) a PAG („phosphoprotein associated with glycosphingolipid-enriched microdomains“) v aktivaci myších žírných buněk. V odborné literatuře existují protikladné studie o úloze proteinu NTAL v aktivační dráze vysoce afinního receptoru pro imunoglobulin E (IgE) (FcεRI). Studie prováděné na žírných buňkách připravených z myší s genovým knockoutem NTALu naznačují, že NTAL je negativní regulátor FcεRI signalizace, zatímco experimenty provedené na lidských žírných buňkách a buňkách bazofilní leukemie potkana s potlačenou expresí proteinu NTAL mu připisují pozitivní regulační roli.

Abychom pochopili zapojení proteinu NTAL v FcεRI zprostředkované signalizaci v myších žírných buňkách a určili, zda různé metodiky delece NTALu mají různé fyziologické následky, použili jsme široké spektrum testů. Jako model jsme použili žírné buňky odvozené z kostní dřeně (BMMC) a připravili jsme BMMC z myší NTAL divokého typu („wild type“) a myší s genovým knockoutem NTALu. Pomocí lentivirových vektorů jsme transdukovali část buněk divokého typu vektorem nesoucím NTAL shRNA („short hairpin RNA“) pro generování buněk s potlačenou expresí NTALu („knockdown“) nebo prázdným vektorem pro přípravu negativní kontroly. Srovnání všech čtyř skupin připravených buněk v našich testech ukázalo, že oba typy NTAL-deficitních BMMC vykazovaly zvýšenou degranulaci, mobilizaci vápníku, chemotaxi, fosforylaci tyrosinu molekul LAT („linker for activation of T cells“) a ERK a depolymeraci filamentárního aktinu. Tyto výsledky prokazují, že NTAL je negativní regulátor FcεRI zprostředkovaných aktivačních dějů v myších BMMC a to nezávisle na případných kompenzačních mechanizmech během vývoje.

Abychom získali další pohled na navazující signalizační děje související s proteinem NTAL, zabývali jsme se transkripčními profily získanými z aktivovaných a neaktivovaných všech čtyř typů připravených BMMCs. Prostřednictvím transkripční analýzy jsme identifikovali několik genů, které byly rozdílně regulované v neaktivovaných a antigenem aktivovaných kontrolních a NTAL-deficitních buňkách. Další rozbor ukázal, že se část těchto genů účastní regulace dějů závislých na cholesterolu v chemotaxi zprostředkované antigenem. Získaná data naznačují multiregulační úlohu proteinu NTAL v genové expresi a fyziologii žírných buněk.

Dále jsme ukázali, že transmembránový adaptorový protein PAG má pozitivní i negativní regulační úlohu při aktivaci žírných buněk v závislosti na regulované signalizační dráze.

Protože obě studie vyžadovaly provedení řady analýz genové exprese pomocí kvantitativní polymerázové řetězové reakce (qPCR), část experimentů byla věnována také vývoji nových reakčních směsí (tzv. master mixů) s akcentem na amplifikaci obtížně amplifikovatelných fragmentů DNA. Zjistili jsme, že zásadního zlepšení lze dosáhnout u směsí s přídavkem 1 M 1,2-propandiolu a 0,2 M trehalózy. Tato reakční směs je nyní komerčně dostupná.

Na závěr jsme provedli recenzi nových přístupů k potlačení onemocnění zprostředkovaných žírnými buňkami nebo s nimi souvisejícími patologiemi. Hlavním zaměřením byly nedávno vyvinuté inhibitory intracelulárních signálních drah a jejich význam pro klinické studie.

ABBREAVIATIONS

BMPCs	basophil/mast cell progenitors
BSA	bovine serum albumin
BSS	buffered salt solution
C/EBPα	CCAAT/enhancer binding protein α
CLPs	common lymphoid progenitors
CMPs	common myeloid progenitors
CRAC	Ca^{2+} release-activated Ca^{2+}
CSK	C-terminal Src kinase
cysLTR	cysteinyl leukotriene receptor
DAG	1,2-diacylglycerol
DOK1	downstream of tyrosine kinase 1
ER	endoplasmic reticulum
FCS	fetal calf serum
FDR	false discovery rate
FLAP	5-lipoxygenase–activating protein
GAB2	GRB2-associated binding protein 2
GADS	GRB2-related adaptor protein
GAPT	GRB2-binding adaptor protein, transmembrane
GEO	Gene Expression Omnibus
GM-CSF	granulocyte/macrophage colony stimulating factor
GMPs	granulocyte/monocyte progenitors
GRB2	growth factor receptor-bound protein 2
HR	histamine receptors
IL	interleukin
IP3	inositol-1,4,5-trisphosphate
ITAM	immunoreceptor tyrosine-based activation motif
ITIM	immunoreceptor tyrosine-based inhibitory motif
LAT	linker for activation of T-cells
LAT	linker for activation of T-cells
LAX	linker for activation of X cells
LTC_4	leukotriene C_4
MAPK	mitogen-activated protein kinase

MCp	mast cell progenitors
MEPs	megakaryocyte/erythrocyte progenitors
MMPs	multipotent progenitors
NFAT	nuclear factor for T cell activation
NGF	nerve growth factor
NTAL	non-T-cell activation linker
PAG	phosphoprotein associated with glycosphingolipid-enriched microdomains
PCA	principal component analysis
PGD_2	prostaglandin D_2
PI(3,4,5)P3	phosphatidylinositol-3,4,5-trisphosphate
PI(4,5)P2	phosphatidylinositol-4,5-bisphosphate
PI3K	phosphatidylinositol 3-kinases
PKC	protein kinase C
PLCγ	phopholipase Cγ
PTEN	phosphatase and tensin homologue deleted on chromosome ten
RasGAP	Ras GTP-binding protein-activating protein
S1P	sphingosine-1-phosphate
SCF	stem cell factor
SH	Src homology
SHIP	SH2-containing inositol 5' phosphatase
SHP	SH2-domain-containing protein tyrosine phosphatase
SLP-76	SH2-domain-containing leukocyte protein of 76 kDA
STIM	stromal interaction molecule 1
SYK	spleen tyrosine kinase
TNF	tumor-necrosis factor
TNP	trinitrophenyl
TRAP	transmembrane adaptor protein
VEGF	vascular endothelial growth factor

INTRODUCTION

Introduction to mast cells

Mast cell discovery

The name mast cell originates from the German word “Mastzellen”. This name was given to these cells by a German scientist Paul Ehrlich in 1878 who was the first person to describe them. In his doctoral thesis “Beiträge zur Theorie und Praxis der histologischen Färbung” (“Contributions to theory and practice of histological coloring") he discussed the chemical and histological properties of the basic aniline dyes and he described aniline-positive cells in human connective tissues. He believed they had a nutritional function because they were full of granules and thus gave them a name related with the “fattening” or “suckling” function [1, 2]. In his other studies he also described neutrophils, eosinophils and basophils which he misleadingly described as blood mast cells [2].

For a long time the real function of mast cells remained unknown. The attention was drawn back to them in the 1950s when they were found to be the main repository of histamine and a key participant in anaphylactic reactions [1]. A polymeric compound known as compound 48/80 was found to induce degranulation of mast cells [3] and became the mainstay for subsequent studies.

In the late 1990s the view on mast cells has changed, from being primarily the mediators of allergic reactions and combatants of parasite infestation, they started to be seen also as important effector cells in innate, as well as acquired, immune responses. They were shown to help to initiate and orchestrate inflammatory responses at sites of pathogen invasion and to function as sentinel cells located in serosal cavities and immediately beneath epithelial surfaces as well as near blood vessels, nerves and glands [4].

Nowadays we look at mast cells as multifunctional cells that do not only play role in initiation of IgE-dependent allergic diseases but also in adaptive and innate immune responses, as well as inflammatory autoimmune diseases. Additionally, mast cells participate in inflammatory responses to tumors where they may function either in facilitating tumor or help suppress the tumor growth depending on the type of cancer. Mast cells function also in promoting angiogenesis, wound healing and tissue remodeling [5].

Origin and development of mast cells

The origin of mast cells remained unclear until the late 1970s when the adaptive transfer of wild type bone marrow cells into mast cell-deficient mice demonstrated that mast cells are of

hematopoietic origin [6]. In contrast to most hematopoietic cells that are released into the blood in an identifiable mature state, mast cell progenitors (MCp) residing in bone marrow enter the blood circulation and home to the tissues in an immature state, where they give a rise to mature mast cells. This process from MCp till mature mast cell residing in tissue is still not fully understood. The migration of MCp to tissues is a regulated process that is stimulated by inflammation and leads to an increase in tissue MCp [7].

Human mast cells are derived from CD34+ pluripotent progenitor cells residing in the bone marrow [8]. However CD34+ cannot be used as a universal specific marker of mast cell precursors. Recently, several studies shed more light onto mast cell development. Results of these studies were recently summarized in a review by Dahlin and Hallgren [7] where they also proposed a model for the development of MCp (Figure 1).

Bone marrow-derived hematopoietic stem cells lose their self-renewing capacity when they develop into multipotent progenitors (MPPs) that further give a rise to either common lymphoid progenitors (CLPs) or common myeloid progenitors (CMPs), to which belong mast cells. CMPs further branch into megakaryocyte/erythrocyte progenitors (MEPs) and granulocyte/monocyte progenitors (GMPs) during their development. Single cells giving rise to neutrophils, basophils and mast cells were found within the classically defined GMP population, verifying that mast cells belong to the granulocyte/monocyte lineage [9]. Moreover, Arinobu et al. identified bipotent basophil/mast cell progenitors (BMCPs) in mice spleen, suggesting a close developmental relationship between the basophil and the mast cell lineage. In agreement with these data, Qi et al. recently isolated within the GMP fraction single progenitors capable of giving rise to both basophils and mast cells [10]. These results and data from others suggest that committed MCp originate from bipotent progenitors with both mast cell and basophil capacity within the GMP population [7]. The process of differentiation of hematopoietic stem cells into mast cells is highly regulated by a complex network of transcription factors. The differentiation from GMPs into mast cells is controlled by CCAAT/enhancer binding protein α (C/EBPα), MITF and GATA-2. C/EBPα, the transcription factor essential for granulocyte development, plays a critical role in their fate decision [9].

After the commitment, the MCp enter blood circulation and reside into peripheral tissues where they undergo maturation under the influence of local factors. Mast cells reside in most tissues, but are especially rich in those exposed to the external environment, including the skin, respiratory, and gastrointestinal tract and thus are likely to be one of the first inflammatory cells, along with dendritic cells, to encounter allergens, pathogens, and other proinflammatory and toxic agents [4].

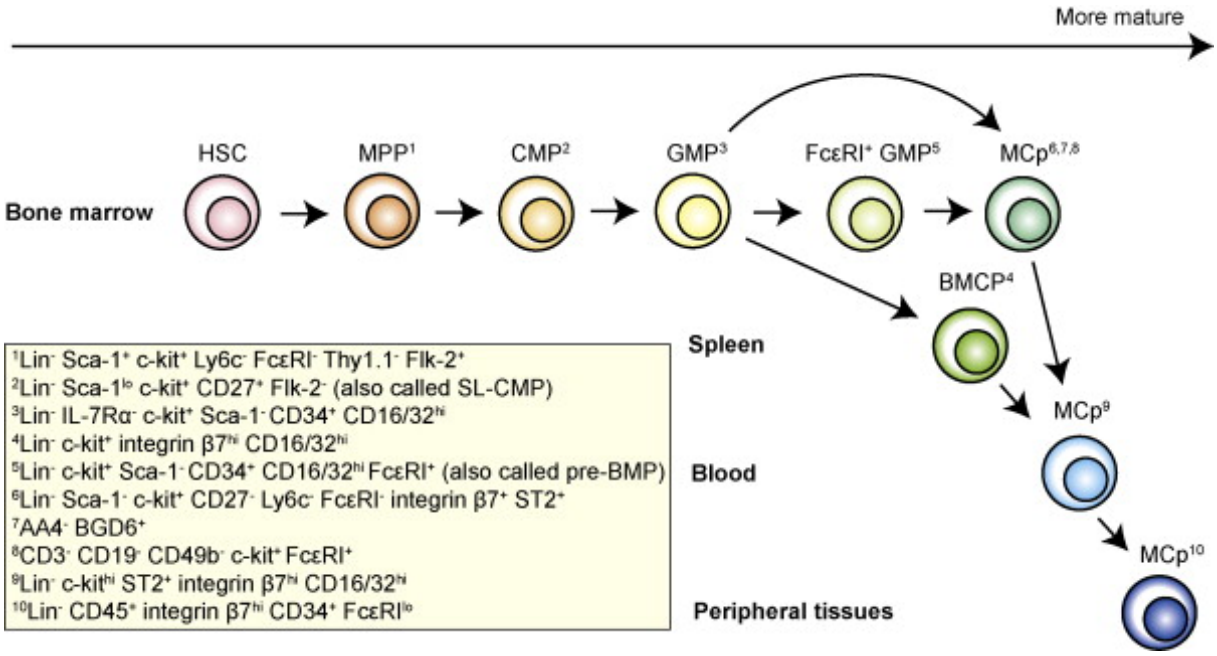

(Dahlin and Hallgren, 2014)

Figure 1. Proposed model for the development of MCp. Mast cells originate from the bone marrow where they develop from the hematopoietic stem cells (HSC) via multipotent progenitors (MPP), common myeloid progenitors (CMPs) and granulocyte/monocyte progenitors (GMPs). The majority of these progenitors is found among the FcεRI$^+$ GMPs. However, progenitors that give rise to mast cells and basophils are also found within the FcεRI$^-$ GMPs. Bipotent basophil/mast cell progenitors (BMCPs) in the spleen are largely negative for FcεRI expression in mice, consistent with the FcεRI$^-$ GMPs in bone marrow. Therefore, mast cells likely develop from both FcεRI$^-$ and FcεRI$^+$ GMPs. MCp exit the bone marrow as FcεRI$^-$ and FcεRI$^+$ cells that can be found in the blood in mice as committed MCp. In the peripheral tissues in mice MCp express FcεRI at low levels. The numbers in superscript at each progenitor stage is repeated in the yellow box to describe the surface markers used to define the particular progenitor stage.

Mast cell subpopulations

In peripheral tissues, the progenitors differentiate into one of two types of mast cells, connective tissue or mucosal tissue mast cells. These types differ in many properties and can be characterized by mediators they release and by staining [11]. Safranin positive cells are connective tissue mast cells and their granules contain heparin and large amount of histamine and serotonin. They are found in the skin, joints, around blood vessels, and in rodents also in peritoneal cavity. The granules of safraninin negative mucosal mast cells contain chondroitin sulfate and little histamine. These cells are localized in the lamina propria of the respiratory tract and in the mucosa of the gastrointestinal system [12].

The bone-marrow derived mast cells, that are widely prepared and used for *in vitro* experiments, resemble more the properties of mucosal mast cells [13]. These cells are prepared from isolated bone-marrow by culturing in the presence of interleukin (IL)-3 and stem cell factor (SCF) for several weeks.

Mast cell function

Mast cell degranulation

After receiving proper activation signals, mast cells degranulate – release mediators from their cytoplasmic granules into exterior area. Mast cells produce three main types of mediators: preformed mediators stored in the granules, newly generated lipid mediators, and various cytokines and chemokines or growth factors.

The secretory granules can be released within minutes after cell activation and these granules contain serine proteases tryptase and chymase, carboxypeptiase A, vasoactive amines, such as histamine, and proteoglycans heparin or chondroitin sulfate E.

The *de novo* synthesis involves eicosanoids such as prostaglandin D_2 (PGD_2) and leukotriene C_4 (LTC_4). Their synthesis is initiated after activation of cytosolic phospholipase A_2, which catalyzes the production of arachidonic acid, the eicosanoid precursor. LTC_4 causes bronchoconstriction and increases vascular permeability [14, 15].

Mast cells produce pro-inflammatory cytokines, such as tumor-necrosis factor (TNF)-α and IL-1β. They can also produce cytokines associated with anti-inflammatory responses, such as IL-10 and transforming growth factor β. TNF-α is the major cytokine of mast cells and they are the only known cells able to store this cytokine and are able to release it immediately after their activation [16]. The production of cytokines and chemokines may vary among species and is also dependent on the obtained stimuli. Other cytokines produced by mast cells are IL-4, IL-5, IL-6, IL-10, IL-13 and others. Mast cells are also source of chemokines, such as CCL5, CXCL8 (IL-8) and CXCL10. They also produce some growth factors such as vascular endothelial growth factor (VEGF), nerve growth factor (NGF) or granulocyte/macrophage colony stimulating factor (GM-CSF) [4].

Mast cell chemotaxis

The migration of mast cells is essential for their localization within the target tissues where they can execute their immunologic functions. Mast cells express various surface receptors that enable them to recognize appropriate chemotactic stimuli that can navigate them to the place of

residing. These receptors bind chemoattractants and chemokines, among them some can be produced by activated mast cells themselves and thus recruit other mast cells. The receptors playing role in chemotaxis include KIT, FcεRI, and group of G protein-coupled receptors. The main chemoattractants are SCF, antigen, sphingosine-1-phosphate (S1P), prostaglandin E_2 and D_2, leukotrienes, chemokines, and many other compounds [17].

The expression pattern of the surface receptors involved in chemotaxis depends on the species and tissue origin of mast cells and also on the conditions of their maturation [7]. Several methods to study mast cell chemotaxis *in vivo* and *in vitro* have been developed and in the recent years more attention is being focused on chemotaxis.

Cross-talk with other immune cells

Benefiting from their localization, mast cells can directly or indirectly sense the presence of pathogens and rapidly respond by releasing proinflammatory and immunoregulatory mediators and cytokines that can attract other cells and further lead to activation of innate and adaptive immune responses [18] The full regulatory role of mast cells and their interactions with other cells of immune system are still not fully understood and are under intense investigation.

Mast cells are able to induce migration of dendritic cells into inflamed tissue and into lymph nodes. Also a direct interaction with dendritic cells was observed [19]. Dendritic cells are important antigen presenting cells and function as a link between the innate and adaptive immunity. Together they are potential partners capable of modulation of immune responses to environmental changes.

Mast cells produce various cytokines and chemokines and other mediators. Recruitment of various cells can be mediated due to production of IL-1 [20], MIP-1α [21], histamine [22] or TNF-α. LTC_4 and TNF-α produced by mast cells were shown to play role in neutrophil recruitment in bacterial infections [23]. Production of MIP-1α can promote migration of T cells [21]. They also promote migration of peripheral lymphocytes, Langerhans cells, and dendritic cells [5].

Mast cells are also known to form immunological synapse with T cells. They can also express ligands for T cell costimulatory molecules, such as OX40L, and enhance T cell activation [24]. Actions of mast cells can subsequently lead to promoting interactions of antigen presenting cells with T helper cells or to activation of cytotoxic T cells.

Figure 2 illustrates some of the actions of mast cells, the consequences of mediator release and the action on other cells.

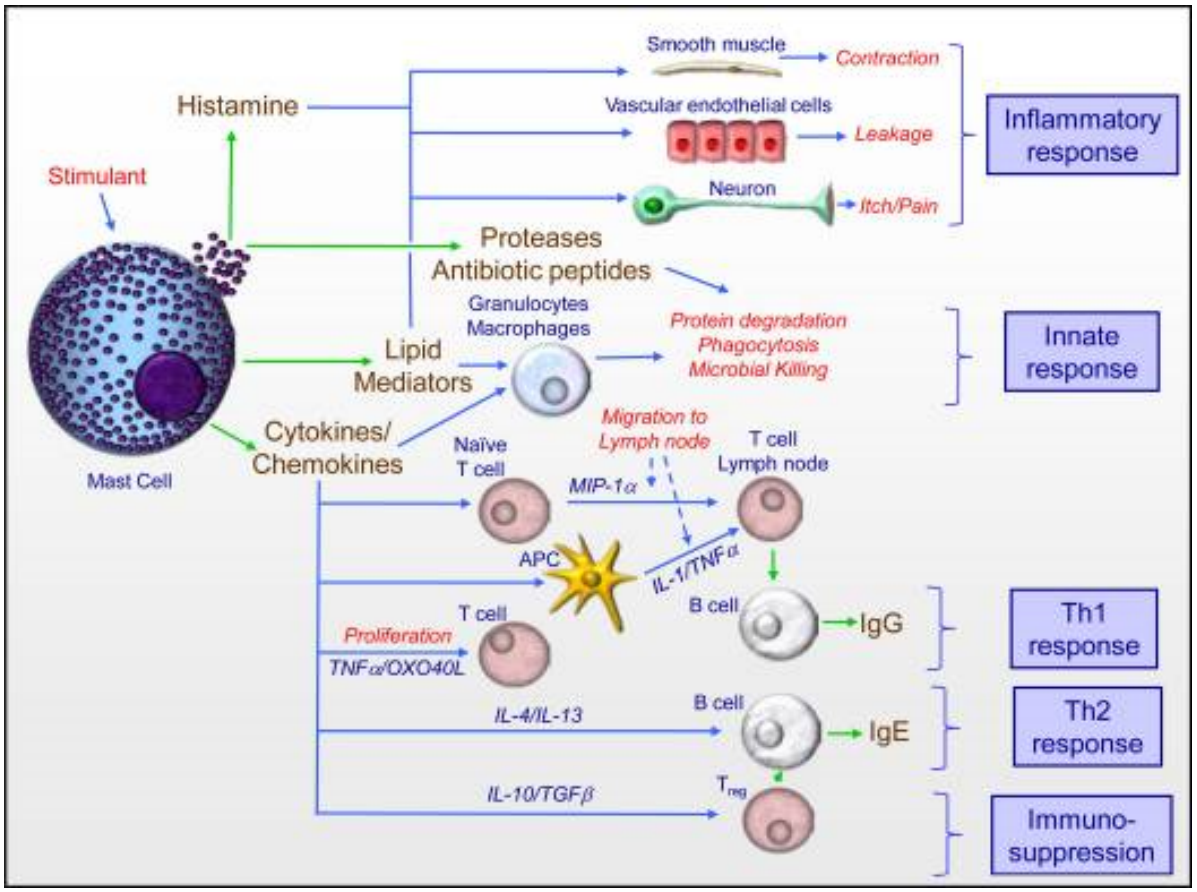

(Gilfillan and Beaven 2011)

Figure 2. Mast cell mediators and their actions in inflammatory and immune responses. Secretion of granules leads to release of histamine and mast-cell specific proteases. Histamine acts through its various receptors to induce smooth muscle contraction or relaxation, enhanced permeability across vascular endothelial cells, and itching or pain by activating sensory neurons, which account for some symptoms of acute allergic reactions. The proteases degrade endogenous and pathogenic proteins and contribute to innate immune responses and tissue remodeling. The lipid mediators are rapidly synthesized and include the arachidonyl-derived prostaglandins and leukotrienes. These compounds also contribute to allergic symptoms such as bronchial constriction, increased vascular permeability, and recruitment of granulocytes and macrophages to facilitate innate and adaptive immune responses. The subsequent production of a wide range of cytokines and chemokines promotes not only the classic delayed allergic reaction but also processes essential for adaptive immune responses and possibly immunosuppression as shown.

The high-affinity IgE receptor (FcεRI)

FcεRI is the most studied receptor on mast cells and its expression on the surface of mast cells together with KIT, a receptor for SCF, is a hallmark for defining mast cell population. FcεRI is expressed also on the surface of basophils. It belongs to the multichain immune receptor family that includes also the T and B cell receptor. The tetrameric structure is composed of one IgE-binding α subunit, one membrane-tetraspanning β subunit and a dimer of disulphide-linked γ

subunits [25]. FcεRI can exist also in a trimeric form lacking the β subunit and is expressed in monocytes, Langerhans cells and dendritic cells [26]. The extracellular α chain belongs to the immunoglobulin superfamily and is responsible for binding the Fc part of IgE at 1:1 ratio [27]. The β chain amplifies the signal of calcium mobilization and spleen tyrosine kinase (SYK) phosphorylation while the γ dimmer functions as an autonomous activation module [28]. The β and γ chains have no role in ligand binding, each contains one immunoreceptor tyrosine-based activation motif (ITAM) located in the cytoplasmic tails. These ITAMs are responsible for signal transduction and after phosphorylation serve as docking sites for molecules containing Src homology (SH) 2 domain [26, 29]. The β and γ chains are shared with other Fc receptors.

FcεRI-mediated signaling

The binding of multivalent antigen to IgE-FcεRI complex on the cell surface causes its crosslinking and triggers a series of activation events starting with the activation of the Src family kinase LYN that is weakly associated with the β chain (Figure 3). The protein tyrosine kinase LYN phosphorylates the aggregated ITAM motives of the adjacent β and γ chains, activates the kinase SYK that is recruited to the γ chain and consequently, additional LYN is recruited to the β chain and enhances the phosphorylation.

Binding of SYK to phosphorylated ITAMs through its SH2 domain enables the kinase a conformational change leading to its increased enzymatic activity [30]. The tyrosine phosphorylation of SYK leads to downstream signal propagation and phosphorylation of many substrates, among them the adaptor proteins linker for activation of T-cells (LAT), non-T-cell activation linker (NTAL) and SH2-domain-containing leukocyte protein of 76 kDA (SLP-76). The adaptors enable the assembly of large signaling complexes that contribute to both degranulation and cytokine production.

A complementary pathway of FcεRI signaling is initiated by the SRC family kinase FYN that also associates with the β chain as LYN. After FcεRI aggregation, FYN phosphorylates the adaptor GRB2-associated binding protein 2 (GAB2) and AKT. Phosphorylated GAB2 serves as a docking site for additional FYN and promotes degranulation by its subsequent association with phosphatidylinositol 3-kinases (PI3K) [31]. PI3K then phosphorylates phosphatidylinositol-4,5-bisphosphate (PI(4,5)P2) to phosphatidylinositol-3,4,5-trisphosphate (PI(3,4,5)P3). FYN is required for normal mast cell degranulation and maintenance and/or amplification of Ca^{2+} signal while LYN is crucial for Ca^{2+} signaling [31-33].

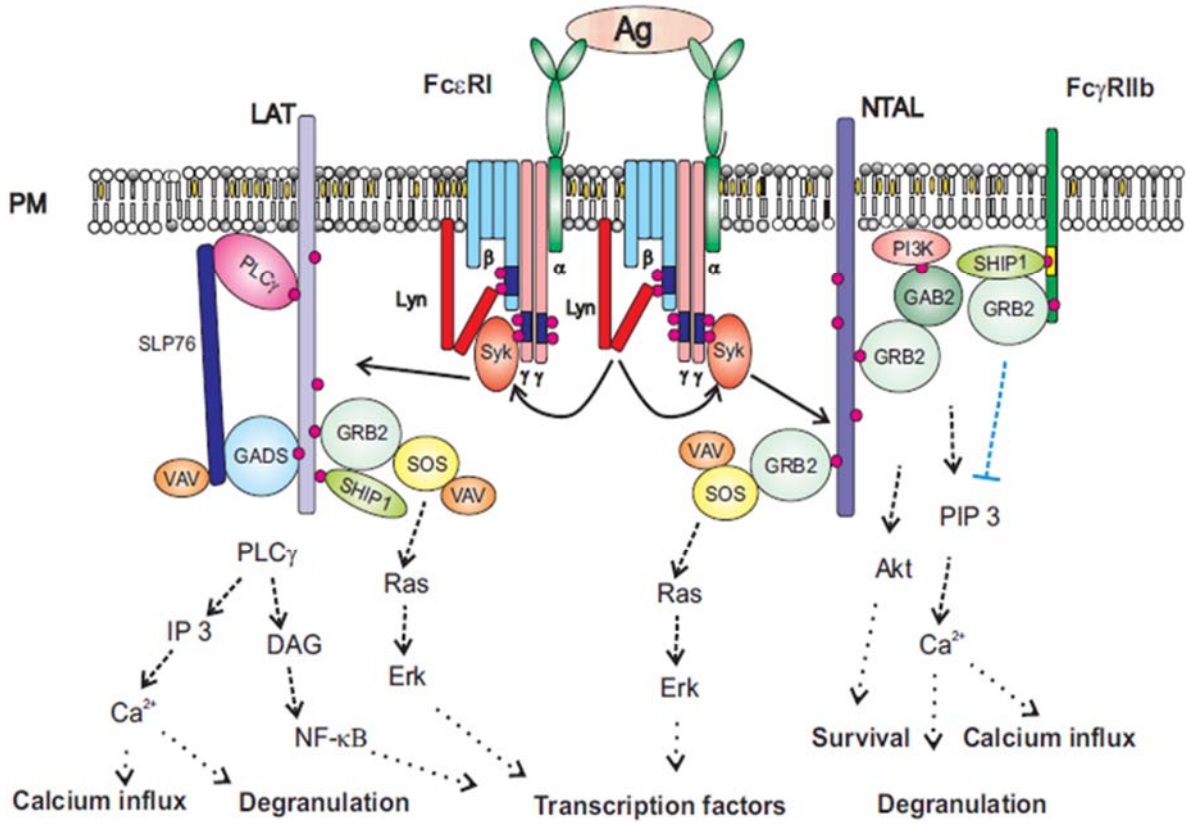

(Draber et al. 2012)

Figure 3. Scheme of FcεRI-mediated signaling. Aggregation of the receptors by multivalent antigen leads to rapid phosphorylation of tyrosine residues in ITAMs by LYN kinase and recruitment of SYK to FcεRI through the interaction of its SH2 domains with the phosphorylated ITAMs. SYK then phosphorylates NTAL and LAT to create binding sites for various SH2-containing proteins. Phosphorylated LAT binds PLCγ1, GRB2, GADS, and SHIP1. GBR2 and GADS enable binding of SLP-76, VAV, and SOS. Activity of PLCγ1 leads to enhanced production of IP3 and DAG, followed by increased Ca^{2+} influx, degranulation, and production of transcription factors. Phosphorylated NTAL also binds GBR2 and other signaling molecules but not PLCγ1. However, NTAL can modulate Ca^{2+} signaling, degranulation, and cell survival through indirect cross-talk with PI3 activation pathway.

The transmembrane adaptor protein LAT, phosphorylated by SYK, recruits cytosolic adaptors, such as GRB2-related adaptor protein (GADS), growth factor receptor-bound protein 2 (GRB2), and SLP76, guanosine triphosphate exchangers VAV and SOS, and the signaling enyzymes phopholipase Cγ (PLCγ)1 and PLCγ2. Assembly of this complex and recruitment of PI3K enables PLCγ activation. PLCγ is phosphorylated by SYK and the Tec family kinase Bruton´s tyrosine kinase BTK. BTK recruitment to the membrane is regulated via its pleckstrin-homology domain-mediated binding to PI(3,4,5)P3, generated by activated PI3K. Activated PLCγ catalyzes the hydrolysis of membrane bound lipid, PI(4,5)P2, to generate two important second messengers, 1,2-diacylglycerol (DAG) and inositol-1,4,5-trisphosphate (IP3). DAG

activates conventional protein kinase C (PKC) isoforms that, together with the free Ca^{2+} released via the action of IP3, initiates the degranulation event and its maximum is reached by sustained high levels of PI(3,4,5)P3 and Ca^{2+} [34-36].

Calcium signaling

IP3 diffuses through the cytosol and induces cytosolic calcium mobilization via binding to its receptors located in the membrane of the endoplasmic reticulum (ER). IP3 receptors are Ca^{2+} channels allowing the release of Ca^{2+} from the ER stores to the cytoplasm. The depletion of Ca^{2+} from intracellular stores, regardless of how stores are depleted, leads to opening of plasma membrane store-operated Ca^{2+} release-activated Ca^{2+} (CRAC) channels that allow a strong Ca^{2+} influx into the cytoplasm. The molecule stromal interaction molecule 1 (STIM1) located on the ER is a Ca^{2+} sensor detecting the ER Ca^{2+} concentration. After ER Ca^{2+} depletion STIM1 forms clusters in the ER membrane which move in the close proximity of the plasma membrane and directly interact with CRAC channel subunit ORAI1 and enable entering of Ca^{2+} into the cells [37]. Mast cell degranulation is critically dependent on increased intracellular calcium and activation of PKC [38]. The Ca^{2+} influx triggers the fusion of mast cell granules to the membrane and is essential for actin cytoskeleton reorganization [39, 40].

Another second messenger for mast cell activation and calcium mobilization is S1P. LYN and FYN kinases also activate sphingosine kinases SPHK1 and SPHK2, which induce conversion of sphingosine into S1P. S1P works as a ligand for a subset of G protein-coupled S1P receptors, which are known to regulate variety of cellular responses including motility, cytoskeletal reorganization, formation of adherent junctions, proliferation, angiogenesis, and the trafficking of immune cells [41]. Mast cells activated via the FcεRI secrete S1P from the cells through transporter ABCC1 (a member of the ATP-binding cassette transporter family) and the extracellular S1P binds to $S1P_1$ and $S1P_2$ receptors [42]. In contrast to murine mast cells, S1P induced degranulation of human mast cells and SPHK1, but not SPHK2, has been shown to play a critical role in antigen-induced degranulation [43]. Direct interaction of SPHK1 with tyrosine kinase LYN but not with SYK causes SPHK1 recruitment to membrane rafts and to FcεRI [43, 44]. The sphingosine kinase activity induced by FcεRI crosslinking plays a role in maintaining the balance between sphingosine and S1P. While high levels of sphingosine are associated with apoptosis, high levels of S1P with cell proliferation [45].

Calcium mobilization has an impact on activation of many adaptors including VAV, GRB2, and SOS, activation of Rho GTPases, ERK, JNK, and the mitogen-activated protein kinase (MAPK) pathway. Phosphorylated adaptor LAT allows direct binding of PLCγ1, GRB2, and

GADS via their SH2 domains. Guanine nucleotide factors VAV and SOS associate with this complex and activate the RAS and Rho family GTPases and thus modulating cytoskeletal rearrangement and vesicle movement as well as initiating MAPKs activation. Activated RAS positively regulates the RAF-dependent pathway and activates the ERK, JNK, and p38 MAPK pathways leading to activation factors FOS and JUN, NFAT, NFκB, ATF2, and ELK1 [5].
The increase in intracellular calcium activates calcineurin by binding a regulatory subunit and activating calmodulin binding. Calcineurin dephosphorylates the nuclear factor for T cell activation (NFAT) and the association between calcineurin and NFAT results in relocalization of NFAT to the nucleus, where it regulates the transcription of several cytokine genes [46].

Regulation of FcεRI-mediated signaling

Mast cells also express inhibitory cell-surface receptors to control the effector functions. These receptors contain in their cytoplasmic part an immunoreceptor tyrosine-based inhibitory motif (ITIM). They use the ITIMs to suppress the activation by promoting the dephosphorylation carried out by the phosphatases of the SH2-domain-containing protein tyrosine phosphatase (SHP) or the SH2-containing inositol 5' phosphatase (SHIP) family. SHIP binds to the low-affinity receptor for IgG, FcγRIIB, and to β and γ subunits of the FcεRI and inhibits the degranulation. Through the ITIMs on inhibitory receptors, the lipid phosphatase SHIP is recruited to the plasma membrane where it degrades PI(3,4,5)P3 to PI(4,5)P2 which leads to reduced BTK activation and PLCγ-mediated Ca^{2+} mobilization. Phosphatase and tensin homologue deleted on chromosome ten (PTEN) opposes PI3K activity. PTEN catalyzes the hydrolysis of PI(3,4,5)P3 to PI(4,5)P2 functioning as a negative regulator of FcεRI-induced calcium flux, degranulation and cytokine production [47].
Reversible phosphorylation of signaling proteins is important in balancing the protein activity and is mediated not only by protein tyrosine phosphatases but also by protein tyrosine kinases. Some molecules may play role not only in initiation of signaling events but also in its termination. LYN, that starts the signaling cascade, negatively regulates the activity of the kinase FYN and thus inhibits the phosphorylation of the GAB2 adaptor. LYN also suppresses signaling by recruiting C-terminal Src kinase (CSK) [48].
Recent study reports that overexpression of β chain of FcεRI in mast cells mainly increased its cytoplasmic expression and slightly up-regulated cell surface FcεRI expression. Some of the β chain in cytoplasm appeared not to be co-localized with α chain of FcεRI. The overexpression of β chain resulted in down-regulation of SYK activation and reduction in Ca^{2+} influx soon after FcεRI aggregation and down-regulation of degranulation, PGD_2 synthesis, and production of a

set of cytokines, including TNF-α. The cytoplasmic β chain can capture LYN preventing its association with functional surface FcεRI tetramers and may thus function as a negative regulator [49].

Negative regulatory function can be also performed by adaptor molecules. The adaptor downstream of tyrosine kinase 1 (DOK1) interacts with negative regulators of FcεRI-mediated signaling. DOK1 is constitutively associated with the Ras GTP-binding protein-activating protein (RasGAP). After SHIP recruitment to the ITIM in a LYN-dependent manner, DOK1 associates with SHIP and the negative regulatory complex SHIP/RasGAP/DOK1 downregulates the IP3 levels and inhibits RAS activation via RasGAP [50, 51].

Recent study by Suzuki et al. [52] reveals how FcεRI modulates the response in mast cells to high- and low-affinity stimulus. The low-affinity stimulation leads to decreased degranulation, reduced leukotriene B_4 and cytokine production but enhanced chemokine production. It shows that the differences are not due to variable receptor phosphorylation but the size of receptor clusters, mobility, and distribution. In the low-affinity stimulation bigger and less mobile receptor clusters are formed. While in high-affinity stimulation LAT, PLCγ1 and PLCγ2 are phosphorylated, in the low-affinity stimulation the signal is shifted to NTAL that is more phosphorylated and colocalizes with FcεRI to higher extend. Also the association of Src family kinase FGR with the receptor is increased.

KIT-mediated signaling

An important receptor localized on the plasma membrane of mast cells is KIT (CD117), a growth factor receptor for SCF. KIT activation is crucial for growth, survival, differentiation and homing of mast cells into target tissues. SCF, existing in two isoforms, soluble and membrane bound, that arise by alternative splicing of one RNA, is produced by different cell types including fibroblasts and endothelial cells. Not only IgE, but also SCF, can be a potent activator of mast cells [53]. In the presence of antigen, SCF markedly increases mast cell degranulation and potentiates and prolongs calcium signal. It also influences mast cell chemotaxis and adhesion [54]. KIT is a single chain receptor with protein-tyrosine kinase activity. Its extracellular part comprises of five immunoglobulin-like domains, from which the first three bind SCF and the fourth is important for the receptor dimerization. The intracellular part has two catalytic domains. SCF binding to KIT leads to dimerization and auto/transphosphorylation at tyrosine residues resulting in the recruitment of various molecules. Phosphorylated residues serve as docking sites for SH2 domain-containing molecules [55, 56].

Signaling pathways elicited by KIT share several similar features with the FcεRI mediated events such as activation of Src kinases, PLCγ1, PI3K, calcium mobilization and MAPK-cascade activation. Though activated KIT does not recruit or activate SYK or phosphorylate LAT. The ability of KIT to potentiate FcεRI dependent degranulation is due to NTAL and BTK and their ability to regulate PLCγ1-dependent calcium mobilization and PKC activation [5]. KIT can directly phosphorylate NTAL and it phosphorylates other tyrosines than SYK when activated in the FcεRI manner [57].

After KIT dimerization and activation of its intrinsic kinase activity, phosphorylated tyrosine residues recruit SH2-domain containing molecules, including cytosolic adaptors SHC and GRB2, kinases LYN and FYN, PLCγ, and PI3K and create signaling complex that further propagates the downstream signaling leading to activation of other signaling molecules. Among them the molecules from the JAK-STAT pathway and RAS-RAF-MAPK pathway are activated and it leads to mast cell growth, differentiation, survival, adhesion and chemotaxis. Other molecules activated include the Tec kinase BTK and the adaptor molecule NTAL, that play role in enhancement of antigen-mediated degranulation and cytokine production. KIT receptor can directly bind the p85α subunit of PI3K which causes subsequent generation of membrane associated PI(3,4,5)P3 [39, 53]. PI3K and BTK were shown to play crucial role in amplification of FcεRI-mediated mast cell signaling and cytokine production by KIT [58, 59].

Transmembrane adaptor proteins

The adaptors play important role as scaffolds enabling the assembly of large temporary signaling complexes that contribute to both degranulation and cytokine production. Organization of activated signaling molecules and directing them to specific cellular compartments is essential for activation of immune cells including mast cells. Adaptors are proteins without intrinsic enzymatic function composed of multiple protein-protein or protein-lipid interacting domains to be able to link molecules to each other. The formation of multimolecular complexes, termed signalosomes, brings together molecules of various activity and creates the necessary machinery to regulate downstream signaling events. These signalosomes must be localized to specific regions to allow interactions with particular molecules and this is mediated by adaptor molecules.

The transmembrane adaptor proteins (TRAP) are anchored scaffolds that provide docking sites through phosphorylation of tyrosine residues. In mast cells five TRAPs have been identified:

LAT, NTAL, PAG, linker for activation of X cells (LAX), and GRB2-binding adaptor protein, transmembrane (GAPT) [60].

TRAPs usually contain a short extracellular domain, a single transmembrane domain, and a long cytoplasmic tail where are localized various tyrosine containing motifs and domains that can be phosphorylated. The hydrophobic transmembrane part anchors the proteins into plasma membrane. Some TRAPs have also juxtamembrane palmitoylation motif, CXXC, for their localization in detergent-resistant membranes. The phosphorylation of the tyrosine residues in the cytoplasmic tail causes the recruitment of downstream effector molecules [61]. The schematic structures, tyrosine motifs, and other domains of all five TRAPs expressed in human and mouse mast cells are illustrated in figure 4.

Cytosolic adaptors usually possess more motifs that allow them to bind other molecules. The cytosolic adaptor proteins lack the hydrophobic transmembrane domain that would anchor them into the plasma membrane; instead they can be associated with cytoskeleton or organelles. They can also be recruited to TRAPs, mainly to LAT and NTAL. LAT brings together two cytosolic adaptors SLP-76 and GADS. Other cytosolic adaptors important in mast cells signaling are GAB2, GRB2, and DOK1 that possesses negative regulatory function [34].

LAT

LAT was the first adaptor described in T-cells playing an important role after T-cell receptor engagement. Because of its crucial role in immunoreceptor signaling it belongs to the most studied adaptor in mast cells. It has the typical TRAP structure and a size of 36-38 kDa. Next to mast cells and T cells, it was found to be expressed also in nature killer cells, megacaryocytes, platelets, and immature B cells [61, 62].

LAT is phosphorylated by SYK in mast cells or ZAP-70 in other cells and associates with GRB2, PLCγ1, VAV, SPL-76, CBL and GADS [60]. LAT-deficient mice are viable and grow normally. LAT deficiency in mast cells causes impaired degranulation, reduced phosphorylation of PLCγ1 and SPL-76, decreased MAPK activity and calcium signaling [63]. Studies with LAT mutants transfected into LAT-deficient cells revealed the key tyrosines in LAT and helped to identify which tyrosines are responsible for docking of other molecules [64].

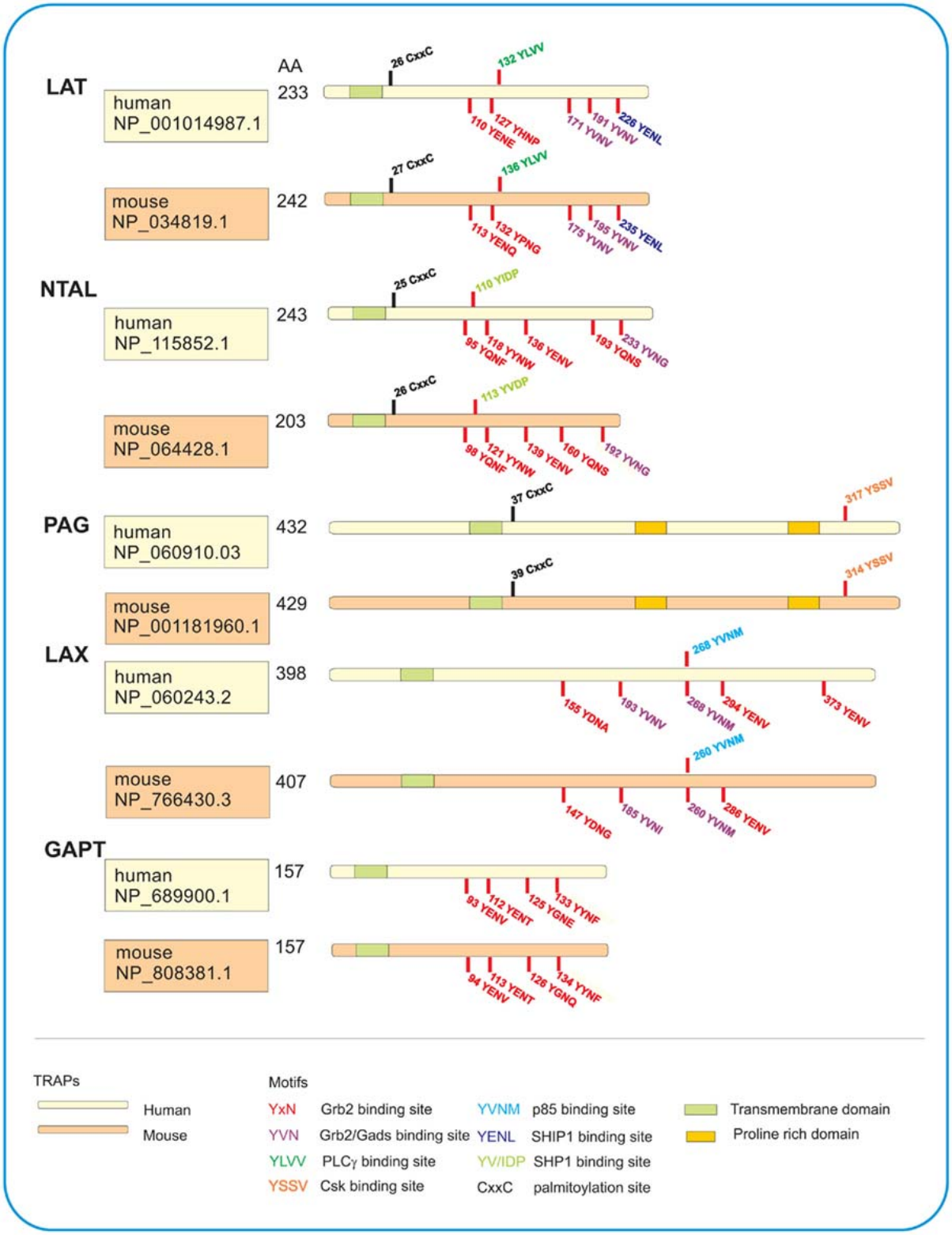

(Draber et al. 2012)

Figure 4. Human and mouse TRAPs in mast cells. Schematic model of TRAPs showing a short extracellular domain, transmembrane domain (green), and cytoplasmic domain with various motifs. After phosphorylation, tyrosine-based motifs serve as binding sites for SH2-containing proteins. The proline-rich domains in PAG serve as anchor for SH3-containing proteins. LAT, NTAL, and PAG possess juxtamembrane CxxC palmitoylation site for their localization in detergent-resistant membranes.

NTAL

NTAL, also termed as LAB or LAT2, was discovered in search for molecule similar to LAT in B cells. It is an adaptor structurally and evolutionary related to LAT but it lacks the PLCγ1 binding motif [65]. The cytoplasmic domain contains 10 tyrosines which are potential targets for tyrosine kinases. Similar to LAT, it has a palmitoylation site adjacent to transmembrane domain but electron microscopy showed that both adaptors occupy different microdomains in the plasma membrane [66]. NTAL is a 30-kDa molecule in humans and 25-kDa in mice. It is expressed in B cells, natural killer cells, monocytes, and mast cells. NTAL is rapidly phosphorylated by SYK and LYN (Iwaki 2008) and it associates with the cytoplasmic signaling molecules GRB2, SOS, VAV, and CBL. Mutation studies to map the phosphorylation and GRB2-binding sites revealed three membrane-distal tyrosines that are primarily phosphorylated in NTAL [67].

The functional similarity between LAT and NTAL was demonstrated by an adoptive transfer of NTAL into LAT-deficient mice. NTAL was able to rescue the thymocyte development but not normal T cell activation [68]. NTAL expressed in the LAT-deficient T cell line became tyrosine phosphorylated and partially rescued the T cell receptor-mediated signaling [65].

There are conflicting results about the function of NTAL in mast cells. NTAL deficiency in mouse mast cells causes enhanced degranulation, calcium mobilization, and phosphorylation of LAT, PLCγ1, and ERK. NTAL-deficient mice exhibit increased IgE-mediated passive systemic anaphylaxis [66, 69]. This is in contrast with results obtained in human mast cells [70]. Using RNA silencing techniques Tkaczyk at al. prepared mast cells with diminished NTAL expression and demonstrated inhibition of degranulation. BMMCs derived from NTAL and LAT null mice exhibit even more decreased degranulation than LAT deficiency alone, suggesting that under certain circumstances NTAL can have also positive regulatory role in mice [66, 69].

Recently, potential developmental alterations of signal transduction pathway in NTAL knock-out mice we excluded by preparing mouse mast cell with silenced NTAL expression. When examining signaling properties of these cells, no differences were found in comparison of these cells to knock-out cells [71].

PAG

PAG, also termed Csk-binding protein, was first described by two parallel studies and each study gave it different name [72, 73]. PAG shows structural similarity with LAT and NTAL and also possesses the palmitoylation motif. PAG was found to be ubiquitously expressed and

is not specific only for hematopoietic cells such as LAT and NTAL. In resting T cells, PAG associates with FYN kinase which constitutively phosphorylates PAG to create a docking site for the CSK SH2 domain. Enhanced CSK catalytic activity leads to phosphorylation of the LCK inhibitory tyrosine. Upon T cell receptor activation, PAG is rapidly dephosphorylated, CSK released from PAG, and LCK dephosphorylated. This increases the activity of LCK, leading to increased phosphorylation of T cell receptor subunits and other substrates.

In mast cells, PAG is phosphorylated by LYN kinase, and following FcεRI triggering, the decrease in PAG phosphorylation is replaced by an increase. Rat basophilic leukemia cells with enhanced PAG expression exhibited lower FcεRI-mediated degranulation and reduced calcium levels [74]. BMMCs derived from PAG-deficient mast cells exhibit impaired degranulation, calcium mobilization, tyrosine phosphorylation of FcεRI subunits and PLCγ (Draberova et al. submitted).

LAX

LAX is another TRAP that was originally found to be expressed in T cells [75], later in B cells [76] and mast cells [77]. LAX does not have significant sequence homology with LAT but it displays similar structural organization. Unlike LAT and NTAL it lacks palmitoylation motif and thus is soluble in non-ionic detergents. LAX is phosphorylated by Src and SYK kinases and it interacts with adaptors GRB2 and GADS. It was suggested that it plays role in negative regulation of PI3K pathway. However, BMMC derived from LAX-deficient mouse exhibited enhanced degranulation, increased phosphorylation of p38 MAPK and AKT but surprisingly no alterations in calcium mobilization. Also modest increase in production of several cytokines was observed. Decrease in NTAL expression on protein and mRNA level was also observed in these cells, suggesting that the ratio of NTAL and LAT is shifted to LAT.

GAPT

Search for other adaptors in human genome database lead also to discovery of GAPT [78]. This adaptor in expressed mainly in B cells and total bone marrow. It was found also in dendritic cells, mast cells and natural killer cells but not in T cells and macrophages. GAPT contains four GRB2-binding motifs. Mast cells generated from GAPT null mice do not show any alterations in degranulation. GAPT was found not to be phosphorylated after FcεRI triggering.

Pharmacological targeting of mast cells

Mast cells in health and disease

Recent research has shown that mast cells can play a key role in innate and adaptive immune responses, autoimmune diseases, and possibly also in tissue homeostasis by producing a range of biologically active products and expressing a variety of receptors. In addition, the responsiveness of mast cells to immunological and pathological stimulants is highly modulated by the tissue cytokine environment and by synergistic, or inhibitory, interactions among the various mast cell receptors. Disrupting this homeostasis can lead to pathology related to mast cells and development of allergies and asthma, contribute to autoimmune diseases, chronic innate immune responses and other mast cells related diseases.

Soluble mediators as targets

Two of the key soluble mediators released by mast cells by different stimuli are histamine and leukotrienes. Both are commonly targeted in clinical practice by various drugs. Other soluble mediators that could possibly be target are β-typtase and chymase, but even though studies in animal models showed promising results none inhibitor has made it to clinical trials.

Histamine is a preformed mediator released from the mast cell granules after activation. There are four known histamine receptors (HR). HR1 is the most targeted in allergies. H1-antihistamines are inverse agonists and are currently the most used antiallergic drugs to treat asthma, urticaria, atopic dermatitis, allergic rhinitis, and conjunctivitis [79]. Recent study reported that a combination of antihistamines targeting H1R and H4R has synergistic therapeutic effects in a mouse model of chronic dermatitis [80].

LTC_4 is a potent bronchoconstrictor and is synthesized *de novo* from arachidonic acid. LTC_4 binds to cysteinyl leukotriene receptor (cysLTR) 1 and 2. Zafirlukast, pranlukast, and montelukast are cysLTR1 specific antagonists and are in clinical use to treat asthma [81, 82]. Inhibitors targeting the synthesis pathway LTC_4 are under investigation. GSK2190915 is an inhibitor of 5-lipoxygenase–activating protein (FLAP), a protein that facilitates the transfer of arachidonic acid to 5-lipoxygenase. Results from patients with mild asthma, show that the drug is well tolerated and effective in inhibiting early and late responses to inhaled allergen [82, 83].

Mast cells produce a variety of cytokines and chemokines but their targeting is not exclusive to mast cells since the same molecules can be produced by other cells too. TNF-α is probably the most proinflammatory cytokine produced by mast cells [84]. Several drugs targeting TNF-α are used in the therapies to treat patients with psoriasis, rheumatoid arthritis, and other serious

chronic inflammatory conditions. Other cytokine under clinical investigations is IL-17 that is predominantly produced by mast cells in patients with inflammatory skin and joint diseases [85].

Use of drugs targeting the soluble mediators is generally seen as a success. But it has to be considered that only the product not the *de novo* synthesis is targeted. Patients with certain diseases do not obtain sufficient relief of their symptoms, not even after administration of high doses. Thus it is desired to target also the production of these mediators.

Intracellular signaling molecules as targets

Activation of mast cells can be blocked by inhibitors that act on signaling pathways transduced from plasma membrane receptors to cytoplasmic effectors. To prevent mast cell activation and production of the mediators released after degranulation, it is possible to inhibit key enzymes involved in signaling pathways leading from the plasma membrane receptors to the cytoplasmic effectors. Most of the signaling pathways used by mast cells are not found exclusively in these cells, and therefore it is a demanding task to find drugs specifically inhibiting the activation of mast cells.

After receiving promising result in mouse model, fostamatinib, an oral SYK inhibitor, has been successfully used in phase II clinical trial for treatment of patients with rheumatoid arthritis [86]. Directly or indirectly, through SYK, the PI3Ks are activated. PI3Ks are used for various signaling pathways in many cell types and are upregulated in cancers and therefor seem not to be ideal targets. However, compounds such as IC87114, its chemical derivate CAL-101, and CAL-263, are highly selective inhibitors of PI3Kδ and have clinical potential to treat allergic rhinitis [87], asthma [88] or rheumatoid arthritis [89]. IPI-145, a small-molecule inhibitor of PI3K-δ and PI3K-γ, showed potent activity in collagen-induced arthritis, ovalbumin-induced asthma, and systemic lupus erythematosus rodent models. IPI-145 was also reported to block neutrophil migration, lymphocyte proliferation, and reduce basophil and mast cell activation [90]. It is in clinical trials for hematologic malignancies and inflammatory diseases, such as asthma and rheumatoid arthritis.

BTK is activated downstream of FcεRI and can be selectively inhibited by ibrutinib that, via its binding to the active site, disables its phosphorylation and thus causes inactivation. It forms a specific covalent bond with a cysteine residue in BTK and abrogates its full activation by inhibiting its tyrosine autophosphorylation [91, 92]. Also the drug AVL-292/CC-292 is designed on the same principle and is under investigation in clinical trials to treat rheumatoid arthritis [93].

Enhancing the negative regulation of degranulation and termination of the activation events can be achieved by stimulating the phosphatase SHIP. Study with AQX-1125, a novel oral SHIP1 activator, reports significantly reduced late response to allergen challenge, with a trend to reduce airway inflammation and claims AQX-1125 a safe and well tolerated drug that merits further investigation in inflammatory disorders [94].

Several diseases including mastocytosis or recurrent anaphylaxis are associated with a gain of function mutation (D816V) in KIT [95]. The known KIT inhibitors are not specific and inhibit also other molecules with tyrosine kinase activity. Inhibition of KIT is mainly desired in myeloid leukemia but would be also desirable for treatment of systemic mastocytosis or arthritis and allergen-induced asthma. Several KIT inhibitors varying in their inhibitory specificity and sensitivity to the activating mutation are available: dasatinib, nilotinib, imatinib, and masitinib [79].

Surface receptors as targets

Third class of drugs focuses on inhibiting mast cell activating receptors or the inhibitory receptors that, after activation, are able to downregulate the stimulatory signaling derived from activating receptors. Blocking FcεRI is already being used as a treatment. However, there are other receptors, such as CD300a, FcγRIIB, and Siglec-8, that might be promising targets for therapy.

The inhibitory receptors CD300a, FcγRIIB, and Siglec-8 contain ITIMs in their cytoplasmic tails and via their activation they can negatively regulate the activation of mast cells. Selective targeting of CD300a receptor with bispecific antibody anti-IgE/anti-CD300a showed promising results in mouse models [96, 97]. Siglec-8 was shown to function not only on human mast cell but also on eosinophils and eosinophiles and is a candidate for further investigation to treat allergy [98, 99]. Bispecific antibodies or fusion proteins targeting FcγRIIB and FcεRI are under development and are tested in mouse models [100-102].

Among the activating receptors only FcεRI is targeted in clinical use. The humanized mAb omalizumab (Xolair) blocks the interaction of IgE with FcεRI by targeting IgE. It binds to IgE in a specific manner that overlaps with receptor binding and thus by itself does not have any activating effect. This antibody has been approved for the treatment of moderate and severe asthma with proven efficacy and safety [103].

Modulating the activity of CD48, a CD2-like molecule expressed on the surfaces of hematopoietic cells, and TSLPR, a thymic stromal lymphopoietin receptor involved in promoting TH2-type immune responses, is currently under investigation in animal models.

AIMS

The main focus of this thesis was to shed light on the role of the transmembrane adaptor protein NTAL in murine mast cells and to clarify the discrepancy in results obtained in mast cells isolated from NTAL knock-out mice and human mast cells with diminished NTAL expression. The second aim was to understand the role of another important transmembrane adaptor protein PAG in mast cell signaling by isolating and studying mast cells from PAG knock-out mice. Furthermore, we attempted to improve the PCR performance, a method widely used in both studies, and to summarize recent approaches in pharmacologic targeting of intracellular signaling pathways in mast cells.

The specific aims were:

1. To examine the regulatory roles of NTAL in murine mast cells signaling and to test the contribution of compensatory developmental alterations in mast cells generated from NTAL KO mice with the following sub-aims:
    1.1. To prepare NTAL knock-down in murine mast cells using the lentiviral delivery of shRNA.
    1.2. To compare lentivirally transduced cells with diminished NTAL expression with mast cells isolated from NTAL knock-out mice and determine degranulation, calcium response, and phosphorylation of several molecules involved in signaling pathway in the course of FcεRI-induced activation.
    1.3. To determine actin polymerization, cell spreading and cell migration in both types of NTAL-deficient cells.
    1.4. To obtain gene expression profiles using the microarray approach.
    1.5. To analyze the microarray data in order to identify differentially-expressed genes in NTAL-deficient cells.
    1.6. To verify the identified genes by real-time PCR.
    1.7. To investigate the role of cholesterol in mast cell migration.
2. To participate in characterization of the role of PAG in murine mast cell immune response by genotyping the mice, analyzing the expression profiles in PAG WT and KO mice and reconstituting expression of PAG in PAG-deficient cells.
3. To contribute to development of new PCR master mixes for amplification of templates which are difficult to amplify and that are also suitable for routine real-time PCR.
4. To review recent pharmacological approaches focused on targeting the intracellular signaling pathways in mast cells with emphasis on clinical trials.

METHODS

Methods used to solve the particular aims of this study are briefly described below. They are described in more details in the result sections in the corresponding publications.

BMMCs preparation

Bone marrow cells were isolated from femurs and tibias of 8-12 week-old mice. The cells were cultured for 6-8 weeks in Iscove's medium supplemented with 10% fetal calf serum (FCS), penicillin, streptomycin, 2-mercaptoethanol, IL-3 (20 ng/ml), and SCF (40 ng/ml). In some experiments BMMCs were cultured for the indicated time intervals in mast cell medium supplemented with 10% cholesterol-depleted FCS instead of FCS.

Mast cell sensitization and degranulation

BMMCs (6 x 10^6/ml) were sensitized in medium without SCF and IL-3, but supplemented with trinitrophenyl (TNP)-specific IgE (1 µg/ml). After 4 hours the cells were washed in buffered salt solution (BSS; 20 mM HEPES, pH 7.4, 135 mM NaCl, 5 mM KCl, 1.8 mM $CaCl_2$, 5.6 mM glucose, and 1 mM $MgCl_2$) supplemented with 0.1% bovine serum albumin (BSA) and stimulated with various concentrations of antigen (TNP-BSA conjugate) and/or SCF. Degree of degranulation was determined by measuring the release of β-glucuronidase from the activated cells in the supernatant. 4-methylumbelliferyl β-D-glucuronide was used as a substrate and the amount of fluorescent product was measured by a plate reader using 365 nm excitation and 460 nm emission filters.

Cholesterol determination

Concentration of cholesterol in cholesterol-depleted FCS and cell samples was determined by the Amplex Red Cholesterol Assay kit (Life Technologies) according to the manufacturer´s instruction. Using this kit, no remaining cholesterol was detectable in delipidated serum. This indicates that cholesterol concentration was reduced from ~80 µg/ml to <15 ng/ml.

Immunoblotting

Cells were solubilized for 30 minutes in ice-cold lysis buffer containing 50 mM Tris-HCl, pH 7.4, 150 mM NaCl, 2 mM EDTA, 10 mM β-glycerophosphate, 1 mM Na_3VO_4, 1 mM PMSF, 1 µg/ml aprotinin, 1 µg/ml leupeptin, 0.2% Triton X-100, 1% Nonidet P-40 and 1% n-dodecyl-β-D-maltoside. After centrifugation (15 minutes at 7.000 x g at 4°C), proteins in postnuclear

supernatants were size fractionated by SDS-polyacrylamide gel electrophoresis and analyzed by direct immunoblotting. Immunoblots were quantified by Luminiscent Image Analyzer LAS 3000 and further analyzed by AIDA image analyzer software.

Measurement of free cytoplasmic Ca^{2+}

Concentration of free intracellular Ca^{2+} was determined using cells labeled with Fura-2-AM. Cells were incubated for 30 minutes with the dye in the presence of probenecid to prevent leakage of the dye from the cells. After proper washing of the cells, Ca^{2+} levels were monitored by means of fluorescence reader Infinite M200 with excitation wavelengths of 340 and 380 nm, and emission wavelength of 510 nm.

Lentiviral vectors and gene transduction

To prepare BMMCs with stable NTAL knock-down in mast cells a set of 5 NTAL shRNA constructs cloned into the pLKO.1 vector was purchased. From these five shRNA constructs two shRNAs that showed reproducibly the highest reduction of NTAL protein expression in mast cells were used in most experiments and produced similar results. Only for microarray gene expression analysis and related qPCR validation, cells with transduced only with one shRNA were used.

Lentiviral transduction was performed accordingly: 21 µl ViraPower lentiviral packaging mix and 14 µg NTAL shRNA or pLKO.1 empty vector as a negative control (in 1.4 ml medium Opti-MEM) were co-transfected into 293T17 packaging cells in the presence of 84 µl Lipofectamine 2000 or 105 µl polyethylenimine (25 kD, linear form; 1 µg/ml). After 2-3 days, the culture supernatants were centrifuged to pellet the viruses, which were then used to infect BMMCs. Stable transfectants were selected in puromycin (5 µg/ml). After one week of selection, cells were analyzed for NTAL expression by immunoblotting. Before the tests, cells were transferred for 2-3 days into fresh media without puromycin.

For rescue experiments in PAG-deficient cells, viruses with Myc-Pag1 cDNA cloned into pCDH-CMV-MCS-EF1-Puro plasmid or empty pCDH-CMV-MCS-EF1-Puro plasmid were produced as described above. Medium with virus was filtered through 0.22 µm filter and divided into two aliquots. The first aliquot was used to transduce the wild type or PAG-deficient cells at day zero, the second one for the repeated transduction at day 3. Stable selection was achieved by culturing the cells for 7 days in the presence of puromycin (2 µg/ml), added 5 days after the first transduction.

F-actin assay

Total amount of F-actin in cells was determined by flow cytometry. Cells in 96-well plates were exposed to various stimuli, fixed with 3% paraformaldehyde in phosphate buffered saline and then permeabilized and stained in a single step by a mixture of lysophosphatidylcholine (200 μg/ml) and 1000x diluted Alexa Fluor 488-phalloidin in phosphate buffered saline. Fluorescence intensity was measured with the help of LSRII flow cytometer.

Cell spreading

8-well multitest slides were coated with fibronectin and Cell-Tak overnight. IgE-sensitized BMMCs were seeded on coated wells and allowed to attach for 1 hour, washed and activated for 30 minutes at 37°C with antigen and/or SCF, fixed with 3% paraformaldehyde in glutamate buffer-EGTA supplemented with 4% polyethylene glycol, and then permeabilized and stained with lysophosphatidylcholine (200 μg/ml) and 100x diluted Alexa Fluor 488-phalloidin. After mounting in Mowiol 4-88 containing Hoechst 33258 (3 μg/ml), fluorescent images were automatically collected using Olympus IX70 inverted microscope equipped with motorized stage and ScanR acquisition software. Cell area was analyzed using ScanR analysis software. At least 500 cells were evaluated in each test.

RNA preparation for microarray and qPCR analysis

Total RNA was isolated from 3 x 10^6 antigen-activated or resting BMMCs using the RNeasy mini kit according to the manufacturer´s protocol. For the NTAL study, three biological replicates were carried out with each cell type: NTAL knock-out, wild type, NTAL knock-down, and control wild type cells infected with empty vector. Cells in each group were cultured in parallel for 24 hours in complete media deprived of SCF and then sensitized with TNP-specific IgE in IL-3- and SCF-deprived medium for 4 hours. After washing, cell suspensions were divided into 2 aliquots; one activated for 2 hours with antigen and the other incubated without. RNA was isolated from all 24 samples and processed under identical conditions. In the case of PAG the process was slightly modified; two biological replicates were carried out with each cell type: wild type and knock-out. Sensitized cells were dived into 3 aliquots; one activated for 2 hours with antigen, second with SCF, and third incubated without. RNA was isolated from all 12 samples.

Microarray gene-expression profiling and data analysis

For the NTAL study, preparation of cRNA, hybridization and gene expression profiling was done by an Affymetrix authorized service provider (AROS Applied Biotechnology A/S) using the Affymetrix GeneTitan HT MG-430 PM 24-array plate with the 3' IVT express labeling kit according to the manufacturer´s protocol. Data analysis was carried out by importing raw data CEL files into Genomic Suite Software Partek 6.4, the Robust Multichip Analysis was applied for background correction, and principal component analysis (PCA) of the normalized microarray expression values was performed as a visualization technique to determine the similarity in the data. Lists of significantly upregulated or downregulated gene transcripts were created based on setting the fold change and false discovery rate (FDR) treshholds. Data were uploaded in the NCBIs Gene Expression Omnibus (GEO) database and are available under the accession number GSE40731.

The expression profiles of wild type and knock-out cells study were obtained in similar manner with some alterations. The profiling was done by a Genomics and Bionformatics core facility at IMG using 12 Affymetrix Mouse Genome 430 2.0 Arrays. The analysis and gene lists were created similarly, but the data were not yet uploaded in GEO.

Reverse transcription quantitative PCR

cDNA was synthesized using M-MLV reverse transcriptase according to manufacturer's instructions. For reverse transcription, 0.3 μg aliquots of total RNA were used from the same samples, which were used for microarray analysis. qPCRs were performed using a PCR mastermix supplemented with 0.2 M trehalose, 1 M 1,2-propanediol and SYBR green I as described in the publication [104]. 10 μl reaction volumes in 384-well plates were processed in LightCycler 480 under the following cycling conditions: initial 3 minutes denaturation at 95°C, followed by 50 cycles at 95°C for 10 s, 60°C for 20 s and 72°C for 20 s. Melting curve analysis was carried out from 72°C to 97°C with 0.2°C increments; Ct values for each sample were determined by automated threshold analysis. Data were normalized to a housekeeping GAPDH mRNA. The qPCRs for each of the biological triplicates was performed in quadruplicates.

DNA polymerase fidelity assay

The fidelity assay was based on streptomycin resistance of *rps*L mutants. Standard PCRs (50 μl) containing master mixes of different composition (salt concentration, additives, DNA dyes) were performed with template DNA (pMOL21 plasmid linearized with ScaI). One of the primers used for template amplification was biotinylated and carried MluI restriction site. The

control high-fidelity PCR reaction with KOD hot start polymerase was performed according to the manufacturer's instruction. The standard PCR conditions were: 94°C for 2 min, followed by 25 cycles at 94°C for 15 s, 58°C for 30 s and 68°C for 5 min. The PCR products were collected using streptavidin magnetic beads (Dynabeads M-280 Streptavidin) under gentle rotation at 22°C. After 30 min, the beads were washed and treated with MluI at 37°C with gentle rotation overnight. Beads were collected and the supernatant was fractionated by electrophoresis in 0.8% agarose gel. The DNA fragment was isolated using TaKaRa Recochi, purified by ethanol precipitation and dissolved in sterile water. After self-ligation with T4 DNA ligase, it was transformed into MF101 competent cells. Half of the transformants was plated on plates with ampicillin (100 μg/ml) to determine the total number of transformed cells; the remaining half on plates with ampicillin and streptomycin (100 μg/ml each) to determine the total number of rpsL mutants. The mutation frequency was determined by dividing the total number of mutants by the total number of transformed cells. The error rate was calculated by dividing the mutation frequency by 130 (the number of amino acids that cause phenotypic changes in rpsL), and the number of template doublings.

PUBLICATIONS

List of publications

1. Polakovicova I, Draberova L, Simicek M, Draber P. Multiple regulatory roles of the mouse transmembrane adaptor protein NTAL in gene transcription and mast cell physiology. PLoS One. 2014 Aug 25;9(8):e105539

2. Draberova L, Bugajev V, Potuckova L, Halova I, Bambouskova M, Polakovicova I, Xavier R, Seed B, Draber P. Transmembrane adaptor protein PAG/CBP is involved in both positive and negative regulation of mast cell signaling. Mol Cell Biol. (submitted)

3. Horáková H, Polakovičová I, Shaik GM, Eitler J, Bugajev V, Dráberová L, Dráber P. 1,2-propanediol-trehalose mixture as a potent quantitative real-time PCR enhancer. BMC Biotechnol. 2011 Apr 18;11:41.

4. Harvima IT, Levi-Schaffer F, Draber P, Friedman S, Polakovicova I, Gibbs BF, Blank U, Nilsson G, Maurer M. Molecular targets on mast cells and basophils for novel therapies. J Allergy Clin Immunol. 2014 Apr 23. pii: S0091-6749(14)00428-X.

Multiple regulatory roles of the mouse transmembrane adaptor protein NTAL in gene transcription and mast cell physiology

PLoS One. 2014 Aug 25;9(8):e105539

Supporting information (Tables S1-5) is available at
http://www.plosone.org/article/info%3Adoi%2F10.1371%2Fjournal.pone.0105539#s5

OPEN ACCESS Freely available online

PLOS ONE

Multiple Regulatory Roles of the Mouse Transmembrane Adaptor Protein NTAL in Gene Transcription and Mast Cell Physiology

Iva Polakovicova, Lubica Draberova, Michal Simicek, Petr Draber*

Department of Signal Transduction, Institute of Molecular Genetics, Academy of Sciences of the Czech Republic, Prague, Czech Republic

Abstract

Non-T cell activation linker (NTAL; also called LAB or LAT2) is a transmembrane adaptor protein that is expressed in a subset of hematopoietic cells, including mast cells. There are conflicting reports on the role of NTAL in the high affinity immunoglobulin E receptor (FcεRI) signaling. Studies carried out on mast cells derived from mice with NTAL knock out (KO) and wild type mice suggested that NTAL is a negative regulator of FcεRI signaling, while experiments with RNAi-mediated NTAL knockdown (KD) in human mast cells and rat basophilic leukemia cells suggested its positive regulatory role. To determine whether different methodologies of NTAL ablation (KO vs KD) have different physiological consequences, we compared under well defined conditions FcεRI-mediated signaling events in mouse bone marrow-derived mast cells (BMMCs) with NTAL KO or KD. BMMCs with both NTAL KO and KD exhibited enhanced degranulation, calcium mobilization, chemotaxis, tyrosine phosphorylation of LAT and ERK, and depolymerization of filamentous actin. These data provide clear evidence that NTAL is a negative regulator of FcεRI activation events in murine BMMCs, independently of possible compensatory developmental alterations. To gain further insight into the role of NTAL in mast cells, we examined the transcriptome profiles of resting and antigen-activated NTAL KO, NTAL KD, and corresponding control BMMCs. Through this analysis we identified several genes that were differentially regulated in nonactivated and antigen-activated NTAL-deficient cells, when compared to the corresponding control cells. Some of the genes seem to be involved in regulation of cholesterol-dependent events in antigen-mediated chemotaxis. The combined data indicate multiple regulatory roles of NTAL in gene expression and mast cell physiology.

Citation: Polakovicova I, Draberova L, Simicek M, Draber P (2014) Multiple Regulatory Roles of the Mouse Transmembrane Adaptor Protein NTAL in Gene Transcription and Mast Cell Physiology. PLoS ONE 9(8): e105539. doi:10.1371/journal.pone.0105539

Editor: Jon C.D. Houtman, University of Iowa, United States of America

Received May 11, 2014; **Accepted** July 21, 2014; **Published** August 25, 2014

Data Availability: The authors confirm that all data underlying the findings are fully available without restriction. All database files are available from the NCBIs Gene Expression Omnibus database under accession number GSE40731.

Funding: This work was supported by project P302/12/G101, P302-14-09807S, and P305-14-00703S from the Grant Agency of the Czech Republic (URL: http://www.gacr.cz/); project LD12073 COST-CZ-MAST from Ministry of Education of the Czech Republic (URL: http://www.msmt.cz/); Institutional project RVO 68378050 from Academy of Sciences of the Czech Republic (URL: http://www.cas.cz/); and Action BM1007 from European Cooperation in Science and Technology (URL: http://www.cost.eu/). I.P. was supported in part by the Faculty of Science, Charles University, Prague (URL: http://www.natur.cuni.cz). The funders had no role in study design, data collection and analysis, decision to publish, or preparation of the manuscript.

Competing Interests: The authors have declared that no competing interests exist.

* Email: draberpe@img.cas.cz

Introduction

Activation of mast cells upon exposure to antigen (Ag) is one of the major events in the allergic reaction. It is initiated by Ag-mediated aggregation of the high-affinity immunoglobulin (Ig) E receptor (FcεRI) armed with Ag-specific IgE, and results in degranulation leading to the release of a number of preformed allergy mediators such as histamine, serotonin, proteases, preformed cytokines, and proteoglycans. Mast cell activation also leads to the synthesis and release of numerous compounds like cytokines and those formed by arachidonic acid metabolism [1]. The first biochemically well-defined step in FcεRI signaling is tyrosine phosphorylation of the immunoreceptor tyrosine-based activation motifs (ITAMs) in the FcεRI β and γ subunits by Src family kinase LYN [2,3]. Phosphorylation of the ITAMs leads to the recruitment and activation of SYK kinase, which phosphorylates tyrosine residues of numerous proteins involved in the intracellular signaling pathways, including two transmembrane adaptor proteins (TRAPs), linker for activation of T cells (LAT) and non-T cell activation linker (NTAL; also called linker for activation of B cells or LAT2). Both these TRAPs possess multiple sites of tyrosine phosphorylation and act as scaffolds for recruitment of various cytosolic adaptors and effector proteins [4–6].

NTAL is expressed in hematopoietic cells such as B cells, natural killer cells, dendritic cells, monocytes, and mast cells but not in resting T cells. NTAL is the product of human WBSCR5 gene located on chromosome 7 encoding a 243 amino acids protein. Its murine ortholog contains 203 amino acids, has a molecular weight of approximately 25 kD and is encoded by a gene located on chromosome 5 [7,8]. NTAL contains a short extracellular domain, a transmembrane domain and a cytosolic tail which possesses a CxxC motif responsible for palmitoylation of the protein and its targeting to detergent-resistant plasma membrane microdomains. The cytoplasmic domain contains 10 tyrosines which are potential targets for tyrosine kinases. NTAL is

structurally similar to another TRAP, LAT; after phosphorylation both molecules are capable of binding a number of cytoplasmic signaling molecules including GRB2, SOS1, GAB1 and C-CBL. NTAL, unlike LAT, is however unable to directly bind the phospholipase Cγ1 [7,8].

Previously we and others showed that bone marrow-derived mast cells (BMMCs) from *Ntal*$^{-/-}$ mice were hyper-responsive to FcεRI stimulation [9,10], whereas BMMCs from *Lat*$^{-/-}$ mice were hypo-responsive [11]. Interestingly, loss of both NTAL and LAT caused stronger inhibitory effect on FcεRI-mediated degranulation than loss of LAT alone. This suggested that NTAL could also have a positive regulatory role in FcεRI signaling, manifested only in the absence of LAT [9,10]. In contrast to studies with cells from mice with NTAL knock out (KO), NTAL knockdown (KD) by RNAi in human mast cells [12] and also in rat basophilic leukemia cells [13] resulted in impaired degranulation; it implies that NTAL has positive regulatory roles in these cells even in the presence of LAT.

To rigorously examine the regulatory role(-s) of NTAL in murine mast cells signaling and to test the contribution of compensatory developmental alterations in mast cells from NTAL KO mice, we prepared BMMCs with NTAL KO or KD and the corresponding controls and cultured them under comparable well-defined conditions. For functional comparison of mast cells with NTAL KO or KD we examined several parameters characteristic for FcεRI signaling including degranulation, calcium mobilization, tyrosine phosphorylation of LAT and ERK, depolymerization of filamentous (F) actin, and chemotaxis. The results obtained with the NTAL KD BMMCs were very similar to those of NTAL KO cells and thus support the notion that in murine mast cells NTAL is predominantly a negative regulator of FcεRI signaling and that compensatory developmental alteration do not contribute to this phenotype.

To gain a better understanding of the genes that are regulated through NTAL-dependent pathways, we further examined the gene expression profiles of resting and Ag-activated BMMCs with NTAL KO or KD and corresponding controls. Several genes have been identified that differ by a factor of 1.8 and higher in their expression in resting and FcεRI-activated NTAL-deficient cells when compared to wild type (WT) cells. Through gene ontology analysis we identified a subset of NTAL-dependent genes, which were related to metabolism and biosynthetic processes. Further analysis showed that some of the genes could be involved in regulation of cholesterol-dependent events in chemotaxis towards antigen.

Materials and Methods

Cells and their activation

Bone marrow cells were isolated from femurs and tibias of 8–12 week-old WT or NTAL KO mice (males and females) of C57BL6 background [9]. Mice were bred and maintained in specific pathogen free facility of the Institute of Molecular Genetics and used in accordance with the Institute guidelines. The protocol, including killing mice by decapitation, was approved by the Institutional Animal Care and Use Committee (Permit number 12135/2010-17210). All efforts were made to minimize suffering. The cells were cultured for 6-8 weeks in mast cell medium [Iscove's modified Dulbecco's medium supplemented with 10% fetal calf serum (FCS), penicillin, streptomycin, 2-mercaptoethanol, recombinant interleukin (IL)-3 (20 ng/ml; Peprotech), and mouse stem cell factor (SCF; 40 ng/ml; Peprotech)]. In some experiments BMMCs were cultured for the indicated time intervals in mast cell medium supplemented with 10% cholesterol-depleted FCS (see below) instead of FCS. For activation, BMMCs (6×10^6/ml) were sensitized in medium without SCF and IL-3, but supplemented with trinitrophenyl (TNP)-specific IgE (IGEL b4 1 monoclonal antibody; 1 μg/ml). After 4 hours the cells were washed in buffered salt solution (BSS; 20 mM HEPES, pH 7.4, 135 mM NaCl, 5 mM KCl, 1.8 mM $CaCl_2$, 5.6 mM glucose, and 1 mM $MgCl_2$) supplemented with 0.1% bovine serum albumin (BSA) and stimulated with various concentrations of Ag (TNP-BSA conjugate) and/or SCF. Degree of degranulation was determined by measuring the release of β-glucuronidase from the activated cells as previously described [14].

Cholesterol-depleted FCS and cholesterol determination

FCS was cleared of cholesterol and other lipids by organic extraction as described [15]. Briefly, 100 ml of FCS was mixed with 200 ml of a mixture n-butanol and diisopropylether at a 40:60 (v/v) ratio. After incubation at room temperature (22°C) for 1 hour in dark, the mixture was centrifuged at 22°C for 15 minutes at 6000 rpm in a JA-10 rotor, Beckman Coulter. The bottom phase containing delipidated serum was recovered and lyophilized. The resulting dry pellet was resuspended in 100 ml deionized H_2O and filter-sterilized through 0.22 μm filter. Concentration of cholesterol in serum and cell samples was determined by the Amplex Red Cholesterol Assay kit (Life Technologies) according to the manufacturer's instruction. Using this kit, no remaining cholesterol was detectable in delipidated serum. This indicates that cholesterol concentration was reduced from ~80 μg/ml to <15 ng/ml. For determination of cellular cholesterol, frozen cell pellet containing 0.35×10^6 cells was lysed in 30 μl of ice cold lysis buffer (10 mM EDTA, 100 mM NaCl, 10 mM Tris-HCl, pH 7.5, 0.2% SDS, 0.5% Nonidet P-40, 0.5% sodium deoxycholate) and 2 μl aliquots were analyzed for cholesterol content using the same kit as above. Protein content in the lysates was determined by BCA protein assay kit (Pierce Chemical Co.) and the amounts of cholesterol were normalized to protein contents.

Antibodies and immunoblotting

All antibodies were purchased from Santa Cruz, except for anti-NTAL (NAP-07; Exbio), anti-phospho-LAT (Upstate Biotechnology) and anti-LAT [16]. Cells were solubilized for 30 minutes in ice-cold lysis buffer containing 50 mM Tris-HCl, pH 7.4, 150 mM NaCl, 2 mM EDTA, 10 mM β-glycerophosphate, 1 mM Na_3VO_4, 1 mM PMSF, 1 μg/ml aprotinin, 1 μg/ml leupeptin, 0.2% Triton X-100, 1% Nonidet P-40 and 1% n-dodecyl-β-D-maltoside. After centrifugation (15 minutes at 7.000×g at 4°C), proteins in postnuclear supernatants were size fractionated by SDS-polyacrylamide gel electrophoresis and analyzed by direct immunoblotting. Immunoblots were quantified by Luminiscent Image Analyzer LAS 3000 (Fuji Photo Film Co.) and further analyzed by AIDA image analyzer software (Raytest).

Measurement of free cytoplasmic Ca^{2+}

Concentration of free cytoplasmic Ca^{2+} $[Ca^{2+}]_i$ was determined using cells labeled with Fura-2-AM (Molecular Probes) as described [9]. Ca^{2+} levels were monitored by means of fluorescence reader Infinite M200 (Tecan) with excitation wavelengths of 340 and 380 nm, and emission wavelength of 510 nm.

Lentiviral vectors and gene transduction

A set of 5 shRNA constructs designed to target murine NTAL (GenBank accession number NM_020044) and cloned into the pLKO.1 vector was purchased from Open Biosystems to prepare

BMMCs with NTAL KD. From these five shRNA constructs (TRCN0000127239, NTAL KD 1; TRCN0000127240, NTAL KD 2; TRCN0000127241, NTAL KD 3; TRCN0000127242, NTAL KD 4; TRCN0000127243, NTAL KD 5), the NTAL KD 3 and NTAL KD 5 showed reproducibly the highest reduction of NTAL protein expression in target cells and were used in most of the experiments with similar results. In all experiments in this study we obtained similar data with these two constructs and therefore the data were pooled and are referred to as NTAL KD. For microarray gene expression analysis and related qPCR validation, cells with the NTAL KD 5 construct were used.

Lentiviral transduction was performed as described previously [17]. Briefly, 21 µl ViraPower packaging mix (Invitrogen Life Technologies) and 14 µg NTAL shRNA or pLKO.1 empty vector as a negative control [in 1.4 ml medium Opti-MEM (Invitrogen)] were co-transfected into 293T17 packaging cells in the presence of 84 µl Lipofectamine 2000 (Invitrogen) or 105 µl polyethylenimine (25 kD, linear form, 1 µg/ml; Polysciences). After 2 3 days, the culture supernatants were centrifuged to pellet the viruses, which were then used to infect NTAL WT BMMCs. Stable transfectants were selected in puromycin (5 µg/ml; InvivoGen). After one week of selection, cells were analyzed for NTAL expression by immunoblotting. Before the tests, cells were transferred for 2 3 days into fresh media without puromycin.

F-actin assay

Total amount of F-actin in nonactivated and activated cells was determined by flow cytometry. Cells in 96-well plates (50 000 cells per well) were exposed to various stimuli at 37°C, fixed with 3% paraformaldehyde in phosphate buffered saline and then permeabilized and stained in a single step by a mixture of lysophosphatidylcholine (200 µg/ml) and 1000x diluted Alexa Fluor 488-phalloidin (Molecular Probes) in phosphate buffered saline. Fluorescence intensity was measured with the help of LSRII flow cytometer (Becton Dickinson). Acquired data were analyzed using FlowJo software (Tree Star Inc).

Cell Spreading

Wells (6 mm in diameter) of 8-well multitest slides (MP Biomedicals) were coated with fibronectin (Sigma Aldrich) and Cell-Tak (BD Biosciences) as described [18]. IgE-sensitized BMMCs were seeded on fibronectin/Cell-Tak-coated wells and allowed to attach for 1 hour. The attached cells were activated for 30 minutes at 37°C with Ag and/or SCF in BSS-0.1% BSA, fixed with 3% paraformaldehyde in glutamate buffer-EGTA (GBE; 137 mM K-glutamate, 2 mM $MgCl_2$, 3 mM EGTA, and 20 mM PIPES-NaOH, pH 6.8) supplemented with 4% polyethylene glycol, molecular weight 3200, and then permeabilized and stained by one-step exposure to lysophosphatidylcholine (200 µg/ml) and 100x diluted Alexa Fluor 488-phalloidin in GBE. Coverslips were mounted in glycerol-based mounting medium containing Mowiol 4-88 reagent (Calbiochem AG) and Hoechst 33258 (3 µg/ml; Sigma). Fluorescent images (25 images/well) were automatically collected using Olympus IX70 inverted microscope (objective LUCPLFLN Ph1 20x) equipped with motorized stage and ScanR acquisition software (Olympus). Cell area was analyzed using ScanR analysis software (Olympus). At least 500 cells were evaluated in each test.

RNA preparation

Total RNA was isolated from 3×10^6 resting or Ag-activated (100 ng/ml TNP-BSA in BSS-0.1% BSA, 37°C, 2 hours) BMMCs using the RNeasy mini kit (Qiagen) according to the manufacturer's protocol. Three biological replicates were carried out with each cell type: NTAL KO, WT, NTAL KD, and mock (empty pLKO.1 vector) infected WT cells (referred to as WT pLKO). Cells in each group were cultured in parallel for 24 hours in complete media deprived of SCF and then sensitized with TNP-specific IgE in IL-3- and SCF-deprived medium for 4 hours. After removal of unbound IgE by washing, cell suspensions were divided into 2 aliquots; one activated for 2 hours with Ag (100 ng/ml) and the other incubated without Ag (nonactivated control cells; 0 hours). RNA was isolated from all 24 samples and processed under identical conditions. For RNA quantification, the absorption at 260 nm was measured using NanoDrop spectrophotometer N-1000 (NanoDrop Technologies).

Microarray gene-expression profiling and data analysis

Preparation of cRNA, hybridization and gene expression profiling was done by an Affymetrix authorized service provider (AROS Applied Biotechnology A/S) using the Affymetrix GeneTitan HT MG-430 PM 24-array plate with the 3′ IVT express labeling kit according to the manufacturer's protocol. Briefly, following fragmentation, 6.5 µg aliquots of cRNA were hybridized for 16 hours at 45°C on the Affymetrix array plate using the Affymetrix GeneTitan system. The array plate was washed, stained and scanned using the Affymetrix GeneTitan system with GCOS 1.4 software. One of the 24 samples analyzed, activated NTAL KO replicate 2, failed during the hybridization, wash and scan step and was removed. Data analysis was carried out by importing raw data CEL files into Genomic Suite Software Partek 6.4 (version 6.09.0602), where the Robust Multichip Analysis was used for background correction. Using the same software, principal component analysis (PCA) of the normalized microarray expression values was performed as a visualization technique to determine the similarity in the data. Lists of significantly upregulated or downregulated gene transcripts were created based on a change greater than 1.8-fold and false discovery rate (FDR) <0.1, with one exception in which activated cells were compared with nonactivated cells (fold change >4; FDR <0.05). Only well annotated probe sets (Affymetrix annotation version from July 2011) are listed in the tables. The microarray study was performed according to the standards of the Microarray Gene Expression Society. Data complying with the Minimum Information About Microarray Experiments (MIAME; [19]) were uploaded in the NCBIs Gene Expression Omnibus (GEO) database and are available under the accession number GSE40731.

Reverse transcription quantitative PCR (RT-qPCR)

cDNA was synthesized using mouse Moloney leukemia virus reverse transcriptase (Invitrogen) according to manufacturer's instructions. For reverse transcription, 0.3 µg aliquots of total RNA were used from the same samples, which were used for microarray analysis. qPCRs were performed using a PCR mastermix supplemented with 0.2 M trehalose, 1 M 1,2-propanediol and SYBR green I as described [20]. Ten µl reaction volumes in 384-well plates sealed with LightCycler 480 sealing foil (Roche Diagnostics) were processed in LightCycler 480 (Roche Diagnostics) under the following cycling conditions: initial 3 minutes denaturation at 95°C, followed by 50 cycles at 95°C for 10 s, 60°C for 20 s and 72°C for 20 s. Melting curve analysis was carried out from 72°C to 97°C with 0.2°C increments; Ct values for each sample were determined by automated threshold analysis. Primer pairs used for cDNA amplification are listed in Table 1. Data were normalized to a housekeeping GAPDH mRNA. The qPCRs for each of the biological triplicates was performed in quadruplicates.

Table 1. Primers used in quantitative RT-PCR.

Gene	Primer	Primer sequence (5′-3′)	Product size (bp)
Dusp5	Forward Reverse	GGGGTATGAGACCTTCTACTCAC GGAGGCTTCTCTCGCCTTC	92
Fdps	Forward Reverse	GCCATCAACGACGCTCTGCT ATGGCCCTGGGGTGCTGTCA	165
Idi1	Forward Reverse	AGCTTCTAGCGGAGATGTGTA CAGCAACTATTGGTGAAACAACC	214
Klhl24	Forward Reverse	TGAAATGGACCCCAAATCTCTG GGACAGCTCGATGGCATGG	170
Lss	Forward Reverse	TCGTGGGGGACCCTATAAAAC CGTCCTCCGCTTGATAATAAGTC	104
Mki67	Forward Reverse	AGAGCCTTAGCAATAGCAACG GTCTCCCGCGATTCCTCTG	145
Mlec	Forward Reverse	GAGGAGGGCGACTATGTGC CATTCAACCGGACATCAAACAC	88
N4bp2l1	Forward Reverse	CCAGAGAAGAGCAAGGAAAGC TCGGGTTCCCGGAATATAACTT	141
Nt5dc2	Forward Reverse	GCCTCATGTACCAGTGGATCG GACCTACCATGTGCCGCATAC	165
Otub2	Forward Reverse	TTCTACAGGGCCTTAGGCTATT AGCACACGCTCTTTGAACTTG	83
Plau	Forward Reverse	ATGGAAATGGTGACTCTTACCGA TGGGCATTGTAGGGTTTCTGA	106
Pmvk	Forward Reverse	TGAGGCTTGAGGGGACGAGCA TTGCTGACCTCGGCTGGGACT	90
Sdf4	Forward Reverse	TGTGGTCTAGCTGCTCATGG TGTGGTCTAGCTGCTCATGG	103
Slain1	Forward Reverse	TCACCAGAGAAATCCCCGAGT CCCCTGGAGGTATAACCTTGC	125
Spink4	Forward Reverse	GCCTTGTTTTCCCCAGAATGCCCTT CGGGTCAGGCAAAGGTGGCA	130
Tmcc3	Forward Reverse	CCCTCAGCCTACCCCTGAA CGCATTGAGTTTGACCTTGTGG	104
NTAL WT	Forward	TGGACACAGCTCCAAACAAG	197
NTAL KO	Forward	CTGCTCACCAGAGTCAGTGG	160
NTAL WT/KO	Reverse	GGAATCGTCGTCTTCTGAGG	
GAPDH	Forward Reverse	AACTTTGGCATTGTGGAAGG ATCCACAGTCTTCTGGGTGG	69

doi:10.1371/journal.pone.0105539.t001

Chemotaxis

The migration of IgE-sensitized BMMCs towards Ag as chemoattractant was determined in a 24-well Transwell system with inserts containing polycarbonate filters having 8-μm diameter pores (Corning). TNP-specific IgE-sensitized BMMCs (0.3×10^6) in 120 μl of chemotaxis medium (RPMI-1640 supplemented with 20 mM HEPES, pH 7.4 and 1% BSA) were added into each Transwell insert and Ag (250 ng/ml TNP-BSA) in 600 μl of chemotaxis medium was added into lower wells of the Transwell system. Cells passing through the polycarbonate filter were counted 8 hours later in 50 μl aliquots with Accuri C6 flow cytometer.

Statistical analysis

Statistical significance of differences was evaluated by Student's t-test, except for microarray gene-expression profiling in which intergroup differences were evaluated by ANOVA test.

Results

Efficient NTAL KD in BMMCs

In order to obtain mast cells with stable reduction of NTAL expression by KD approach, five different shRNAs were introduced into *Ntal*$^{+/+}$ BMMCs by lentiviral-mediated infection, followed by selection in puromycin. To minimize the effect of variables other than the presence of NTAL, target *Ntal*$^{+/+}$ cells were the same as those which served as WT littermate controls to BMMCs isolated from *Ntal*$^{-/-}$ mice (KO). Controls for NTAL KDs were the same *Ntal*$^{+/+}$ BMMCs infected with empty pLKO.1 vector and selected in puromycin. Immunoblotting with NTAL-specific monoclonal antibody confirmed that all five shRNAs inhibited NTAL expression to different degrees (Figure 1A, B). Two of them, namely NTAL KD 3 and NTAL KD 5, showed the highest (>90%), reproducible and highly significant inhibition of NTAL expression and were therefore selected for further experiments. No decrease in NTAL expression was observed in cells infected with empty pLKO.1 vector (WT pLKO; Figure 1A, B). Flow cytometry analysis showed that BMMCs with NTAL KD expressed FcεRI (>95% cells positive) and KIT (>95% positive) at levels comparable to those in WT cells and WT pLKO cells (not shown).

NTAL KD results in enhanced degranulation and Ca^{2+} response

As described in Introduction, there are conflicting reports on the role of NTAL in mast cell signaling in mammalian systems. To address these discrepancies, we compared under well-defined conditions the effect of NTAL KO and KD on mast cell signaling. First we evaluated degranulation. The cells were sensitized with IgE and stimulated with various concentrations of Ag. Degranulation was then determined as the amount of β-glucuronidase released into the supernatant. Data presented in Figure 2A indicate that BMMCs with both NTAL KD and NTAL KO showed enhanced degranulation when compared to the corresponding controls (WT pLKO and WT). The difference between NTAL-deficient cells (KD or KO) and controls (WT pLKO and WT) was more pronounced at suboptimal concentrations of Ag (100 and 200 ng/ml) and was not significant at supraoptimal concentration (1000 ng/ml). Our results show a similar trend for both NTAL KD and KO BMMC. To check for possible off-target effects of lentiviral infection and puromycin selection we also examined antigen-induced degranulation of NTAL KO cells transduced with NTAL shRNA vectors and found no significant difference between infected and noninfected cells (data not shown).

It is known that degranulation is enhanced in cells simultaneously triggered via FcεRI and KIT, a receptor for SCF [21]. We

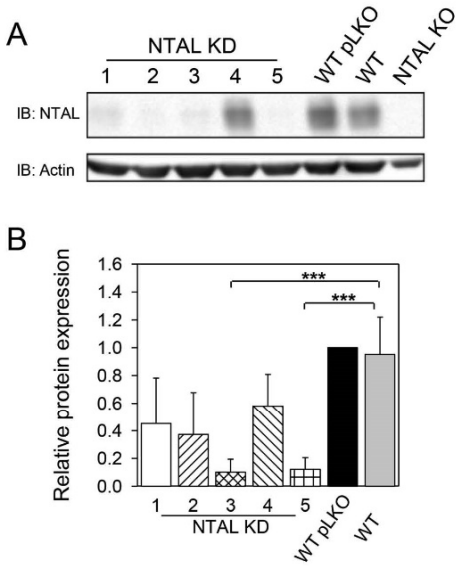

Figure 1. Decreased NTAL expression after shRNA silencing. (A) BMMCs were infected with five lentiviral shRNA constructs (NTAL KD 1–5) or empty pLKO.1 construct (WT pLKO). After selection in puromycin, the amount of NTAL was assessed by immunoblotting. For comparison, NTAL in noninfected WT and NTAL KO cells was also evaluated. Actin was used as a loading control. (B) Densitometry analysis of NTAL immunoblots. The data were normalized to the amount of NTAL in WT pLKO cells and that of actin. Means ± SD were calculated from 3–7 independent experiments. ***$p<0.001$.
doi:10.1371/journal.pone.0105539.g001

found degranulation not only after exposure of the cells to IgE-antigen complexes, but also after triggering with SCF alone. This is probably due to the fact that mast cells were differentiated from their precursors in the presence of IL-3 and SCF [22]. NTAL KO has no effect on degranulation induced by SCF alone and SCF enhances Ag- induced degranulation in both WT and NTAL KO cells [18]. We therefore investigated degranulation of cells with NTAL KD and the corresponding controls activated by Ag and/or SCF. Compared to separate activation by Ag (100 or 500 ng/ml) or SCF (40 ng/ml), simultaneous activation by Ag and SCF raised degranulation in *Ntal*$^{+/-}$ controls (WT and WT pLKO; Figure 2B). In cells with NTAL KD, the enhanced degranulation induced by Ag was further increased if the cells were simultaneously activated with SCF (Ag + SCF), even though the difference between NTAL-KD and control cells transduced with empty pLKO was not significant. Similar data were obtained in BMMCs from NTAL KO mice.

Calcium mobilization is another hallmark of mast cell activation. We therefore activated IgE-sensitized BMMCs with Ag in the presence of extracellular Ca^{2+} and evaluated calcium mobilization by means of Ca^{2+}-sensitive fluorophore Fura-2-AM. Both *Ntal*$^{+/+}$ controls (WT and WT pLKO) showed a comparable increase in $[Ca^{2+}]_i$ peaking at 50–60 s after exposure to Ag (Figure 2C). NTAL KO cells showed the expected [9,10] long-lasting increase in Ca^{2+} mobilization. Within 120–600 s this response significantly ($P<0.01$) differed from that seen in WT cells. Significant increase in calcium response was also observed in NTAL KDs between 180–450 s. No significant difference in Ca^{2+} response between NTAL-deficient cells and controls was observed after stimulation with SCF (Figure 2D). Exposure of all cell types to a mixture of Ag and SCF resulted in an accelerated increase in the $[Ca^{2+}]_i$, and again, BMMCs with NTAL KO and KD cells showed higher Ca^{2+} mobilization than the controls, WT and WT pLKO (Figure 2E). These data indicate that negative regulatory roles of NTAL on FcεRI-mediated degranulation and Ca^{2+} response are due to the absence of NTAL rather than possible compensatory developmental changes induced in NTAL KO.

NTAL depletion and deletion induce tyrosine phosphorylation of ERK and LAT

Mast cell activation is initiated by tyrosine phosphorylation of the β and γ subunits of FcεRI, followed by phosphorylation of numerous substrates, including ERK and LAT [23,24]. It has been suggested that enhanced tyrosine phosphorylation of LAT and some other substrates in *Ntal*$^{-/-}$ cells could reflect a better accessibility of kinases to LAT in the absence of competition between NTAL and LAT as substrates [9]. This process could be subjected to compensatory developmental alterations. We therefore decided to determine phosphorylation of ERK and LAT in cells with NTAL KD. Immunoblotting experiments showed an increase of tyrosine phosphorylation of ERK (Figure 3A) and LAT (Figure 3B) in NTAL KD cells when compared to WT cells. WT pLKO cells showed similar phosphorylation profile as WT cells (data not shown). Since the same enhanced phosphorylation of LAT and ERK was observed in NTAL KO and NTAL KD cells, developmental compensation mechanisms are unlikely to be responsible for enhanced phosphorylation of the targets.

Effect of NTAL on cell spreading and chemotaxis

Activation through FcεRI or KIT results in enhanced spreading of BMMCs on fibronectin [25,26]. Our previous studies with NTAL KO BMMCs showed that full-value spreading on fibronectin was dependent on the presence of NTAL in FcεRI-activated, but not KIT activated, cells [18]. Spreading on fibronectin requires expression of intact integrins and signaling pathways, which could be developmentally regulated. Therefore, we analyzed spreading of BMMC on fibronectin in controls and cells with NTAL KD after exposure to Ag and/or SCF. Data presented in Figure 4A show that in relation to WT and WT pLKO cells, cells with NTAL KD exhibited decreased spreading after activation with Ag. Activation with both Ag and SCF also reduced the spreading of cells with NTAL KD, which showed similar response as cells from NTAL KO mice. No inhibition of spreading was observed in NTAL-deficient cells after activation with SCF. Quantitative analysis of the data obtained is shown in Figure 4B. The area of individual cells was measured and normalized to that of nonactivated cells. Compared to corresponding controls, NTAL KDs and KOs exhibited a significant decrease in surface area after triggering with Ag. Similarly, clear inhibition of cell spreading was observed in both NTAL KOs and KDs activated with Ag + SCF. The difference between NTAL KDs and WT pLKO control, stimulated with Ag + SCF was, however, not significant, mainly because of slight decrease in the spreading of cells with WT pLKO.

We also tested the chemotactic response of NTAL-deficient cells in comparison to WT cells. Data presented in Figure 4C indicate that BMMCs with NTAL KD exhibited significantly enhanced Ag-mediated chemotaxis, similarly as cells with NTAL KO. There was no significant difference between the two cells types.

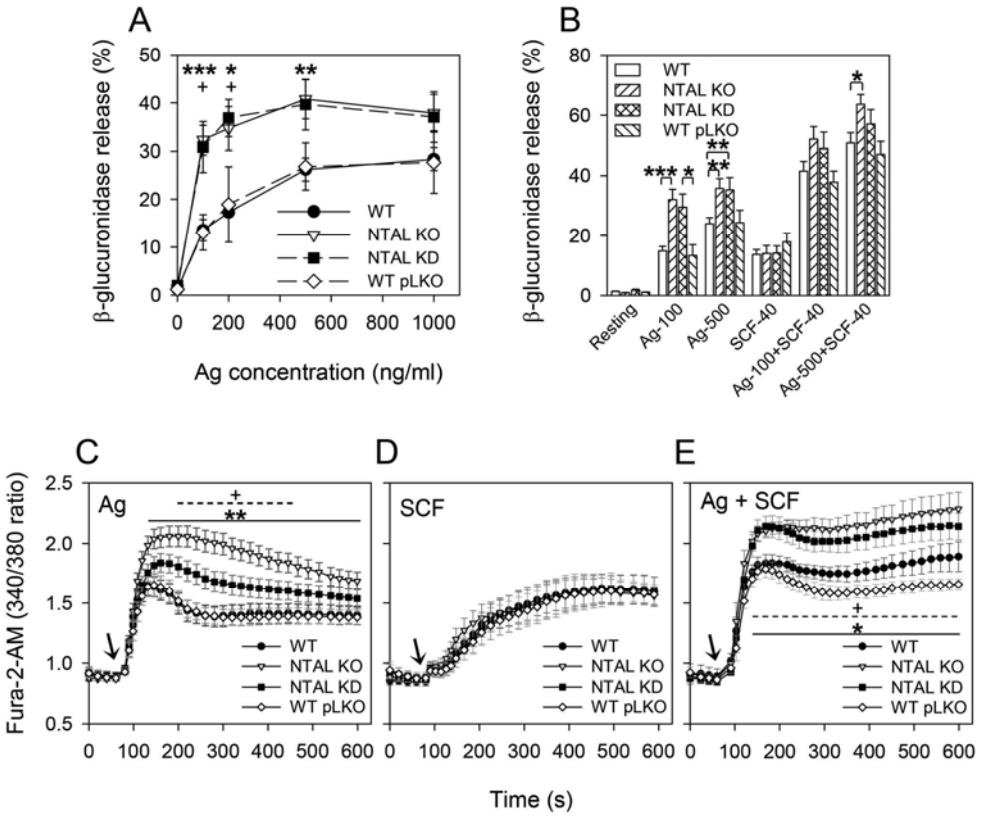

Figure 2. BMMCs with NTAL KD exhibit increased degranulation and calcium response. (A) IgE-sensitized BMMCs (WT, NTAL KO, NTAL KD, and WT pLKO) were stimulated for 30 minutes with various concentrations of Ag (TNP-BSA), and β-glucuronidase released into supernatant was determined as described in Materials and Methods. Data represent means ± SE from 7–17 independent experiments performed in duplicates or triplicates). (B) IgE-sensitized BMMCs were stimulated with Ag [TNP-BSA at a concentration 100 ng/ml (Ag-100) or 500 ng/ml (Ag-500)], SCF (40 ng/ml), or both activators together. Data represent means ± SE from 6–20 independent experiments). (C–E) BMMCs were sensitized with IgE, loaded with Fura-2-AM (1 μg/ml), then stimulated with Ag (100 ng/ml TNP-BSA; C), SCF (40 ng/ml; D) or both activators together (E) and free intracellular Ca^{2+} was monitored by measuring fluorescence emission at 510 nm after excitation at 340 and 380 nm. Arrows indicate addition of Ag and/or SCF. Data are means ± SE from 11 (C), 7 (D) or 6 (E) independent experiments performed in duplicates. All data presented in A–E were obtained with BMMCs isolated from 3–5 mice. *,+$p<0.05$; **$p<0.01$; ***$p<0.001$; in A, C and E, significant differences between NTAL KOs and WTs (asterisks) and NTAL KDs and WT pLKOs (crosslets) are shown.
doi:10.1371/journal.pone.0105539.g002

NTAL KD increases F-actin depolymerization

FcεRI-induced activation of BMMCs is accompanied by rapid F-actin depolymerization [27]. To determine whether F-actin depolymerization is similarly regulated in NTAL KDs, we activated cells with NTAL KD or NTAL KO and corresponding controls with Ag and/or SCF for the indicated time intervals, and determined the amount of F-actin by flow cytometry. Data presented in Figure 5A show that triggering with Ag stimulated both NTAL KOs and KDs to significantly higher F-actin depolymerization when compared to WT cells. We also observed that SCF activation induced clear increase in F-actin formation, rather than actin depolymerization, and no difference between NTAL KOs and KDs was noticed (Figure 5B). Cells activated by both activators (Ag + SCF) responded by stronger depolymerization than cells activated with Ag alone, and again no difference between cells with NTAL KO and KD was observed (Figure 5C).

Transcriptome profiles of cells with NTAL KO or KD

To better understand the role of NTAL in mast cell physiology and Ag-induced signaling pathways, we compared gene expression profiles of nonactivated and Ag-activated NTAL-deficient BMMCs with the corresponding controls. Four groups of cells (NTAL KO, NTAL KD, WT, and WT pLKO) were prepared and maintained under comparable culture conditions. Each group consisted of BMMCs isolated from three mice to account for variability of cell donors and procedures of BMMCs isolation.

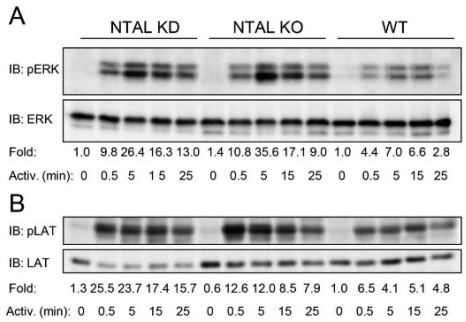

Figure 3. FcεRI-activated BMMCs with NTAL KD show enhanced tyrosine phosphorylation of ERK and LAT. NTAL-deficient cells and WT controls were sensitized with IgE and stimulated with Ag (100 ng/ml TNP-BSA). After the indicated time intervals, the cells were solubilized in lysis buffer and postnuclear supernatants were analyzed by immunoblotting for tyrosine phosphorylated ERK (pERK; A) or LAT (pLAT; B), followed by stripping and immunoblotting for total ERK (A) or LAT (B). Fold inductions of protein tyrosine phosphorylation, normalized to nonactivated WT cells and corrected for the amount of protein in each lysate, are also included. Each immunoblot is a typical result from three independent experiments.
doi:10.1371/journal.pone.0105539.g003

RNA was isolated from IgE-sensitized nonactivated cells or cells activated for 2 hours with Ag. The same RNA was used for microarray analysis and for later confirmation of the gene expression by qPCR. First, we compared expression profiles of nonactivated NTAL KO cells with nonactivated littermate WT controls; from 209 differentially expressed genes (258 probe sets), 70 showed more than 1.8 fold upregulation in NTAL KO cells (Table S1). When focused on biological processes and molecular functions of the genes (Table 2), a large group of the genes involved in metabolic and biosynthetic processes as well as in transcription, translation, and mRNA and rRNA processing was present. The gene list contains about 60 genes with DNA, RNA, or nucleotide binding functions involved in regulation of transcription, replication, and splicing, 21 genes with protein binding function, but, surprisingly, only 6 genes with receptor or signal transducer activity [*Il12rb1* (0.36 fold decrease in KO cells), *Pdcd1lg2*, (3.22 fold increase), *Lgr4* (2.31), *Calca* (2.70), *Lrp8* (0.47) and *Bzrap1* (0.39)]. Other differentially regulated genes are involved in protein phosphorylation and dephosphorylation [*Mlkl* (0.48), *Cdkl2* (2.79), *Ptp4a3* (0.33), *Dusp5* (2.19), *Ppp1r14b* (0.43)] and MAPK kinase kinase cascade [*Map3k7* (0.42) and *Pebp1* (0.49)]. In a group of genes involved in metabolic and biosynthetic processes we found downregulated genes in steroid biosynthetic processes and lipid metabolism.

When comparing transcriptomes of nonactivated NTAL KD cells with their WT controls, infected with empty pLKO.1 vector, 162 differentially expressed genes (200 probe sets) were identified (Table S2). Some of these genes are involved in protein phosphorylation and dephosphorylation [*Dusp4* (3.55), *Ptpn2* (0.55), *Ptpn3* (1.81) *Dusp5* (2.33), *Epha5* (2.58) and *Mylk3* (0.39)] and signal transduction [*Tmem123* (0.47), *Rasal3* (2.00), *Mmd* (2.70), *Il1r2* (2.90), *Sema4b* (1.81), *Lphn1* (0.42), and *Ogfrl1* (0.52)]. Interestingly, among differentially expressed genes was *Idi*, which was also downregulated in NTAL KO cells.

Numbers of differentially expressed genes in nonactivated NTAL KO and KD cells and their overlaps are schematically depicted in Figure 6A. Expression levels of the overlapping genes were verified by qPCR. The data presented in Figure 6B show that from 9 differentially expressed genes showing overlap between KO and KD, 5 genes were upregulated in NTAL KO cells (*Spink4*, *Plau*, *Otub2*, *Dusp5* and *Sdf4*). Two of them were also upregulated in NTAL KD cells (*Plau* and *Dusp5*); one gene, *Otub2*, was dowregulated in NTAL KD cells, and *Spink4* and *Sdf4* gave in NTAL KD cells results which were not consistent between microarray analysis and qPCR. Downregulated genes involved *Mlec*, *Slain1*, *Idi1* and *Nt5dc2* and were comparably reduced in both NTAL KO and KD cells.

Analysis of gene expression in Ag-activated cells revealed 194 genes (235 probe sets) differentially expressed between NTAL KO cells and WT cells (Table S3). Among them, 83 genes showed more than 1.8 fold upregulation. Most of the genes are involved in transcription, other genes are involved in metabolic processes, production and function of cytokines and in cytoskeleton organization and function. Analysis of Ag-activated NTAL KDs revealed 165 genes (203 probe sets; Table S4).

Numbers of differentially expressed genes in Ag-activated NTAL KO and KD cells and their overlaps are schematically shown in Figure 6C. Expression levels of the overlapping genes were verified by qPCR. Data presented in Figure 6C and D show that from the 5 overlapping genes in activated KD and KO, 4 of them showed transcriptional regulation in the same direction. In NTAL KO cells, *N4bp2l1* gene was upregulated but *Klhl24* gave results which were not consistent between microarray analysis and qPCR. In NTAL KD cells both these genes were upregulated. In both NTAL KO and KD cells *Mki67* and *Tmcc3* were downregulated in both cells types.

We also looked at changes of gene expression profiles after FcεRI triggering of NTAL KO, NTAL KD, WT and WT pLKO BMMCs. With a more stringent cut-off point of >4 fold up- or down-regulated gene expression and with FDR <0.05, we obtained a list of 308 probe sets representing 244 genes which are shown in Table S5. It is noteworthy that when performing PCA using all probe sets, differences between activated NTAL-deficient cells and the corresponding nonactivated controls were preserved. The highest clustering according to the treatment was found for the first principal component (PC; Figure 7; PC#1) demonstrating that activation of mast cells is a robust process with high impact on transcriptional changes. Smaller clustering was shown according to the type of cells along the second principal component (Figure 7; PC#2).

In this context it was also of interest to determine the contribution of lentiviral infection and selection procedure. We therefore focused on differences in gene expression between WT and WT pLKO cells. In nonactivated cells we found about 100 genes with different expression at the cut-off >1.8 fold change (FDR <0.1), but no difference was found between Ag-activated WT and WT pLKO cells. This was also corroborated by PCA as closer clustering of activated WT and WT pLKO cells (Figure 7).

NTAL-cholesterol crosstalk in regulation of Ag-mediated chemotaxis

Detailed analysis of the microarray data and gene sorting with the help of Gene Onthology Molecular Function and Biological Process (a module incorporated in the Partek software), suggested that NTAL KO led, among others, to decreased expression of several genes involved in cholesterol synthesis. The genes included isopenthyl-diphosphate delta isomerase1 (*Idi1*), farnesyl diphosphate synthase (*Fdps*), lanosterol synthase (*Lss*) and the phosphomevalonate kinase (*Pmvk*; Table S1 and Figure 6B). Decreased expression of the genes in NTAL KO cells was confirmed by RT-

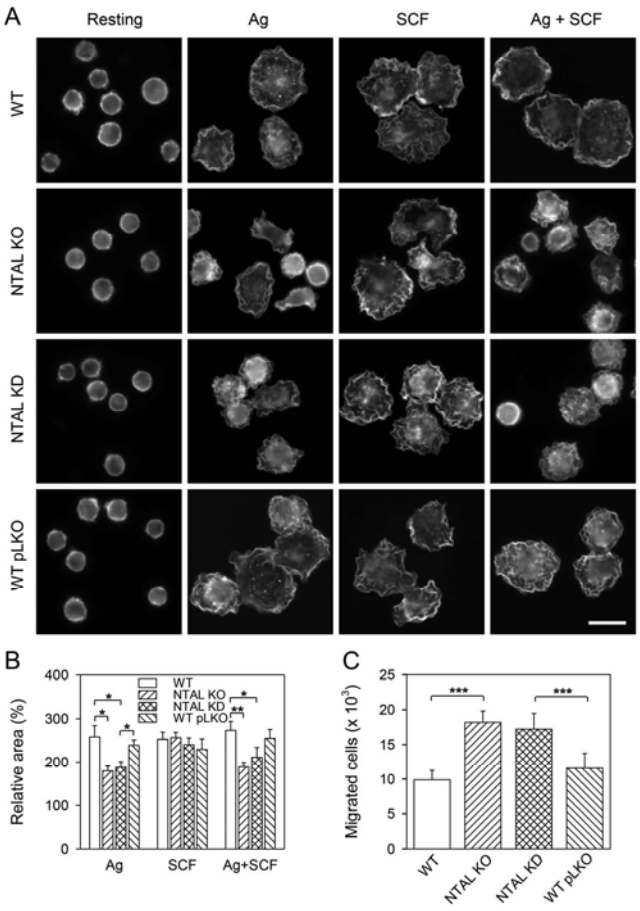

Figure 4. BMMCs with NTAL KD exhibit reduced spreading on fibronectin after stimulation with Ag or Ag + SCF, and enhanced chemotaxis towards Ag. (A) NTAL deficient cells and controls were sensitized with IgE, attached to fibronectin/Cell-Tak–coated glass for 1 hour at 37°C and then challenged or not (Resting) with Ag (250 ng/ml TNP-BSA), SCF (40 ng/ml) or both (Ag + SCF) for 30 minutes. Afterwards the cells were fixed and stained for actin with Alexa Fluor 488 phalloidin. Scale bar 10 μm. All images are depicted in the same scale. (B) Cell areas were determined using ScanR analysis software and data were normalized to nonactivated cells. Means ± SE were calculated from 6 independent experiments with at least 500 cells evaluated in each test. (C) Chemotactic response of IgE-sensitized BMMCs (WT, NTAL KO, NTAL KD and WT pLKO) towards Ag (250 ng/ml TNP-BSA) was evaluated by means of Transwell system with polycarbonate membrane. Numbers of the cells migrating through the membrane after 8 hours were determined by flow cytometry. Means ± SD were calculated from 4 independent experiments performed in duplicates. *$p<0.05$; **$p<0.01$; ***$p<0.001$.

doi:10.1371/journal.pone.0105539.g004

qPCR (Figure 6B). In further experiments we therefore investigated whether NTAL-deficient cells exhibit any change in amount of cellular cholesterol. Using Amplex Red Cholesterol Assay kit we found, however, no significant differences in total amount of cholesterol in both NTAL-deficient cells and corresponding control cells whether the cells were activated or not (data not shown).

Experiments with macrophages showed that local redistribution of cholesterol from inner to outer leaflet of the plasma membrane is of key significance for chemotaxis [28]. We therefore compared chemotaxis of NTAL-deficient and control cells cultured for 66 h in media supplemented with FCS or cholesterol-depleted FCS. This latter approach has been previously shown to decrease cholesterol level in BMMCs by ~25% ([29] and our unpublished data). We found (Figure 8A) that if WT cells grew in media containing cholesterol-deprived FCS, they exhibited lower chemotaxis towards antigen than cells cultured in cholesterol-containing medium (decrease to 78.8%±10.5%, mean ± SD; n = 8). When NTAL KO cells were used the inhibitory effect of cholesterol deprivation was more pronounced (decrease to

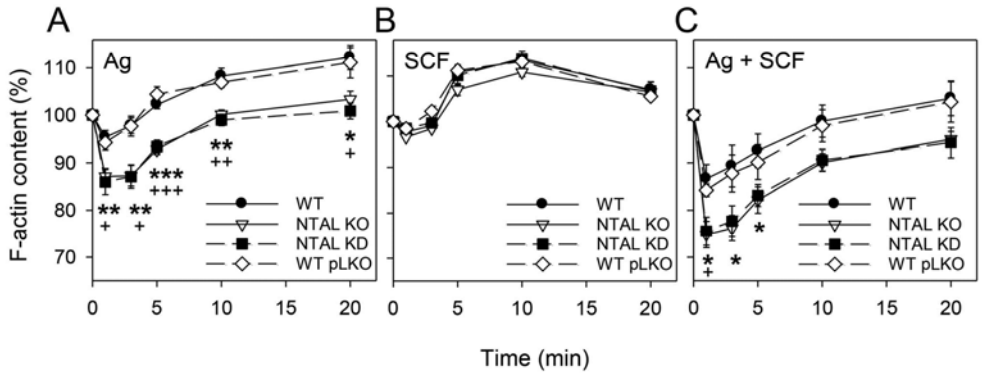

Figure 5. BMMCs with NTAL KD exhibit enhanced actin depolymerization after stimulation with Ag or Ag + SCF. Cells were activated with Ag (250 ng/ml TNP-BSA; A), SCF (40 ng/ml; B) or Ag + SCF (C). At the indicated times, the cells were fixed, stained for F-actin with Alexa Fluor 488-phalloidin and analyzed by flow cytometry. Data were normalized to fluorescence of resting cells (similar in all cell types). Values indicate mean ± SE ($n = 6$). $^{*,+}p<0.05$; $^{**,++}p<0.01$; $^{***,+++}p<0.001$; significant differences between NTAL KOs and WTs (asterisks) and NTAL KDs vs WT pLKOs (crosslets) are shown.
doi:10.1371/journal.pone.0105539.g005

Table 2. Differences in transcriptional regulation between NTAL KO and WT cells.

Biological processes different in NTAL KO vs WT cells			**Molecular functions different in NTAL KO vs WT cells**		
Biological process	**Genes in non-activated cells**	**Genes in activated cells**	**Molecular function**	**Genes in non-activated cells**	**Genes in activated cells**
metabolic processes	24	17	nucleotide binding	38	41
biosythetic processes	15	2	protein binding	21	31
transcription and its regulation	12	15	DNA binding	14	20
mRNA/rRNA processing and translation	11	2	catalytic activity	12	5
transport	11	3	RNA binding	8	1
protein phosphorylation and dephosphorylation	8	9	nucleic acid binding	7	5
cell cycle	7	14	receptor and signal transducer activity	6	3
ATP catabolic process	5	5	binding	5	5
DNA replication	5	6	magnesium ion binding	4	0
apoptosis	4	5	phosphoprotein phosphatase activity	4	2
signal transduction	4	6	chromatin binding	2	0
mitosis	3	9	peptidyl-prolyl cis-trans isomerase activity	2	1
DNA repair	3	7	actin binding	2	3
protein folding	3	1	serine-type endopeptidase inhibitor activity	2	1
microtubule organization and depolymerization	1	4	iron ion binding	2	1
cell proliferation	0	4	calcium ion binding	2	0
ubiquitin-dependent processes	0	4	structural molecule activity	1	2
cytokinesis and cytokine production	0	4	ubiquitin thiolesterase activity	0	2
other process	51	31	other function	44	28
unknown process	42	46	unknown function	33	43
total number of genes	**209**	**194**	**total number of genes**	**209**	**194**

doi:10.1371/journal.pone.0105539.t002

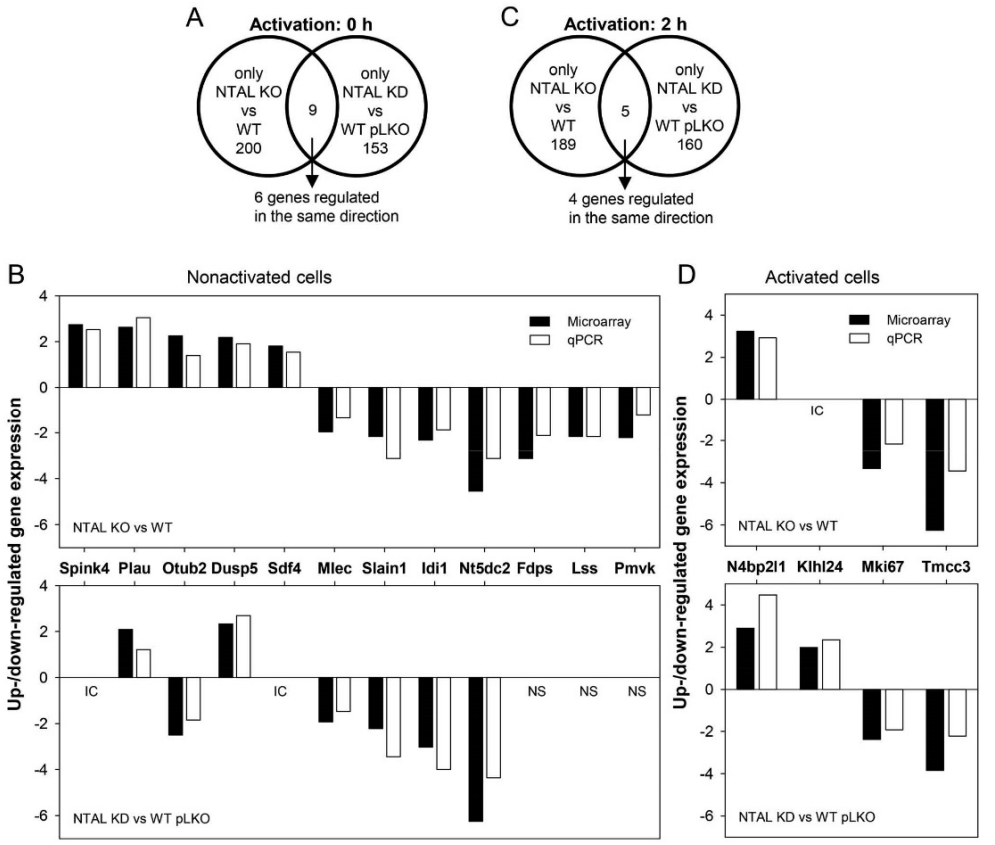

Figure 6. NTAL-dependent up- or down-regulated gene transcripts in resting and Ag-activated BMMCs. (A) Venn diagram illustrating number of genes with expression significantly (>1.8 x) up- or down-regulated in nonactivated cells with NTAL KO vs WT cells and NTAL KD vs WT pLKO cells; only 9 genes showed overlap. (B) Fold up- or down-regulation of overlapping genes in cells with NTAL KO and NTAL KD as determined by microarray data and qPCR analysis. Not shown are genes where qPCR data were inconsistent (IC) with microarray data and data with no significant p-values in microarray data analysis (NS). Four down-regulated genes involved in cholesterol synthesis in NTAL KO cells are also included (*Idi1, Fdps, Lss* and *Pmvk*). (C) Venn diagram as in A but documenting genes in Ag-activated NTAL KO and KD cells; only 5 genes showed overlap. (D) Microarray data and qPCR analysis of the overlapping genes in Ag-activated NTAL KO and KD cells as described in C; only 4 genes showing transcriptional regulation in the same direction are shown.
doi:10.1371/journal.pone.0105539.g006

66.8%±7.1%, mean ± SD; n = 8). The observed difference in chemotaxis decrease between WT cell and NTAL KO cells was significant (P = 0.004). These data indicate that chemotaxis of NTAL-deficient cells is more sensitive to decreased cholesterol levels than chemotaxis of WT cells.

In parallel experiments we compared chemotaxis of NTAL-deficient and control cells after treatment with various concentrations of methyl-β-cyclodextrin (MβCD), a compound which has been previously shown to reduce cellular cholesterol in mast cells [14,30]. In accord with previous findings (Figure 4C), Ag-driven chemotactic response was higher in NTAL-deficient cells than that of WT cells (Figure 8B). When NTAL KO BMMCs were exposed to increasing concentrations of MβCD (0.1–2.5 mM), significant decrease in chemotactic response was observed at all concentrations of MβCD tested (Figure 8B). In contrast, WT cells showed no decrease in chemotaxis after exposure to 0.5–2.5 mM MβCD. When exposed to 0.1 mM MβCD even a small but significant increase in chemotactic response to Ag was observed in WT BMMCs. These data suggest that low concentrations of MβCD change distribution of the plasma membrane cholesterol in NTAL KO cells in such a way that their chemotactic response is reduced.

Discussion

This study was initiated because of long-standing discrepancies in published data indicating that NTAL in mouse mast cells is a negative regulator of FcεRI signaling [9,10], whereas in human or rat mast cells is a positive regulator [12,13]. However, it was not

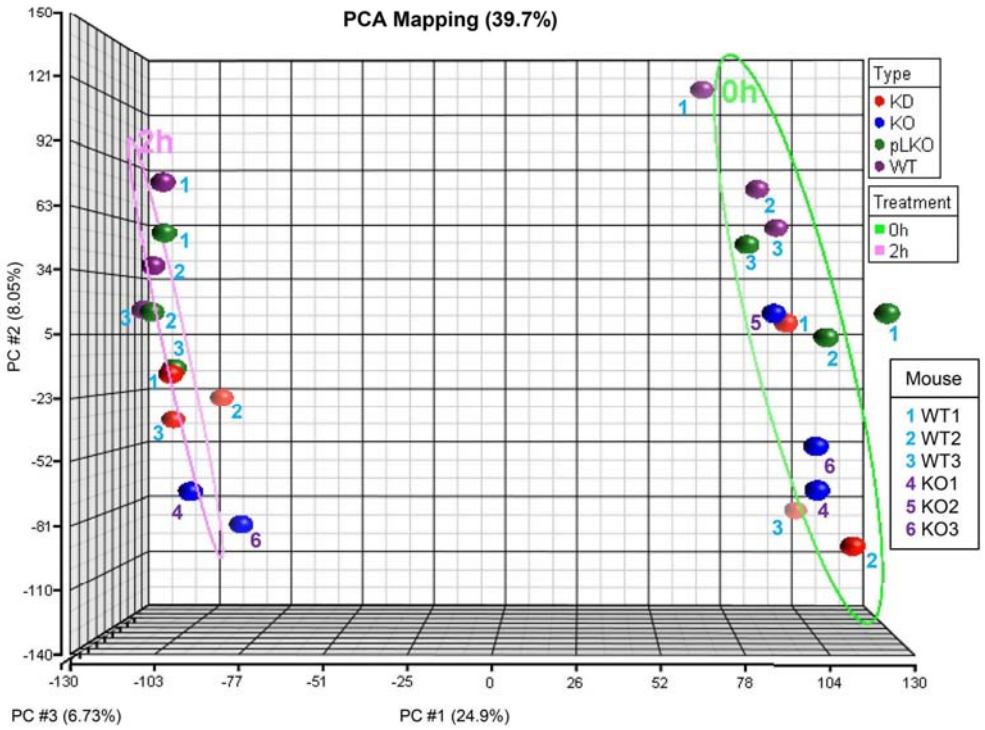

Figure 7. Principal component analysis of the microarrays. Each colored circle represents different cell type: NTAL KD (KD; red), NTAL KO (KO; blue), WT pLKO (pLKO; green), and WT (lilac). Each mouse from which the cells originated is identified by a colored numbers. The WT BMMCs isolated from mice 1–3 (blue numbers) were used not only as controls for NTAL KO cells, but also for obtaining NTAL KD and WT pLKO cells after lentiviral infection with NTAL shRNA or empty pLKO vector, respectively. The BMMC isolated from *Lat*$^{-/-}$ mice 4–6 (lilac numbers) were used only as cells with NTAL KO. Treatment [Ag-activated cells (2h, pink) and nonactivated cells (0h, green)] is distinguished by ellipsoids. The arrays cluster according to the treatment groups showing separation along PC #1 and according to the type of cells showing separation along PC #2. The percentage values indicate the proportion of total variance described by each PC; PC #1 (X-axis), PC #2 (Y-axis), and PC #3 (Z-axis).
doi:10.1371/journal.pone.0105539.g007

clear whether these discrepancies reflect different methods/strategies used for NTAL down-regulation (NTAL KO in mice, whereas NTAL KD in human and rat mast cells) and developmental alterations in KO mice as described in other systems where absence of a given gene is compensated for by enhanced transcriptional activity of other genes [31–34]. In attempt to understand the contribution of the compensatory mechanisms, we investigated for the first time the properties of mouse BMMCs with NTAL KD and compared them with BMMCs from mice with NTAL KO and well-matched controls. Several lines of evidence obtained in this study, indicate expressive similarities between the properties of BMMCs with NTAL KD or KO, and support the concept that NTAL is mostly a negative regulator of FcεRI signaling, independently of possible compensatory developmental alterations.

First, BMMCs with both NTAL KO and NTAL KD showed comparable increase in degranulation induced by FcεRI triggering. Compared to WT cells, NTAL KDs showed the highest increase in degranulation at suboptimal concentrations of Ag, similarly to NTAL KOs. At optimal and supraoptimal Ag concentrations the differences were less pronounced. Interestingly, activation through KIT was not potentiated by the absence of NTAL, even though NTAL is tyrosine phosphorylated in KIT-activated mast cells [12,35] and activation through KIT enhances degranulation of FcεRI-activated WT cells, and even more so of cells with NTAL KO or KD.

Second, Ag-activated BMMCs with NTAL KD exhibited higher Ca^{2+} response when compared to WT pLKO cells, but lower when compared to NTAL KO cells. Similarly to degranulation, down-regulation of NTAL had no effect on Ca^{2+} response after KIT triggering, even though KIT activation enhanced Ca^{2+} response in Ag-activated WT cells, and even more so in NTAL-deficient cells.

Third, when compared to WT cells, Ag activation of cells with NTAL KD resulted in enhanced tyrosine phosphorylation of ERK and LAT. Similar enhancement was also observed in Ag-activated NTAL KOs ([9,10] and this study). These data support the hypothesis that competition between NTAL and LAT as kinase substrates could attenuate the response in WT cells through decreased tyrosine phosphorylation of LAT, followed by decreased

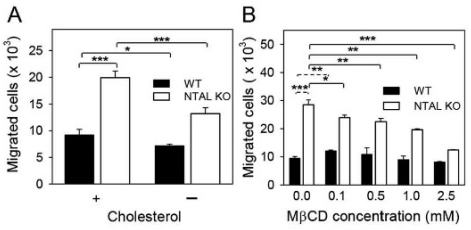

Figure 8. Different sensitivity of Ag-mediated chemotactic response of WT and NTAL KO BMMCs to cholesterol depletion. (A) BMMCs were cultured in media supplemented with IL-3 (without SCF) and 10% FCS with (+) or without (-) cholesterol. After 52 hours the cells were washed, suspended in medium with 10% FCS or cholesterol-depleted FCS and sensitized with TNP-specific IgE (1 μg/ml). After 14 hours, the cells were washed in chemotaxis medium and transferred into Transwell inserts, which were then immersed into the wells of the Transwell system with 600 μl of chemoattractant (250 ng/ml TNP-BSA) in chemotaxis medium. The number of cells passing through the filter was counted 8 hours later with flow cytometer. (B) The cells were cultured in medium supplemented with 10% FCS and IL-3 for 52 hours and then sensitized with TNP-specific IgE (1 μg/ml). After 14 hours, the cells were washed in chemotaxis medium containing various concentrations of MβCD and incubated at 37°C. After 30 min, the cells were washed in chemotaxis medium and transferred into Transwell inserts, which were then immersed into the wells of the Transwell system with 600 μl of chemoattractant (250 ng/ml TNP-BSA) in chemotaxis medium. The number of cells passing through the filter was counted 8 hours later with flow cytometer. Means and SD were calculated from data obtained in 3–4 independent experiments performed in duplicates. *$p<0.05$; **$p<0.01$; ***$p<0.001$.
doi:10.1371/journal.pone.0105539.g008

binding and activation of phospholipase Cγ1 and subsequent events [6,9,36].

Fourth, BMMCs with both NTAL KD and NTAL KO exhibited enhanced F-actin depolymerization after stimulation with Ag alone and even more after simultaneous triggering with both Ag + SCF. F-actin depolymerization precedes degranulation [27,37] and the observed decrease in amount of F-actin could account for the observed higher degranulation in NTAL-deficient cells than in WT cells after simultaneous activation with Ag + SCF.

Fifth, cells activated through FcεRI or KIT exhibited enhanced spreading on fibronectin. In cells with NTAL KD spreading was significantly decreased after activation with antigen, but was unaffected after SCF triggering. The observed data suggest that positive regulatory role of NTAL on Ag-mediated spreading ([18] and this study) is not the result of developmental compensatory events. Rather, spreading could be related to transient actin depolymerization which was observed in Ag-activated WT cells and even more in NTAL-deficient cells, but not in SCF-activated cells, WT or NTAL-deficient.

Sixth, BMMCs with NTAL KD exhibited migration towards Ag comparable with that seen in NTAL KO cells, and significantly higher than in WT cells. We recently showed that the level of active RhoA in resting NTAL KO BMMCs is at least twice as high as in WT cells [18]. Although active RhoA transiently decreased after FcεRI triggering, more in NTAL KO cells than in WT cells, it is likely that differences in regulation of RhoA activity in NTAL-deficient cells and WT cells are responsible for the enhanced NTAL-regulated chemotaxis. It should be stressed that previous reports have shown that RhoA regulates chemotaxis in other cell types, such as neutrophils [38–40], macrophages [41], dendritic cells [42] and lymphocytes [43].

The data presented in this study, together with those obtained in mice experiencing systemic anaphylaxis [9] indicate that in mouse mast cells NTAL is a negative regulator of FcεRI signaling. In contrast to mouse cells, NTAL in human mast cells and rat basophilic leukemia (RBL)-2H3 cells was described as a positive regulator of mast cells signaling [12,13,35]. The observed differences could have several causes. Thus, NTAL could play different roles in mast cells of different origin. It has been shown that human mast cells differ from mouse mast cells in cytokine production, immunoglobulin receptor expression, and the ability of different stimuli to cause degranulation and release of mediators [44]. Furthermore, when total tyrosine phosphorylated proteins were compared between RBL-2H3 cells and freshly isolated peritoneal and pleural rat mast cells, dramatic differences were observed [45]. These differences could reflect tumor origin of RBL-2H3 cells and could be responsible for the observed properties of NTAL. Importantly, mouse and human mast cells were obtained after differentiation under different cell culture conditions, which could modify their responsiveness. Mouse BMMCs were obtained by culturing bone marrow precursors in the presence of IL-3 and SCF (this study; [9]) or IL-3 alone [10], whereas human mast cells were derived from CD34+ pluripotent peripheral blood progenitors cultured in the presence of human SCF, IL-6 and IL-3 [12,35]. Previous study showed that differentiation of mast cells from their precursors in the presence of various cytokines could result in different responsiveness of the cells to various activators [22]. Finally, one cannot exclude the possibility that silencing vectors used for NTAL KD in human and/or RBL-2H3 mast cells exhibited off-target effects, which modified responsiveness of the cells to FcεRI triggering.

To clarify the role of NTAL in FcεRI signaling and to find out whether absence or decreased expression of NTAL has any effect on transcriptional regulation of genes, we compared under thoroughly controlled conditions RNA expression profiles of resting and Ag-activated BMMCs with NTAL KO or KD and the corresponding controls. We found that number of genes were up- or down-regulated, in BMMCs with NTAL KO or KD when compared to WT cells; most of the genes were not related to known immunoreceptor signaling pathways. The exact mechanisms and pathways through which NTAL causes changes in transcription of these genes remains to be determined. As expected, FcεRI activation induced robust changes in gene expression in all four types of mast cells studied (NTAL KO, NTAL KD, WT and WT pLKO). At the given cut-off level (>1.8-fold difference from proper controls), 209 genes showed different expression in nonactivated NTAL KO cells. It is remarkable that no differences in gene expression were noticed between Ag-activated WT and WT pLKO when similar criteria for analysis of differential gene expression were used. This confirms that infection and puromycin selection had no significant effect on the data obtained from lentivirally infected and activated cells. This is in marked contrast with comparison of RNA from activated cells with NTAL KO vs WT and NTAL KD vs WT pLKO, where 194 and 165 genes, respectively, were found differentially expressed.

When comparing expression levels in various cell types we noticed that the degree of overlap between nonactivated and activated NTAL KO and KD cells was rather modest. This could be due to methodological differences in production of NTAL-deficient cells. However, it should be kept in mind that although lentiviral infection itself and puromycin selection caused differential expression of some genes, as can be deduced from the observed differences in gene expression between nonactivated WT and WT

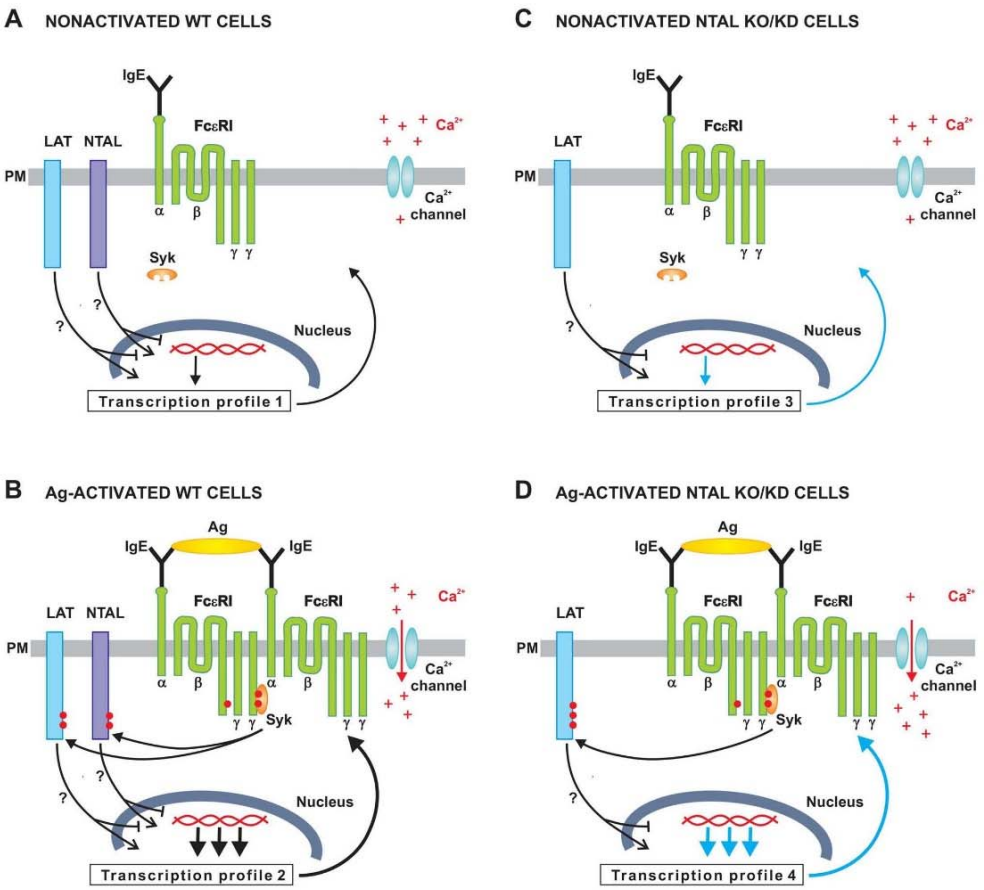

Figure 9. A hypothetical model on the role of NTAL in mast cell activation and transcriptional regulation. (A) In nonactivated WT cells both adaptor proteins, LAT and NTAL, and FcεRI β and γ subunits only exhibit weak phosphorylation, low $[Ca^{2+}]_i$ and transcription corresponding to nonactivated cells (Transcription profile 1). (B) After Ag-mediated aggregation of the FcεRI-IgE complex, β and γ subunits of the FcεRI are tyrosine phosphorylated by LYN and SYK. SYK then phosphorylates NTAL and LAT and this leads to enhanced Ca^{2+} uptake and further propagation of the signal, including dramatic changes in transcriptional regulation (Transcription profile 2). (C) In nonactivated NTAL-deficient cells, LAT and FcεRI subunits are only weakly tyrosine phosphorylated and the cells exhibit slightly different transcriptional regulation when compared to WT cells (Transcription profile 3). (D) After FcεRI triggering of NTAL-deficient cells, β and γ subunits of the FcεRI are tyrosine phosphorylated as in B, but because of the absence of NTAL, LAT is more phosphorylated by SYK. This leads to enhanced mobilization of Ca^{2+} and other signaling events and transcriptional regulation which differs from the one in activated WT cells (Transcription profile 4).
doi:10.1371/journal.pone.0105539.g009

pLKO cells, this difference disappeared in activated cells. Thus, lentiviral infection and puromycin selection did not contribute to the differences observed, at least in activated cells.

A hypothetical simplified model on the role of NTAL in mast cell activation and transcriptional regulation in WT and NTAL-deficient cells is shown in Figure 9. In nonactivated WT cells both adaptor proteins, NTAL and LAT, as well as FcεRI β and γ subunits are only weakly tyrosine phosphorylated, because of the equilibrium between kinases and phosphatases and/or decreased access of the kinase to their substrates [46]. Quiescent cells also exhibit low $[Ca^{2+}]_i$ and standard gene expression (Transcription profile 1; Figure 9A). After Ag-mediated activation there is enhanced tyrosine phosphorylation of FcεRI β and γ subunits by LYN and SYK kinase. Activated SYK phosphorylates NTAL and LAT and this leads to further propagation of the activation signal, increased $[Ca^{2+}]_i$ and dramatic changes in gene expression by so far not fully understood mechanism (Transcription profile 2; Figure 9B). In cells with decreased expression of NTAL due to NTAL KO or NTAL KD, gene expression is changed when compared to WT cells (Transcription profile 3; Figure 9C). After activation of NTAL-deficient cells, LAT is phosphorylated by SYK. However, because of NTAL absence, LAT is more

phosphorylated than in WT cells. This leads to increased $[Ca^{2+}]_i$ and transcriptional regulation which is different from WT cells (Transcription profile 4; Figure 9D). These processes contribute to enhanced response to Ag in NTAL-deficient cells, including enhanced degranulation, calcium response, chemotaxis and depolymerization of F-actin.

Unexpected findings in this study were NTAL-dependent changes in the expression of a number of genes related to metabolism and biosynthetic processes. A subgroup of these genes was involved in lipid metabolism, including synthesis of cholesterol. Although decreased transcription of several genes involved in cholesterol synthesis was confirmed by RT-qPCR, no significant difference in total amount of cellular cholesterol was detected between WT and NTAL-deficient cells. Yet, surprisingly, we found that pretreatment of BMMCs with MβCD had different effect on NTAL KO and WT cells. In NTAL KO cells MβCD significantly inhibited chemotaxis at all concentrations of MβCD tested (0.1 2.5 mM), whereas in WT cells MβCD either slightly, but reproducibly increased chemotaxis at a low concentration (0.1 mM) or had no significant effect at higher concentrations (0.5 2.5 mM). MβCD is known to remove cholesterol from the cells [47,48] and therefore one can hypothesize that enhanced chemotaxis in NTAL-deficient cells is regulated in part by plasma membrane cholesterol distribution. Molecular mechanism of the cholesterol-dependent regulations of chemotaxis is poorly understood, but could be related to differences in synthesis and/or distribution of cholesterol into plasma membrane sheets. One such possible mechanism has been recently described in macrophages with defect in ATP-binding cassette transporters ABCA1 and ABCG1, which are involved in the movement of cholesterol from the inner to the outer leaflet of the plasma membrane and play role in chemotaxis towards C5a chemoattractant [28]. Regulation of chemotactic response by cholesterol has been described in other cell types including T cells [49], monocytes [50] and neutrophils [51]. Molecular mechanisms of the cross-talk between NTAL and cholesterol remains to be determined.

In summary, the results based on functional studies of BMMCs with NTAL KD and the corresponding controls indicate that NTAL is a negative regulator of FcεRI-mediated signaling pathways. Because similar findings were observed in BMMCs with NTAL KD or KO, no significant role of compensatory developmental alterations appear to account for FcεRI signaling in BMMCs from *Ntal*$^{-/-}$ mice. Expression profiles of nonactivated or FcεRI activated BMMCs with NTAL KO, NTAL KD, and the corresponding controls identified several genes which were up- or down-regulated in NTAL-deficient cells. The data indicate that some of these genes could be involved in regulation of cholesterol-dependent events in Ag-mediated chemotaxis.

Supporting Information

Table S1 Differentially expressed gene transcripts in nonactivated NTAL KO cells when compared with nonactivated WT cells. The table represents a list of probe sets for the corresponding genes that were up- or down-regulated in nonactivated (0 h) NTAL KO cells (KO) when compared to corresponding nonactivated WT cells (WT) and passed the filter of FDR <0.1 and 1.8 fold change (ratio). Probe sets are sorted in ratio descending order. Those probe sets that also show significant up- or down-regulation in noactivated NTAL-KD cells are in bold. For comparison purposes (in grey) are shown p-values and ratios of the selected probe sets from comparison of nonactivated NTAL KD cells (KD) vs nonactivated WT pLKO cells (pLKO), activated (2 h) NTAL KO cells vs activated WT cells, and activated NTAL KD cells vs activated WT pLKO cells.
(XLSX)

Table S2 Differentially expressed gene transcripts in nonactivated NTAL KD cells when compared with nonactivated WT pLKO cells. The table represents a list of probe sets for the corresponding genes that were up- or down-regulated in nonactivated NTAL KD cells when compared to the corresponding nonactivated WT pLKO cells and passed the filter of FDR < 0.1 and 1.8 fold change (ratio). Probe sets are sorted in ratio descending order. Those probe sets that also show significant up- or down-regulation in NTAL-KO cells are in bold. For comparison purposes (in grey) are shown p-values and ratios of the selected probe sets from comparison of nonactivated NTAL KO cells vs nonactivated WT cells, activated NTAL KO cells vs activated WT cells, and activated NTAL KD cells vs activated WT pLKO cells.
(XLSX)

Table S3 Differentially expressed gene transcripts in Ag-activated NTAL KO cell when compared with Ag-activated WT cells. The table represents a list of probe sets for the corresponding genes that were up- or down-regulated in Ag-activated NTAL KO cells when compared to the corresponding activated WT cells and passed the filter of FDR <0.1 and 1.8 fold change (ratio). Probe sets are sorted in ratio descending order. Those probe sets that also show significant up- or down-regulation in NTAL KD cells are in bold. For comparison purposes (in grey) are shown p-values and ratios of the selected probe sets from comparison of activated NTAL KD cells vs activated WT pLKO cells, nonactivated NTAL KO cells vs nonactivated WT cells, and nonactivated NTAL KD cells vs nonactivated WT pLKO cells.
(XLSX)

Table S4 Differentially expressed gene transcripts in Ag-activated NTAL KD cells when compared with Ag-activated WT pLKO cells. The table represents a list of probe sets for the corresponding genes that were up- or down-regulated in Ag-activated NTAL KD cells when compared to the corresponding WT pLKO cells and passed the filter of FDR <0.1 and 1.8 fold change (ratio). Probe sets are sorted in ratio descending order. Those probe sets that also show significant up- or down-regulation in NTAL-KO cells are in bold. For comparison purposes (in grey) are shown p-values and ratios of the selected probe sets from comparison of activated NTAL KO cells vs activated WT cells, nonactivated NTAL KO cells vs nonactivated WT cells, and nonactivated NTAL KD cells vs nonactivated WT pLKO cells.
(XLSX)

Table S5 Differentially expressed gene transcripts in all four groups of cells after Ag activation when compared to their noinactivated forms. The table represents a list of probe sets for the corresponding genes that were up- or down-regulated among all four groups of cells when the same Ag-activated (2 h) and nonactivated (0 h) cells were compared. Table shows probe sets that passed the filter of FDR <0.05 and 4 fold change (ratio). Probe sets are sorted in ratio descending order. Correspondig unadjusted p-values and ratios of these probe sets from comparison of activated WT cells vs nonactivated WT cell, activated NTAL KO cells vs nonactivated NTAL KO cells, activated NTAL KD cells vs nonactivated NTAL KD, and activated WT pLKO cells vs nonactivated WT pLKO cell are shown.
(XLSX)

Acknowledgments

The authors thank Hana Mrazova, Lukas Kocanda and Romana Budovicova for technical assistance and Petr Simecek for help with microarray data analysis.

Author Contributions

Conceived and designed the experiments: PD IP LD. Performed the experiments: IP LD MS. Analyzed the data: IP LD MS PD. Contributed reagents/materials/analysis tools: LD PD. Contributed to the writing of the manuscript: IP PD LD.

References

1. Kinet JP (1999) The high-affinity IgE receptor (FcεRI): from physiology to pathology. Annu Rev Immunol 17: 931 972.
2. Eiseman E, Bolen JB (1992) Signal transduction by the cytoplasmic domains of FcεRI-γ and TCR-ζ in rat basophilic leukemia cells. J Biol Chem 267: 21027 21032.
3. Rivera J, Gilfillan AM (2006) Molecular regulation of mast cell activation. J Allergy Clin Immunol 117: 1214 1225.
4. Lindquist JA, Simeoni L, Schraven B (2003) Transmembrane adapters: attractants for cytoplasmic effectors. Immunol Rev 191: 165 182.
5. Horejsi V, Zhang W, Schraven B (2004) Transmembrane adaptor proteins: organizers of immunoreceptor signalling. Nat Rev Immunol 4: 603 616.
6. Draber P, Halova I, Levi-Schaffer F, Draberova L (2012) Transmembrane adaptor proteins in the high-affinity IgE receptor signaling. Frontiers Immunol, 2: 1 11.
7. Brdička T, Imrich M, Angelisová P, Brdičková N, Horváth O, et al. (2002) Non-T cell activation linker (NTAL): a transmembrane adaptor protein involved in immunoreceptor signaling. J Exp Med 196: 1617 1626.
8. Janssen E, Zhu M, Zhang W, Koonpaew S, Zhang W (2003) LAB: a new membrane-associated adaptor molecule in B cell activation. Nat Immunol 4: 117 123.
9. Volná P, Lebduška P, Dráberová L, Šimová S, Heneberg P, et al. (2004) Negative regulation of mast cell signaling and function by the adaptor LAB/NTAL. J Exp Med 200: 1001 1013.
10. Zhu M, Liu Y, Koonpaew S, Granillo O, Zhang W (2004) Positive and negative regulation of FcεRI-mediated signaling by adaptor protein LAB/NTAL. J Exp Med 200: 991 1000.
11. Saitoh S, Arudchandran R, Manetz TS, Zhang W, Sommers CL, et al. (2000) LAT is essential for FcεRI-mediated mast cell activation. Immunity 12: 525 535.
12. Tkaczyk C, Horejsi V, Shoko I, Draber P, Samelson LE, et al. (2004) NTAL phosphorylation is a pivotal link between the signaling cascades leading to human mast cell degranulation following kit activation and FcεRI aggregation. Blood 104: 207 214.
13. Dráberová L, Shaik GM, Volná P, Heneberg P, Tůmová M, et al. (2007) Regulation of Ca^{2+} signaling in mast cells by tyrosine-phosphorylated and unphosphorylated non-T cell activation linker. J Immunol 179: 5169 5180.
14. Surviladze Z, Dráberová L, Kovářová M, Boubelík M, Dráber P (2001) Differential sensitivity to acute cholesterol lowering of activation mediated via the high-affinity IgE receptor and Thy-1 glycoprotein. Eur J Immunol 31: 1 10.
15. Cham BE, Knowles BR (1976) A solvent system for delipidation of plasma or serum without protein precipitation. J Lipid Res 17: 176 181.
16. Tolar P, Tůmová M, Dráber P (2001) New monoclonal antibodies recognizing the adaptor protein LAT. Folia Biol (Praha) 47: 215 217.
17. Hájková Z, Bugajev V, Dráberová E, Vinopal S, Dráberová L, et al. (2011) STIM1-directed reorganization of microtubules in activated mast cells. J Immunol 186: 913 923.
18. Tůmová M, Koffer A, Šimíček M, Dráberová L, Dráber P (2010) The transmembrane adaptor protein NTAL signals to mast cell cytoskeleton via the small GTPase Rho. Eur J Immunol 40: 3235 3245.
19. Brazma A, Hingamp P, Quackenbush J, Sherlock G, Spellman P, et al. (2001) Minimum information about a microarray experiment (MIAME)-toward standards for microarray data. Nat Genet 29: 365 371.
20. Horáková H, Polakovičová I, Shaik GM, Eitler J, Bugajev V, et al. (2011) 1,2-propanediol-trehalose mixture as a potent quantitative real-time PCR enhancer. BMC Biotechnol 11: 41.
21. Gilfillan AM, Tkaczyk C (2006) Integrated signalling pathways for mast-cell activation. Nat Rev Immunol 6: 218 230.
22. Nocka KH, Levine BA, Ko JL, Burch PM, Landgraf BE, et al. (1997) Increased growth promoting but not mast cell degranulation potential of a covalent dimer of c-Kit ligand. Blood 90: 3874 3883.
23. Paz PE, Wang S, Clarke H, Lu X, Stokoe D, et al. (2001) Mapping the Zap-70 phosphorylation sites on LAT (linker for activation of T cells) required for recruitment and activation of signalling proteins in T cells. Biochem J 356: 461 471.
24. Zhu M, Janssen E, Zhang W (2003) Minimal requirement of tyrosine residues of linker for activation of T cells in TCR signaling and thymocyte development. J Immunol 170: 325 333.
25. Thompson HL, Thomas L, Metcalfe DD (1993) Murine mast cells attach to and migrate on laminin-, fibronectin-, and matrigel-coated surfaces in response to FcεRI-mediated signals. Clin Exp Allergy 23: 270 275.
26. Dastych J, Metcalfe DD (1994) Stem cell factor induces mast cell adhesion to fibronectin. J Immunol 152: 213 219.
27. Frigeri L, Apgar JR (1999) The role of actin microfilaments in the down-regulation of the degranulation response in RBL-2H3 cells. J Immunol 162: 2243 2250.
28. Pagler TA, Wang M, Mondal M, Murphy AJ, Westerterp M, et al. (2011) Deletion of ABCA1 and ABCG1 impairs macrophage migration because of increased Rac1 signaling. Circ Res 108: 194 200.
29. Kovarova M, Wassif CA, Odom S, Liao K, Porter FD, et al. (2006) Cholesterol deficiency in a mouse model of Smith-Lemli-Opitz syndrome reveals increased mast cell responsiveness. J Exp Med 203: 1161 1171.
30. Sheets ED, Holowka D, Baird B (1999) Critical role for cholesterol in Lyn-mediated tyrosine phosphorylation of FcεRI and their association with detergent-resistant membranes. J Cell Biol 145: 877 887.
31. Reaume AG, de Sousa PA, Kulkarni S, Langille BL, Zhu D, et al. (1995) Cardiac malformation in neonatal mice lacking connexin43. Science 267: 1831 1834.
32. Thyagarajan T, Totey S, Danton MJ, Kulkarni AB (2003) Genetically altered mouse models: the good, the bad, and the ugly. Crit Rev Oral Biol Med 14: 154 174.
33. Fernandes AR, Easton AC, De Souza Silva MA, Schumann G, Muller CP, et al. (2012) Lentiviral-mediated gene delivery reveals distinct roles of nucleus accumbens dopamine D2 and D3 receptors in novelty- and light-induced locomotor activity. Eur J Neurosci 35: 1344 1353.
34. Wright J, Morales MM, Sousa-Menzes J, Ornellas D, Sipes J, et al. (2008) Transcriptional adaptation to Clcn5 knockout in proximal tubules of mouse kidney. Physiol Genomics 33: 341 354.
35. Iwaki S, Spicka J, Tkaczyk C, Jensen BM, Furumoto Y, et al. (2008) Kit- and FcεRI-induced differential phosphorylation of the transmembrane adaptor molecule NTAL/LAB/LAT2 allows flexibility in its scaffolding function in mast cells. Cell Signal 20: 195 205.
36. Orr SJ, McVicar DW (2011) LAB/NTAL/Lat2: a force to be reckoned with in all leukocytes? J Leukoc Biol 89: 11 19.
37. Tolarová H, Dráberová L, Heneberg P, Dráber P (2004) Involvement of filamentous actin in setting the threshold for degranulation in mast cells. Eur J Immunol 34: 1627 1636.
38. Lecut C, Frederix K, Johnson DM, Deroanne C, Thiry M, et al. (2009) P2X1 ion channels promote neutrophil chemotaxis through Rho kinase activation. J Immunol 183: 2801 2809.
39. Liu L, Das S, Losert W, Parent CA (2010) mTORC2 regulates neutrophil chemotaxis in a cAMP- and RhoA-dependent fashion. Dev Cell 19: 845 857.
40. Cavnar PJ, Berthier E, Beebe DJ, Huttenlocher A (2011) Hax1 regulates neutrophil adhesion and motility through RhoA. J Cell Biol 193: 465 473.
41. Fan H, Hall P, Santos LL, Gregory JL, Fingerle-Rowson G, et al. (2011) Macrophage migration inhibitory factor and CD74 regulate macrophage chemotactic responses via MAPK and Rho GTPase. J Immunol 186: 4915 4924.
42. Wang Z, Kumamoto Y, Wang P, Gan X, Lehmann D, Smrcka AV, et al. (2009) Regulation of immature dendritic cell migration by RhoA guanine nucleotide exchange factor Arhgef5. J Biol Chem 284: 28599 28606.
43. Ishizaki H, Togawa A, Tanaka-Okamoto M, Hori K, Nishimura M, et al. (2006) Defective chemokine-directed lymphocyte migration and development in the absence of Rho guanosine diphosphate-dissociation inhibitors α and β. J Immunol 177: 8512 8521.
44. Finkelman FD (2007) Anaphylaxis: lessons from mouse models. J Allergy Clin Immunol 120: 506 515.
45. Dráberová L, Dráber P (1995) Aggregation of Thy-1 glycoprotein induces tyrosine phosphorylation of different proteins in isolated rat mast cells and rat basophilic leukemia cells. In: Mestecky J, McGhee J, Tláskalová H, Šterzl J, editors. Advances in Mucosal Immunology. New York, N.Y.: Plenum Press. pp. 297 301.
46. Bugajev V, Bambouskova M, Draberova L, Draber P (2010) What precedes the initial tyrosine phosphorylation of the high affinity IgE receptor in antigen-activated mast cell? FEBS Lett 584: 4949 4955.
47. Kilsdonk EP, Yancey PG, Stoudt GW, Bangerter FW, Johnson WJ, et al. (1995) Cellular cholesterol efflux mediated by cyclodextrins. J Biol Chem 270: 17250 17256.
48. Yancey PG, Rodrigueza WV, Kilsdonk EPC, Stoudt GW, Johnson WJ, et al. Phillips MC, Rothblat GH (1996) Cellular cholesterol efflux mediated by cyclodextrins. Demonstration of kinetic pools and mechanism of efflux. J Biol Chem 271: 16026 16034.
49. Nguyen DH, Espinoza JC, Taub DD (2004) Cellular cholesterol enrichment impairs T cell activation and chemotaxis. Mech Ageing Dev 125: 641 650.
50. Murphy AJ, Woollard KJ, Hoang A, Mukhamedova N, Stirzaker RA, et al. (2008) High-density lipoprotein reduces the human monocyte inflammatory response. Arterioscler Thromb Vasc Biol 28: 2071 2077.
51. Pierini LM, Eddy RJ, Fuortes M, Seveau S, Casulo C, et al. (2003) Membrane lipid organization is critical for human neutrophil polarization. J Biol Chem 278: 10831 10841.

Transmembrane adaptor protein PAG/CBP is involved in both positive and negative regulation of mast cell signaling

Mol Cell Biol. (submitted)

Transmembrane adaptor protein PAG/CBP is involved in both positive and negative regulation of mast cell signaling

Lubica Draberova[1], Viktor Bugajev[1], Lucie Potuckova[1], Ivana Halova[1], Monika Bambouskova[1], Iva Polakovicova[1], Ramnik J. Xavier[2,3], Brian Seed[2], and Petr Draber[1#]

[1]Department of Signal Transduction, Institute of Molecular Genetics, Academy of Sciences of the Czech Republic, Prague, Czech Republic

[2]Center for Computational and Integrative Biology, Massachusetts General Hospital, Harvard Medical School, Boston, MA 02114

[3]Broad Institute of Harvard University and Massachusetts Institute of Technology, Cambridge, MA 02142

Running title: Regulation of mast cell signaling by PAG/CBP adaptor

[#]Correspondence:
Petr Draber, PhD,
Department of Signal Transduction,
Institute of Molecular Genetics,
Academy of Sciences of the Czech Republic,
Videnska 1083,
CZ-142 20 Prague 4,
Czech Republic

Tel.: +420-241062468;
Fax: +420-241470339;
E-mail: draberpe@img.cas.cz

Materials and Methods: 3121 words
Introduction, Results, Discussion: 4932 words

ABSTRACT

The transmembrane adaptor protein PAG/CBP (hereafter PAG) is expressed in multiple cell types. Tyrosine phosphorylated PAG serves as an anchor for C-terminal SRC kinase, an inhibitor of SRC family kinases. The role of PAG as a negative regulator of immunoreceptor signaling has been examined in several model systems, but no functions *in vivo* have been determined. Here, we examine the activation of bone marrow-derived mast cells (BMMCs) with PAG knockout, PAG knockdown, and corresponding controls. Our data show that PAG-deficient BMMCs exhibit impaired antigen-induced degranulation, extracellular calcium uptake, tyrosine phosphorylation of several key signaling proteins (including the high affinity IgE receptor subunits, spleen tyrosine kinase, and phospholipase C), production of several cytokines and chemokines, and chemotaxis. Enzymatic activities of the LYN and FYN kinases were increased in non-activated cells, suggesting the involvement of a LYN- and/or FYN-dependent negative regulatory loops. When BMMCs from PAG knockout mice were activated via KIT receptor, enhanced degranulation and tyrosine phosphorylation of the receptor were observed. *In vivo* experiments showed that PAG is a positive regulator of passive systemic anaphylaxis. The combined data indicate that PAG can function as both a positive or negative regulator of mast cell signaling depending upon the signaling pathway involved.

48 **INTRODUCTION**

49 Mast cells are widely distributed in the body, where they play important roles in innate as
50 well as adaptive immune responses (1). To fulfill their role in adaptive immune responses, the
51 cells express the high affinity IgE receptor (FcεRI) on their plasma membranes. Aggregation of
52 this tetrameric immunoreceptor, $\alpha\beta\gamma 2$, induces cell signaling events leading to release of
53 preformed inflammatory mediators and *de novo* synthesis and release of leukotrienes, cytokines,
54 and chemokines. The first well-defined biochemical step after FcεRI triggering is tyrosine
55 phosphorylation of the immunoreceptor tyrosine-based activation motifs in the cytoplasmic tail
56 of the FcεRI β and γ subunits by SRC family protein tyrosine kinase (PTK) LYN (2, 3). The
57 phosphorylated β and γ subunits then serve as binding and activation sites for LYN kinase and
58 spleen tyrosine kinase (SYK), respectively. These two enzymes, together with FYN and other
59 kinases, then phosphorylate various adaptor proteins and enzymes with a variety of functions in
60 signal transduction pathways. The exact molecular events preceding LYN-mediated tyrosine
61 phosphorylation of the FcεRI β subunit are not clear and several models have been proposed,
62 including the transphosphorylation model (4), lipid raft model (5), and the PTK-protein tyrosine
63 phosphatase (PTP) interplay model (6).

64 Our previous study with murine bone marrow-derived mast cells (BMMCs) showed that
65 FcεRI triggering induced transient hyperphosphorylation of LYN kinase on its C-terminal
66 regulatory tyrosine (Tyr 487), leading to the formation of a closed inactive conformation where
67 SRC homology (SH)2 domain interacts with phospho-Tyr 487 and transiently decreases LYN
68 enzymatic activity (7). This finding was surprising because in T cells the corresponding SRC
69 family kinase (SFK), LCK, showed decreased tyrosine phosphorylation of the C-terminal
70 regulatory tyrosine and enhanced enzymatic activity after activation through T cell
71 immunoreceptors (8, 9). Phosphorylation of the C-terminal inhibitory tyrosine in SFKs is

72 catalyzed by the C-terminal SRC kinase (CSK) (10), a cytoplasmic PTK that can be anchored
73 through its SH2 domain to PAG (11), also termed CBP (12). PAG/CBP (hereafter PAG) is a
74 ubiquitously expressed transmembrane adaptor protein containing a short extracellular domain, a
75 transmembrane domain, and a long cytoplasmic tail with multiple tyrosine-based motifs.
76 Phosphorylated Tyr 314 in mouse PAG has been shown to be essential for CSK binding. PAG
77 also possesses two proline-rich sequences that serve as binding sites for proteins with SH3
78 domains, and a C-terminal VTRL motif for interaction with the PDZ domain of the cytoskeletal
79 linker ezrin/radixin/moesin-binding protein of 50 kDa (13). Similar to some other
80 transmembrane adaptor proteins, such as the non-T cell activation linker and linker for activation
81 of T cells (LAT), PAG has two conserved cysteine residues located in the vicinity of the
82 transmembrane domain, which are the subject of post-translational palmitoylation and which
83 contribute to poor solubility of the proteins in nonionic detergents and their presumable
84 localization in membrane microdomains called lipid rafts (14, 15).
85 PAG in resting T cells associates with FYN kinase, which constitutively phosphorylates
86 PAG on Tyr 314 to create a docking site for the CSK SH2 domain. This binding brings CSK to
87 the vicinity of its substrate, SFK LCK, and enhances CSK catalytic activity leading to
88 phosphorylation of the LCK inhibitory C-terminal tyrosine. Upon T cell receptor activation,
89 PAG is rapidly dephosphorylated, CSK is released from PAG, and LCK is dephosphorylated on
90 its C-terminal tyrosine. This modification increases the activity of LCK, leading to increased
91 tyrosine phosphorylation of T cell receptor subunits and other substrates. A negative regulatory
92 role of PAG in T cell signaling was confirmed in experiments with PAG knockdowns (KDs)
93 (16), but not with PAG KOs (17, 18), suggesting that developmental compensatory mechanisms
94 are involved.

In mast cells, PAG is phosphorylated by LYN kinase instead of FYN kinase, and following FcεRI triggering, the decrease in PAG phosphorylation is replaced by an increase (19, 20). Overexpression of PAG has been reported to inhibit FcεRI-mediated degranulation in rat basophilic leukemia (RBL) cells (21). Further experiments showed that FcεRI activation of BMMCs from LYN-deficient mice resulted in enhanced degranulation, whereas FYN-deficient cells showed the opposite effect (22-24). This finding supports the concept that SFKs are tightly regulated in the course of mast cell activation and important differences exist between early regulatory events induced by engagement of the T cell receptors and FcεRI. The exact role of PAG in mast cell activation remains to be determined.

Herein we present data on FcεRI-mediated activation events in BMMCs derived from mice deficient in PAG (PAG-KO) and from the corresponding WT mice. We also attempted to determine whether any differences in activation are detectable between BMMCs in which PAG is down-regulated by RNA interference and corresponding control cells. Furthermore, we examined the role of PAG in cells activated through another important mast cell surface receptor, KIT. The combined data indicate that PAG functions as a positive or negative regulator of mast cell signaling, and that the specific effect depends on the particular signaling pathway. We also show that PAG-deficient mice have a distinct phenotype *in vivo* as assessed by passive systemic anaphylaxis response.

MATERIALS AND METHODS

Mice and cells. Mice deficient in PAG were generated by modified bacterial artificial chromosome technology as previously described (25, 26). Briefly, the bacterial artificial chromosome clones were electroporated into strain 129Sv/J embryonic stem cells. Targeting in clone 7 was confirmed by fluorescence *in situ* hybridization. PAG-KO mice derived from clone 7 were born in the expected Mendelian frequency and were healthy. Transgenic founders were backcrossed to C57BL/6 mice for more than eight generations. For experiments, PAG-KO mice were mated with C57BL/6 mice and their F1 descendants were genotyped by PCR using the following primers: PAG 1 F (5´- GAC AGC ACA GGA AAG GCC AAG -3´), PAG 2 R (5´- GTG TCC ACC GGT CCC TTC TG -3´) and PAG ZEO R (5´- CCA GGG TGT TGT CCG GCA C -3´), giving PCR products of 498 and 390 bps for the wild-type (WT) and PAG KO allele, respectively. Bone marrow cells were isolated from the femurs and tibias of 6 – 8-week-old PAG-KO mice or their WT littermates (PAG-WT). All animal studies were performed in compliance with the US Department of Health and Human Services Guide for the Care and Use of Laboratory Animals and were approved by the Animal Care and Usage Committee of the Institute of Molecular Genetics. Cells were cultured in RPMI-1640 medium supplemented with 100 U/ml penicillin, 100 µg/ml streptomycin, 71 µM 2-mercaptoethanol, minimum essential medium (MEM) non-essential amino acids, 0.7 mM sodium pyruvate, 2.5 mM L-glutamine, 12 mM D-glucose, recombinant mouse stem cell factor (SCF; 20 ng/ml, PeproTech EC), mouse recombinant interleukin (IL)-3 (20 ng/ml, PeproTech EC) and 10% fetal calf serum (FCS).

Antibodies and reagents. The following monoclonal antibodies (mAbs) were used: anti-LAT (27), anti-LYN (28), anti-FcεRI β chain (29), and trinitrophenol (TNP)-specific immunoglobulin

(Ig)E mAb (IGEL b4 1) (30), and anti-hypoxanthine-guanine phosphoribosyltransferase (HPRT) (Santa Cruz Biotechnology Inc.). Anti-paxillin was obtained from BD Transduction Laboratories. Polyclonal antibodies specific for LYN and LAT were prepared in our laboratory in Prague by immunization of rabbits with the corresponding recombinant proteins or their fragments (31). Rabbit anti-IgE was prepared by immunization with whole IGEL b4.1. Polyclonal antibodies specific for FYN, actin, phospholipase C (PLC)γ1, PLCγ2, GRB2, CSK, KIT, STAT5, SHIP1, phospho-KIT (Y568/570), phospho-focal adhesion kinase (FAK; Y925), as well as horseradish peroxidase (HRP)-conjugated donkey anti-goat IgG, goat anti-mouse IgG, and goat anti-rabbit IgG, were obtained from Santa Cruz Biotechnology Inc. Antibodies specific for phospho-SYK (Y525/Y526), phospho-STAT5 (Y694), phospho-SH2-containing inositol 5'-phosphatase 1 (SHIP1; Y1020), and Myc-Tag were obtained from Cell Signaling. PAG-specific rabbit polyclonal antibody was from Exbio. HRP-conjugated anti-phosphotyrosine mAb (PY-20) was obtained from BD Biosciences. Antibodies specific for tumor necrosis factor (TNF)-α, IL-6, and IL-13 were purchased from PeproTech EC. Anti-mouse FcεRI labeled with fluorescein isothiocyanate (FITC) and anti-mouse KIT-allophycocyanin (APC) conjugates were obtained from eBiosciences. ^{45}Ca (specific activity 773 MBq/mg Ca^{2+}) and adenosine 5′-[γ-^{32}P]triphosphate (specific activity 222 TBq/mmol) were purchased from the Institute of Isotopes Co., Ltd (Budapest). Donkey anti-rabbit-Alexa Fluor 488 conjugate and thapsigargin were obtained from Invitrogen. Mowiol 4-88 was from Merck. Colloidal gold nanoparticles (Au-NPs; 30 nm in diameter), containing approximately 2×10^{11} Au-NPs/ml, were obtained from BBInternational. All other reagents were from Sigma-Aldrich.

Lentivirus short hairpin (sh)RNA constructs and cells transduction. A set of four murine Pag1 (SwissProt ID: Q3U1F9) shRNA constructs based on the pLKO.1 vector

(TRCN0000124814 [shRNA14], TRCN0000124815 [shRNA15], TRCN0000124816 [shRNA16], and TRCN0000124817 [shRNA17]) were obtained from Open Biosystems. Each of the Pag1 shRNA constructs (14 µg) was mixed with Opti-MEM (1 ml; Invitrogen), 21 µl of ViraPower Lentiviral Packaging Mix (Invitrogen), and 82 µl of Lipofectamine 2000 (Invitrogen). The mixture was homogenized by vortexing 10 s and then incubated at room temperature for 20 min before it was added to semi-confluent (70 %) HEK-293FT packaging cells growing in 20 ml of freshly added Dulbecco's medium supplemented with antibiotic and 10% FCS in 150 cm^2 tissue- culture flasks. Three days later, viruses in culture supernatant were concentrated by centrifugation at 25,000 rpm for 2 h using a JA-25.50 rotor (Beckman Coulter). The pellets were resuspended in 1 ml of culture medium and added to 29 ml of culture medium containing 5 x 10^7 BMMCs. After two days, medium was changed to virus-free medium and the cells were cultured for additional two days (recovery period). Stable selection was achieved by culturing transduced cells for one week in the presence of puromycin (5 µg/ml). Cells were pooled and analyzed for PAG expression by immunoblotting. Cells with the highest reduction of PAG, obtained with shRNA14 and shRNA15, were used for further experiments. Cells transfected with empty pLKO.1 vector were used as negative controls. For rescue experiments, mouse Pag1 cDNA (Ref. Seq. BC145761; 40131064, Open Biosystems) was amplified using forward primer 5´-AAAGAATTCGCCGCCACCAT**GGGCCCTGCAGGAAGCGT**-3´ (EcoRI restriction site underlined, coding sequence in bold) and reverse primer 5´-TTTGTCGAC**GAGCCTGGTGACATCTCTGC**-3´ (SalI restriction site underlined, coding sequence in bold). The amplified DNA was cloned via EcoRI and SalI restriction sites (upstream of Myc) into pFLAG-CMV™-5a expression vector (Sigma-Aldrich) modified to express Myc-tag (kindly provided by V. Korinek). The cassette encoding the Myc-tagged Pag1 sequence was then amplified with the same forward primer as above and reverse primer 5´-

186 TTTGCGGCCGCTTA**CAGGTCCTCCTCTGAGA**-3´ (NotI restriction site underlined, coding
187 sequence in bold) and recloned via EcoRI and NotI restriction sites into pCDH-CMV-MCS-EF1-
188 Puro expression lentivector (pCDH; System Biosciences, CD510B-1). The construct was verified
189 by DNA sequencing. Viruses with pCDH-Pag-myc or empty pCDH were produced as described
190 above. Medium with virus (30 ml) was filtered through 0.22 μm filter and divided into two
191 aliquots. The first aliquot was used to transduce the WT or PAG-KO BMMCs at day zero. The
192 second aliquot was preserved at 4°C and used for the second transduction of the same cells at day
193 3. Stable selection was achieved by culturing the cells for 7 days in the presence of puromycin (2
194 μg/ml), added 5 days after the first transduction.
195
196 **Flow cytometry.** To determine the surface expression of FcεRI, cells were exposed to FITC-
197 conjugated anti-FcεRI (1 μg/ml). The samples were evaluated by flow cytofluorometry using a
198 FACSCalibur instrument (BD Biosciences). For rescue experiments, cells were sensitized with
199 TNP-specific IgE during 20 h incubation in culture medium without IL-3 and SCF. Then they
200 were washed and activated by antigen [TNP-bovine serum albumin (BSA) conjugate; 15-25 mol
201 of TNP/mol of BSA; 100 ng/ml] for 90 min and fixed in 4% paraformaldehyde for 10 min at
202 37°C. The cells were washed once in phosphate-buffered saline (PBS) and free binding sites
203 were blocked with 5% normal donkey serum (Jackson ImmunoResearch Laboratories) in PBS.
204 After washing the cells were incubated for 45 min with anti-TNF antibody diluted 1:100 in PBS
205 with 0.5% BSA. After repeated washing the cells were incubated for 30 min with secondary
206 donkey anti-rabbit Alexa Fluor 488 antibody conjugate, washed and analyzed by flow cytometry
207 using LSRII (Becton Dickinson). For analysis of peritoneal mast cells, mice were sacrificed and
208 injected intraperitoneally with 5 ml of PBS supplemented with 1% FCS. The peritoneal cavity
209 was gently massaged for 30 s, and the injected PBS with free peritoneal fluid cells was

withdrawn. One ml of PBS with peritoneal cells was spun down (400 x g, 5 min), the cells were washed in cold PBS and stained for FcεRI (as above) or KIT using the anti-mouse KIT-APC conjugate.

Cell activation. Before experiments, BMMCs were cultured for 48 h in medium without SCF, followed by incubation for 12-16 h in SCF- and IL-3-free medium supplemented with IgE (1 µg/ml). Sensitized cells were washed in buffered salt solution (BSS; 20 mM HEPES, pH 7.4, 135 mM NaCl, 5 mM KCl, 1.8 mM $CaCl_2$, 5.6 mM glucose, 1 mM $MgCl_2$, and 0.1% BSA). To quantify degranulation, the cells (0.15×10^6) in 30 µl aliquots were transferred into wells of a 96-well plate and challenged with 30 µl of antigen (TNP-BSA conjugate), thapsigargin, or SCF at the concentrations indicated in Results. The degree of degranulation was determined as the amount of β-glucuronidase released into the supernatant as described (32). Briefly, 40 µl aliquots of the cell supernatants were mixed in white wells of a 96-well plate (Nunc) with 40 µl of β-glucuronidase substrate (40 µM 4-methylumbelliferyl β-D-glucuronide hydrate). After incubation for 60 min at 37ºC, the reaction was stopped by adding 200 µl of ice-cold 0.2 M glycine buffer, pH 10.0, and fluorescence was determined in a microtiter plate reader Infinite M200 (TECAN) with 355 nm excitation and 460 nm emission filters. Total cell content of the enzyme was evaluated in the supernatant from cells lysed in 1% Triton X-100.

Extracellular calcium uptake. Calcium uptake was determined by a modified previously described procedure (33). Briefly, IgE-sensitized BMMCs (2×10^6) were resuspended in 100 µl BSS-BSA with 1 mM Ca^{2+}, mixed with 100 µl of BSS-BSA supplemented with $^{45}Ca^{2+}$ and various concentrations of antigen or thapsigargin, and incubated for selected time intervals at 37°C. The reactions were terminated by placing the tubes on ice and then suspending 100 µl

234 aliquots on the walls of the microtest tubes to make them separated by air space from the 12%
235 BSA in PBS (300 µl) at the bottoms. Cells with bound $^{45}Ca^{2+}$ were separated from free $^{45}Ca^{2+}$ by
236 centrifugation through 12% BSA at 3220 x g for 15 min at 4°C. The cell pellets were recovered
237 by freezing the tubes, slicing off the tube bottom, and solubilization with 1 ml of 1% Triton X-
238 100. The radioactivity was counted in 10 ml scintillation liquid (EcoLite TM, ICN Biomedicals)
239 in a scintillation counter with QuantaSmart software (PerkinElmer).
240
241 **Immunoprecipitation and immunoblotting.** Cells were pelleted and solubilized in ice-cold
242 lysis buffer for immunoprecipitation (25 mM Tris-HCl, pH 8.0, 140 mM NaCl, 1 mM Na_3VO_4, 2
243 mM EDTA, 1 µg/ml aprotinin, 1 µg/ml leupeptin, 1 mM phenylmethylsulfonyl fluoride)
244 supplemented with 1% n-dodecyl β-D-maltoside and 1% Nonidet P-40 (for most experiments),
245 0.2% Triton X-100 (for FcεRI immunoprecipitation), or 1% Brij 96 (for kinase assays). After
246 incubation (30 min on ice) the lysates were spun down (16,000 x g for 5 min at 4°C) and
247 postnuclear supernatants were immunoprecipitated with the corresponding antibodies prebound
248 to UltraLink-immobilized protein A or G (Pierce, Thermo Scientific). The immunoprecipitates
249 were size-fractionated by sodium dodecyl sulfate-polyacrylamide gel electrophoresis (SDS-
250 PAGE) and immunoblotted with phosphotyrosine-specific PY-20-HRP conjugate or with
251 protein-specific antibodies followed by HRP-conjugated anti-mouse or anti-rabbit IgG antibody.
252 Some phosphorylated proteins were determined by direct immunoblotting with phospho-protein
253 specific antibodies, followed by corresponding secondary HRP-conjugated anti-mouse or anti-
254 rabbit IgG. The HRP signal was detected by chemiluminescence. Immunoblots were quantified
255 by luminescent image analyzer LAS-3000 (Fuji Photo Film Co., Tokyo, Japan) and further
256 analyzed by Aida image analyzer software (Raytest). The amount of phosphorylated proteins was
257 normalized to the amount of immunoprecipitated proteins after stripping off the membranes,

258 followed by development with the corresponding antibodies. In some experiments parallel
259 immunoblots were used instead of stripped membranes.
260
261 **Sucrose density gradient fractionation.** Sucrose density gradient separations were performed
262 as previously described (34) with some modifications. Briefly, BMMCs (30 x 10^6) were lysed
263 with 0.8 ml ice-cold lysis buffer (20 mM Tris-HCl, pH 8.0, 100 mM NaCl, 10 mM EDTA, 1 mM
264 Na_3VO_4, 10 mM glycerophosphate, 1 mM phenylmethylsulfonyl fluoride, 100 x diluted protease
265 inhibitor cocktail, 5 mM iodoacetamide) supplemented with 1% Brij 96. The lysates were
266 homogenized by passing ten times through a 27-gauge needle and adjusted to 40% (w/v) using
267 80% stock sucrose in 25 mM Tris-HCl pH 7.5, 125 mM NaCl, and 2 mM EDTA. The gradient
268 was prepared by adding 0.5 ml 80% sucrose at the bottom of the polyallomer tube (11 x 60 mm,
269 Beckman Instruments) followed by 1.5 ml of 40 % sucrose containing the cell lysate, 2 ml 30%,
270 and 1 ml 10% sucrose. The gradient was ultracentrifuged at 210,000 x g for 4 h at 4°C using an
271 SW55 Ti rotor (Beckman Instruments) and 0.5 ml fractions were collected from the top.
272
273 **Immunocomplex kinase assay.** The *in vitro* kinase assays were performed as previously
274 described (35) with some modifications. FcεRI, LYN and FYN were immunoprecipitated from
275 non-activated or antigen-activated cells lysed in lysis buffer for immunoprecipitation. Proteins
276 immobilized to antibody-armed protein A beads were washed with kinase buffer (25 mM
277 HEPES-NaOH, pH 7.2, 3 mM $MnCl_2$, 0.1% Nonidet P-40, 100 mM Na_3VO_4, 20 mM $MgCl_2$)
278 and then resuspended in 25 µl kinase buffer supplemented with 2.5 µCi (92.5 kBq) of [γ-
279 ^{32}P]ATP, 100 µM ATP and 0.5 µg/µl of acid-denatured enolase as exogenous substrate. After
280 incubation for 30 min at 37°C, the immunoprecipitates were eluted from the beads with reducing
281 2x concentrated SDS-PAGE sample buffer and boiled for 7 min. The ^{32}P-labeled proteins were

size-fractionated by SDS-PAGE, transferred to nitrocellulose membrane, and visualized by autoradiography. Films were quantified with Aida image analyzer software.

Cytokine and chemokine detection. IgE-sensitized BMMCs were activated with different concentrations of antigen. One hour later, mRNA was extracted using the TurboCapture 96 mRNA kit (Qiagen). Single-stranded cDNA was synthesized with M-MLV reverse transcriptase (Invitrogen) according to the manufacturer's instructions. Real-time PCR amplifications of cDNAs were performed in 10 µl reaction volumes of qPCR mix containing 1 M 1,2-propanediol, 0.2 M trehalose and SYBR green 1 (36) in 384-well plates sealed with LightCycler 480 sealing foil (Roche Diagnostics) and analyzed in LightCycler 480 (Roche Diagnostics). The following primer sets were used for amplification of different cDNA fragments (with sizes of the amplified fragments in bps in square brackets; sense/antisense): actin, 5´-GATCTGGCACCACACCTTCT-3'/5´GGGGTGTTGAAGGTCTCAAA-3' [138]; glyceraldehyde 3-phosphate dehydrogenase (GAPDH), 5´-AACTTTGGCATTGTGGAAGG-3'/5´-ATCCACAGTCTTCTGGGTGG-3' [69]; ubiquitin, 5´-ATGTGAAGGCCAAGATCCAG-3'/ 5´TAATAGCCACCCCTCAGACG/3' [160]; TNF-α, 5´-CCCTCACACTCAGATCATCTTCT-3'/5´-GCTACGACGTGGGCTACAG-3' [61]; IL-6, 5´-GAGGATACCACTCCCAACAGACC-3'/5´-AAGTGCATCATCGTTGTTCATACA-3' [141]; IL-13, 5´-AGACCAGACTCCCCTGTGCA-3'/5´-TGGGTCCTGTAGATGGCATTG-3' [123]; CCL3, 5´-CATCGTTGACTATTTTGAAACCAG-3'/5´-GCCGGTTTCTCTTAGTCAGGAA-3' [72]; CCL4, 5´-CTTGGAGTTGAACTGAGCAGC-3'/5-AGAGGGGCAGGAAATCTGAA-3' [126]. The following cycling conditions were used: 3 min at 95°C, followed by 50 cycles of 10 s at 95°C, 20 s at 60°C, and 20 s at 72°C. Threshold cycle (Ct) values were determined by automated threshold analysis of the cycler. Specificity of the PCR was evaluated by examining

306 melting curves. Actin, GAPDH, and ubiquitin were used as reference genes and the expression
307 levels of all mRNAs were normalized to the geometrical mean of these genes. The relative
308 increase in the expression level of a cytokine was normalized to the one of non-activated WT
309 cells in each experiment.

310 For detection of cytokines, the immuno-PCR method was used as described (37). Briefly,
311 anti-TNF-α (1 μg/ml), anti-IL-6 (2 μg/ml), or anti-IL-13 (1 μg/ml) in 100 mM borate buffer (pH
312 9.5) were dispensed in 50 μl aliquots into wells of a real-time 96-well plate (Eppendorf). After
313 overnight incubation at 4°C, each well was washed four times with 200 μl of Tris-buffered saline
314 (10 mM Tris-HCl, pH 7.4, 150 mM NaCl) containing 0.05% Tween 20 (TBST) and the
315 remaining binding sites were blocked by 2 h incubation at 37°C with TBST supplemented with
316 2% BSA. After washing, 50 μl of serial dilutions (0.1-100 ng/ml) of recombinant TNF-α, IL-6,
317 or IL-13 (all from PeproTech) or the tested samples diluted in PBS-1% BSA were added. The
318 samples were incubated for 1 h at 37°C and after washing with TBST, 50 μl of Au-NPs armed
319 with thiolated DNA oligonucleotide template [5′-(5ThioMC6-
320 D//iSp18)CCTTGAACCTGTGCCATTTGAATATATTAAGACTATACGCGGGAACA-3′] and
321 with the corresponding cytokine-specific antibody were applied into each well. The wells were
322 incubated for 1 h at 37°C and washed with TBST and deionized water. Fifty μl aliquots of qPCR
323 master mix solution (see above) supplemented with 60 nM oligonucleotide primers, 5′-
324 CCTTGAACCTGTGCCATTTG-3′ and 5′-
325 GTCCCTCCATCTTCCTACTGTTCCACATGTTCCCGCGTATAGTCTT-3′ were then
326 dispensed into each well. Plates were sealed and the amount of template DNA bound to antigen-
327 anchored functionalized Au-NPs was evaluated by real-time PCR using Realplex4 Mastercycler
328 (Eppendorf) with the following cycling conditions: 2 min at 94°C, followed by 40 cycles of 20 s

329 at 94°C, 20 s at 53°C, and 20 s at 72°C. For the calculation of TNF-α, IL-6, and IL-13
330 concentrations, the corresponding Ct values were substituted into the regression equations
331 obtained from the calibration curves constructed from the concentration series of appropriate
332 recombinant proteins.
333
334 **Chemotaxis assay.** Chemotaxis responses were assayed in 24-well Transwell chambers
335 (Corning) with 8 μm polycarbonate filters in upper wells. Chemoattractants (antigen or SCF) in
336 0.6 ml chemotaxis medium (RPMI-1640 supplemented with 1% BSA and 20 mM HEPES, pH
337 7.4) were added to the lower wells. IgE-sensitized BMMCs (0.3×10^6 in 120 μl chemotactic
338 media) were added to the upper wells. Cells migrating into lower wells during the 8 h incubation
339 (37°C, 5% CO_2) were counted using the Accuri C6 Flow Cytometer (BD Biosciences).
340
341 **Confocal microscopy.** BMMCs (3×10^5) were attached to fibronectin-coated multitest slides
342 (MP Biomedicals). Cells were fixed with 4% paraformaldehyde for 15 min at room temperature
343 and permeabilized in 0.3% Triton X-100 for 20 min. Free binding sites were blocked with 5%
344 normal donkey serum and the cells were stained with rabbit anti-Myc-Tag antibody followed by
345 labeling with secondary antibody (donkey anti-rabbit IgG-Alexa Fluor 488 conjugate). After 60
346 min, the cells were washed and mounted in Mowiol 4-88 supplemented with Hoechst 33258
347 nucleic acid stain (1 μg/ml, Molecular Probes) to label nuclei. Samples were examined with a
348 confocal laser scanning microscope Leica TCS SP5 equipped with an X63/1.4.N.A. oil-
349 immersion objective.
350
351 **Passive systemic anaphylaxis.** The systemic anaphylactic reaction is accompanied by the
352 release of histamine from activated mast cells leading to decreased body temperature (38). The

353 body temperature was measured with an accuracy of ± 0.1°C using the VitalView data
354 acquisition system with ER-4000 energizer receivers, G2 E-mitter transponders, and VitalView
355 software (Mini Mitter). G2 probes were implanted intra-abdominally under systemic anesthesia
356 with isoflurane (Abbott Laboratories). Monitoring of body temperature was initiated nine days
357 after the surgery. Mice aged 11-18 weeks were sensitized by tail vein injection of TNP-specific
358 IgE (3 µg in 100 µl PBS per mouse) and 24 h later anaphylaxis was induced by intravenous
359 administration of antigen (500 µg in 100 µl PBS per mouse). Body temperature was recorded at
360 1 min intervals for at least 3 h after antigen challenge.
361

362 **Serum IgE quantification.** ELISA 96-well plates (Nunc) were coated for 16 h at 4°C with rat
363 antibody specific for mouse IgE (BD Biosciences; 1 µg/ml in PBS; 50 µl/well). Wells were
364 washed (four times with TBST) and blocked by incubation at 22°C with TBST-2% BSA. After 2
365 h, the plates were washed and incubated for 1 h at 22°C with various concentrations of mouse
366 IgE standard (BD Biosciences; 1.95 - 125 ng/ml in PBS-1% BSA) or mouse serum samples
367 (diluted 1:5 in PBS-1% BSA). Then, the wells were washed and the captured IgE was detected
368 with biotinylated rat anti-mouse IgE antibody (BD Bioscience; 2 µg/ml in PBS-1% BSA),
369 washed and incubated for 30-min incubation with streptavidin-HRP conjugate (BD Biosciences;
370 diluted 1:1000 in PBS-1% BSA). Peroxidase substrate solution (0.5 mg/ml o-phenylenediamine
371 and 0.015% H_2O_2 in 0.1 M NaH_2PO_4, pH 6.0) was used for colorimetric reaction. The reaction
372 was stopped by adding 50 µl of 4M H_2SO_4 and absorbance was determined at 492 nm using
373 Infinite M200 plate reader (TECAN).
374

375 **Statistical analysis.** The significance of intergroup differences was evaluated by Student's t-test;

376 *, $P<0.05$; **, $P<0.01$, ***, $P<0.001$

377

RESULTS

Positive regulatory role of PAG on antigen-induced degranulation. To examine the role of PAG in mast cell signaling, we isolated bone marrow cells from homozygous F1 descendant PAG-KO and PAG-WT mice and cultured them in the presence of IL-3 and SCF to obtain BMMCs. Cells with or without PAG exhibited comparable growth parameters under *in vitro* conditions (not shown), suggesting that PAG had no effect on the growth response of mast cells to IL-3 and SCF. The same PAG-WT BMMCs were used for production of PAG-KDs after transduction with lentiviral vectors containing PAG shRNA constructs based on a pLKO vector (shRNA14 - 17), followed by selection in puromycin. PAG-WT BMMCs infected with empty lentiviral vector were used as a negative control (pLKO). PAG-KO and PAG-WT cells expressed comparable amounts of surface FcεRI as detected by flow cytometry (Fig. 1 A). Similarly, no difference in surface FcεRI was observed among various PAG-KDs and controls (not shown). As expected, we found no detectable PAG in PAG-KO cells using immunoblotting with PAG-specific antibody (Fig. 1 B). The amount of PAG in PAG-KD cells was substantially reduced when compared to control (pLKO) cells. The strongest inhibition was observed in the cells infected with shRNA14 and 15 constructs, which reduced PAG expression by 73 % and 75 %, respectively (Fig. 1 C). Infection with constructs containing shRNA16 and 17 reduced PAG expression by 25 % and 51 %, respectively. Guided by these data, we used viruses containing shRNA14 and 15 for further experiments with BMMCs. Because of the similar knockdown characteristics of these constructs, data from BMMCs infected with these shRNAs were combined and are presented under the common heading of PAG-KDs.

Using BMMCs with PAG-KO, PAG-KD, and corresponding controls, we first investigated whether PAG deficiency has any effect on mast cell degranulation after FcεRI triggering. Degranulation was estimated by the amount of β-glucuronidase released from

activated cells. BMMCs were sensitized with TNP-specific IgE and then exposed to various concentrations of antigen. After 30 min, PAG-KO cells exhibited significantly lower degranulation compared to WT cells at all concentrations of the antigen tested (0.05 – 1.0 μg/ml; Fig. 1 D); the total amount of β-glucuronidase released from both cell types by Triton X-100 was similar (data not shown). These data indicated that the absence of PAG reduces antigen-induced degranulation but does not interfere with production of β-glucuronidase present in secretory vesicles. Significant inhibition of degranulation was also observed in PAG-KO cells activated with various concentrations of thapsigargin (0.1 – 2.0 μM; Fig. 1 E). Thapsigargin induces the release of Ca^{2+} from intracellular stores by inhibiting the endoplasmic reticulum (ER) ATPase (39). The combined data suggested that PAG is involved not only in CSK-mediated FcεRI-proximal regulation of SFKs but could still have other functions distal to FcεRI.

To test whether compensatory developmental alterations could be responsible for the unexpected properties of PAG-KO BMMCs, we examined antigen- and thapsigargin-induced degranulation in cells with PAG-KD and the corresponding controls. Data shown in Fig. 1 F and G demonstrate that stimulation of PAG-KD cells with antigen or thapsigargin decreased degranulation when compared to pLKO controls, supporting previous findings that PAG is a positive regulator of mast cell degranulation.

Positive regulatory role of PAG on Ca^{2+} response. Early events in mast cell signaling involve the release of Ca^{2+} from intracellular stores followed by influx of extracellular Ca^{2+} through store-operated Ca^{2+} (SOC) channels in the plasma membrane (40). To determine whether PAG has a role in this process, we quantified Ca^{2+} uptake in PAG-deficient and control BMMCs. Data presented in Fig. 2 A show that stimulation with antigen causes significantly lower uptake of extracellular $^{45}Ca^{2+}$ in PAG-KO cells than in PAG-WT cells, reaching a peak at approximately 5

426 min after triggering in both cell types. Inhibition of Ca^{2+} uptake in PAG-KO cells 5 min after
427 triggering was observed at all concentrations of the antigen tested (Fig. 2 B). Significant
428 inhibition of Ca^{2+} uptake in PAG-KO cells was also seen after stimulation for various time
429 intervals (Fig. 2 C) or with various concentrations of thapsigargin (Fig. 2 D). A positive
430 regulatory role of PAG in calcium uptake after antigen (Fig. 2 E) or thapsigargin (Fig. 2 F)
431 activation was also evident when PAG-KD cells were compared to the corresponding PAG-
432 expressing controls (pLKO). These data imply that the observed inhibition of degranulation in
433 PAG-deficient cells could be at least in part attributable to decreased calcium mobilization.
434
435 **Localization of CSK in lipid rafts depends on PAG.** Previous studies localized PAG almost
436 exclusively to lipid rafts, where it could interact with CSK, and through this interaction
437 negatively regulate lipid raft-associated SFKs (15). This conclusion was based on data evaluating
438 the distribution of PAG in fractions after sucrose density gradient ultracentrifugation of lysates
439 from cells disintegrated in nonionic detergents (11, 12) or 0.5 M $NaHCO_3$ (21). However, there
440 are inconsistencies regarding the role of PAG in the localization of CSK in lipid rafts. One study
441 found lipid raft-associated CSK in thymocytes greatly reduced in the absence of PAG (18),
442 whereas another concluded that PAG is dispensable for localization of CSK in lipid rafts (17). To
443 determine whether PAG contributes to the localization of CSK in lipid rafts in BMMCs, non-
444 activated or antigen-activated PAG-WT and PAG-KO BMMCs were solubilized in a buffer
445 supplemented with 1% Brij 96, fractionated by sucrose density gradient ultracentrifugation, and
446 their presence in individual fractions was analyzed by immunoblotting. Distribution of LYN
447 kinase, a well-known lipid raft marker in BMMCs, was also examined. In accordance with
448 previous data (41), most of the LYN (88%) in non-activated cells was associated with detergent-
449 resistant membranes (DRM; Fr. 1 – 3). Five minutes after activation with antigen, this amount

450 was reduced approximately by half (Fig. 3 A). In the same gradient fractions, less PAG was
451 found in DRMs (55%) and no significant changes were observed after stimulation with antigen.
452 Only a small fraction of CSK was found in DRM fractions (4 %) and no significant changes were
453 observed after activation with antigen. When lysates from PAG-KO BMMCs were analyzed, no
454 CSK was found in DRM fractions from activated and non-activated cells even after longer
455 exposure (Fig. 3 B), suggesting that PAG is involved in localization of CSK in DRMs.
456
457 **PAG and tyrosine phosphorylation of signal transduction proteins**. The first biochemically
458 defined step after FcεRI triggering is tyrosine phosphorylation of the FcεRI subunits by SFK
459 LYN, followed by engagement of other kinases and phosphorylation of a number of signal
460 transduction proteins. To specify the role of PAG in these processes we examined tyrosine
461 phosphorylation of FcεRI and several selected proteins involved in early stages of antigen-
462 induced mast cell signaling (SYK, LAT, ERK) (42), as well as proteins involved in cell
463 movement (FAK and paxillin) (43). In initial experiments we looked for proteins phosphorylated
464 on tyrosine in total cellular lysates. We found that PAG-WT cells differ from PAG-KO cells in
465 several tyrosine phosphorylated proteins not only after antigen stimulation, but also in non-
466 activated state (Fig. 4 A). Further analysis showed that FcεRI triggering caused an increase in
467 tyrosine phosphorylation of FcεRI β and γ chains in WT cells and that this process was
468 significantly reduced in PAG-KO cells (Fig. 4 B). Tyrosine phosphorylation of SYK (Fig. 4 C)
469 and its substrates LAT (Fig. 4 D) and ERK (Fig. 4 E) were also impaired in PAG-deficient cells.
470 In contrast, FAK (Fig. 4 F) and focal adhesion-associated adaptor protein paxillin (Fig. 4 G)
471 showed elevated basal levels of tyrosine phosphorylation in PAG-KO cells; this difference was
472 maintained after FcεRI triggering (Fig. 4, F and G).

The observed decrease in tyrosine phosphorylation of FcεRI β and γ subunits in antigen-activated PAG-KO cells suggested an imbalance between PTKs and PTPs in the vicinity of the receptor. To examine FcεRI-associated PTK activity towards its endogenous substrate, FcεRI was immunoprecipitated from non-activated and antigen-activated PAG-WT and PAG-KO cells and the immunocomplexes were analyzed by *in vitro* kinase assays with [γ-^{32}P]ATP. Using PAG-WT cells, we observed a significant increase in radioactivity bound to FcεRI β and γ receptor subunits after activation with antigen (Fig. 5, A and B). Surprisingly, when the receptor was precipitated from PAG-KO cells, strong phosphorylation of the receptor β and γ subunits was observed in non-activated cells and was decreased after FcεRI triggering. These data, together with the results of immunoblotting experiments showing weak and comparable tyrosine phosphorylation of β and γ subunits of FcεRI isolated from non-activated PAG-WT and PAG-KO cells, suggested that the activity of PTKs bound to FcεRI isolated from PAG-KO cells are enhanced.

To determine enzymatic activities of total LYN and FYN, the kinases were immunoprecipitated and their activities were assessed by *in vitro* kinase assay. To overcome the problem with possible variation in the extent of non-phosphorylated residues in the target proteins, we used acid-denatured enolase as exogenous substrate in immunocomplex kinase assays. Data in Fig. 5, C - F show low but significantly higher autophosphorylation of LYN and FYN kinases immunoprecipitated from PAG-KO cells than from PAG-WT cells. Importantly, enolase phosphorylation was also enhanced in LYN and FYN immunoprecipitates obtained from PAG-KO cells. In contrast to previous studies (3, 19), we did not observe any increase in activity of the kinases after FcεRI triggering, which is probably due to different culture condition used (44).

LYN is a positive regulator of PTPs (45, 46), which could be responsible for decreased tyrosine phosphorylation of several substrates as shown in Fig. 4, A - E. One of the phosphatases involved in the regulation of mast cell degranulation and calcium responses is SHIP1. LYN kinase phosphorylates SHIP1 and thus enhances its enzymatic activity and down-regulates degranulation (46, 47). In further experiments we therefore examined tyrosine phosphorylation of SHIP1 in BMMCs from PAG-WT and PAG-KO mice. In non-activated WT cells, SHIP1 showed baseline phosphorylation which was enhanced after FcεRI triggering (Fig. 5, G and H). When compared to PAG-WT cells, non-activated PAG-KO cells exhibited significantly higher SHIP1 tyrosine phosphorylation. After activation with antigen, the difference between PAG-WT and PAG-KO cells became insignificant.

Different regulatory roles of PAG in SCF signaling. An important surface receptor of mast cells is KIT, which binds SCF and thereby triggers mast cell activation and enhances activation induced by FcεRI (48). However, no data are available on the involvement of PAG in SCF-induced activation. To determine a possible role of PAG in KIT-mediated activation, PAG-WT and PAG-KO BMMCs were activated with different concentrations of SCF and degranulation was examined. PAG-WT cells released increasing amounts of β-glucuronidase when activated with 25 - 200 ng/ml SCF. The extent of SCF-induced degranulation was higher than that described in previous studies (49, 50) and was apparently related to the growth of bone marrow cells in the presence of both IL-3 and SCF. When BMMCs were derived from cultures containing IL-3 alone, their SCF-induced degranulation was low (44). PAG-KO cells released significantly more β-glucuronidase than PAG-WT cells at all concentrations of SCF tested (Fig. 6 A). This effect was associated with higher KIT tyrosine phosphorylation in PAG-KO cells (Fig. 6, B and C). However, an opposite effect of PAG on FcεRI- and KIT-mediated signaling

520 events was absent when tyrosine phosphorylation of PLCγ1 was examined. Stimulation of PAG-
521 WT cells with antigen as well as with SCF resulted in tyrosine phosphorylation of PLCγ1, even
522 though it was slower in SCF-activated cells. Similar findings have been previously described
523 (49) and indicate that FcεRI-activated PTKs are more potent to phosphorylate PLCγ1 than KIT.
524 In PAG-KO cells the extent of PLCγ1 tyrosine phosphorylation was significantly inhibited in
525 both antigen- and SCF-triggered cells (Fig. 6, D and E). A similar effect was observed when
526 PLCγ2 was examined (data not shown). No significant effect of PAG was observed when
527 tyrosine phosphorylation of several other signaling molecules (SYK, LAT, FAK, paxillin) was
528 examined in PAG-WT and PAG-KO cells. Furthermore, no effect of PAG on calcium response
529 was observed in SCF-activated BMMCs (not shown).
530 An important aspect of mast cell physiology is chemotaxis directed by various ligands
531 (51). Here we compared chemotaxis towards antigen or SCF in cells differing in PAG
532 expression. In transwell migration assays, PAG-WT BMMCs exhibited faster migration towards
533 the antigen than PAG-KO cells. The difference was almost two-fold and was significant (Fig. 6
534 F). When SCF was used as a chemoattractant, both cell types migrated faster and no significant
535 difference between them was evident. To exclude possible compensatory developmental
536 alterations in PAG-KO cells, we also compared chemotaxis of BMMCs with PAG-KD and their
537 corresponding controls (pLKO). We found significantly lower migration of PAG-KD cells after
538 exposure to antigen when compared to pLKO cells. Again, no significant difference between the
539 two cell types was observed when SCF was used as a chemoattractant (Fig. 6 G).
540
541 **Positive regulatory role of PAG in cytokine and chemokine production**. Previous studies
542 showed that activation of mast cells resulted in rapid tyrosine phosphorylation of several
543 transcription factors. We selected STAT5 as the transcription factor, which has been extensively

544 studied in FcεRI- or KIT-activated cells (52, 53). To elucidate the role of PAG in this process,
545 we examined tyrosine phosphorylation of STAT5 in non-activated and antigen- or SCF-activated
546 PAG-WT and PAG-KO cells (Fig. 7, A and B). Antigen-induced tyrosine phosphorylation of
547 STAT5 was positively regulated by PAG. Significantly lower phosphorylation of STAT5 in
548 PAG-KO cells was observable even without activation, but activation intensified the difference.
549 Phosphorylation of STAT5 was also observed in cells stimulated with SCF (Fig. 7, A and B).
550 However, no significant difference between PAG-WT and PAG-KO cells was observed.
551 Decreased phosphorylation of STAT5 in antigen-stimulated PAG-KO cells suggested
552 reduced production of cytokines and chemokines in such cells (54). Detailed analysis at protein
553 and mRNA levels showed that indeed three selected cytokines, TNF-α, IL-6, and IL-13, were
554 significantly reduced in antigen-stimulated PAG-KO cells than in PAG-WT cells at both the
555 protein and mRNA level (Fig. 7 C). Antigen-activated PAG-KO BMMCs also exhibited
556 significant inhibition of transcription of two chemokines, CCL3 and CCL4 (Fig. 7 D).
557
558 **Phenotype rescue of PAG-KO cells**. Next, we attempted to confirm the role of PAG as a
559 positive regulator of cytokine production. We prepared a PAG-myc construct in the pCDH
560 vector and transfected it into PAG-KO BMMCs. Control cells were transfected with empty
561 pCDH vector and puromycin-resistant cells were further analyzed. Staining for myc after cell
562 permeabilization and confocal microscopy showed association of the PAG-myc with the plasma
563 membrane (Fig. 8 A). No signal was observed in cells transduced with empty pCDH (Fig. 8 B).
564 Furthermore, immunoblotting analysis with Myc-Tag-specific antibody confirmed expression of
565 PAG-myc in cells transduced with pCDH-PAG-myc vector but not pCDH empty vector (Fig. 8
566 C). These data suggested that PAG-myc was expressed as expected. Next, we examined the
567 production of TNF-α in antigen-activated PAG-WT and PAG-KO cells transfected with empty

568 pCDH, and PAG-KO cells transfected with pCDH-PAG-myc. For this analysis we selected flow
569 cytometry, which allowed us to evaluate TNF-α positive cells, after gating-out cellular debris
570 detected in forward and side scatter plot. This eliminated the problem with different proportions
571 of living cells and debris in various transduction experiments. Data presented in Fig. 8 D indicate
572 that production of TNF-α in cells transfected with empty pCDH vector was significantly lower in
573 PAG-KO than in PAG-WT cells. PAG-KO cells transfected with pCDH-PAG-myc produced
574 significantly more TNF-α than pCDH transfectants. These data confirm the phenotype rescue in
575 PAG-KO cells.
576
577 **Impaired passive systemic anaphylaxis in PAG-KO mice**. Finally, we examined degranulation
578 in antigen-activated mast cells under *in vivo* conditions. We induced passive systemic
579 anaphylaxis in PAG-KO and PAG-WT mice by sensitizing them with TNP-specific IgE mAb
580 and subsequent challenge with antigen. In control mice, the decrease in body temperature was
581 observable within the first 60 min and was followed by slow recovery for more than 180 min
582 after antigen injection (Fig. 9 A). In PAG-KO mice, the decrease in body temperature was less
583 pronounced and recovery was faster, being complete 150 min after antigen administration. The
584 difference in body temperature between PAG-WT and PAG-KO mice was significant in the
585 interval ranging from 45 to 170 min after antigen administration. The observed decrease in
586 systemic anaphylaxis was not likely attributable to decreased numbers of mast cells in PAG-KO
587 mice, as inferred from comparable mast cell (KIT- and FcεRI-positive) counts in peritoneal
588 lavage of PAG-WT and PAG-KO cells (Fig. 9 B). Furthermore, we found no significant
589 difference in serum IgE levels between PAG-WT and PAG KO mice (Fig. 9 C). This finding
590 indicates that production of IgE is not affected by the absence of PAG and that the decreased

591 anaphylactic response in PAG-KO mice is not caused by enhanced production of IgE, which

592 might preclude sensitization with antigen-specific IgE.

593 **DISCUSSION**

594 In this study, we used BMMCs derived from PAG-KO and PAG-WT mice to understand the role
595 of PAG in FcεRI and SCF signaling. To minimize the possible effect of compensatory
596 developmental alterations in PAG-KO cells, we also used BMMCs with PAG-KD and
597 corresponding controls. Several lines of evidence indicate that PAG has positive as well as
598 negative regulatory roles in FcεRI- or KIT-mediated signaling depending on the receptor
599 triggered and the signaling pathway involved.

600 First, when stimulated with antigen, mast cells derived from PAG-KO mice exhibited
601 decreased degranulation. In view of previous results obtained with other immunoreceptors (17,
602 18, 26), this was an unexpected finding because phosphorylated PAG was regarded as a plasma
603 membrane anchor of CSK, a negative regulator of SFKs. Furthermore, overexpression of PAG
604 reportedly resulted in decreased degranulation in RBL-2H3 cells (21). The positive regulatory
605 role of PAG in FcεRI-mediated signaling described here was not the consequence of
606 developmental changes caused by the absence of PAG, since a similar phenotype was also
607 observed in PAG-KD BMMCs where PAG expression was down-regulated by RNA
608 interference. Neither was the decreased degranulation caused by reduced production of β-
609 glucuronidase or reduced expression of FcεRI in PAG-KO and PAG-KD cells. Interestingly, a
610 defect in degranulation was also observed in PAG-deficient cells activated by thapsigargin, a
611 non-competitive inhibitor of ER Ca^{2+} ATPase.

612 Second, antigen-activated PAG-KO cells exhibited decreased tyrosine phosphorylation of
613 FcεRI β and γ subunits. This change implies that the reduced degranulation in PAG-deficient
614 cells is caused at least in part by inhibition of the earliest stages of mast cell signaling, starting
615 from reduced phosphorylation of the FcεRI β and γ subunits, followed by impaired membrane
616 anchoring, phosphorylation and activation of SYK. The exact molecular mechanism of the

617 impaired phosphorylation of FcεRI in PAG-deficient cells is unknown and is likely connected
618 with local changes in the activity and/or topography of SFKs and PTPs within the FcεRI
619 signalosome. Our finding that FcεRI immunocomplexes isolated from nonionic detergent-
620 solubilized non-activated PAG-KO cells show kinase activity higher than those from PAG-WT
621 cells would be compatible with this hypothesis, provided that PTKs are more stably associated
622 with isolated FcεRI immunocomplexes than PTPs. Furthermore, we found that tyrosine
623 phosphorylation of SHIP1, a negative regulator of mast cell activation (47, 55), is increased in
624 non-activated PAG-KO cells. This could be caused by enhanced enzymatic activity of LYN,
625 which phosphorylates and activates SHIP1 (46), and in this manner could contribute to decreased
626 calcium and degranulation responses (47, 55).
627 In contrast to FcεRI and several other signaling proteins involved in calcium response
628 (SYK, LAT, PLCγ), the FAK and at least one of its substrates, the multi-domain scaffolding
629 adaptor protein paxillin, showed enhanced tyrosine phosphorylation in PAG-KO cells. The
630 molecular mechanism of enhanced phosphorylation of FAK and paxillin in PAG-KO cells
631 remains to be determined but apparently reflects changes in the activity of SFKs and PTPs which
632 use FAK and paxillin as a substrate (56, 57).
633 Third, PAG-deficient BMMCs showed reduced calcium uptake after activation with
634 antigen. This could be attributed to reduced tyrosine phosphorylation and activity of PLCγ,
635 which cleaves the plasma membrane-bound phosphatidylinositol 4,5-bisphosphate into diacyl-
636 glycerol and inositol 1,4,5-trisphosphate; the latter binds to its receptors and regulates release of
637 calcium from intracellular organelles. Increases in cytoplasmic calcium lead to the influx of
638 extracellular calcium into the cytoplasm through SOC channels. Reduced calcium uptake in
639 PAG-KO cells was observed not only after exposure to antigen, but also after activation with
640 thapsigargin, a non-competitive inhibitor of ER Ca^{2+} ATPase. This could be related to previous

findings documenting that PLCγ is involved in thapsigargin-induced Ca^{2+} entry (58-60) and reduced phosphorylation of PLCγ in PAG-deficient cells. Furthermore, it has been shown that STIM1, which is indispensable for opening SOC channels in mast cells (61, 62), needs for its function expression and phosphorylation of SYK and LYN kinases (63). Enhanced tyrosine phosphorylation of SHIP1 and presumably its increased enzymatic activity (44, 45) could also contribute to decreased calcium mobilization in activated PAG-KO cells.

Fourth, PAG-KO cells exhibited higher degranulation when activated by SCF. SCF binds to KIT, a type III plasma membrane receptor tyrosine kinase. After SCF binding, the receptor forms a dimer that stimulates its intrinsic tyrosine kinase activity, creating phosphotyrosine binding sites for FYN (64) and LYN (65) kinases, and many other signaling molecules, including SHIP1 and PLCγ (66). These molecules are apparently integrated into signaling circuits regulated by PAG.

Fifth, it has been previously shown that activation through FcεRI as well as KIT rapidly stimulates STAT5 tyrosine phosphorylation and that STAT5 deficiency greatly reduces early and late mast cell responses (67). PAG-KO cells exhibited lower tyrosine phosphorylation of STAT5 when activated via FcεRI but not via KIT. This difference could be explained by different kinases involved in STAT5 phosphorylation. In SCF-activated cells, KIT activates STAT5 partly through the tyrosine kinase JAK2 (68). In contrast, JAK2 is dispensable in IgE-activated cells, which use FYN for STAT5 phosphorylation (52). Phosphorylated STAT5 serves as a transcription factor for a number of inflammatory genes (54). Reduced transcription of genes for cytokines (TNF-α, IL-6, and IL-13) and chemokines (CCL3 and CCL4) and reduced production of TNF-α, IL-6, and IL-13 in antigen-activated PAG-KO cells could be a direct consequence of impaired STAT5 tyrosine phosphorylation.

664 Sixth, IgE-sensitized PAG-KO cells exhibited decreased chemotaxis towards antigen.
665 Mast cell chemotaxis is a complex process dependent on numerous signaling molecules and cell
666 signaling pathways (51). The observed inhibition of tyrosine phosphorylation of the FcεRI β and
667 γ subunits, SYK, and LAT in antigen-activated PAG-deficient cells could partly explain the
668 reduced antigen-induced chemotaxis (69). In contrast, PAG-KO BMMCs showed no inhibition
669 of KIT and LAT tyrosine phosphorylation after SCF triggering and this could be related to
670 normal chemotaxis response towards SCF in these cells. These findings indicate that either PAG
671 is not involved in the regulation of KIT-mediated chemotaxis or the positive regulatory roles of
672 PAG are compensated by activation of other molecules, such as PTPs, which also bind to KIT
673 (70, 71).
674 Seventh, experiments *in vivo* showed that PAG is a positive regulator of passive systemic
675 anaphylaxis, manifested by decreased body temperature after administration of antigen into IgE-
676 sensitized mice. It is widely accepted that the anaphylactic reaction is initiated by inflammatory
677 mediators released from mast cells (72, 73). Experiments with mice deficient in histidine
678 decarboxylase, and therefore lacking histamine, suggested that histamine released from mast
679 cells controls body temperature (38). Our finding of impaired degranulation in PAG-KO cells
680 could thus be directly related to the impaired anaphylactic response. A positive regulatory role of
681 PAG in passive systemic anaphylaxis is the first well-defined *in vivo* trait that is regulated by
682 PAG.
683 Although previous data using other cell types have implicated phosphorylation of PAG
684 and PAG-CSK interactions as an important regulatory step in immunoreceptor signaling (11, 12),
685 no dramatic changes in tyrosine phosphorylation of PAG were observed in the course of FcεRI-
686 mediated activation of BMMCs [(19) and our unpublished data]. Furthermore, only a small
687 fraction of CSK co-localized with PAG in lipid raft fractions in PAG-WT BMMCs. In PAG-KO

688 cells, CSK was not detected in lipid raft fractions, suggesting that in mast cells PAG could be a
689 major anchor of CSK in lipid rafts. These data corroborate the results of a previous study
690 documenting that PAG in lipid rafts from mouse thymocytes is a major anchor of CSK (18). On
691 the other hand, they stand in contrast to another study (17) showing that the amount of lipid raft-
692 associated CSK in thymus cells is not affected by the absence of PAG. However, we would like
693 to point out that different detergents and cell/detergent ratios were used in these various studies
694 and that association of proteins with lipid rafts is sensitive to these parameters (74, 75).
695 In summary, the data reported in this study provide compelling evidence that PAG
696 functions both as a positive and negative regulator of mast cell signaling, depending on the
697 signaling pathway involved. It seems that through interaction with CSK, PAG serves as a
698 negative regulator of SFKs, which are involved in both positive and negative regulatory loops in
699 mast cell activation. Furthermore, we show for the first time that PAG-deficient mice exhibit a
700 distinct phenotype in terms of passive systemic anaphylaxis response.
701
702 **ACKNOWLEDGMENTS**
703 We thank H. Mrazova, L. Kocanda and R. Budovicova for technical assistance.
704 This work was supported by projects 301/09/1826, P302/10/1759, P302-14-09807S,
705 P302/12/G101, P305-14-00703S, and 204/09/H084 from the Czech Science Foundation; Action
706 BM1007 from European Cooperation in Science and Technology; project LD12073 COST-CZ-
707 MAST from the Ministry of Education Youth and Sports of the Czech Republic, and by the
708 Institute of Molecular Genetics of the Acad. Sci. Czech Republic (RVO 68378050). L. P., M. B.
709 and I. P. were supported in part by the Faculty of Science, Charles University, Prague. The
710 authors have no conflicting financial interests.
711

712 **REFERENCES**

713

714

715 1. **Galli SJ, Borregaard N, Wynn TA**. 2011. Phenotypic and functional plasticity of cells
716 of innate immunity: macrophages, mast cells and neutrophils. Nat. Immunol. **12**:1035-
717 1044.

718 2. **Eiseman E, Bolen JB**. 1992. Engagement of the high-affinity IgE receptor activates *src*
719 protein-related tyrosine kinases. Nature **355**:78-80.

720 3. **Yamashita T, Mao S-Y, Metzger H**. 1994. Aggregation of the high-affinity IgE receptor
721 and enhanced activity of p53/p56^{lyn} protein-tyrosine kinase. Proc. Natl. Acad. Sci. USA
722 **91**:11251-11255.

723 4. **Pribluda VS, Pribluda C, Metzger H**. 1994. Transphosphorylation as the mechanism by
724 which the high-affinity receptor for IgE is phosphorylated upon aggregation. Proc. Natl.
725 Acad. Sci. USA **91**:11246-11250.

726 5. **Field KA, Holowka D, Baird B**. 1995. FcεRI-mediated recruitment of p53/56^{lyn} to
727 detergent-resistant membrane domains accompanies cellular signaling. Proc. Natl. Acad.
728 Sci. USA **92**:9201-9205.

729 6. **Heneberg P, Dráberová L, Bambousková M, Pompach P, Dráber P**. 2010. Down-
730 regulation of protein tyrosine phosphatases activates an immune receptor in the absence
731 of its translocation into lipid rafts. J. Biol. Chem. **285**:12787-12802.

7. **Tolar P, Dráberová L, Tolarová H, Dráber P**. 2004. Positive and negative regulation of Fcε receptor I-mediated signaling events by Lyn kinase C-terminal tyrosine phosphorylation. Eur. J. Immunol. **34**:1136-1145.

8. **Bergman M, Mustelin T, Oetken C, Partanen J, Flint NA, Amrein KA, Autero M, Burn P, Alitalo K**. 1992. The human p50 csk tyrosine kinase phosphorylates p56 lck at tyr-505 and down regulates its catalytic activity. EMBO J. **11**:2919-2924.

9. **Plas DR, Thomas ML**. 1998. Negative regulation of antigen receptor signaling in lymphocytes. J. Mol. Med. (Berl) **76**:589-595.

10. **Nada S, Okada M, MacAuley A, Cooper JA, Nakagawa H**. 1991. Cloning of a complementary DNA for a protein tyrosine kinase associated that specifically phosphorylates a negative regulatory site for p60 c- src. Nature **351**:69-72.

11. **Brdička T, Pavlistová D, Leo A, Bruyns E, Kořínek V, Angelisová P, Scherer J, Shevchenko A, Hilgert I, Černý J, Drbal K, Kuramitsu Y, Kornacker B, Hořejší V, Schraven B**. 2000. Phosphoprotein associated with glycosphingolipid-enriched microdomains (PAG), a novel ubiquitously expressed transmembrane adaptor protein, binds the protein tyrosine kinase csk and is involved in regulation of T cell activation. J. Exp. Med. **191**:1591-1604.

12. **Kawabuchi M, Satomi Y, Takao T, Shimonishi Y, Nada S, Nagai K, Tarakhovsky A, Okada M**. 2000. Transmembrane phosphoprotein Cbp regulates the activities of Src-family tyrosine kinases. Nature **404**:999-1003.

13. **Brdičková N, Brdička T, Anděra L, Špička J, Angelisová P, Milgram SL, Hořejší V.** 2001. Interaction between two adapter proteins, PAG and EBP50: a possible link between membrane rafts and actin cytoskeleton. FEBS Lett. **507**:133-136.

14. **Draber P, Halova I, Levi-Schaffer F, Draberova L.** 2012. Transmembrane adaptor proteins in the high-affinity IgE receptor signaling. Frontiers Immunol. , **2**:1-11.

15. **Hrdinka M, Horejsi V.** 2013. PAG - a multipurpose transmembrane adaptor protein. Oncogene **doi: 10.1038/onc.2013.485**.

16. **Smida M, Cammann C, Gurbiel S, Kerstin N, Lingel H, Lindquist S, Simeoni L, Brunner-Weinzierl MC, Suchanek M, Schraven B, Lindquist JA.** 2013. PAG/Cbp suppression reveals a contribution of CTLA-4 to setting the activation threshold in T cells. Cell Commun. Signal. **11**:28.

17. **Dobenecker MW, Schmedt C, Okada M, Tarakhovsky A.** 2005. The ubiquitously expressed Csk adaptor protein Cbp is dispensable for embryogenesis and T-cell development and function. Mol. Cell Biol. **25**:10533-10542.

18. **Xu S, Huo J, Tan JE, Lam KP.** 2005. Cbp deficiency alters Csk localization in lipid rafts but does not affect T-cell development. Mol. Cell Biol. **25**:8486-8495.

19. **Odom S, Gomez G, Kovarova M, Furumoto Y, Ryan JJ, Wright HV, Gonzalez-Espinosa C, Hibbs ML, Harder KW, Rivera J.** 2004. Negative regulation of immunoglobulin E-dependent allergic responses by Lyn kinase. J. Exp. Med. **199**:1491-1502.

772 20. **Kitaura J, Kawakami Y, Maeda-Yamamoto M, Horejsi V, Kawakami T**. 2007.
773 Dysregulation of Src family kinases in mast cells from epilepsy-resistant ASK versus
774 epilepsy-prone EL mice. J. Immunol. **178**:455-462.

775 21. **Ohtake H, Ichikawa N, Okada M, Yamashita T**. 2002. Cutting Edge: Transmembrane
776 phosphoprotein Csk-binding protein/phosphoprotein associated with glycosphingolipid-
777 enriched microdomains as a negative feedback regulator of mast cell signaling through
778 the FcεRI. J. Immunol. **168**:2087-2090.

779 22. **Nishizumi H, Horikawa K, Mlinaric-Rascan I, Yamamoto T**. 1998. A double-edged
780 kinase Lyn: a positive and negative regulator for antigen receptor-mediated signals. J.
781 Exp. Med. **187**:1343-1348.

782 23. **Kawakami Y, Kitaura J, Satterthwaite AB, Kato RM, Asai K, Hartman SE, Maeda-**
783 **Yamamoto M, Lowell CA, Rawlings DJ, Witte ON, Kawakami T**. 2000. Redundant
784 and opposing functions of two tyrosine kinases, Btk and Lyn, in mast cell activation. J.
785 Immunol. **165**:1210-1219.

786 24. **Parravicini V, Gadina M, Kovarova M, Odom S, Gonzalez-Espinosa C, Furumoto**
787 **Y, Saitoh S, Samelson LE, O'Shea JJ, Rivera J**. 2002. Fyn kinase initiates
788 complementary signals required for IgE-dependent mast cell degranulation. Nat.
789 Immunol. **3**:741-748.

790 25. **Yang Y, Seed B**. 2003. Site-specific gene targeting in mouse embryonic stem cells with
791 intact bacterial artificial chromosomes. Nat. Biotechnol. **21**:447-451.

792 26. **Lindquist S, Karitkina D, Langnaese K, Posevitz-Fejfar A, Schraven B, Xavier R,**
793 **Seed B, Lindquist JA**. 2011. Phosphoprotein associated with glycosphingolipid-enriched
794 microdomains differentially modulates SRC kinase activity in brain maturation. PLoS.
795 One. **6**:e23978.

796 27. **Tolar P, Tůmová M, Dráber P**. 2001. New monoclonal antibodies recognizing the
797 adaptor protein LAT. Folia Biol. (Praha) **47**:215-217.

798 28. **Dráberová L, Amoui M, Dráber P**. 1996. Thy-1-mediated activation of rat mast cells:
799 the role of Thy-1 membrane microdomains. Immunology **87**:141-148.

800 29. **Rivera J, Kinet J-P, Kim J, Pucillo C, Metzger H**. 1988. Studies with a monoclonal
801 antibody to the β subunit of the receptor with high affinity for immunoglobulin E. Mol.
802 Immunol. **25**:647-661.

803 30. **Rudolph AK, Burrows PD, Wabl MR**. 1981. Thirteen hybridomas secreting hapten-
804 specific immunoglobulin E from mice with Ig^a or Ig^b heavy chain haplotype. Eur. J.
805 Immunol. **11**:527-529.

806 31. **Kovářová M, Tolar P, Arudchandran R, Dráberová L, Rivera J, Dráber P**. 2001.
807 Structure-function analysis of Lyn kinase association with lipid rafts and initiation of
808 early signaling events after Fcε receptor I aggregation. Mol. Cell Biol. **21**:8318-8328.

809 32. **Surviladze Z, Dráberová L, Kovářová M, Boubelík M, Dráber P**. 2001. Differential
810 sensitivity to acute cholesterol lowering of activation mediated via the high-affinity IgE
811 receptor and Thy-1 glycoprotein. Eur. J. Immunol. **31**:1-10.

812 33. **Dráberová L**. 1990. Cyclosporin A inhibits rat mast cell activation. Eur. J. Immunol.
813 **20**:1469-1473.

814 34. **Surviladze Z, Dráberová L, Kubínová L, Dráber P**. 1998. Functional heterogeneity of
815 Thy-1 membrane microdomains in rat basophilic leukemia cells. Eur. J. Immunol.
816 **28**:1847-1858.

817 35. **Amoui M, Dráber P, Dráberová L**. 1997. Src family-selective tyrosine kinase inhibitor,
818 PP1, inhibits both FcεRI- and Thy-1-mediated activation of rat basophilic leukemia cells.
819 Eur. J. Immunol. **27**:1881-1886.

820 36. **Horáková H, Polakovičová I, Shaik GM, Eitler J, Bugajev V, Dráberová L, Dráber**
821 **P**. 2011. 1,2-propanediol-trehalose mixture as a potent quantitative real-time PCR
822 enhancer. BMC. Biotechnol. **11**:41.

823 37. **Potůčkova L, Franko F, Bambousková M, Dráber P**. 2011. Rapid and sensitive
824 detection of cytokines using functionalized gold nanoparticle-based immuno-PCR,
825 comparison with immuno-PCR and ELISA. J. Immunol. Methods **371**:38-47.

826 38. **Makabe-Kobayashi Y, Hori Y, Adachi T, Ishigaki-Suzuki S, Kikuchi Y, Kagaya Y,**
827 **Shirato K, Nagy A, Ujike A, Takai T, Watanabe T, Ohtsu H**. 2002. The control effect
828 of histamine on body temperature and respiratory function in IgE-dependent systemic
829 anaphylaxis. J. Allergy Clin. Immunol. **110**:298-303.

830 39. **Thastrup O, Dawson AP, Scharff O, Foder B, Cullen PJ, Drobak BK, Bjerrum PJ,**
831 **Christensen SB, Hanley MR**. 1989. Thapsigargin, a novel molecular probe for studying
832 intracellular calcium release and storage. Agents Actions **27**:17-23.

40. **Putney JW, Jr.** 2005. Capacitative calcium entry: sensing the calcium stores. J. Cell Biol. **169**:381-382.

41. **Volná P, Lebduška P, Dráberová L, Šímová S, Heneberg P, Boubelík M, Bugajev V, Malissen B, Wilson BS, Hořejší V, Malissen M, Dráber P**. 2004. Negative regulation of mast cell signaling and function by the adaptor LAB/NTAL. J. Exp. Med. **200**:1001-1013.

42. **Gilfillan AM, Rivera J**. 2009. The tyrosine kinase network regulating mast cell activation. Immunol. Rev. **228**:149-169.

43. **Huang C, Jacobson K, Schaller MD**. 2004. MAP kinases and cell migration. J. Cell Sci. **117**:4619-4628.

44. **Nocka KH, Levine BA, Ko JL, Burch PM, Landgraf BE, Segal R, Lobell R**. 1997. Increased growth promoting but not mast cell degranulation potential of a covalent dimer of c-Kit ligand. Blood **90**:3874-3883.

45. **Heneberg P, Dráber P**. 2002. Nonreceptor protein tyrosine and lipid phosphatases in type I Fcε receptor-mediated activation of mast cells and basophils. Int. Arch. Allergy Immunol. **128**:253-263.

46. **Hernandez-Hansen V, Smith AJ, Surviladze Z, Chigaev A, Mazel T, Kalesnikoff J, Lowell CA, Krystal G, Sklar LA, Wilson BS, Oliver JM**. 2004. Dysregulated FcεRI signaling and altered Fyn and SHIP activities in Lyn-deficient mast cells. J. Immunol. **173**:100-112.

47. **Huber M, Helgason CD, Damen JE, Liu L, Humphries RK, Krystal G**. 1998. The src homology 2-containing inositol phosphatase (SHIP) is the gatekeeper of mast cell degranulation. Proc. Natl. Acad. Sci USA **95**:11330-11335.

48. **Gilfillan AM, Tkaczyk C**. 2006. Integrated signalling pathways for mast-cell activation. Nat. Rev. Immunol. **6**:218-230.

49. **Iwaki S, Tkaczyk C, Satterthwaite AB, Halcomb K, Beaven MA, Metcalfe DD, Gilfillan AM**. 2005. Btk plays a crucial role in the amplification of FcεRI-mediated mast cell activation by kit. J. Biol. Chem. **280**:40261-40270.

50. **Iwaki S, Spicka J, Tkaczyk C, Jensen BM, Furumoto Y, Charles N, Kovarova M, Rivera J, Horejsi V, Metcalfe DD, Gilfillan AM**. 2008. Kit- and FcεRI-induced differential phosphorylation of the transmembrane adaptor molecule NTAL/LAB/LAT2 allows flexibility in its scaffolding function in mast cells. Cell Signal. **20**:195-205.

51. **Halova I, Draberova L, Draber P**. 2012. Mast cell chemotaxis - chemoattractants and signaling pathways. Front Immunol. **3**:119.

52. **Pullen NA, Barnstein BO, Falanga YT, Wang Z, Suzuki R, Tamang TD, Khurana MC, Harry EA, Draber P, Bunting KD, Mizuno K, Wilson BS, Ryan JJ**. 2012. Novel mechanism for FcεRI-mediated signal transducer and activator of transcription 5 (STAT5) tyrosine phosphorylation and the selective influence of STAT5B over mast cell cytokine production. J. Biol. Chem. **287**:2045-2054.

53. **Grange M, Verdeil G, Arnoux F, Griffon A, Spicuglia S, Maurizio J, Buferne M, Schmitt-Verhulst AM, Auphan-Anezin N**. 2013. Active STAT5 regulates T-bet and

874 eomesodermin expression in CD8 T cells and imprints a T-bet-dependent Tc1 program
875 with repressed IL-6/TGF-beta1 signaling. J. Immunol. **191**:3712-3724.

876 54. **Pullen NA, Falanga YT, Morales JK, Ryan JJ**. 2012. The Fyn-STAT5 Pathway: A
877 New Frontier in IgE- and IgG-Mediated Mast Cell Signaling. Front Immunol. **3**:117.

878 55. **Huber M, Helgason CD, Scheid MP, Duronio V, Humphries RK, Krystal G**. 1998.
879 Targeted disruption of SHIP leads to Steel factor-induced degranulation of mast cells.
880 EMBO J. **17**:7311-7319.

881 56. **Deakin NO, Turner CE**. 2008. Paxillin comes of age. J. Cell Sci. **121**:2435-2444.

882 57. **Fang X, Lang Y, Wang Y, Mo W, Wei H, Xie J, Yu M**. 2012. Shp2 activates Fyn and
883 Ras to regulate RBL-2H3 mast cell activation following FcεRI aggregation. PLoS. One.
884 7:e40566.

885 58. **Broad LM, Braun FJ, Lievremont JP, Bird GS, Kurosaki T, Putney JW, Jr.** 2001.
886 Role of the phospholipase C-inositol 1,4,5-trisphosphate pathway in calcium release-
887 activated calcium current and capacitative calcium entry. J. Biol. Chem. **276**:15945-
888 15952.

889 59. **Litjens T, Nguyen T, Castro J, Aromataris EC, Jones L, Barritt GJ, Rychkov GY**.
890 2007. Phospholipase C-γ1 is required for the activation of store-operated Ca^{2+} channels in
891 liver cells. Biochem. J. **405**:269-276.

892 60. **Antigny F, Jousset H, Konig S, Frieden M**. 2011. Thapsigargin activates Ca^{2+} entry
893 both by store-dependent, STIM1/Orai1-mediated, and store-independent,

894 TRPC3/PLC/PKC-mediated pathways in human endothelial cells. Cell Calcium **49**:115-
895 127.

896 61. **Baba Y, Nishida K, Fujii Y, Hirano T, Hikida M, Kurosaki T**. 2008. Essential
897 function for the calcium sensor STIM1 in mast cell activation and anaphylactic responses.
898 Nat. Immunol. **9**:81-88.

899 62. **Hájková Z, Bugajev V, Dráberová E, Vinopal S, Dráberová L, Janáček J, Dráber P,**
900 **Dráber P**. 2011. STIM1-directed reorganization of microtubules in activated mast cells.
901 J. Immunol. **186**:913-923.

902 63. **Chung SC, Limnander A, Kurosaki T, Weiss A, Korenbrot JI**. 2007. Coupling Ca^{2+}
903 store release to Icrac channel activation in B lymphocytes requires the activity of Lyn and
904 Syk kinases. J. Cell Biol. **177**:317-328.

905 64. **Timokhina I, Kissel H, Stella G, Besmer P**. 1998. Kit signaling through PI 3-kinase and
906 Src kinase pathways: an essential role for Rac1 and JNK activation in mast cell
907 proliferation. EMBO J. **17**:6250-6262.

908 65. **Linnekin D, DeBerry CS, Mou S**. 1997. Lyn associates with the juxtamembrane region
909 of c-Kit and is activated by stem cell factor in hematopoietic cell lines and normal
910 progenitor cells. J. Biol. Chem. **272**:27450-27455.

911 66. **Lennartsson J, Ronnstrand L**. 2012. Stem cell factor receptor/c-Kit: from basic science
912 to clinical implications. Physiol Rev. **92**:1619-1649.

913 67. **Barnstein BO, Li G, Wang Z, Kennedy S, Chalfant C, Nakajima H, Bunting KD,**
914 **Ryan JJ**. 2006. Stat5 expression is required for IgE-mediated mast cell function. J.
915 Immunol. **177**:3421-3426.

916 68. **Morales JK, Falanga YT, Depcrynski A, Fernando J, Ryan JJ**. 2010. Mast cell
917 homeostasis and the JAK-STAT pathway. Genes Immun. **11**:599-608.

918 69. **Hálová I, Dráberová L, Bambousková M, Machyna M, Stegurová L, Smrž D,**
919 **Dráber P**. 2013. Crosstalk between tetraspanin CD9 and transmembrane adaptor protein
920 non-T cell activation linker (NTAL) in mast cell activation and chemotaxis. J. Biol.
921 Chem. **288**:9801-9814.

922 70. **Samayawardhena LA, Hu J, Stein PL, Craig AW**. 2006. Fyn kinase acts upstream of
923 Shp2 and p38 mitogen-activated protein kinase to promote chemotaxis of mast cells
924 towards stem cell factor. Cell Signal. **18**:1447-1454.

925 71. **Samayawardhena LA, Kapur R, Craig AW**. 2007. Involvement of Fyn kinase in Kit
926 and integrin-mediated Rac activation, cytoskeletal reorganization, and chemotaxis of
927 mast cells. Blood **109**:3679-3686.

928 72. **Metcalfe DD, Baram D, Mekori YA**. 1997. Mast cells. Physiol Rev. **77**:1033-1079.

929 73. **Williams CM, Galli SJ**. 2000. The diverse potential effector and immunoregulatory
930 roles of mast cells in allergic disease. J. Allergy Clin. Immunol. **105**:847-859.

931 74. **Schuck S, Honsho M, Ekroos K, Shevchenko A, Simons K**. 2003. Resistance of cell
932 membranes to different detergents. Proc. Natl. Acad. Sci. U. S. A **100**:5795-5800.

933 75. **Garner AE, Smith DA, Hooper NM**. 2008. Visualization of detergent solubilization of
934 membranes: implications for the isolation of rafts. Biophys. J. **94**:1326-1340.
935
936

937

938 **FIGURE LEGENDS**

939

940 **FIG. 1.** Positive regulatory role of PAG in antigen- or thapsigargin-induced degranulation. (A)
941 BMMCs derived from WT mice (PAG-WT) or PAG-deficient mice (PAG-KO) were stained for
942 surface FcεRI by anti-FcεRI-FITC conjugate. Unstained WT cells were used as negative
943 controls. Samples were analyzed by flow cytometry. (B, C) The presence of PAG in lysates from
944 PAG-WT and PAG-KO BMMCs (B) or WT BMMCs infected with empty pLKO lentiviral
945 vector (pLKO) or shRNA14 - 17 lentiviral vectors (C) was determined by immunoblotting (IB).
946 As loading controls, the membranes were also developed for LYN (B) or actin (C). The amount
947 of PAG normalized to its amount in cells infected with empty pLKO vector and actin loading
948 control is also shown in C (Fold). For each panel, one representative experiment out of a
949 minimum of three performed is shown. (D, E) PAG-WT or PAG-KO BMMCs were sensitized
950 (D) or not (E) with TNP-specific IgE (1 μg/ml) and then stimulated for 30 min with various
951 concentrations of antigen (Ag; D) or thapsigargin (Th; E). (F, G) PAG-WT BMMCs were
952 infected with empty pLKO lentiviral vector (pLKO) or with PAG shRNAs14 and 15 vectors
953 (PAG-KD) and stable transfectants were activated with antigen (F) or thapsigargin (G) as above.
954 The amount of β-glucuronidase released from the cells was determined 30 min after triggering.
955 Data represent means ± SE calculated in D and E from 11 independent experiments, and in F and
956 G from 6 - 8 independent experiments performed in duplicates or triplicates. Statistical
957 significance of differences between PAG-WT and PAG-KO or pLKO and PAG-KD cells is
958 shown.

959

960 **FIG. 2.** Positive regulatory role of PAG on antigen- or thapsigargin-induced calcium uptake. (A,
961 B) PAG-WT and PAG-KO BMMCs were sensitized with IgE and then stimulated for various
962 time intervals with antigen (Ag; 0.5 μg/ml; A) or with various concentrations of antigen for 5
963 min (B) in the presence of 1 mM extracellular $^{45}Ca^{2+}$. The reactions were terminated by
964 centrifugation of the cells through BSA gradient and cell-bound radioactivity (in sediment) was
965 determined. (C, D) PAG-WT and PAG-KO BMMCs were activated for various time intervals
966 with 1 μM thapsigargin (C) or with various concentrations of thapsigargin for 5 min (D) and the
967 uptake of $^{45}Ca^{2+}$ was determined as above. (E, F) PAG-WT BMMCs were infected with empty
968 pLKO lentiviral vector (pLKO) or with PAG shRNAs vectors (PAG-KD) and stable
969 transfectants were activated with antigen (E) or thapsigargin (F) and analyzed as above. Data
970 represent means ± SE from 3 - 6 independent experiments performed in duplicates or triplicates.
971
972 **FIG. 3.** Localization of CSK in lipid rafts depends on PAG. IgE-sensitized PAG-WT BMMCs
973 (A) or PAG-KO BMMCs (B) were non-activated (Control) or activated for 5 min with antigen
974 (Ag; 250 ng/ml). After solubilization in lysis buffer containing 1% Brij 96 the whole cell lysates
975 were fractionated by sucrose density gradient ultracentrifugation as described in Materials and
976 Methods. Individual fractions were collected and analyzed by immunoblotting for the presence
977 of PAG, CSK, and LYN. Fractions containing DRMs are indicated. Representative data from
978 three independent experiments are shown.
979
980 **FIG. 4.** Antigen-induced tyrosine phosphorylation of signal transduction proteins is dependent
981 on PAG. (A - G) IgE-sensitized PAG-WT and PAG-KO cells were activated for the indicated
982 time intervals with antigen (250 ng/ml). The cells were lysed, and total cellular lysates were
983 analyzed by immunoblotting with the tyrosine-specific mAb PY-20-HRP conjugate (PY).

Alternatively, FcεRI (B), LAT (D), and paxillin (G) were immunoprecipitated from the lysates and examined by immunoblotting with tyrosine-specific mAb as in A. For SYK (C), ERK (E), and FAK (F), size-fractionated proteins in cell lysates were directly analyzed by immunoblotting with the corresponding phosphoprotein-specific antibodies. For loading controls the membranes were analyzed by immunoblotting for LYN kinase (A), FcεRI β chain (B), SYK (C), LAT (D), ERK (E), FAK (F) and paxillin (G). Data in A and in upper parts of B-G are representative immunoblots from at least 3 experiments. Data in bottom parts of B - G show densitometry analysis of the corresponding immunoblots in which signals from tyrosine-phosphorylated proteins in activated cells were normalized to the signal in non-activated cells and loading control proteins. Means ± SE were calculated from a minimum of four independent experiments. Statistical significance of differences between PAG-WT and PAG-KO cells are also shown.

FIG. 5. PAG-dependent regulation of LYN and FYN kinase activities and SHIP1 tyrosine phosphorylation. (A) IgE-sensitized PAG-WT and PAG-KO BMMCs were activated or not for 2 min with antigen (250 ng/ml) and then solubilized with lysis buffer containing 1% Brij 96. FcεRI-IgE complexes were immunoprecipitated and incubated in a kinase buffer containing [γ-^{32}P]ATP. After kinase assay ^{32}P-labeled proteins were size-fractionated, transferred to nitrocellulose membranes and examined by autoradiography. Relative amounts of FcεRI β chain were determined by immunoblotting. Positions of FcεRI β and γ chains are indicated. (B) Autoradiograms obtained as in A were quantified and the signals corresponding to FcεRI β and γ chains were normalized to the signals in non-activated PAG-WT cells and the amount of FcεRI β chain immunoprecipitated. (C - F) The cells were activated and solubilized as in A. LYN (C and D) and FYN (E and F) were immunoprecipitated and incubated in kinase buffer supplemented with [γ-^{32}P]ATP and acid-denatured enolase used as exogenous substrate. Kinase assays and

1008 further analyses were performed as in A. Autoradiograms were quantified and the signals
1009 corresponding to LYN, FYN and enolase were normalized to the signals in non-activated PAG-
1010 WT cells and the amount of immunoprecipitated LYN (D) or FYN (F). (G and H) IgE-sensitized
1011 PAG-WT and PAG-KO BMMCs were activated for the indicated time intervals with antigen as
1012 above. The cells were lysed and analyzed by immunoblotting with phospho-SHIP1-specific
1013 antibody (p-SHIP1). The amount of SHIP1 was used as loading control. (H) Densitometry
1014 analysis of the immunoblots in which the signal for p-SHIP1 was normalized to the signal in
1015 non-activated PAG-WT cells and the amount of SHIP1. Representative experiments are shown in
1016 A, C, E, and G. Means ± SE in B, D, F and H were calculated from 3 - 5 independent
1017 experiments. Statistical significance of intergroup differences is indicated.
1018
1019 **FIG. 6.** Different regulatory roles of PAG in KIT and FcεRI signaling. (A) PAG-WT and PAG-
1020 KO BMMCs were stimulated for 30 min with various concentrations of SCF and the amount of
1021 β-glucuronidase released into supernatant was determined. (B) PAG-WT and PAG-KO cells
1022 were exposed for different time intervals to SCF (50 ng/ml), lysed, and tyrosine phosphorylation
1023 of KIT was analyzed by immunoblotting with p-KIT-specific antibody. Immunoblotting with
1024 KIT-specific antibody served as a loading control. One representative experiment out of three
1025 performed is shown. (C) The immunoblots obtained as in B were analyzed by densitometry and
1026 the amounts of tyrosine phosphorylated KIT were normalized to KIT phosphorylation in non-
1027 activated PAG-WT cells and loading controls. (D and E) PAG-WT and PAG-KO BMMCs were
1028 activated for different time intervals with antigen (250 ng/ml) or SCF (50 ng/ml), lysed, and
1029 PLCγ1 was immunoprecipitated. The immunoprecipitates were analyzed by immunoblotting
1030 with tyrosine-specific mAb PY-20-HRP conjugate (PY; D). As loading controls, the membranes
1031 were also analyzed by immunoblotting for PLCγ1. Representative immunoblots out of three

performed are shown. The immunoblots obtained were analyzed by densitometry and the relative amounts of tyrosine phosphorylated proteins were normalized to the amounts of the proteins immunoprecipitated and to their phosphorylation in non-activated PAG-WT cells (E). (F) IgE-sensitized PAG-WT or PAG-KO BMMCs were analyzed in chemotactic assay with chemotaxis medium alone (Control) or supplemented with antigen (250 ng/ml) or SCF (100 ng/ml) in lower wells. Numbers of cells migrating into lower wells were determined after 8 h. (G) The experiments were performed as in F, except that cells with PAG-KD and corresponding controls (pLKO) were used. Means ± SE were calculated from a minimum of nine independent experiments performed in triplicates (A), three independent experiments (C, E and G) or six independent experiments (F). Statistical significance of differences between PAG-WT/PAG-KO cells (A, C, E, and F) and pLKO/PAG-KD cells (G) is shown.

FIG. 7. Decreased tyrosine phosphorylation of STAT5 and production of cytokines and chemokines in antigen-activated PAG-KO BMMCs. (A) Cells were activated for different time intervals with antigen (250 ng/ml) or SCF (50 ng/ml), lysed, and analyzed for STAT5 tyrosine 694 phosphorylation by immunoblotting. As loading controls, the membranes were also immunoblotted with STAT5-specific antibody. Representative immunoblots are shown. (B) The immunoblots were analyzed by densitometry and the relative amount of tyrosine-phosphorylated STAT5 was normalized to its amount in non-activated cells and the corresponding loading control. (C, D) Production of cytokines (TNF-α, IL-6, and IL-13) at the protein level (C, upper part) and mRNA level (C, lower part) and chemokines (CCL3 and CCL4; D) at the mRNA level were evaluated in PAG-WT and PAG-KO BMMCs activated with various concentrations of antigen for 1 h (mRNA) or 6 h (protein). Specific proteins and mRNAs were quantified by immuno-PCR and qPCR, respectively. Means ± SE were calculated from 4-12 independent

1056 experiments. Statistical significance of differences between PAG-WT and PAG-KO cells are
1057 shown.
1058
1059 **FIG. 8.** Phenotype rescue of PAG-KO BMMCs. (A, B) PAG-KO BMMCs were transfected with
1060 the pCDH-PAG-myc vector (A) or control empty vector (pCDH; B). Puromycin-resistant
1061 transfectants were isolated and attached to fibronectin-coated slides. Then the cells were fixed,
1062 permeabilized and labeled for PAG-myc with anti-Myc-Tag/anti-IgG-Alexa Fluor 488 conjugate
1063 (green) and Hoechst 33258 (blue). Scale bar, 10 µm. (C) Puromycin-resistant pCDH-PAG-myc
1064 or empty pCDH vector transfected cells were solubilized and the presence of PAG-myc was
1065 determined by immunoblotting with anti-Myc-Tag antibody. As loading controls, the membranes
1066 were developed for HPRT. (D) PAG-WT or PAG-KO BMMCs stably transfected with pCDH
1067 vector or PAG-KO BMMCs transfected with pCDH-PAG-myc were sensitized overnight with
1068 IgE and then activated with antigen (100 ng/ml). After 90 min the cells were fixed and stained
1069 with TNF-specific rabbit antibody, followed by anti-rabbit-Alexa Fluor 488 conjugate. The cells
1070 were analyzed by flow cytometry and the ratios of mean fluorescence intensity between activated
1071 and non-activated cells were normalized to PAG-WT+pCDH controls. Data show means ± SE
1072 calculated from three independent experiments. Statistical significance of differences is
1073 indicated.
1074
1075 **FIG. 9.** Decreased passive systemic anaphylaxis in PAG-KO mice. (A) PAG-WT (n = 17) and
1076 PAG-KO mice (n = 16) were passively sensitized with TNP-specific IgE (3 µg/mouse) and 24 h
1077 later challenged with antigen (500 µg per mouse) to induce systemic anaphylaxis. Body
1078 temperature responses at various time intervals after antigen administration were recorded.
1079 Means ± SE are shown. Statistically significant differences ($P<0.05$) between PAG-WT and

1080 PAG-KO mice are indicated by black line below the curves. (B) Percentage of mast cells (KIT-
1081 and FcεRI-positive) in peritoneal lavage of PAG-WT and PAG-KO mice. (C) Serum IgE levels
1082 in PAG-WT and PAG-KO mice. Data are means ± SE calculated from three (B) or four (C)
1083 animals in each group.

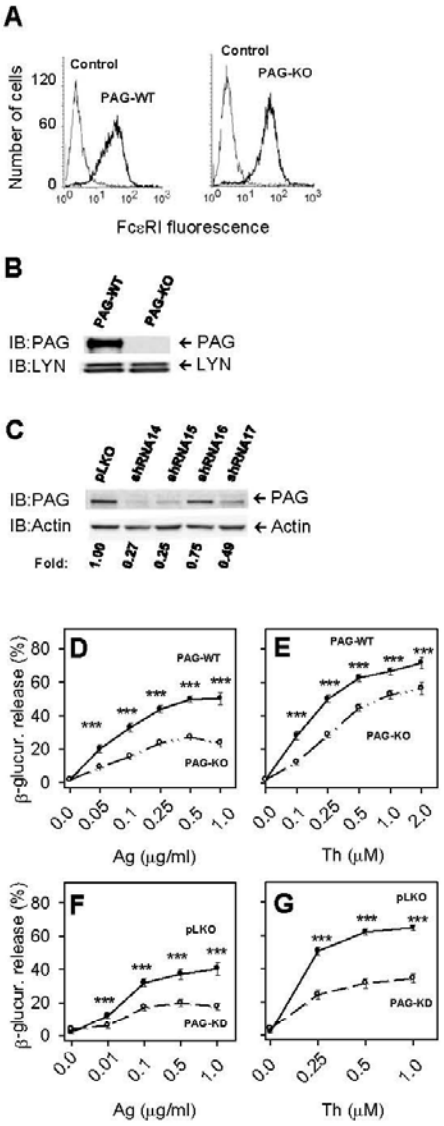

Figure 1
Draberova et al.

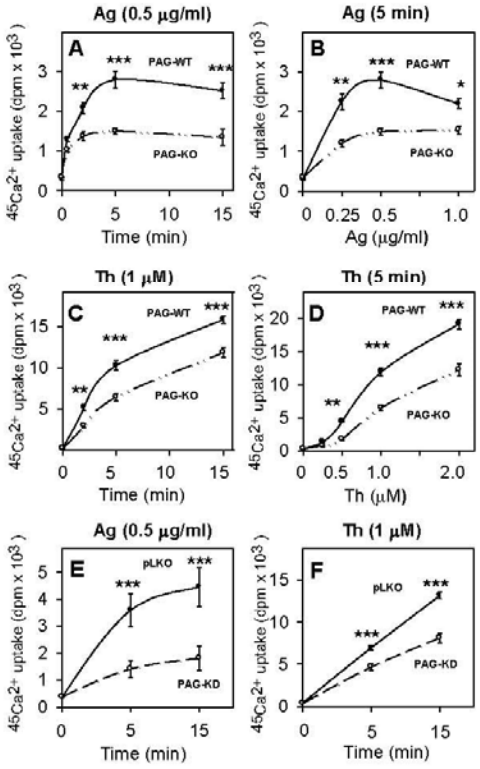

Figure 2
Draberova et al.

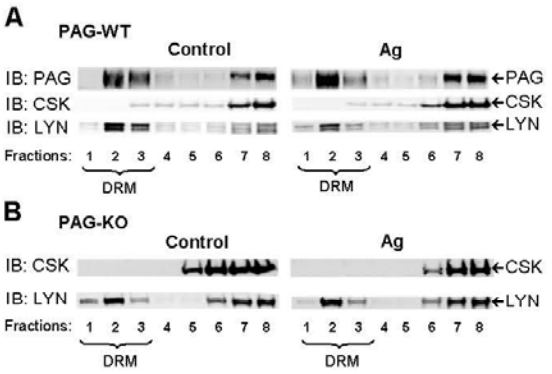

Figure 3
Draberova et al.

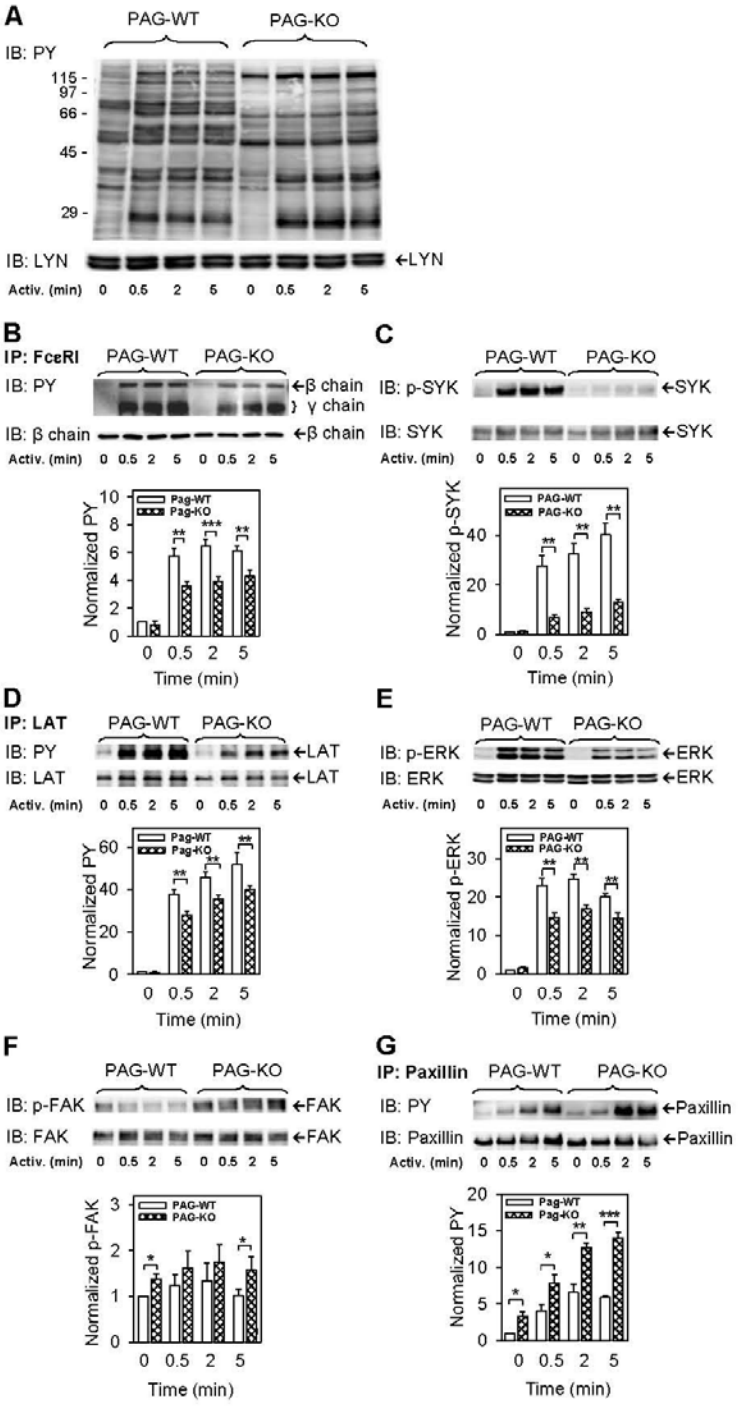

Figure 4
Draberova et al.

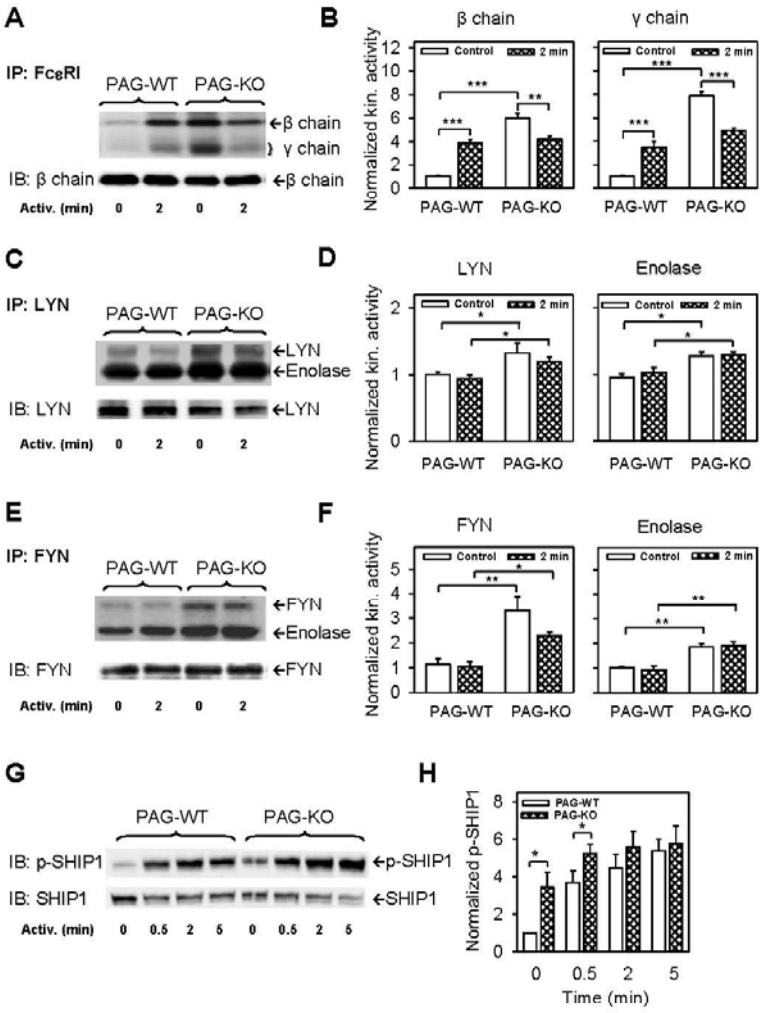

Figure 5
Draberova et al.

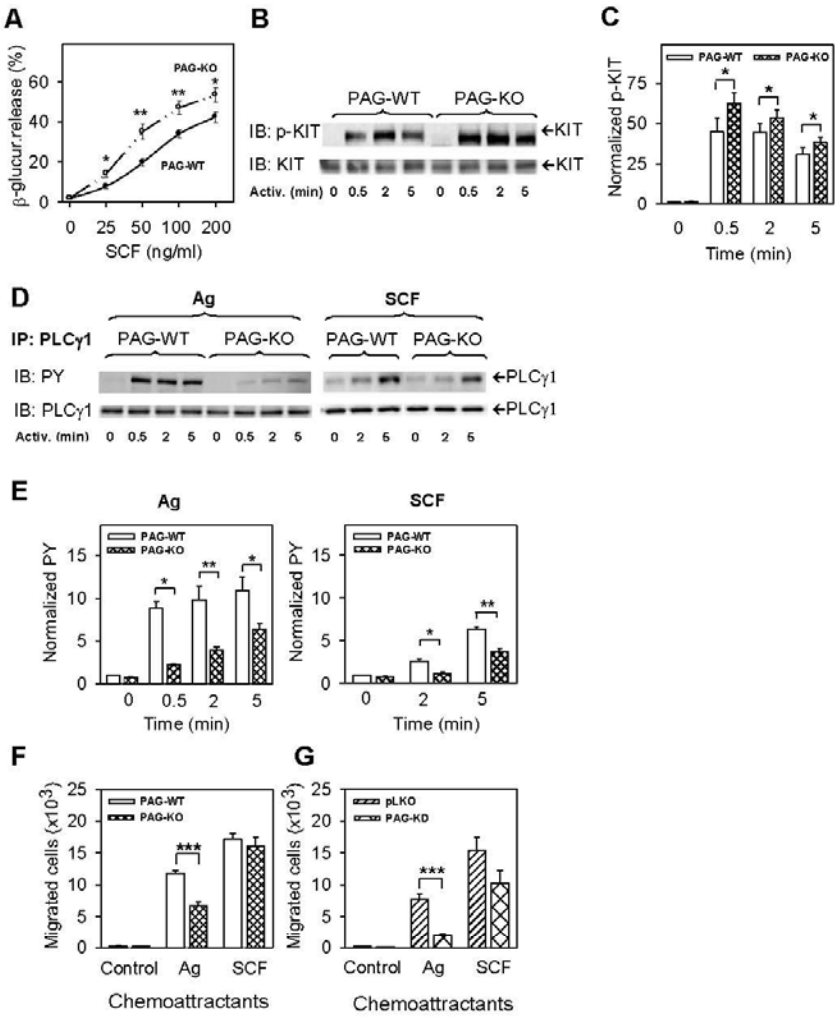

Figure 6
Draberova et al.

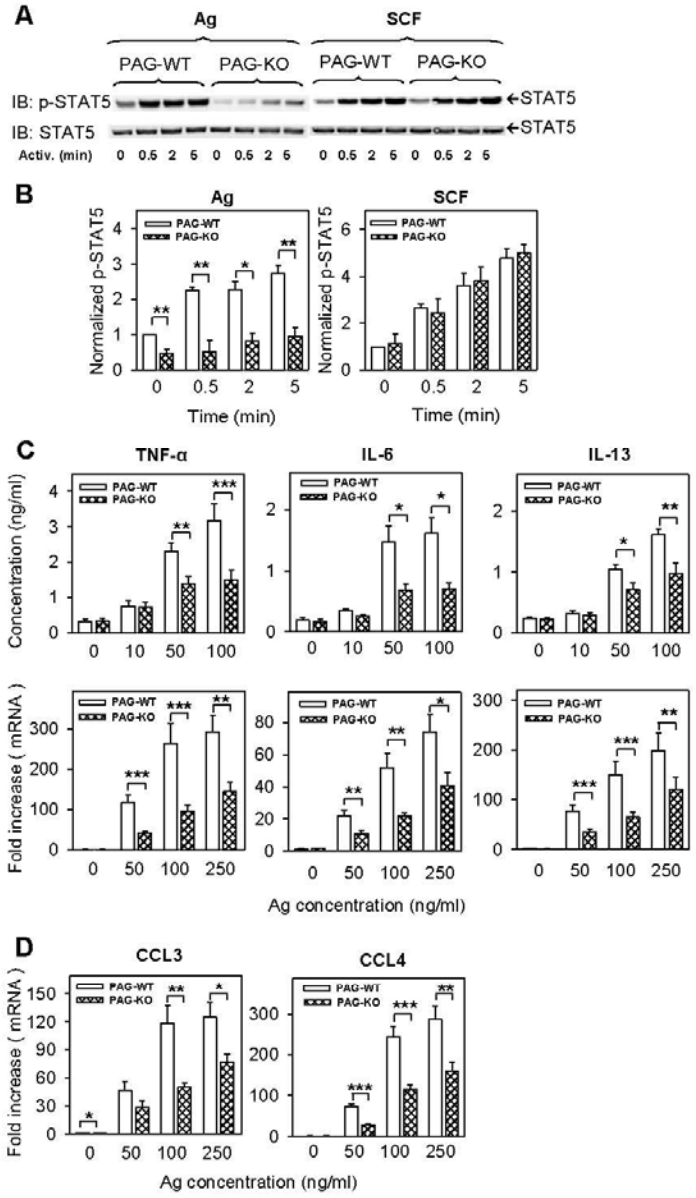

Figure 7
Draberova et al.

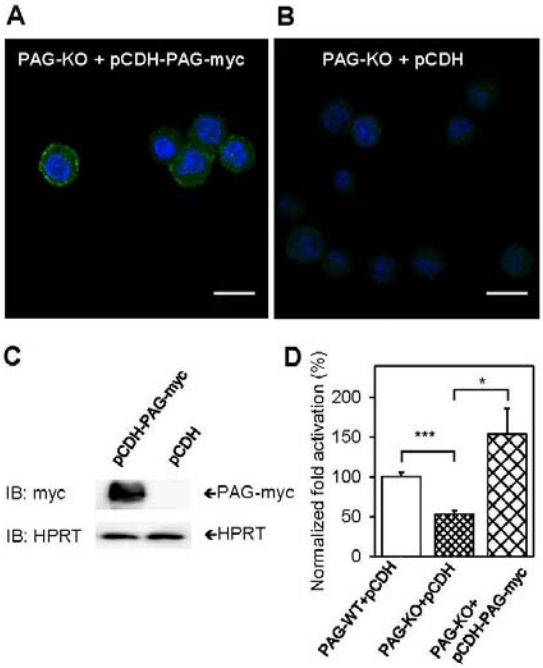

Figure 8
Draberova et al.

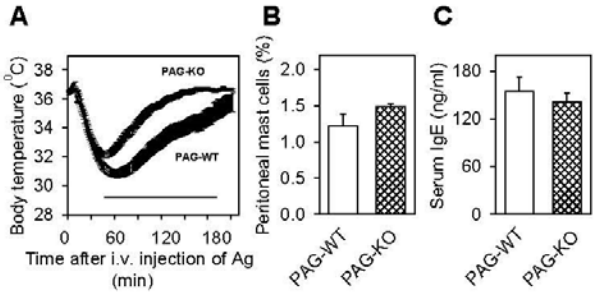

Figure 9
Draberova et al.

1,2-propanediol-trehalose mixture as a potent quantitative real-time PCR enhancer

BMC Biotechnol. 2011 Apr 18;11:41

Horáková et al. BMC Biotechnology 2011, 11:41
http://www.biomedcentral.com/1472-6750/11/41

BMC Biotechnology

METHODOLOGY ARTICLE Open Access

1,2-propanediol-trehalose mixture as a potent quantitative real-time PCR enhancer

Helena Horáková, Iva Polakovičová, Gouse M Shaik, Jiří Eitler, Viktor Bugajev, Lubica Dráberová and Petr Dráber*

Abstract

Background: Quantitative real-time PCR (qPCR) is becoming increasingly important for DNA genotyping and gene expression analysis. For continuous monitoring of the production of PCR amplicons DNA-intercalating dyes are widely used. Recently, we have introduced a new qPCR mix which showed improved amplification of medium-size genomic DNA fragments in the presence of DNA dye SYBR green I (SGI). In this study we tested whether the new PCR mix is also suitable for other DNA dyes used for qPCR and whether it can be applied for amplification of DNA fragments which are difficult to amplify.

Results: We found that several DNA dyes (SGI, SYTO-9, SYTO-13, SYTO-82, EvaGreen, LCGreen or ResoLight) exhibited optimum qPCR performance in buffers of different salt composition. Fidelity assays demonstrated that the observed differences were not caused by changes in Taq DNA polymerase induced mutation frequencies in PCR mixes of different salt composition or containing different DNA dyes. In search for a PCR mix compatible with all the DNA dyes, and suitable for efficient amplification of difficult-to-amplify DNA templates, such as those in whole blood, of medium size and/or GC-rich, we found excellent performance of a PCR mix supplemented with 1 M 1,2-propanediol and 0.2 M trehalose (PT enhancer). These two additives together decreased DNA melting temperature and efficiently neutralized PCR inhibitors present in blood samples. They also made possible more efficient amplification of GC-rich templates than betaine and other previously described additives. Furthermore, amplification in the presence of PT enhancer increased the robustness and performance of routinely used qPCRs with short amplicons.

Conclusions: The combined data indicate that PCR mixes supplemented with PT enhancer are suitable for DNA amplification in the presence of various DNA dyes and for a variety of templates which otherwise can be amplified with difficulty.

Background

Advances in the methodology of qPCR contributed significantly to a widespread use of this method for DNA genotyping, gene expression analysis and mutational scanning. Several different systems have been developed for continuous monitoring of the production of PCR amplicons and characterization of their properties. Widely used are sequence-specific probes which facilitate a highly sensitive detection of specific PCR products. However, these probes are difficult to prepare and are relatively expensive [1]. An alternative to the probe-based methods is the use of DNA-intercalating dyes which at concentrations compatible with PCR-mediated DNA amplification exhibit enhanced fluorescence after binding to double-stranded (ds)DNA. These dyes are less expensive, but they are also less specific because they bind to all dsDNAs present in PCR mixtures, including nonspecific products and primer-dimers. Although some of these unwanted DNA species can be distinguished by analysis of the melting curves of PCR amplicons, their presence reduces the sensitivity of qPCR and requires a proper adjustment of PCR conditions. Biophysical studies showed that DNA dyes bind to dsDNA by intercalation and external binding, and that these interactions could interfere with PCR [2-4]. Furthermore, it has been shown that the dyes also react with single-stranded (ss)DNA oligonucleotide primers [2] and that this binding could inhibit annealing of the

* Correspondence: petr.draber@img.cas.cz
Department of Signal Transduction, Institute of Molecular Genetics, Academy of Sciences of the Czech Republic, Vídeňská 1083, 142 20 Prague 4, Czech Republic

primers to the template during PCR [5]. This could account for some difficulties in amplifying certain DNA fragments, which are otherwise easily amplified in the absence of the dyes.

In initial studies, real-time accumulation of PCR amplicons was evaluated with ethidium bromide [6]. This dye was later substituted with SGI [7], which quickly became the most-widely used DNA dye for qPCR monitoring. Recently, several other DNA dyes have been introduced giving a strong fluorescence signal with dsDNA at concentrations not inhibiting PCR. These include YO-PRO-1 [8], BEBO [9], LCGreen [10], SYTO-9 [4,11], EvaGreen [3], SYTO-13, SYTO-82 [11] and LightCycler 480 ResoLight dye [12,13].

We have found that SGI inhibits amplification of medium-size genomic DNA fragments and that this inhibitory effect can be reduced by using a PCR mix, denoted here as mix IV, with modified salt composition [5]. In this study, we compared qPCR performance of seven DNA dyes (Table 1) in the mix IV and three other widely used PCR mixes of different salt composition. We found that amplification in the presence of SGI was optimal in mix IV, whereas all other dyes performed better in a mix marked here as mix II. To find out conditions which would allow efficient amplification of difficult-to-amplify DNA templates, such as those in whole blood and/or GC-rich and compatible with various DNA dyes, we tested various additives and their combinations. Excellent performance was found when PCR mix II was supplemented with PT enhancer. Extensive testing showed that PT enhancer-containing mix II could be used for efficient amplification of various DNA templates known to resist amplification under various routinely used conditions. The data have implications for a more rational design and routine use of qPCR assays.

Table 2 PCR mixes used and their composition

Component**	PCR mixes*			
	I	II	III	IV
Tris-HCl (mM) [pH]***	10 [8.0]	75 [8.8]	10 [8.0]	20 [8.8]
KCl (mM)	50	-	50	10
$(NH_4)_2SO_4$ (mM)	-	20	-	10
$MgSO_4$ (mM)	-	-	-	2
Triton X-100 (%)	0.1	-	0.1	0.1
Tween 20 (%)	-	0.01	-	-
$MgCl_2$ mM	2.5	2.5	2.5	-
DMSO (%)	-	-	5	-
dNTPs μM	200	200	200	200
Taq DNA pol. (U/ml)	25	25	25	25
anti-Taq mAb (nM)	22	22	22	22

* Final concentrations of the component during PCR.

** Components present at the same concentrations in all mixes include 200 μM dNTPs, Taq DNA pol. (25 U/ml) and anti-Taq mAb (22 nM). Oligonucleotide primers, DNA templates, DNA dyes and additives/enhancers were added immediately before the assay.

*** pH at 21°C.

Results

PCR with difficult-to-amplify templates

In our previous study we showed that amplification of the 864 base pairs (bp) genomic fragment of mouse Thy-1 can be achieved only in a PCR mix denoted here as mix IV [5]. In this study, we first tested whether the mix IV was also optimal for qPCR analysis with other DNA dyes. We compared amplification of Thy-1 genomic DNA fragment in mix IV and in three other widely used PCR mixes combined with seven DNA dyes. Properties of all DNA dyes and composition of all PCR mixes used are shown in Table 1 and 2, respectively. When SGI was combined with PCR mix IV, amplification was observed at all dilutions of the template DNA with reasonable regression coefficient (R^2 = 0.996 ± 0.003; mean ± SD; n = 6) and efficiency (E = 0.88 ±

Table 1 DNA dyes, their origin and properties

DNA dye	Origin	Stock concentration	Final concentration	Absorption maximum	Emission maximum
SGI	Invitrogen	10 mM in DMSO*	0.33 μM	497	520
SYTO-9	Invitrogen	5 mM in DMSO	2 μM	485	498
SYTO-13	Invitrogen	5 mM in DMSO	2 μM	488	509
SYTO-82	Invitrogen	5 mM in DMSO	2 μM	541	560
EvaGreen	Biotium	25 mM in DMSO	1.33 μM	500	530
LCGreen	Idaho	10 × concentrated	1×	440-470	470-520
ResoLight	Roche	20 × concentrated	1×	450-500	487

* [3]

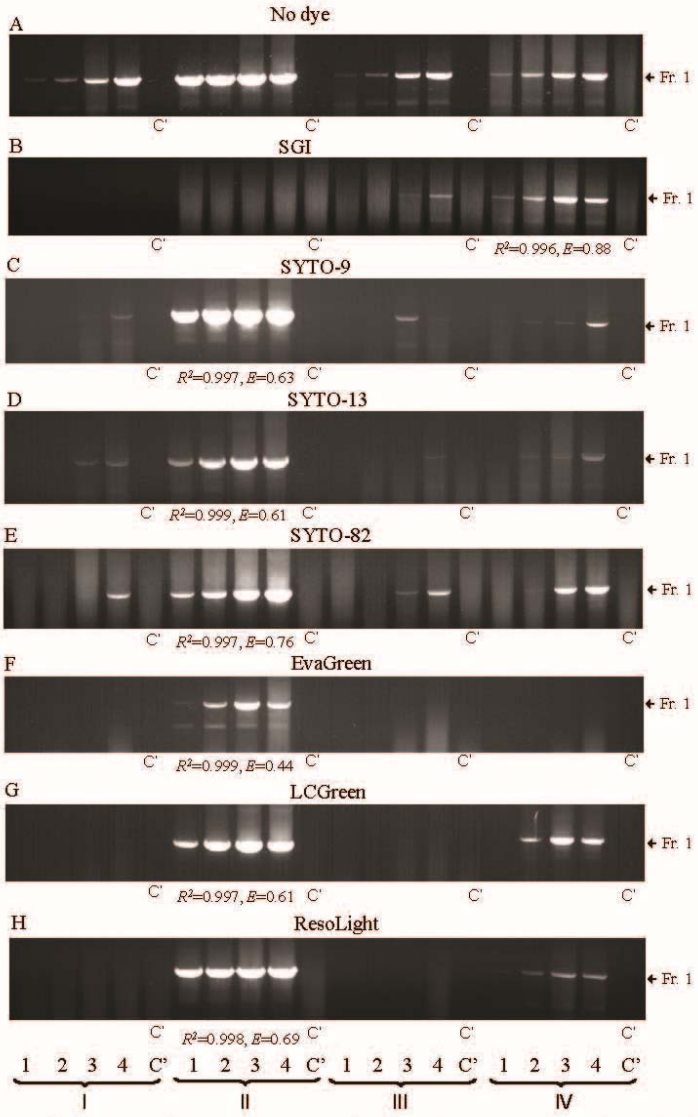

Figure 1 Amplification of genomic DNA fragments in various combinations of PCR mixes and DNA dyes. Isolated genomic DNA was diluted to contain 47 (1), 141 (2), 423 (3) 1269 (4) or none (Control; C') copies of Thy-1 gene per one μl of different PCR mixes (I - IV) supplemented without (A) or with (B - H) various DNA-binding dyes. The samples were analyzed by PCR (A) or qPCR (B - H) followed by agarose gel electrophoresis; DNA fragments were visualized by ethidium bromide staining. Migration of the specific DNA fragment (864 bp) is indicated by an arrow (Fr. 1). Regression coefficients (R^2) and efficiencies (E) were calculated from plots of Cq values versus log copy numbers, and are presented only for samples with the expected melting temperature at all template dilutions. All samples were analyzed in 3 - 7 independent experiments with similar results.

0.11). In all other mixes amplification of the fragment was either absent (mix I and II) or poor (mix III). These data were confirmed by agarose gel electrophoresis (Figure 1B). Poor amplification in PCR mixes I - III was obviously caused by the presence of SGI, since Thy-1 was reproducibly amplified in its absence (Figure 1A). Changing the Mg^{2+} concentration or optimizing the annealing temperature failed to improve the reaction in mixes I - III. It should be noted that the amount of Thy-1 amplicons in mix IV was similar regardless of the presence or absence of SGI (compare Figure 1A and 1B), indicating that the salt composition of PCR mixes has a decisive role on the inhibitory effect of SGI.

When the same fragment was amplified in SYTO-9-supplemented PCR mixes, a different profile was obtained: strong amplification (R^2 = 0.997, E = 0.63) was observed in mix II, but only week and variable amplification, as detected by melting curve analysis and gel electrophoresis, was observed in mixes I, III and IV (Figure 1C). Mix II was also optimal for other DNA dyes (SYTO-13, SYTO-82, EvaGreen, LCGreen and ResoLight; Figure 1D - H). Interestingly, inhibition of PCRs by different dyes varied in different mixes. In mix I, for example, amplification of Thy-1 DNA fragment was only observed at high concentrations of the template in the following order: SYTO-82 > SYTO-9 = SYTO-13. In mix III, some reactivity was observed with the following dyes: SYTO-82 > SGI = SYTO-9 = SYTO-13. In mix IV, Thy-1 amplification was seen in mixes supplemented with SGI > LCGreen > SYTO-82 > ResoLight > SYTO-9 = SYTO-13. In several combinations of PCR mixes and DNA dyes, complete inhibition of amplification was noted: SGI in mixes I and II, EvaGreen in mixes I, III and IV and LCGreen and ResoLight in mixes I and III. This inhibition persisted even when concentration of $MgCl_2$ was raised up to 5 mM (data not shown).

Fidelity assays

The observed difficulties with amplification of medium-size genomic DNA fragments in some PCR mixes might in part reflect an enhanced mutagenesis interfering with the synthesis of DNA fragments [14]. To find out whether salt composition of PCR mixes and the presence of DNA dyes could affect the fidelity of PCRs, we used an assay system based on streptomycin resistance of *rps*L mutants [15]. Data presented in Table 3 show that in mix I the error rate was 3.88×10^{-7}. A similar error rate was observed in mix II and an approximately two-fold increase in mix III and IV. To prove the sensitivity of the fidelity assay, we also amplified the template using KOD polymerase in a reaction mix of undisclosed composition provided by the manufacturer of the enzyme. As expected, amplification with KOD polymerase resulted in substantially lower error rate (7.6×10^{-5}), which is in agreement with the manufacturer's data. When PCR mix II was supplemented with SYTO-9, SYTO-13, EvaGreen, LCGreen or ResoLight, no dramatic changes in mutation frequencies were observed (Table 3). These findings indicate that different mutation frequencies in different PCR mixes cannot by themselves explain the observed changes in amplification efficiency caused by various DNA dyes.

New universal PCR master mix

In an attempt to develop a universal PCR master mix compatible with all the DNA dyes and suitable for amplification of DNA templates that cannot be readily amplified due to dye interference, presence of inhibitory substances and/or secondary structure formation, we tested several additives combined with mixes I - IV and various DNA dyes. As a template we used GC-rich DNA fragment of Q8N1R6 gene (Table 4; 806 bp, 73.3% GC) in human heparinized blood which escaped

Table 3 Effect of the tested PCR mixes and selected DNA dyes on DNA polymerase fidelity

Sample	Colonies mutant/total	Template doubling[a]	Mutation frequency[b]	Error rate ($\times 10^{-6}$)[c]
Taq in mix I	362/5789	12.5	0.063	38.8
Taq in mix II	990/16342	10.9	0.061	43.0
Taq in mix III	2760/21433	12.4	0.129	80.0
Taq in mix IV	951/8273	11.7	0.115	75.6
KOD in mix K[d]	30/25006	12.1	0.0012	0.76
Various DNA dyes in PCR mix II				
SYTO-9	318/4845	9.1	0.066	46.0
SYTO-13	640/10087	9.2	0.063	44.7
EvaGreen	307/5607	9.2	0.054	38.6
LCGreen	211/4068	9.0	0.052	35.8
ResoLight	64/1243	9.1	0.052	36.2

[a] Template doublings (d) were calculated using the equation 2^d = (amount of PCR product)/(amount of starting target).

[b] Mutation frequency = (mutant colonies)/(total colonies).

[c] Error rate = (mutation frequency)/(130 × d).

[d] PCR mix provided by KOD enzyme manufacturer

Table 4 Oligonucleotide primer sets and PCR amplicon properties

No	Gene*	Chromosome			Amplicon	Primer (5'-3')
	Name	No.	Position (Start-End)**	%GC	Fragment (bp)/name	Forward/reverse
Pr. 1	Thy-1	9	43854065-43854933	53.6	864/Fr. 1	ATGAACCCAGCCATCAGCG/GGGTAAGGACCTTGATATAGG
Pr. 2	NTAL	5	135085842-135086225	50.8	384/Fr. 2	CTAGGGAGCTGAGTGTTCTCA/GAACGGCTAGAACTACACAGAG
Pr. 3	NP_660313.1	16	613645-614375	71.5	731/Fr. 3	GGTCGCCGACATCCACTC/TGCTCCGGGAACAGAACCT
Pr. 4	Q8WZ58	11	2292033-2292813	71.7	781/Fr. 4	CCTGACCGTCCTGGCACA/CTGGCGAAATCTGCGAGTTC
Pr. 5	NP_060193.2	9	140174905-140175662	72.4	758/Fr. 5	CCCCTCACTCAGGTCGTGTTTT/CCCTCTGAGCCCCTTTCG
Pr. 6	Q8N4X1	16	2029023-2029774	72.6	752/Fr. 6	CGGTCCATCCCCTCATCG/ACCCCTCACGCCACCAC
Pr. 7	NP_001035158.1	16	33961629-33962363	73.1	735/Fr. 7	CGGCGAACCGGACATCC/GGCTCGTGAGGCGGGTCT
Pr. 8	Q8N1R6	13	111267817-111268622	73.3	806/Fr. 8	GACACGGCCCTGCTCC/GGGTGTGATTGAGCGAGTTG
Pr. 9	NM_020975	10	43572333-43572724	79.1	392/Fr. 9	CCCGCACTGAGCTCCTACAC/GGACGTCGCCTTCGCCATCG

* Homo_sapiens LATESTGP database was used, except for Thy-1 and NTAL for which Mus_musculus LATESTGP database was used.
** Primer sets Pr. 3 - Pr. 9. are based on Ensembl release 56 - Sept 2009

detection under standard conditions using various commercial PCR master mixes such as iQ™ SYBR Green Supermix and LightCycler 480 SYBR Green I Master (LC 480 SGI). In pilot experiments various mixes were combined with several additives and/or procedures, which have been reported to allow amplification of GC-rich fragments and/or neutralize PCR inhibitory components present in the blood (hemoglobin, lactoferrin and immunoglobulin G [16,17]). These included 0.1 - 0.5 M trehalose (final concentration) [18], 5 - 15% dimethyl sulfoxide (DMSO) [19,20], 0.5 - 2.5 M N,N,N-trimethylglycine monohydrate (betaine) [21,22], combinations of 5 - 15% DMSO and 2.2 M betaine [23], 5 - 25 mM tetrapropylammonium chloride [5], 0.5 - 1.5 M 1,2-propanediol, 0.5 - 1.5 M ethyleneglycol [24], 50 - 150 μM 7-deaza-2'-deoxyguanosine 5'-triphosphate [25,26], PCR-enhancing coctail containing 0.3 M D-(+)-trehalose, 0.24 M L-carnitine, and 0.4% Nonidet P-40 (TCN) [27] and antibody-mediated hot start PCR [5] combined with "touchdown" procedure [28,29]. Yet, none of these additives and/or procedures improved PCR to get specific signal determined by agarose gel electrophoresis (data not shown). Interestingly, specific amplicons were observed in PCR mix II supplemented with both 1 M 1,2-propanediol and 0.2 M trehalose (mix II-PT); higher or lower concentrations of these two additives resulted in inhibition of production of the specific amplicons and/or enhanced formation of nonspecific DNA fragments (Figure 2).

Mix II-PT allowed efficient amplification of numerous gene fragments in heparin-treated whole blood, including mouse Thy-1 and NTAL (data not shown) and, as shown in Figure 3 (mix II-PT), GC-rich fragments of the human genes NP_660313.1 (Table 4; 71.5% GC, 731 bp), Q8WZ58 (71.7% GC, 781 bp), NP_060193.2 (72.4% GC, 758 bp), Q8N4X1 (72.6% GC, 752 bp), NP_001035158.1 (73.1% GC, 735 bp), and Q8N1R6 (73.3% GC, 806 bp). PT enhancer also allowed efficient amplification of 392 bp DNA fragment with 79.1% GC (Table 4; [26]) from whole blood which was resistant to amplification under standard conditions (data not shown). In its enhancing capacity mix II-PT surpassed the TCN enhancer [27], which was capable of amplifying only one of the six GC-rich templates tested (Figure 3, mix II-TCN). Similar results were obtained when blood samples were treated with other commonly used anticoagulants, 2.7 mM EDTA or 0.38% sodium citrate (data not shown).

Next we tested qPCR performance of various DNA dyes in mix II-PT during amplification of the GC-rich fragment (72.6% GC, 752 bp) of Q8N4X1 gene in whole human blood. Pilot experiments indicated that different dilutions of whole human blood in water, followed by qPCR in mix II-PT with SGI resulted in poor regression coefficients. This was probably caused by simultaneous dilution of the DNA templates and the inhibitory (e.g. hemoglobin [17]) and/or stimulatory (e.g. heparin [30]) components present in the whole blood samples. However, when human blood was diluted with mouse blood

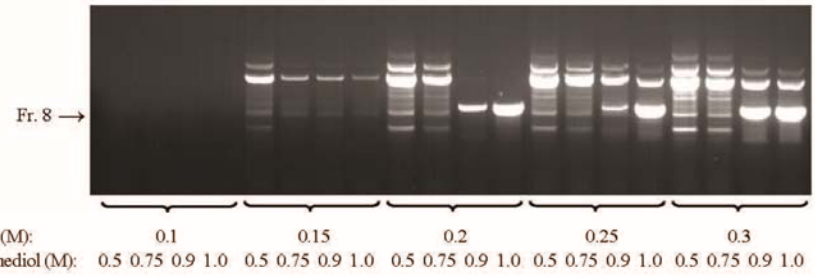

Figure 2 Amplification of medium-size GC-rich DNA fragment using whole blood as a source of the template. 806 bp fragment of human Q8N1R6 gene (73.3% GC) in heparinized human blood (2% final concentration) was amplified in PCR mix II containing various concentrations of trehalose (0.1 - 0.3 M) and 1,2-propanediol (0.5 - 1.0 M). Position of the specific product (Fr. 8) is shown by an arrow. A typical result of three independently performed experiments is shown.

to keep the concentration of human/mouse blood in PCR constant (2%), reasonable regression coefficients (R^2 = 0.986 ± 0.006; mean ± S.D.; n = 4) and efficiencies (E = 0.95 ± 0.03) were obtained. Amplification of non-specific fragments after 40 cycles of PCR was low, as determined by agarose gel electrophoresis (Figure 4, top, left). Under the same conditions other DNA dyes also gave satisfactory results in the following order (based on regression coefficients): SGI > ResoLight > SYTO-9 > LCGreen > SYTO-13 > EvaGreen (Figure 4). Thus, Mix II-PT is unique in its capability to serve as universal qPCR mix for all DNA dyes tested.

PCR mix II-PT could be used with advantage not only for amplification of DNA fragments from crude blood samples that are difficult to amplify, but also for routine qPCR analysis of cDNA fragments without time-consuming adjustment of qPCR conditions for individual primer sets. Data presented in Figure 5A show that for amplification of 138 bp fragment of actin cDNA (58% GC) mix II-PT supplemented with SGI gave comparable regression coefficients and efficiencies as the routinely used LC 480 SGI. Similar results were obtained when GAPDH cDNA fragment was analyzed (Figure 5B; 52% GC, 69 bp). However, when low abundant cDNA fragments were amplified, such as ORMDL1_Fr.a

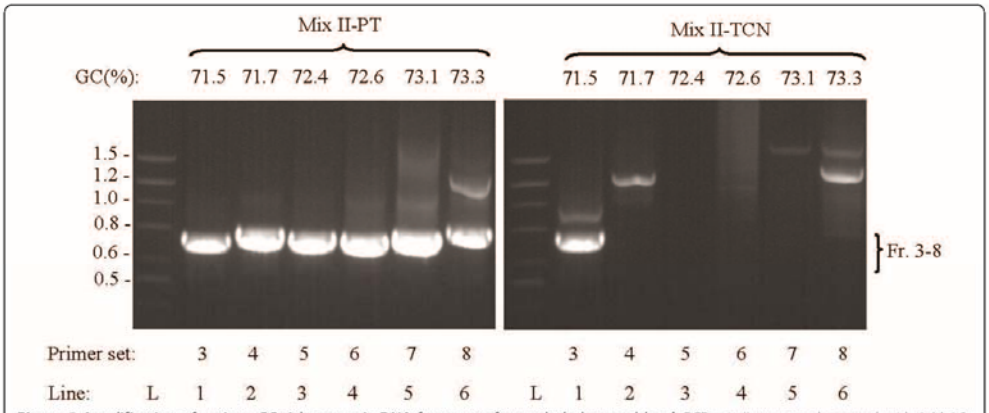

Figure 3 Amplification of various GC-rich genomic DNA fragments from whole human blood. PCR mix II was supplemented with 1 M 1,2-propanediol and 0.2 M trehalose (final concentrations; Mix II-PT) or 0.3 M trehalose, 0.24 M L-carnitine, and 0.4% Nonidet P-40 (Mix II-TCN). Various GC-rich templates from heparinized whole human blood (~100 copies of the template/μl of PCR mixture) were amplified in the two PCR mixes using primer sets specified in Table 4. Positions of the specific fragments (731-806 bp in size) are indicated on the right (Fr. 3-8). Lane L, DNA standard ladder with sizes indicated in kbp on the left. The numbers at the top indicate percentages of GCs in specific amplicons. A typical experiment of at least four performed is shown.

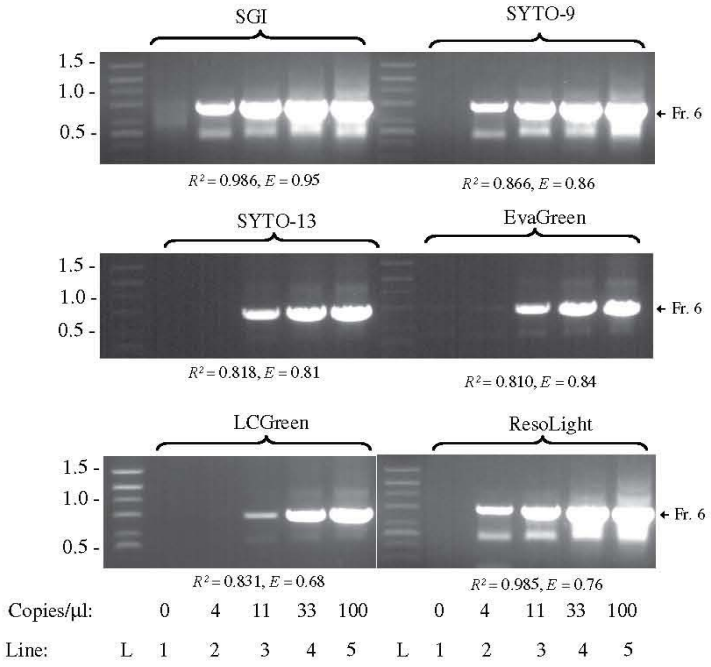

Figure 4 Amplification of GC-rich DNA fragment from whole blood in the presence of various DNA dyes. Human blood was diluted with mouse blood to yield 0, 4, 11, 33 and 100 copies of human Q8N4X1 gene per 1 µl of PCR reaction mix II supplemented with PT enhancer and various DNA dyes. Final concentration of human/mouse blood was 2% in all mixes. The samples were analyzed by qPCR followed by agarose gel electrophoresis and staining with ethidium bromide. Position of the specifically amplified DNA fragment is indicated by an arrow (Fr. 6). Lane L, DNA standard ladder with sizes indicated in kbp on the left. Regression coefficients (R^2) and efficiencies (E) were calculated from plots of Cq values versus log copy numbers. All samples were analyzed in 3-4 independent experiments with similar results.

(Figure 5C; 43% GC, 171 bp) or ORMDL1_Fr.b (Figure 5D; 47% GC, 205 bp), detectable amplification at all concentrations of template cDNA and reasonable regression coefficients and efficiencies were obtained only in mix II-PT-supplemented samples. Interestingly, addition of 1,2-propanediol and/or trehalose at various concentrations to LC 480 SGI containing chemically modified Taq DNA polymerase did not improve performance of this PCR mix, but instead had an inhibitory effect (data not shown).

Fluorescence measurements and melting temperatures

In our previous study we showed that SGI bound to ssDNA primers and suggested that the binding could at least in part contribute to the inhibitory effect of SGI in qPCR assays [5]. In further studies we evaluated whether trehalose and/or 1,2-propanediol could interfere with interaction of various DNA dyes with ssDNA, as reflected by changes in fluorescence signal. Data presented in Figure 6A indicate that interaction of various DNA dyes (at concentrations used for qPCR) with ssDNA oligonucleotide primer for tumor necrosis factor (TNF; 45.5% GC) induced fluorescence in the following order: SGI < SYTO-13 < LCGreen < SYTO-9 < EvaGreen < ResoLight. Addition of 0.2 M trehalose had little to no inhibitory effect on this fluorescence. In contrast, 1,2-propanediol significantly ($P < 0.05$; $n = 3$-5) decreased fluorescence in all DNA dyes used, except for SGI. Combination of both 1,2-propanediol and trehalose had a similar effect as 1,2-propanediol alone. When ssDNA primer No. 7, reverse (Table 4; 72.2% GC) was used, basal level of fluorescence was increased in all DNA dye-enhancer combinations and again trehalose had no significant effect on fluorescence intensity. In contrast to trehalose, 1,2-propanediol significantly ($P < 0.05$; $n = 4$) decreased fluorescence, except for SGI and ResoLight (Figure 6B).

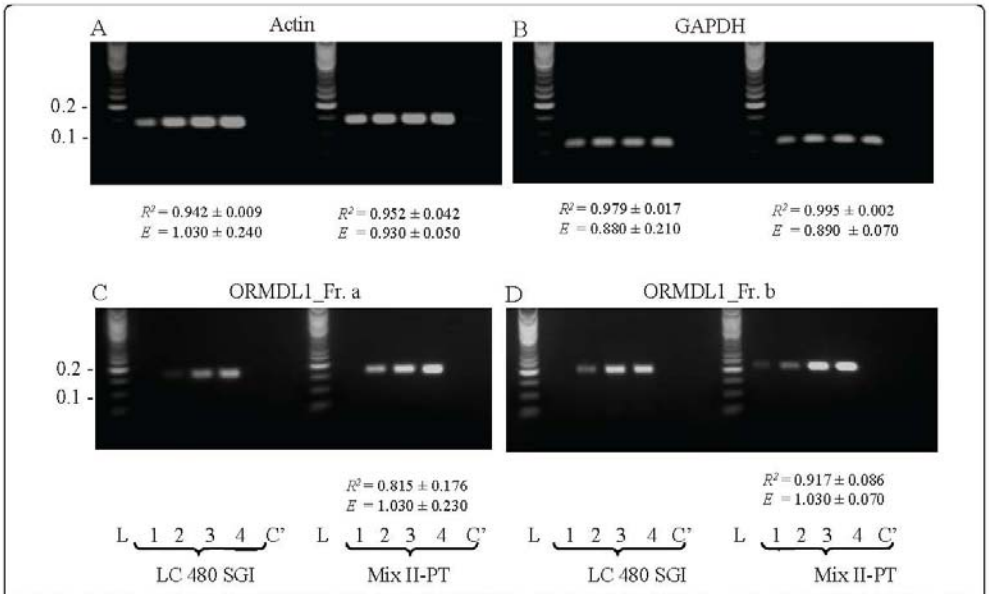

Figure 5 Enhanced performance of PCR mix II-PT in routine qPCR amplifications. cDNA from mouse bone marrow-derived mast cells was prepared, diluted 1:10^5 (1), 1:10^4 (2), 1:10^3 (3) or 1:10^2 (4) and amplified in SGI-supplemented PCR mix II-PT or LC 480 SGI using primer sets for Actin, GAPDH, ORMDL1_Fr. a or ORMDL1_Fr. b. In controls (C'), cDNA was replaced by H_2O. The samples were analyzed by qPCR followed by agarose gel electrophoresis and staining with ethidium bromide. Lane L, DNA standard ladder with sizes indicated in kbp on the left. Regression coefficients (R^2) and efficiencies (E) were calculated from the plots of Cq values versus log copy numbers and are presented only for samples with the expected melting temperature at all template dilutions. Data are presented as means ± S.D. calculated from three independent experiments performed in triplicates.

In an attempt to understand the enhancing effect of trehalose and 1,2-propanediol on qPCR performance, we also evaluated the melting temperatures of short dsDNA oligonucleotides. When dsDNA of TNF and anti-TNF (45.5% GC) was used, the melting temperature depended on DNA dye used (Figure 6C). The highest melting temperature was observed in control mix II supplemented with EvaGreen, followed by SGI > ResoLight > Syto-9 > LCGreen > Syto-13. Addition of 0.2 M trehalose decreased the melting temperature by 0.7 - 1.5°C, whereas addition of 1 M 1,2-propanediol decreased it by 4.9 - 5.9°C. When both trehalose and 1,2-propanediol were used, further decrease by 1.1 - 1.5°C was observed. Using dsDNA oligonucleotide with 72.2% GC, melting temperature was increased but a similar effect of trehalose and 1,2-propanediol was observed (Figure 6D).

Cooperative effect of 1,2-propanediol and trehalose

The above data suggested that 1,2-propanediol and trehalose have different roles in promoting DNA amplification of GC-rich DNA fragments from crude blood samples: trehalose mainly acts by neutralizing the inhibitory components present in blood, whereas 1,2-propanediol mainly acts by decreasing melting temperature. To prove this, we compared the effect of the enhancers on amplification of GC-rich fragments from whole blood or isolated DNA. As expected, efficient amplification of DNA template in whole blood, occurred only in samples supplemented with both 1,2-propanediol and trehalose (Figure 7A, line 3). In contrast, when isolated GC-rich DNA fragment was used as a template, comparable amplification was observed in samples supplemented with 1,2-propanediol alone or together with trehalose (Figure 7A, lines 6 and 7). Trehalose alone was not able to promote amplification of the DNA templates (Figure 7A, lines 1 and 5).

When PCR mix was supplemented with SGI and isolated DNA was amplified, a different picture was observed. SGI partially inhibited amplification in 1,2-propanediol-supplemented samples (Figure 7B, line 2). This inhibition was caused by SGI as indicated by no inhibition in samples containing vehicle (DMSO) instead of SGI (Figure 7B, line 6). PCR mixes supplemented with both 1,2-propanediol and trehalose exhibited an

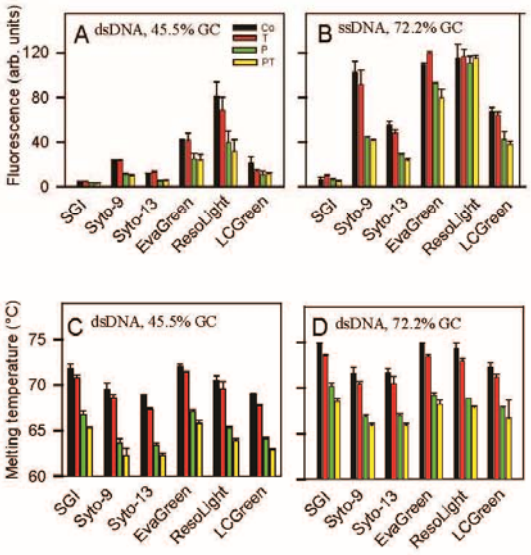

Figure 6 The effect of various DNA dyes and enhancers on ssDNA fluorescence and dsDNA melting temperature. (A) TNF-1 oligonucleotide (ssDNA, 45.5% GC; 1 μM final concentration) in PCR mix II (without dNTPs, Taq DNA polymerase and anti-Taq) was mixed with H_2O (Control; Co) or enhancers [0.2 M trehalose (T; final concentration), 1 M 1,2-propanediol (P) or both 1 M 1,2-propanediol and 0.2 M trehalose (PT)] and various DNA dyes at final concentrations as indicated in Table 1. After heating at 95°C for 2 min the samples were cooled to 50°C and fluorescence was determined using Mastercycler ep realplex. (B) Oligonucleotide primer No 7, reverse (ssDNA; 72.2% GC; 1 μM final concentration) in PCR mix II was combined with various additives and DNA dyes, and fluorescence at 50°C was determined as in A. (C) Oligonucleotide mixture of TNF-1 and anti-TNF-1 (dsDNA, 45.5% GC; 1 μM final concentration) was prepared in mix II supplemented with various additives and DNA dyes. The samples were heated to 95°C for 2 min, then cooled to 30°C and temperature-dependent changes in fluorescence were obtained during heating from 30 to 95°C (0.2°C increments) in Mastercycler ep realplex. Melting temperatures were determined from the melting curves. (D) Oligonucleotide mixture of the primer No 7, reverse, and the anti-primer 7 (dsDNA, 72.2% GC; final concentration 1 μM) was combined in mix II with additives and DNA dyes and analyzed as in C. Means ± S.D. were calculated from 3 - 5 measurements.

improved amplification in SGI-supplemented samples (Figure 7B, line 3) indicating cooperative effect of the enhancers in SGI-supplemented samples.

Next we tested the effect of trehalose and 1,2-propanediol on amplification of isolated DNA in samples supplemented with hemoglobin. Pilot experiments showed that hemoglobin completely inhibited PCR at concentrations 25 μM and higher (data not shown). Data in Figure 8A indicate that the inhibitory effect of hemoglobin (37.5 μM) was removed by addition 1,2-propanediol and trehalose together but not by trehalose or 1,2-propanediol alone.

To understand the effect of the enhancers on amplification in the presence of blood inhibitors, we analyzed melting temperatures of dsDNA. We found that hemoglobin at the inhibitory concentration (37.5 μM) significantly decreased melting temperature of short dsDNA fragments by 5.8 ± 0.6°C (mean ± S.D.; n = 4). Addition of trehalose, 1,2-propanediol or both enhancers to hemoglobin-supplemented samples further decreased Tm by 2.1 ± 1.6°C, 4.4 ± 0.6°C and 4.8 ± 0.6°C, respectively (Figure 8B). These data suggested direct or indirect interaction of hemoglobin with DNA. The direct interaction was however weak, if any, as indicated by similar mobility in agarose gel of DNA fragments alone and DNA fragments mixed with hemoglobin (37.5 μM; data not shown).

Finally, we tested whether blood inhibitors could interfere with enzymatic activity of Taq DNA polymerase as determined by incorporation of [α-^{32}P]dATP into activated salmon testes DNA. Data presented in Figure 8C indicate that blood at the inhibitory concentration (10%) significantly reduced activity of Taq DNA polymerase. Addition of trehalose significantly ($P < 0.05$) decreased the enzymatic activity of Taq DNA polymerase in control samples (- blood), but slightly increased the activity in blood-supplemented samples, leading to statistically non-significant differences between the

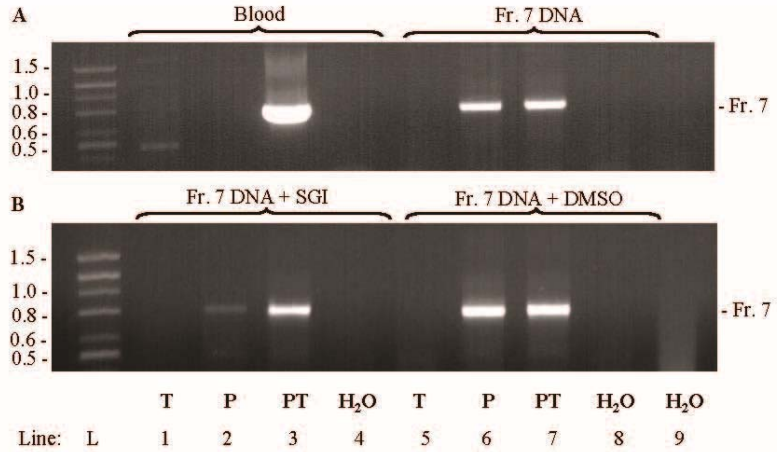

Figure 7 Cooperative effect of 1,2-propanediol and trehalose on amplification of difficult-to-amplify DNA templates. (A) DNA fragment of the human gene NP_001035158.1 (Fr. 7; 735 bp; 73.1% GC) was amplified from the whole blood (2% final) in PCR mix II supplemented with 0.2 M trehalose (T, final concentration), 1M 1,2-propanediol (P) or mixture of both (PT). Alternatively, PCR-amplified DNA (Fr. 7) was diluted in H_2O and used as a template for PCRs performed under various conditions as above. PCR mixes supplemented with H_2O instead of enhancers (line 4 and 8) and a mix without enhancers and template (line 9) served as controls. After amplification the fragments were analyzed by agarose gel electrophoresis and stained with ethidium bromide. (B) PCR amplified DNA (Fr. 7) was re-amplified and analyzed as in A, except that PCR mix II was supplemented with SGI (left) or vehicle (DMSO) alone (right). After amplification the fragments were analyzed by agarose gel electrophoresis and stained with ethidium bromide. Numbers to the left indicate migration of DNA ladder (L; in kbp). Gels from a typical experiment of at least four performed are shown.

control and blood-supplemented samples. 1,2-propanediol decreased enzymatic activity of Taq DNA polymerase in both control and blood-supplemented samples; the difference between these two groups was statistically significant. Addition of trehalose to 1,2-propanediol-supplemented control samples (PT) further significantly decreased ($P < 0.05$) the activity of Taq polymerase. In contrast, in blood-supplemented samples there was small (insignificant) increase in activity of Taq DNA polymerase in PT-containing samples compared to samples containing 1,2-propanediol alone. This led to non-significant differences between control and blood-containing samples with PT. These data indicate that trehalose has a different effect on activity of Taq polymerase in control and blood containing samples. This could explain at least in part the enhancing effect of trehalose in samples containing blood inhibitors.

Discussion

The aim of this study was to develop new qPCR mixes capable of amplifying difficult DNA templates, such as those in whole blood, of medium size and/or GC-rich, in the presence of various DNA dyes. First, we assessed the properties of seven different DNA dyes in four widely used PCR buffers differing in salt composition. Our data indicate that the performance of various DNA dyes in qPCR is differently affected by salt composition of the PCR mixes. When genomic DNA fragment of mouse Thy-1 (864 bp) was amplified, SGI completely inhibited PCR in most of the PCR mixes. The only PCR mix which allowed efficient amplification of the Thy-1 fragment in the presence of SGI was mix IV, which differed from other mixes by the presence of both KCl and $(NH_4)_2SO_4$ and the substitution of $MgSO_4$ for $MgCl_2$. This mix had pH 8.8, which also contributed to its performance; when pH of this mix was decreased to 8.0, SGI-mediated inhibition of PCR was noticed (data not shown). Besides pH, salt composition also plays a role because SGI completely inhibited amplification in PCR mix II, which has the same pH as mix IV. When other dyes were tested, amplification in mix IV was completely (EvaGreen) or partially (SYTO-9, SYTO-13, ResoLight) inhibited or remained unchanged (LCGreen and SYTO-82). In contrast to SGI, other dyes allowed amplification of the Thy-1 genomic fragment when present in PCR mix II. This mix is unique among others by containing 20 mM $(NH_4)_2SO_4$ instead of KCl, enhanced concentration of Tris-HCl (75 mM) and inclusion of Tween 20 instead of Triton X-100 (Table 2). It should be mentioned that all PCRs were run under identical cycling

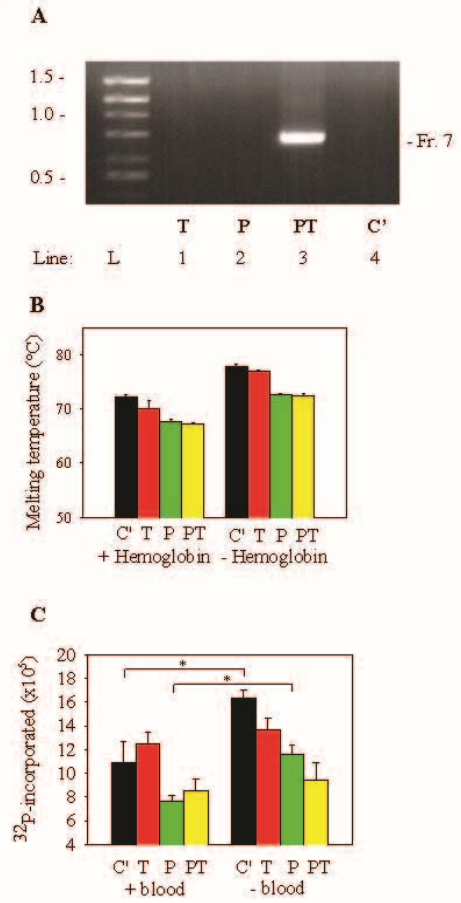

Figure 8 The effect of blood inhibitors and enhancers on PCR, melting temperature, and polymerase activity. (A) DNA fragment of NP_001035158.1 gene (Fr. 7; 735 bp; 73.1% GC) was amplified in PCR mix II supplemented with the corresponding primers, 37.5 μM hemoglobin and 0.2 M trehalose alone (T), 1 M 1,2 propanediol alone (P) or their combination (PT). PCR mix supplemented with H_2O instead of enhancers served as a control (C'). A typical experiment of four performed is shown. (B) Melting temperature of GC rich dsDNA oligonucleotide primer No 7, reverse, and the anti primer (72.2% GC; 1 μM final concentration) in the presence (+) or absence (-) of hemoglobin (37.5 μM) and various enhancers (as in A). Melting temperature was determined as in Figure 6, except that SGI was used at higher concentration (1.32 μM). (C) Enzymatic activity of Taq DNA polymerase in PCR mix II buffer supplemented with (+) or without (-) 10% blood and various enhancers (as in A). Samples supplemented with H_2O instead of enhancers (C') served as controls. Data in B and C indicate means ± S.D. (n = 4). Asterisks indicate statistically significant differences ($P < 0.05$).

conditions. Optimization of annealing temperature and cycling conditions for individual SGI-supplemented PCR mixes, however, resulted in no substantial improvement of PCR efficiency (data not shown). Neither was any improvement achieved by varying the concentration of Mg^{2+}. Since the concentrations of deoxynucleotide triphosphates (dNTPs), DNA polymerase and anti-Taq monoclonal antibody (mAb) were identical in all PCR mixes tested, it is likely that an interaction of DNA dye with ionic environment is responsible for the observed differences in qPCR performance. Both divalent and monovalent cations bind to DNA and affect its physical properties [31]. Thus, ionic environment and DNA dyes could affect DNA denaturation, annealing of oligonucleotide primers to the DNA template and/or activity of Taq DNA polymerase, including its enhanced mutation frequency which could inhibit PCR [14]. Our data indicate, however, that error rate was not dramatically affected and therefore it is unlikely that it could contribute to the observed differences in PCR mixes of different salt composition. Neither was fidelity of the Taq DNA polymerase affected by the presence of various DNA dyes.

Under more stringent conditions, such as amplification of medium-size GC-rich genomic fragments from crude blood samples, no amplification was observed in various commercial and home-made PCR mixes with or without DNA dye, and no dramatic improvement was achieved with additives and/or procedures recommended for amplification of GC-rich templates. These included supplementing PCR mixes with DMSO, betaine, trehalose, 1,2-propanediol or 7-deaza-2'-deoxyguanosine 5'-triphosphate, performing hot-start PCR under "touchdown" conditions, or with recently introduced PCR enhancing coctail containing trehalose, L-carnitin and Nonidet P-40 (Figure 3). It is likely that PCR product formation under such conditions was compromised by the presence of inhibitors present in blood (e g. hemoglobin), concurrently with inadequate strand separation due to higher GC content and/or formation of secondary structures reflecting Hoogsteen base pairing between successive guanosine bases. Furthermore, DNA templates may create intramolecular stem loops formed during initial cycles of amplification, leading to formation of hairpin structures that are resistant to amplification by Taq DNA polymerase in subsequent cycles of PCR [32].

Interestingly, strong and specific amplification was observed when PCR mix II was supplemented with both 1 M 1,2-propanediol and 0.2 M trehalose. This mix allowed efficient amplification in the presence of all DNA dyes tested, including SGI. Trehalose has been previously shown to enhance the yield of the amplified PCR products, and it has been speculated that it acts

through its thermostabilizing effect and/or lowering the template melting temperature [18,33]. However, it is unlikely that any of these two factors contributed individually to the observed effect of trehalose. In fact, the enzymatic activity of Taq DNA polymerase preincubated for 15 min at 95°C in mix II supplemented with 0.2 M trehalose (without blood inhibitors) was slightly decreased, rather than increased. Furthermore, although 0.2 M trehalose decreased melting temperature, this decrease was only marginal compared to the effect of other additives like DMSO or betaine which are routinely used as PCR enhancers.

1,2-propanediol at a final concentration 0.816 M has been recognized as an effective enhancer for amplification of medium-size GC-rich DNA sequences [24,34]. Although 1,2-propanediol surpassed 2.2 M betaine in its ability to amplify GC-rich templates [24] and decreased the melting temperature of dsDNA fragments (this study), it was unable on its own to surpass the inhibitory effect caused by the components present in the whole blood. Efficient amplification of such difficult-to-amplify templates was only achieved when 1,2-propanediol was combined with trehalose. It should be noted, that 1,2-propanediol slightly decreased enzymatic activity of Taq DNA polymerase. This inhibitory effect was however fully compensated by beneficial effects of 1,2-propanediol on PCR performance. Our finding of significant decrease of Taq DNA polymerase activity in samples supplemented with blood and even more with blood and 1,2-propanediol, and removal of this inhibitory effect after addition of trehalose suggest that trehalose acts by protecting the enzyme from negative interference of the blood inhibitors. Similarly, trehalose protected against the inhibitory effect of SGI, as indicated by enhanced amplification in the presence of both 1,2-propanediol and trehalose, compared to 1,2-propanediol alone.

In our previous study we found that SGI bound to ssDNA primers and interfered with annealing of the primers to DNA template; in this way SGI could, at least in part, contribute to its inhibitory effect on PCR [5]. In the present study we extended these tests to other DNA dyes and found that all of them bound to ssDNA oligonucleotides, as reflected by enhanced fluorescence. Importantly, for most of the dyes this binding was decreased by 1 M 1,2 propanediol. Extent of the inhibition depended on a combination of DNA dye used and GC content of the primers.

One of the PCR inhibitors present in blood is hemoglobin [17]. The inhibitory effect of hemoglobin on amplification of GC-rich DNA fragments was counteracted by addition of PT enhancer but not by 1,2-propanediol or trehalose alone. Although hemoglobin decreased melting temperature of dsDNA which was further decreased by the addition of 1,2-propanediol, it was still not sufficient for removal of its inhibitory effect. Interestingly, hemoglobin-containing samples supplemented with 1,2-propanediol or 1,2-propanediol and trehalose exhibited similar melting temperature, suggesting again that PT enhancer does not increase PCR performance solely by decreasing melting temperature.

Zhang and collaborators recently described a TCN coctail which in combination with inhibitor-resistant Taq DNA polymerase mutants enabled efficient amplification of high-GC content DNA targets directly from crude blood samples [27]. However, when wild-type Taq DNA polymerase was used for PCR with TCN, only a fraction of GC-rich DNA templates in whole blood was amplified. Under identical conditions, PCR mix supplemented with PT enhancer efficiently amplified all fragments analyzed in this study. These data indicate that PT is a superior enhancer for amplification of difficult templates when wild type Taq DNA polymerase is used. PT enhancer can be used as a universal enhancer suitable for normal targets, GC-rich targets (up to 79% GC) and/or targets in the presence of PCR inhibitors. PCR mix II supplemented with PT enhancer is suitable for DNA genotyping from whole blood without DNA extraction and is compatible with various DNA dyes. In order to get reasonable regression coefficients based on qPCR analyses of crude blood samples it is adviceable to dilute DNA templates present in human blood with e.g. mouse blood to keep the amount of the blood components in PCR constant. This will eliminate the problems with simultaneous dilution of the inhibitory (e.g. hemoglobin, immunoglobulins) and/or stimulatory (e.g. heparin) components which interfere with PCR performance, and/or recording of the fluorescence signal.

Conclusions

This study shows that a combination of 1 M 1,2-propanediol and 0.2 M trehalose represents a unique enhancer which can be combined with various DNA dyes. The enhancer can be used for amplification of various DNA templates, including those which are GC-rich and present in crude specimens, where other enhancers such as DMSO or betaine fail.

Methods

Reagents, antibodies and plasmids

The origin and properties of DNA dyes are specified in Table 1. DMSO was obtained from Fluka Chemie Gmbh (Buchs, Switzerland). Taq DNA polymerase was produced as described [5] or obtained together with buffers of various composition from several manufacturers (Fermentas, Vilnius, Lithuania; Sigma-Aldrich, Prague, Czech Republic; Promega, Madison, USA). All other

chemicals were from Sigma-Aldrich. The production of anti-Taq mAb which inhibits Taq DNA polymerase activity and is suitable for hot-start PCR has already been described [5]. The plasmid pMOL21 (4 kbp), carrying the *bla* gene for ampicillin resistance and *rpsL* gene, and *E. coli* K12 strain, MF101 [15], were obtained from Hisaji Maki (University of Tokyo, Japan).

qPCR

Most of the experiments were conducted with Mastercycler ep realplex (Eppendorf, AG, Hamburg, Germany) according to the manufacturer's instructions. Reactions were performed in 20 or 25 μl volumes in twin.tec 96 real-time PCR plates (Eppendorf) sealed with heat sealing film (Eppendorf). Amplifications of cDNAs were performed in 5 μl reaction volumes in 384-well plates sealed with LightCycler 480 sealing foil (Roche Diagnostics) using LightCycler 480 (Roche Diagnostics, Mannheim, Germany). PCR mixes of different salt composition (Table 2) were prepared according to Taq DNA polymerase manufacturer's protocols and/or literature data [5]. Oligonucleotide primers, DNA template, DNA dyes and additives/enhancers were added immediately before the assay. For comparison, we also used iQ™ SYBR Green Supermix (Bio-Rad Laboratories, Hercules, CA, USA) and LC 480 SGI (Roche Diagnostics). DNA dyes were prepared from stock solutions as recommended by manufacturers and/or previous studies [2,3] and as summarized in Table 1. Primers used for amplification of genomic DNA fragments are indicated in Table 4. For cDNA amplification, the following primers were used (forward/reverse, [accession number; fragment size, GC content]): actin, 5'-GATCTGGCACCACACCTTCT-3'/5'-GGGGTGTTGAAGGTCTCAAA-3', [NM_007393.2; 138 bp, 58% GC]; GAPDH, 5'-AACTTTGGCATTGTGGAAGG-3'/5'-ATCCACAGTCTTCTGGGTGG-3', [XM_001473623.1; 69 bp, 52% GC]; ORMDL1_Fr.a, 5'-GGATCAGGGTAGAGCAAGG-3'/5'-AGCAGAGAAGCTGTGTTTAGG-3', [NM_145517.4; 171 bp, 43% GC]; ORMDL1_Fr.b, 5'-ACTCGTGTAATGAACAGCCG-3'/5'-GCCTTGCTCTACCCTGATCC-3', [NM_145517.4; 205 bp, 47% GC]. For amplification of 864 bp genomic DNA fragment of mouse Thy-1 gene, thermal cycling consisted of 94°C/1 min | 30 × [94°C/15 s | 56°C/15 s | 72°C/1 min]. For amplification of human or mouse genomic DNA fragments from crude blood samples, the cycling conditions were: 95°C/10 min | 40 × [94°C/15 s | 58°C/30 s | 72°C/1 min]. For cDNA amplification the cycling conditions were: 95°C/3 min | 40 × [95°C/10 s | 60°C/20 s | 72°C/20 s]. Melting curve analysis was carried out from 50°C to 95°C with 0.2°C increments. In some experiments, DNA amplicons were size-fractionated in 1% or 2% agarose gels stained with ethidium bromide (0.5 μg/ml) and evaluated as described [35]. Quantification cycle (Cq) values [36] were determined by automated threshold analysis. PCR efficiencies (E) were determined from dilutions of DNA and calculated from the slopes of the standard curves according to the equation $E = 10^{-1/a} - 1$, where a is the slope of the corresponding standard curve.

Genomic DNA

Mouse genomic DNA was isolated from tails of C57BL/6J mice as previously described [37]. As a source of human genomic DNA, whole human blood was collected into heparin (20 U/ml), 0.38% sodium citrate or 2.7 mM EDTA, and stored in small aliquots at -70°C. All these experiments were approved by the ethical committee of the Institute of Molecular Genetics. The mass of the haploid mouse and human genome (C-value) is ~3.3 pg and ~3.5 pg, respectively [38]; this indicates that 1 ng of mouse or human genomic DNA contains approximately 303 and 286 copies of a single-copy gene. These numbers were used for generation of standard curve of Cq values from amplification plots versus log copy number.

RNA extraction and cDNA synthesis and analysis

RNA was extracted from mouse bone marrow-derived mast cells cultured under standard conditions [39] using RNeasy Mini Kit (Qiagen, Hilden, Germany). The amount of RNA was determined by spectrophotometer ND-100 (NanoDrop Technologies, Wilmington, DE). Single-stranded cDNA was synthesized by means of mouse moloney leukemia virus reverse transcriptase (Invitrogen, Carlsbad, CA, USA) according to manufacturer's instructions using 10 μg of isolated RNA and 50 ng of random hexamers per reaction.

Fluorescence measurements and melting temperature determination

PCR mix II without Taq DNA polymerase, dNTPs and anti-Taq antibody was supplemented with various additives/enhancers, DNA dyes and ssDNA oligonucleotide PCR primer TNF, 5'- TAAAACGACGGCCAGTGAATTC-3' (45.5% GC) or primer No 7, reverse (Table 4; 72.2% GC). The mixtures (25 μl) were transferred into white wells of the 96-well PCR plate, heat-sealed, and fluorescence reading was carried out on Mastercycler ep realplex (SGI filter set). The samples were heated at 95°C for 2 min, then cooled to 50°C and subjected to fluorescence reading. For determination of melting temperatures, the samples were prepared as above except that dsDNA was formed by adding oligonucleotide mixture of TNF and anti-TNF (5'-GAATTCACTGGCCGTCGTTTTA-3') or primer No 7, reverse (Table 4) and anti-primer No 7, reverse (5'-

AGACCCGCCTCACGAGCC-3'). In some experiments human hemoglobin (Sigma-Aldrich) at a final concentration 37.5 μM was also added. The samples were heated at 95°C for 2 min and then cooled to 30°C. Temperature-dependent changes in fluorescence obtained during heating from 30°C to 95°C (0.2°C increments) were determined by Mastercycler ep realplex. Melting temperatures were determined from melting curves.

DNA polymerase fidelity assay

The fidelity assay was based on streptomycin resistance of *rps*L mutants [15]. Standard PCRs (50 μl) containing mixes of different composition, as indicated in Table 2, were supplemented with 0.2 μM of each primer and 1 ng of template DNA (pMOL21 plasmid linearized with ScaI). In some experiments various DNA dyes at concentrations specified in Table 1 were also added. The PCR with KOD hot start polymerase was performed according to the manufacturer's instruction (Novagen, Darmstadt, Germany). The following primers were used: biotin-5'-AAAAACGCGTCACCAGTCACAGAAAAG-CATCTTAC-3' (forward sequence) and 5'-AAAAACGCGTCAACCAAGTCATTCTGAGAA-TAGT-3' (reverse sequence) [40]; MluI restriction sites are underlined. The standard PCR conditions were: 94°C for 2 min, followed by 25 cycles at 94°C for 15 s, 58°C for 30 s and 68°C for 5 min. The concentration of amplified DNA was determined by means of Quant-iT dsDNA HS Assay Kit (Invitrogen), and the number of template doublings was estimated. The PCR products were collected using streptavidin magnetic beads (Dynabeads M-280 Streptavidin, Invitrogen). Briefly, 100 μl aliquots of the beads were rinsed with washing solution (5 mM Tris-HCl, pH 7.5, 0.5 mM EDTA, 1 M NaCl), resuspended in 180 μl washing solution, combined with 20 μl of the PCR amplified DNA, and incubated under gentle rotation at room temperature. After 30 min, the beads were washed, resuspended in 100 μl of the corresponding enzyme mix and treated with 10 units of MluI at 37°C with gentle rotation overnight. The beads were collected using magnetic stand, and the supernatant was fractionated by electrophoresis in 0.8% agarose gel. The DNA fragment was isolated using TaKaRa Recochip (TaKaRa Biomedicals, Kyoto, Japan), precipitated in ethanol, lyophilized and dissolved in 20 μl of sterile water purified with Milli-Q Advantage A10 (Millipore, Molsheim, France). The purified DNA was self-ligated with T4 DNA ligase and transformed into MF101 competent cells. Half of the transformants were plated with ampicillin (100 μg/ml) to determine the total number of transformed cells; the remaining half on plates with ampicillin and streptomycin (100 μg/ml each) to determine the total number of *rps*L mutants. The mutation frequency was determined by dividing the total number of mutants by the total number of transformed cells. The error rate was calculated by dividing the mutation frequency by 130 (the number of amino acids that cause phenotypic changes in *rps*L), and the number of template doublings [15].

DNA polymerase activity

Activity of Taq DNA polymerase was assayed by measuring the conversion of radiolabeled dATP into acid insoluble DNA as previously described [41] with some modifications. Activated salmon testes DNA (Sigma-Aldrich) was prepared by exposing the DNA to low concentrations of pancreatic DNase [42]. Reaction mixture (100 μl) contained DNA polymerase 50 U/ml, 75 mM Tris-HCl, pH 8.8, 20 mM $(NH_4)_2SO_4$, 0.01% Tween 20, 2.5 mM $MgCl_2$, 100 μM dATP, 200 μM dGTP, 200 μM dCTP, 200 μM dTTP, activated salmon testes DNA (0.2 mg/ml), and various additives [10% (final concentration) human sodium citrate-treated blood, 0.2 M trehalose and/or 1 M 1,2-propanediol]. The samples were denatured for 15 min at 95°C then cooled to 72°C and supplemented with [α-^{32}P]dATP (14.8 kBq; 111TBq/mmol; MP Biomedicals, Irvine, CA). The mixtures were incubated for 30 min at 72°C and the reactions were then stopped by the addition of 100 μl of stop solution (150 mM sodium pyrophosphate and 100 mM EDTA, pH 8.0). DNA was precipitated by the addition of 150 μl of ice-cold 25% trichloracetic acid. After 15 min on ice, the samples were vacuum filtered on type A/E glass fiber filters (25 mm; Pall Corporation, Ann Arbor, MI) pre-wet with stop solution. Precipitated DNA retained on the disc was washed with 5 ml ice-cold 10% trichloracetic acid followed by 10 ml of ice-cold 96% ethanol. The filters were air dried and the radioactivity was measured in 10 ml scintillation fluid BetaMax ES (MP Biomedicals) in a scintillation counter with QuantaSmart software (Perkin Elmer, Waltham, MA).

Statistical analysis

Statistical analysis of intergroup differences was performed using Student's t-test.

List of abbreviations

qPCR: quantitative real-time PCR; SGI: SYBR green I; PT enhancer: 1 M 1,2-propanediol and 0.2 M trehalose; ds: double-stranded; ss: single-stranded; bp: base pairs; LC 480 SGI: LightCycler 480 SYBR Green I Master; DMSO: dimethyl sulfoxide ; TCN: 0.3 M D-(+)-trehalose, 0.24 M L-carnitine, and 0.4% Nonidet P-40; TNF: tumor necrosis factor; dNTP: deoxynucleotide triphosphate; mAb: monoclonal antibody; Cq: quantification cycle; E: efficiency.

Acknowledgements

This project was supported by the Academy of Sciences of the Czech Republic [KAN200520701, M200520901, Institutional Project AVOZ50520514] and grant 204/09/H084, 301/091826 and P302/10/1759 from Grant Agency of the Czech Republic. I. P. was supported by a stipend from the Ministry of Education, Youth, and Sports of the Czech Republic and Specific University

Research Project No. 33779266 awarded by Charles University, Prague. The authors thank Hisaji Maki for kindly providing the pMOL21 plasmid and MF101 competent cells, and Lukáš Kocanda and Hanka Mrázová for skilled technical assistance.

Authors' contributions

HH carried out experiments with PT enhancers. IP performed DNA polymerase fidelity assays and wrote the corresponding part of the manuscript. GMS carried out the experiments presented in Figure 1. JE performed the experiments presented in Figure 5. VB conceived the experiments with cDNA analysis and wrote the corresponding part. LD and PD conceived the study and wrote the manuscript. All authors read and approved the final manuscript.

Competing interests

The authors declare that they have no competing interests.

Received: 4 December 2010 Accepted: 18 April 2011
Published: 18 April 2011

References

1. Bustin SA: *A-Z of Quantitative PCR* International University Line. La Jolla, California; 2004.
2. Zipper H, Brunner H, Bernhagen J, Vitzthum F: **Investigations on DNA intercalation and surface binding by SYBR Green I, its structure determination and methodological implications.** *Nucleic Acids Res* 2004, **32**(12):e103.
3. Mao F, Leung WY, Xin X: **Characterization of EvaGreen and the implication of its physicochemical properties for qPCR applications.** *BMC Biotechnol* 2007, **7**:76.
4. Monis PT, Giglio S, Saint CP: **Comparison of SYTO9 and SYBR Green I for real-time polymerase chain reaction and investigation of the effect of dye concentration on amplification and DNA melting curve analysis.** *Anal Biochem* 2005, **340**(1):24-34.
5. Shaik GM, Draberova L, Draber P, Boubelik M, Draber P: **Tetraalkylammonium derivatives as real-time PCR enhancers and stabilizers of the qPCR mixtures containing SYBR Green I.** *Nucleic Acids Res* 2008, **36**(15):e93.
6. Higuchi R, Dollinger G, Walsh PS, Griffith R: **Simultaneous amplification and detection of specific DNA sequences.** *Biotechnology (N Y)* 1992, **10**(4):413-7.
7. Wittwer CT, Herrmann MG, Moss AA, Rasmussen RP: **Continuous fluorescence monitoring of rapid cycle DNA amplification.** *BioTechniques* 1997, **22**(1):130-8.
8. Ishiguro T, Saitoh J, Yawata H, Yamagishi H, Iwasaki S, Mitoma Y: **Homogeneous quantitative assay of hepatitis C virus RNA by polymerase chain reaction in the presence of a fluorescent intercalater.** *Anal Biochem* 1995, **229**(2):207-13.
9. Bengtsson M, Karlsson HJ, Westman G, Kubista M: **A new minor groove binding asymmetric cyanine reporter dye for real-time PCR.** *Nucleic Acids Res* 2003, **31**(8):e45.
10. Wittwer CT, Reed GH, Gundry CN, Vandersteen JG, Pryor RJ: **High-resolution genotyping by amplicon melting analysis using LCGreen.** *Clin Chem* 2003, **49**(6):853-60.
11. Gudnason H, Dufva M, Bang DD, Wolff A: **Comparison of multiple DNA dyes for real-time PCR: effects of dye concentration and sequence composition on DNA amplification and melting temperature.** *Nucleic Acids Res* 2007, **35**(19):e127.
12. Takano EA, Mitchell G, Fox SB, Dobrovic A: **Rapid detection of carriers with BRCA1 and BRCA2 mutations using high resolution melting analysis.** *BMC Cancer* 2008, **8**:59.
13. Mackay JF, Wright CD, Bonfiglioli RG: **A new approach to varietal identification in plants by microsatellite high resolution melting analysis: application to the verification of grapevine and olive cultivars.** *Plant Methods* 2008, **4**:8.
14. Barnes WM: **PCR amplification of up to 35-kb DNA with high fidelity and high yield from λ bacteriophage templates.** *Proc Natl Acad Sci USA* 1994, **91**(6):2216-20.
15. Fujii S, Akiyama M, Aoki K, Sugaya Y, Higuchi K, Hiraoka M, Miki Y, Saitoh N, Yoshiyama K, Ihara K, Seki M, Ohtsubo E, Maki H: **DNA replication errors produced by the replicative apparatus of Escherichia coli.** *J Mol Biol* 1999, **289**(4):835-50.
16. Al-Soud WA, Jönsson LJ, Rådström P: **Identification and characterization of immunoglobulin G in blood as a major inhibitor of diagnostic PCR.** *J Clin Microbiol* 2000, **38**(1):345-50.
17. Al-Soud WA, Rådström P: **Purification and characterization of PCR-inhibitory components in blood cells.** *J Clin Microbiol* 2001, **39**(2):485-93.
18. Spiess AN, Mueller N, Ivell R: **Trehalose is a potent PCR enhancer: lowering of DNA melting temperature and thermal stabilization of Taq polymerase by the disaccharide trehalose.** *Clin Chem* 2004, **50**(7):1256-9.
19. Sidhu MK, Liao MJ, Rashidbaigi A: **Dimethyl sulfoxide improves RNA amplification.** *BioTechniques* 1996, **21**(1):44-7.
20. Jung M, Muche JM, Lukowsky A, Jung K, Loening SA: **Dimethyl sulfoxide as additive in ready-to-use reaction mixtures for real-time polymerase chain reaction analysis with SYBR Green I dye.** *Anal Biochem* 2001, **289**(2):292-5.
21. Weissensteiner T, Lanchbury JS: **Strategy for controlling preferential amplification and avoiding false negatives in PCR typing.** *BioTechniques* 1996, **21**(6):1102-8.
22. Henke W, Herdel K, Jung K, Schnorr D, Loening SA: **Betaine improves the PCR amplification of GC-rich DNA sequences.** *Nucleic Acids Res* 1997, **25**(19):3957-8.
23. Baskaran N, Kandpal RP, Bhargava AK, Glynn MW, Bale A, Weissman SM: **Uniform amplification of a mixture of deoxyribonucleic acids with varying GC content.** *Genome Res* 1996, **6**(7):633-8.
24. Zhang Z, Yang X, Meng L, Liu F, Shen C, Yang W: **Enhanced amplification of GC-rich DNA with two organic reagents.** *BioTechniques* 2009, **47**(3):775-9.
25. Motz M, Paabo S, Kilger C: **Improved cycle sequencing of GC-rich templates by a combination of nucleotide analogs.** *BioTechniques* 2000, **29**(2):268-70.
26. Musso M, Bocciardi R, Parodi S, Ravazzolo R, Ceccherini I: **Betaine, dimethyl sulfoxide, and 7-deaza-dGTP, a powerful mixture for amplification of GC-rich DNA sequences.** *J Mol Diagn* 2006, **8**(5):544-50.
27. Zhang Z, Kermekchiev MB, Barnes WM: **Direct DNA amplification from crude clinical samples using a PCR enhancer cocktail and novel mutants of taq.** *J Mol Diagn* 2010, **12**(2):152-61.
28. Don RH, Cox PT, Wainwright BJ, Baker K, Mattick JS: **'Touchdown' PCR to circumvent spurious priming during gene amplification.** *Nucleic Acids Res* 1991, **19**(14):4008.
29. Hubé F, Reverdiau P, Iochmann S, Gruel Y: **Improved PCR method for amplification of GC-rich DNA sequences.** *Mol Biotechnol* 2005, **31**(1):81-4.
30. Kermekchiev MB, Kirilova LI, Vail EE, Barnes WM: **Mutants of Taq DNA polymerase resistant to PCR inhibitors allow DNA amplification from whole blood and crude soil samples.** *Nucleic Acids Res* 2009, **37**(5):e40.
31. Owczarzy R, Moreira BG, You Y, Behlke MA, Walder JA: **Predicting stability of DNA duplexes in solutions containing magnesium and monovalent cations.** *Biochemistry* 2008, **47**(19):5336-53.
32. McDowell DG, Burns NA, Parkes HC: **Localised sequence regions possessing high melting temperatures prevent the amplification of a DNA mimic in competitive PCR.** *Nucleic Acids Res* 1998, **26**(14):3340-7.
33. Carninci P, Nishiyama Y, Westover A, Itoh M, Nagaoka S, Sasaki N, Okazaki Y, Muramatsu M, Hayashizaki Y: **Thermostabilization and thermoactivation of thermolabile enzymes by trehalose and its application for the synthesis of full length cDNA.** *Proc Natl Acad Sci USA* 1998, **95**(2):520-4.
34. Chakrabarti R, Schutt C: **Chemical PCR: Composition for enhancing polynucleotide amplification reactions.** *US patent 7772383* 2004.
35. Kovárová M, Dráber P: **New specificity and yield enhancer of polymerase chain reactions.** *Nucleic Acids Res* 2000, **28**(13):e70.
36. Bustin SA, Benes V, Garson JA, Hellemans J, Huggett J, Kubista M, Mueller R, Nolan T, Pfaffl MW, Shipley GL, Vandesompele J, Wittwer CT: **The MIQE guidelines: minimum information for publication of quantitative real-time PCR experiments.** *Clin Chem* 2009, **55**(4):611-22.
37. Wolff R, Gemmill R: **Purifying and Analyzing Genomic DNA.** In *Genome Analysis: A Laboratory Manual.* Edited by: Birren B, Green ED, Klapholz S, Myers RM, Roskams J. Cold Spring Harbor, New York, NY, Cold Spring Harbor Laboratory Press; 1977:1-81.
38. Gregory TR: **Animal Genome Size Database.** 2010 [http://www.genomesize.com].
39. Volná P, Lebduška P, Dráberová L, Šimová S, Heneberg P, Boubelik M, Bugajev V, Malissen B, Wilson BS, Hořejší V, Malissen M, Dráber P: **Negative**

Regulation of Mast Cell Signaling and Function by the Adaptor LAB/NTAL. *J Exp Med* 2004, **200(8)**:1001-13.
40. Lackovich KK, Lee JE, Chang P, Rashtchian A: Measuring the fidelity of Platinum Pfx DNA polymerase. *Focus* 2001, **23**:6-7.
41. Scalice ER, Sharkey DJ, Daiss JL: Monoclonal antibodies prepared against the DNA polymerase from Thermus aquaticus are potent inhibitors of enzyme activity. *J Immunol Methods* 1994, **172(2)**:147-63.
42. Aposhian HV, Komberg A: Enzymatic synthesis of deoxyribonucleic acid. IX. The polymerase formed after T2 bacteriophage infection of Escherichia coli: a new enzyme. *J Biol Chem* 1962, **237(2)**:519-25.

doi:10.1186/1472-6750-11-41
Cite this article as: Horáková *et al.*: 1,2-propanediol-trehalose mixture as a potent quantitative real-time PCR enhancer. *BMC Biotechnology* 2011 11:41.

Molecular targets on mast cells and basophils for novel therapies

J Allergy Clin Immunol. 2014 Apr 23. pii: S0091-6749(14)00428-X.

Molecular targets on mast cells and basophils for novel therapies

Ilkka T. Harvima, MD, PhD,[a] Francesca Levi-Schaffer, PharmD, PhD,[b] Petr Draber, PhD,[c] Sheli Friedman, MSc,[b] Iva Polakovicova, MSc,[c] Bernhard F. Gibbs, PhD,[d] Ulrich Blank, PhD,[e,f] Gunnar Nilsson, PhD,[g] and Marcus Maurer, MD[h]

Kuopio, Finland, Jerusalem, Israel, Prague, Czech Republic, Kent, United Kingdom, Paris, France, Stockholm, Sweden, and Berlin, Germany

Mast cells and basophils (MCs/Bs) play a crucial role in type I allergy, as well as in innate and adaptive immune responses. These cells mediate their actions through soluble mediators, some of which are targeted therapeutically by, for example, H1- and H2-antihistamines or cysteinyl leukotriene receptor antagonists. Recently, considerable progress has been made in developing new drugs that target additional MC/B mediators or receptors, such as serine proteinases, histamine 4-receptor, 5-lipoxygenase–activating protein, 15-lipoxygenase-1, prostaglandin D_2, and proinflammatory cytokines. Mediator production can be abrogated by the use of inhibitors directed against key intracellular enzymes, some of which have been used in clinical trials (eg, inhibitors of spleen tyrosine kinase, phosphatidylinositol 3-kinase, Bruton tyrosine kinase, and the protein tyrosine kinase KIT). Reduced MC/B function can also be achieved by enhancing Src homology 2 domain–containing inositol 5′ phosphatase 1 activity or by blocking sphingosine-1-phosphate. Therapeutic interventions in mast cell–associated diseases potentially include drugs that either block ion channels and adhesion molecules or antagonize antiapoptotic effects on B-cell lymphoma 2 family members. MCs/Bs express high-affinity IgE receptors, and blocking their interactions with IgE has been a prime goal in antiallergic therapy. Surface-activating receptors, such as CD48 and thymic stromal lymphopoietin receptors, as well as inhibitory receptors, such as CD300a, FcγRIIb, and endocannabinoid receptors, hold promising therapeutic possibilities based on preclinical studies. The inhibition of activating receptors might help prevent allergic reactions from developing, although most of the candidate drugs are not sufficiently cell specific. In this review recent advances in the development of novel therapeutics toward different molecules of MCs/Bs are presented. (J Allergy Clin Immunol 2014;134:530-44.)

Key words: *Mast cell, basophil, mediator, receptor, signaling protein, survival protein, drug, therapy*

Mast cells and basophils (MCs/Bs) have traditionally been associated with the induction of symptoms of type I type allergies, such as rhinitis, asthma, and urticaria, through the release of soluble proinflammatory mediators. However, this notion is an oversimplification given the growing evidence during the last 2 decades that both cell types can contribute to

From [a]the Department of Dermatology and Cancer Center of Eastern Finland, University of Eastern Finland and Kuopio University Hospital; [b]the Department of Pharmacology and Experimental Therapeutics, School of Pharmacy, Institute for Drug Research, Faculty of Medicine, Hebrew University of Jerusalem; [c]the Department of Signal Transduction, Institute of Molecular Genetics, Academy of Sciences of the Czech Republic, Prague; [d]the Medway School of Pharmacy, University of Kent; [e]INSERM UMRS 699, Paris; [f]Université Paris Diderot, Sorbonne Paris Cité, Laboratoire d'excellence INFLAMEX, Paris; [g]Clinical Immunology and Allergy, Department of Medicine, Karolinska Institutet, Stockholm; and [h]the Department of Dermatology and Allergy, Allergie-Centrum-Charité, Charité-Universitätsmedizin Berlin.

Supported by the COST Action BM1007 "Mast cells and Basophils: targets for innovative therapies." I.T.H. was supported, in part, by the Cancer Center of Eastern Finland and VTR funding of Kuopio University Hospital. F.L.-S.'s research is supported, in part, by grants from the Israel Science Foundation (grant 213/05); the MAARS (Microbes in Allergy and Autoimmunity Related to the Skin) EU 7th framework (grant no. HEALTH-F2-2011-261366); and the Aimwell Charitable Trust (London, United Kingdom). P.D. and I.P. were supported, in part, by project COST CZ LD12073 from Ministry of Education of the Czech Republic and grants 14-00703S, 14-09807S, and P302/12/G101 from the Czech Science foundation and by the Institute of Molecular Genetics ASCR (RVO 68378050). I.P. was supported in part by the Faculty of Science, Charles University, Prague. U.B is supported by the French National Research Agency (ANR-12-ISV3-0006-01), the Investissements d'Avenir programme ANR-11-IDEX-0005-02, Sorbonne Paris Cite, Laboratoire d'excellence INFLAMEX.

Disclosure of potential conflict of interest: I. T. Harvima has received travel support from the European Union COST action BM1007 and is employed by the University of Eastern Finland and Kuopio University Hospital. F. Levi-Schaffer has received research support from the Israel Science Foundation and the European Union FP7 Collaborative Project; has received travel support from the European Union COST action BM1007; has a patent for CD48 as a novel target for antiasthmatic and antiallergic therapy and as a marker for early prediction of allergy issued; has a patent for bispecific complexes for targeting cells involved in allergic-type reactions, compositions, and uses thereof issued; and has a patent on sialic acid–binding immunoglobulin-like lectin 7 and treatment of mast cell–related pathologies pending. P. Draber has received research support from the Ministry of Education of the Czech Republic, the Czech Science Foundation, and the Institute of Molecular Genetics ASCR and has received travel support from the European Union COST action BM1007. I. Polakovicova has received research support from the Ministry of Education of the Czech Republic, the Czech Science Foundation, and the Faculty of Science of Charles University and has received travel support from the European Union COST action BM1007. B. F. Gibbs has received travel support from the European Union COST action BM1007; is employed by the University of Kent; has received research support from Leverhulme Trust; and has received payment for lectures from the University of Virginia, Southampton, Kings College London, and ALK-Abelló. U. Blank has received research support from the French National Research Agency and the Investissements d'Avenir programme ANR-11-IDEX-0005-02, Sorbonne Paris Cite, Laboratoire d'excellence INFLAMEX and has received travel support from the European Union COST action BM1007. G. Nilsson has received research support from the Swedish Research Council and has received travel support from the European Union COST action BM1007. M. Maurer has received research support from Charit; has received travel support from the European Union COST action BM1007; has consultant arrangements from Almirall, Bayer, Biofrontera, FAES, Genentech, GlaxoSmithKline, Recordati, Novartis, Sanofi Aventis, Merck Sharp Dohme, Moxie, UCB, and Uriach; is employed by Charité–Universitätsmedizin Berlin; and has received research support from FAES, Genentech, Novartis, Merck Sharp Dohme, Moxie, UCB, and Uriach. S. Friedman declares no relevant conflicts of interest.

Received for publication December 20, 2013; revised February 24, 2014; accepted for publication March 7, 2014.

Available online April 24, 2014.

Corresponding author: Ilkka T. Harvima, MD, PhD, Department of Dermatology, Kuopio University Hospital, POB 100, 70029 KYS, Kuopio, Finland. E-mail: ilkka.harvima@kuh.fi.

0091-6749/$36.00

http://dx.doi.org/10.1016/j.jaci.2014.03.007

Abbreviations used
BCL-2: B-cell lymphoma 2
BH: BCL-2 homology
Bs: Basophils
BTK: Bruton tyrosine kinase
CB: Endocannabinoid receptor
CRAC: Calcium release–activated calcium
cysLTR: Cysteinyl leukotriene receptor
DP: D-type prostanoid receptor
FLAP: 5-Lipoxygenase–activating protein
ITIM: Immunoreceptor tyrosine–based inhibitory motif
5-LO: 5-Lipoxygenase
15-LO-1: 15-Lipoxygenase-1
LT: Leukotriene
MC: Mast cell
MC/B: Mast cell and basophil
MMP: Matrix metalloproteinase
PGD_2: Prostaglandin D_2
PI3K: Phosphatidylinositol 3-kinase
SHIP-1: Src homology 2 domain-containing inositol 5′ phosphatase 1
Siglec: Sialic acid–binding immunoglobulin-like lectin
S1P: Sphingosine-1-phosphate
SPHK: Sphingosine kinase
SYK: Spleen tyrosine kinase
TRP: Transient receptor potential
TSLP: Thymic stromal lymphopoietin
TSLPR: Thymic stromal lymphopoietin receptor

inflammation, autoimmunity, chronic innate immune responses, and other conditions, as well as performing immunomodulatory roles.[1-3]

Two of the key soluble mediators released by MCs/Bs on activation by different stimuli are histamine and leukotrienes (LTs). Both are commonly targeted in clinical practice by various drugs, such as H1- and H2-antihistamines and LTC_4 synthesis inhibitors or receptor antagonists. Indeed, the treatment of different diseases or symptoms with these classes of drugs has generally been regarded as a success. However, there are numerous patients with MC/B-driven diseases who do not obtain sufficient relief of their symptoms, even after administration of high doses of the above drug classes. One of the reasons for this is that MCs/Bs release other preformed and *de novo*–synthesized mediators that also contribute to the pathogenesis of MC/B-mediated conditions.[1-3]

Approaches to improve the treatment of MC/B-driven conditions include the development of inhibitors of additional MC/B mediators and their receptors and of inhibitors of MC/B-activating receptors and signal transduction pathways. Recently, MCs/Bs have been shown to express inhibitory receptors that, on activation, are able to downregulate the stimulatory signaling derived from activating receptors. For example, FcγRIIB, CD300, endocannabinoid receptor (CB) 1, CD72, and sialic acid–binding immunoglobulin-like lectins (Siglecs) have been described on mast cells (MCs) and might be promising targets for therapy.[4] In addition, MC/B activation can be blocked by inhibitors that act on signaling pathways transduced from plasma membrane receptors to cytoplasmic effectors. However, most of the signaling pathways used by MCs/Bs are not found exclusively in these cells.[5,6]

A therapy for disease should target only those cells and molecules that are specifically involved in the pathogenesis of that particular disease. However, in patients with allergy, as in those with many other diseases, several different cell types are involved in causing symptoms, and therefore a number of potential targets exist. The problem of selectivity and trying to hit multiple targets simultaneously increases potential side effects and adverse drug reactions. Despite this, in allergic patients the main *primum movens* are the MCs,[1] but growing evidence indicates an important role for Bs as well.[2]

During the last decade, considerable progress has been made targeting soluble mediators released from MCs/Bs. In addition, promising target molecules have been discovered among cell-surface receptors and intracellular signaling or survival molecules. Therefore in this review we focus on these mediators, receptors, and signaling molecules of MCs/Bs as targets for pharmacotherapy, especially those that are close to clinical application.

SOLUBLE MEDIATORS AS TARGETS

Proteinases

β-Tryptase, a tetrameric serine proteinase, is the major protein within the secretory granules of MCs. However, Bs can contain a small amount of β-tryptase.[1,7] The pathophysiologic role of β-tryptase is not clear, but the enzyme has been associated with the promotion of inflammation and matrix remodeling.[1,8] An essential new proteolytic target of β-tryptase is the proteinase-activated receptor 2, which is expressed by different inflammatory cells.[1,8] Several synthetic inhibitors have been produced since the 1990s,[9,10] such as APC-366 and dibasic APC-2059, which have been used in clinical trials. In a randomized, double-blind cross-over study of 16 atopic asthmatic patients, inhaled APC-366 significantly inhibited allergen-induced late asthmatic responses.[11] In an open-label phase 2 pilot study, subcutaneously injected APC-2059 displayed efficacy in the treatment of ulcerative colitis.[12] Nafamostat mesilate, a drug used in the therapy of disseminated intravascular coagulation and pancreatitis, is a further candidate for inhibiting tryptase because of its inhibitory potency toward this proteinase, although it is not specific.[13] Nevertheless, despite positive expectations in the 1990s, specific tryptase inhibitors have thus far not appeared on the market. Future therapeutic approaches to inhibit tryptase might include designing molecules that are able to displace tryptase from heparin, leading to dissociation of the tryptase tetramer into monomers with low catalytic activity.[14]

Chymase is a chymotrypsin-like serine proteinase stored in high quantities in the secretory granules of the MC_{TC} (tryptase$^+$, chymase$^+$) type of MCs.[8] Unlike tryptase, chymase can be inactivated by endogenous protease inhibitors, and therefore chymase is under the control of protease inhibitors in inflamed tissue.[15,16] If left uncontrolled by inhibitors, chymase is a potent enzyme that causes matrix destruction[8,16] and inflammation, as well as producing angiotensin II from angiotensin I, suggesting a role in hypertension and cardiac failure.[8,17] Several potent chymase inhibitors have been synthesized and tested in a variety of animal and *ex vivo* models with proven physiologic effect.[17,18] However, clinical studies with chymase inhibitors are still lacking. The secretory granules of MC_{TC} cells also contain another chymotrypsin-like serine proteinase, cathepsin G,[8] and several existing chymase inhibitors also inhibit cathepsin G to some

extent.[17] Because chymase and cathepsin G share many similar biological functions, it might be therapeutically useful to develop inhibitors that inactivate both enzymes simultaneously, such as RWJ-355871, which has shown efficacy in rat, mouse, and sheep models of lung or paw inflammation.[19]

Human MCs can be a source of matrix metalloproteinases (MMPs), especially MMP-1 and MMP-9.[20,21] The clinical trials performed thus far with MMP inhibitors have been rather disappointing, especially in patients with cancer, because of their adverse effects, low specificity, or both.[22] However, targeting chymase in therapy might prevent the activation of the latent forms of MMP-1 and MMP-9.[23,24] Additionally, targeting tryptase might prevent the activation of prostromelysin to stromelysin (MMP-3) and subsequent activation of MMP-1.[25]

Histamine and histamine receptors

Histamine, a preformed mediator in MCs/Bs, has long been proven to be a critical factor in the cause and therefore treatment of allergy. Histamine has 4 distinct G protein–coupled receptors, histamine receptors 1-4 (H1-4R). H1R, discovered in 1937 by Bovet and Staub, is the major histamine receptor in allergies, whereas H4R was discovered some 12 years ago and has not been studied extensively as a therapeutic target.[26] H1-antihistamines are inverse agonists and are currently the most used antiallergic drugs, such as in patients with urticaria, atopic dermatitis, allergic rhinitis, and conjunctivitis, as well as in asthmatic patients.

In addition to its effects on vascular endothelial cells, T cells, and other cells, histamine also has autocrine effects on MCs through H1R and H4R. It has recently been shown that a combination of antihistamines targeting H1R and H4R has synergistic therapeutic effects in a mouse model of chronic dermatitis.[27] At high doses, H1-antihistamines can also reduce MC functions, acting as MC stabilizers.[28-30]

H2R agonists have been shown to mimic the inhibitory effects of histamine on MCs activated by compound 48/80, actions that were reversed by an H2R blocker.[31] The H2R-mediated inhibitory actions of histamine seem to be more prominent in Bs than in MCs,[32-34] where the receptor has been shown to be involved in early suppression of the release of all known major mediator classes during venom-specific allergen immunotherapy.[35]

H3R and H4R share high sequence homology, and some pharmacologic agonists and antagonists affect both receptors. In Bs H3R does not seem to affect function.[36,37] Although H4R expression has been shown on mature human MCs/Bs,[38,39] thus far, there is no clear evidence for a role of this receptor in controlling mediator release. Nevertheless, several experimental models suggest that H4R can modulate the function of MCs, Bs, or both.[39-41] H4R antagonists/inverse agonists are plausible new drugs for treating allergic diseases,[42] even though contradictory results in experimental models of atopic dermatitis have recently been published.[43] Systemic treatments are currently being tested in clinical trials (reviewed by Salcedo et al[44]), although the research has been progressing rather slowly. Future therapeutic applications might include combinations with H1-antihistamines, such as in the treatment of allergic inflammation.

De novo–synthesized lipid mediators

LTC_4 is synthesized *de novo* in MCs/Bs from arachidonic acid through the consecutive action of 5-lipoxygenase (5-LO) and LTC_4 synthase, followed by conversion to LTD_4 and LTE_4.[45,46] LTC_4 and LTD_4 are potent bronchoconstrictors and play an important role in asthma through binding to cysteinyl leukotriene receptor (cysLTR) 1 and 2. Several specific cysLTR1 antagonists have been developed and are in clinical use, including zafirlukast, pranlukast, and montelukast.[45,46] Even though the stable product LTE_4 does not bind to traditional cysLTRs, it might cause clinical reactions in asthmatic patients by possibly binding to the purinergic $P2Y_{12}$ receptor and/or to another, yet uncharacterized LTE_4 receptor.[45,46]

The current cysLTR1 antagonists do not antagonize cysLTR2, the LTE_4 receptors, and/or the effects of LTB_4, with the latter binding to its receptors BLT1 and BLT2,[45,46] which might explain their variability in efficacy. However, this problem can be overcome by using an inhibitor of 5-LO, such as zileuton, which was introduced in the 1990s and has been used for the prevention and chronic treatment of asthma in the United Kingdom and United States.[45,46] A recent randomized head-to-head trial on chronic persistent asthma comparing the zileuton extended-release tablet with the montelukast tablet suggests that the zileuton extended-release tablet (2400 mg/d) is well tolerated and probably more efficacious than montelukast (10 mg/d).[47] Another strategy is to target the 5-lipoxygenase–activating protein (FLAP), a protein that facilitates the transfer of arachidonic acid to 5-LO.[45] In fact, several FLAP inhibitors have been developed and tested in clinical trials, although they have not yet reached the market.[45] In a recent study investigating the efficacy, safety, and pharmacodynamics of the new and potent FLAP inhibitor GSK2190915 in patients with mild asthma, results show that the drug is well tolerated and effective in inhibiting both the early and late responses to inhaled allergen.[48]

MCs in human skin and lung tissue express 15-lipoxygenase-1 (15-LO-1), an enzyme that produces substantial amounts of the arachidonic acid metabolite 15-ketoeicosatetraenoic acid, as well as smaller amounts of 15-hydroxyeicosatetraenoic acid, in IL-4–stimulated cord blood–derived human MCs.[49] This enzyme might play a role in chronic inflammation, atherosclerosis, diabetes, and carcinogenesis. Several potent inhibitors of the enzyme, such as PD146176, have been developed and shown to have efficacy in animal models.[50,51]

Prostaglandin D_2 (PGD_2) is another soluble lipid mediator produced *de novo* predominantly by MCs and in small amounts also by Bs.[52-55] The characterization of PGD_2 receptors, namely D-type prostanoid receptor (DP) 1 and 2 (also known as CRTH2) and the thromboxane receptor, has uncovered novel roles for PGD_2 in allergic inflammation given their expressions on endothelial and airway smooth muscle cells, as well as on eosinophils, T_H2 cells, and Bs.[53,54,56] PGD_2 induces bronchoconstriction through thromboxane receptors on airway smooth muscle cells, vasodilatation through DP1 receptors on endothelial cells, and activation of immune cells through DP2. These findings have promoted intense research on developing specific antagonists for these receptors, as well as dual DP1-DP2 antagonists, some of which have proceeded to clinical trials.[53,54,56] For example, the DP2 antagonist OC000459 has shown promising clinical effects in phase 2 studies in patients with rhinoconjunctivitis, asthma, and eosinophilic esophagitis.[57-59] In contrast, the dual DP1-DP2 antagonist AMG 853 was not effective at improving the symptoms of patients with moderate-to-severe asthma as an add-on to inhaled corticosteroid therapy.[60] Likewise, the results of a phase 2 clinical trial with the DP1 antagonist

laropiprant (MK-0524) in patients with asthma and allergic rhinitis were disappointing.[61] Another possibility is to specifically inhibit the formation of PGD_2 by designing an inhibitor of hematopoietic prostaglandin D synthase, as shown in experimental models of allergic rhinitis in guinea pigs,[62,63] although clinical trials are currently lacking. However, PGD_2 can display both proinflammatory and anti-inflammatory functions or even a protective role in infections,[53,54] attributes that need to be clarified in future studies.

Cytokines and chemokines

Both MCs and Bs synthesize and release a variety of cytokines and chemokines.[1,2,64] Even though these proinflammatory factors are not exclusively produced by these cells, drugs can be designed to specifically target different cytokines or chemokines secreted from MCs/Bs. TNF-α is one of the most relevant proinflammatory cytokines produced by MCs/Bs on activation,[1,65,66] and biological drugs (eg, infliximab, adalimumab, and etanercept) that target TNF-α are well established in the therapy of patients with psoriasis, rheumatoid arthritis, and other chronic inflammatory conditions. IL-6 is another proinflammatory cytokine that is produced by MCs/Bs and numerous other cell types.[64,67] Blocking the interaction between IL-6 and its receptor has been under clinical investigation, although most phase 2 and 3 clinical trials have been conducted with tocilizumab, a biological drug targeting the IL-6 receptor.[68] During recent years, the "T_H17" cytokine IL-17 has received considerable attention because of its key role in different inflammatory and autoimmune diseases. Recently, MCs were found to be the predominant cell type producing IL-17 in patients with inflammatory skin and joint diseases.[69,70] IL-17–targeted therapies are currently being investigated in phase 3 trials with secukinumab (a fully humanized anti–IL-17A $IgG_{1\kappa}$ mAb), ixekizumab (a humanized, hinge-modified anti–IL-17A IgG_4 mAb), and brodalumab (a fully humanized anti–IL-17RA receptor IgG_2 mAb) in patients with psoriasis, psoriatic arthritis, uveitis, and/or rheumatoid arthritis.[71] CXCL8/IL-8 is a chemokine that attracts neutrophils and is produced by different cell types, including MCs[72] and Bs (Gibbs et al, unpublished observations). Because of its plausible role in patients with diseases characterized by neutrophil accumulation, such as psoriasis and palmoplantar pustulosis, fully humanized anti–IL-8 mAbs have been produced and tested in clinical drug trials with efficacy.[73,74] MCs/Bs are also thought to play a key immunomodulatory role by releasing IL-4 and IL-13, which promote T_H2-associated allergies and certain autoimmune diseases.[2,75,76] IL-4 is a particularly important cytokine in this regard, and clinical trials are currently in progress to test the efficacy of neutralizing mAbs against this cytokine.[77] Even though the ability of isolated human MCs to generate these cytokines in relevant levels is not clear,[2,75] human Bs are important early sources of both IL-4 and IL-13.[78]

MCs/Bs are also known to release the angiogenic cytokine vascular endothelial growth factor A,[79] which is thought to be involved in tissue remodeling associated with chronic allergic inflammation (especially in asthma), as well as in tumor progression. This cytokine is usually generated by various leukocytes under hypoxic conditions that result in the stabilization of hypoxia-inducible factor 1α.[80-82] However, it remains to be determined whether anti–vascular endothelial growth factor approaches can actually reverse the pathology associated with chronic allergic inflammation.

NOVEL THERAPEUTICS THAT TARGET INTRACELLULAR SIGNALING AND SURVIVAL PATHWAYS

Activation of MCs/Bs can be blocked by inhibitors that act on signaling pathways transduced from plasma membrane receptors to cytoplasmic effectors. Most of the signaling pathways used by MCs/Bs are not found exclusively in these cells, and therefore it is a demanding task to find drugs specifically inhibiting the activation of MCs/Bs. Here we will focus on several cytoplasmic signaling proteins that have been targeted with pharmacologic inhibitors to suppress antigen-induced degranulation. Specifically, we will deal with spleen tyrosine kinase (SYK), phosphatidylinositol 3-kinases (PI3Ks), Src homology 2 domain-containing inositol 5′ phosphatase 1 (SHIP-1), Bruton tyrosine kinase (BTK), the protein tyrosine kinase KIT, and sphingosine kinases (SPHKs).

SYK

The cytosolic nonreceptor protein tyrosine kinase SYK is recruited to FcεRI after tyrosine phosphorylation of its γ chain immunoreceptor tyrosine–based activation motifs by the Src family kinase LYN. SYK is involved in the tyrosine phosphorylation of numerous substrates, degranulation, and production and secretion of LTC_4 and cytokines after FcεRI triggering.[83] Targeting SYK is desirable because of its role in several diseases, including asthma, allergic rhinitis, and rheumatoid arthritis.[84] There are several SYK inhibitors that have been tested in clinical trials. Fostamatinib (also called R-788) is a prodrug of the active compound tamatinib (R-406).[85] Fostamatinib passed the phase 2 clinical trial for treatment of patients with rheumatoid arthritis.[86] However, the phase 3 clinical trials investigating fostamatinib as an oral treatment for rheumatoid arthritis have recently been terminated. Another SYK inhibitor, PRT062607 (P505-15), seems to be more selective for SYK, safer, and better tolerated than other compounds in development. PRT062607 reduced inflammation in a dose-dependent manner in several preclinical *in vivo* models,[87] but a phase 2 clinical trial for the treatment of rheumatoid arthritis has been withdrawn. R343, an inhaled SYK inhibitor, was tested as a potential therapeutic drug for patients with allergic asthma but also failed in a recently completed phase 2 clinical study. Another SYK inhibitor unsuccessfully tested in a phase 2 study is the compound R112, which was used to treat allergic rhinitis.[88,89]

PI3Ks

PI3Ks are enzymes involved in catalysis of ATP-dependent phosphorylation of phosphoinositides and generation of the lipid-based second messenger phosphatidylinositol 3,4,5-trisphosphate (PI[3,4,5]P3) from phosphatidylinositol 4,5-bisphosphate (PI[4,5]P2).[90] This enzymatic step is crucial for the development of inflammatory responses.[91] Several compounds inhibiting the class I PI3K isoforms γ and δ have been identified as possible targets in patients with inflammatory diseases. One of them, IC87114, is a highly selective inhibitor of PI3Kδ with potential for treatment of rheumatoid arthritis and allergic asthma.[92,93]

CAL-101 (GS1101), a chemical derivative of IC87114, has increased potency and inhibits the δ isoform of PI3K with 40- to 300-fold higher selectivity than other class I PI3K isoforms.[94] Oral inhibitors of the P13Kδ isoform, CAL-101 and CAL-263, completed phase 1 clinical trials for the treatment of allergic rhinitis.[95,96] Currently, a potent oral inhibitor of both isoforms of PI3K, δ and γ, IPI-145, is in phase 2 clinical trials for the treatment of allergic asthma and rheumatoid arthritis.[97]

SHIP-1

Activation of MCs/Bs can be also inhibited by activation of enzymes involved in termination of the signaling pathways. One such enzyme is the lipid phosphatase SHIP-1, which dephosphorylates the inositol ring of PI(3,4,5)P3 to yield phosphatidylinositol 3,4-bisphosphate (PI[3,4]P2). Reduction of PI(3,4,5)P3 levels leads to inhibition of calcium influx, followed by changes in gene transcription and downregulated production of cytokines.[98] It has been shown that SHIP-1–deficient mice exhibit progressive inflammation[99] and that enhanced activity of SHIP-1 suppresses MC activation.[100] In accordance with these findings, the small molecule AQX-1125, which has been shown to increase the catalytic activity of human SHIP-1, inhibited activation of MCs and chemotaxis of leukocytes. Furthermore, AQX-1125 decreased passive cutaneous anaphylaxis, LPS-mediated pulmonary neutrophilic infiltration, and ovalbumin-mediated airway inflammation.[101,102] This highly active and selective small-molecule allosteric activator of SHIP1 demonstrated a favorable safety profile and anti-inflammatory activity in phase 2 clinical studies for the treatment of mild and moderate asthma and is now being investigated in a phase 2 clinical trial for the treatment of chronic obstructive pulmonary disease.

BTK

An important target downstream of SYK is the Tec family tyrosine kinase BTK, which has been shown to play important roles in antigen-activated MCs/Bs.[103] BTK is selectively inhibited by ibrutinib (PCI-32765), which binds covalently to the noncatalytic Cys-481 residue in the active site of BTK and thereby inhibits its phosphorylation on Tyr-223. Structural alignments revealed that only 10 kinases have a Cys at this position, contributing to significant selectivity of the drug.[104] Ibrutinib has been shown to block MC degranulation[105] and inhibit IgE-mediated activation of human Bs[106] and appears to have therapeutic potential for arthritis treatment.[107] AVL-292/CC-292 is a novel, orally available, irreversible inhibitor of BTK with clinical potential for treatment of patients with rheumatoid arthritis and some other autoimmune diseases.[108] AVL-292/CC-292 is in clinical development and has successfully completed 2 phase 1a clinical studies.[109]

KIT

KIT is an MC surface receptor with tyrosine kinase activity. Binding of stem cell factor, a KIT ligand, to its receptor leads to MC activation, proliferation, differentiation, and survival. There are several small inhibitors of KIT that have been considered for treatment of asthma, anaphylaxis, or systemic mastocytosis. Patients with mastocytosis often carry a gain-of-function mutation of KIT (D816V), and most KIT inhibitors cannot sufficiently block the mutated KIT.[110] Imatinib and nilotinib are 2 compounds with inhibitory effects on the KIT-mediated MC response, but they are not suitable for the treatment of patients with mastocytosis carrying mutated KIT (D816V).[111,112] Imatinib has been reported to be efficient in the treatment of arthritis and mastocytosis,[110,113-115] whereas nilotinib has recently been shown to have an antiallergic effect on MC-mediated anaphylaxis.[116] Dasatinib is a drug that inhibits not only KIT but also several other tyrosine kinases, including BTK. Dasatinib has been shown to inhibit FcεRI-induced histamine release in Bs and allergen-induced release of histamine in sensitized subjects.[117] Masitinib is a potent tyrosine kinase inhibitor that seems to be promising for the treatment of asthma and systemic or cutaneous mastocytosis.[118,119] Its combined inhibition of KIT and LYN/FYN kinases makes it particularly efficient in controlling MC activity. Clinical phase 2 studies focused on mastocytosis or corticosteroid-dependent asthma have shown sustainable improvement and acceptable tolerability for long-term treatment.[118,119] Midostaurin inhibits several tyrosine kinases, including KIT, and *in vitro* studies have shown its efficacy also against the D816V mutation. First results from a phase 2 clinical trial showed efficacy in patients with this mutation.[120] However, none of the above-mentioned inhibitors is specific for KIT; they also inhibit platelet-derived growth factor receptors and some other proteins with tyrosine kinase activity. Imatinib, nilotinib, and dasatinib also inhibit the protein tyrosine kinase BCR/ABL and are therefore used mainly in the treatment of chronic myeloid leukemia.[110]

SPHKs

Sphingosine-1-phosphate (S1P) is a bioactive sphingolipid mediator produced and secreted by activated MCs and plays an important role in allergic reactions within the respiratory system.[121] S1P levels have been found to be increased in the airways of asthmatic patients but not healthy control subjects after antigen challenge.[122] There are 2 kinases responsible for the production of S1P, SPHK1, and SPHK2. SPHK1, but not SPHK2, has been shown to play a critical role in antigen-induced degranulation.[123] Targeting S1P through inhibition of SPHKs, use of S1P-neutralizing antibodies, or administration of S1P receptor antagonists are possible strategies to treat allergic disorders, anaphylactic reactions, or asthma. Several specific S1P receptor agonists and antagonists have recently been described.[124] FTY720 (fingolimod) is phosphorylated by SPHK2 to function as an agonist for S1P receptors.[125] FTY720 promotes endocytosis and degradation of S1P receptors, thereby resulting in functional antagonistic effects. It has been shown to be highly effective in reducing the severity of autoimmune diseases in several animal models and has recently been approved as an oral treatment for relapsing forms of multiple sclerosis.[126,127]

Ion channels

Calcium ions are essential for MC/B activation and degranulation. Calcium release–activated calcium (CRAC) channels are important for the influx of extracellular Ca^{2+} into the cytoplasm and have been considered potential targets for the treatment of diseases caused by activation of MCs/Bs. Experiments with MCs derived from mice deficient in Orai1 or stromal interaction molecule 1, the proteins forming the CRAC channel pores, or functioning as Ca^{2+} sensors in the endoplasmic reticulum and interacting with Orai1, respectively, showed an important role of

CRAC channels in degranulation, cytokine secretion, and LT production *in vitro*. These structures are also involved as positive regulators of IgE-mediated immediate-phase anaphylactic responses *in vivo*.[128,129] Several compounds blocking CRAC channels have been described, including 2-aminophenylborane and SFK96365. The channels can be also blocked by low concentrations of trivalent cations Gd^{3+}[130] or by Synta compound 66, which do not interfere with potassium channels or ATPase pumps.[131] However, these compounds are not specific for MCs.[132] To solve this problem, it has been suggested that CRAC channels can be inhibited more specifically by combining low concentrations of CRAC channel inhibitors and an LT receptor antagonist.[133] Further studies showed that the 3,5-bis(trifluoromethyl) pyrazole derivate BTP2 (YM-58483) blocks CRAC channels, facilitates the activity of the nonselective transient receptor potential (TRP) M4 channel,[134] and inhibits the activity of TRPC3 and TRPC5.[135] BTP2 exhibited inhibitory effects in allergy asthma models in rats and guinea pigs.[136] Membrane potential and calcium signaling in MCs and other cells is also regulated by the calcium-activated potassium channel KCa3.1. A potent blocker of the human KCa3.1 channel ICA-17043 (senicapoc, PF-05416266) showed good pharmacokinetic properties and was well tolerated in human subjects. However, clinical phase 2 trials did not show any improvement after administration of ICA-17043 in asthmatic patients.[137]

Regulation of survival/apoptosis

MCs express proteins of the B-cell lymphoma 2 (BCL-2) family, which are involved in regulation of cell apoptosis. The family consists of proteins with proapoptotic and antiapoptotic functions, and balance between these proteins determines cellular fate through protein-protein interactions.[138] The proapoptotic effector proteins, including BAX and BAK, are crucial for the induction of permeabilization of the outer mitochondrial membrane and irreversible onset of apoptotic cell death. The antiapoptotic proteins (BCL-2, BCL-XL, BFL-1/A1, MCL-1, and BCL-W among others) inhibit apoptosis through direct interactions with effector proteins.[139] Members of the BCL-2 family share 1 or more of the 4 characteristic domains of homology named BCL-2 homology (BH) domains. BH3-only proteins, such as BIM, PUMA, BAD, and NOXA, are capable of inducing apoptosis by binding to and neutralizing the antiapoptotic proteins. Activation of human MCs through FcεRI leads to upregulation of the antiapoptotic BCL-2 family members MCL-1 and BFL-1.[140] Further studies showed that BFL-1 is a major effector in activation-induced human MC survival.[141] In recent years, several small molecular compounds mimicking the BH3 domain have been developed in the frame of anticancer research. These included ABT-737, TW-37, and ABT-263 (navitoclax).[142-145] Experiments in mice showed that intraperitoneal administration of ABT-737 resulted in selective abolishment of MCs in the peritoneum. Furthermore, *ex vivo* treatment of human skin biopsy specimens with ABT-737 demonstrated increased MC apoptosis.[146] Recent experiments with the novel BH3 mimetic obatoclax (GX015-070) showed that this drug induces growth arrest in primary human MCs and MC lines and exerts synergistic antineoplastic effects on MCs when combined with other targeted drugs, such as dasatinib.[147] The combined data suggest that BH3-only mimetic compounds are good candidate drugs for treatment of MC-associated diseases, such as mastocytosis, allergy, asthma, and chronic inflammatory diseases.

SURFACE RECEPTORS AS TARGETS

Targeting surface inhibitory and activating receptors on different cell types is a valid means of therapeutic intervention. In allergic patients considerable efforts are being made to control the activity of effector cells through their functional receptors. Blocking FcεRI is already being used as a treatment and is the basis of many ongoing studies. However, there are also several less developed yet promising new candidate receptors as targets for treatment of MC/B-mediated diseases.

Inhibitory receptors

Among the inhibitory receptors, we decided to focus on 3 receptors that have been shown to be expressed on MCs/Bs with promising preclinical results: CD300a, FcγRIIB, and Siglec-8. CD300a contains 4 immunoreceptor tyrosine–based inhibitory motifs (ITIMs) in its cytoplasmic tail and belongs to the immunoglobulin superfamily. Although CD300a is not expressed only on MCs,[148] eosinophils,[149] and Bs,[150,151] selective targeting of this receptor has been shown to be feasible for treatment of allergies and other diseases mediated by MCs/Bs.[152]

FcγRIIB is one of the most studied IgG receptors, which was found to be expressed on MCs (except from human skin[153]) and Bs both of human and mouse origin[154] and shown to negatively regulate the activation of these cells through ITIM-mediated signaling after allergen binding to IgE.[155,156]

Siglec-8 is the most characterized receptor among the Siglecs that are expressed on MCs and inhibits their activation through ITIMs located in its intracellular domain. Siglec-8 is a promising candidate for treating allergy because it was shown to be functional not only on human MCs but also on eosinophils and Bs.[157-159]

We also briefly introduce the cannabinoid receptors, which in recent years were shown to play a role in the regulation of the immune system in general and of MCs in particular. Although the mechanism for this regulation is not fully understood, growing evidence suggests that these receptors probably inhibit MC activation.[160]

CD300a receptor

The inhibitory function of CD300a was demonstrated in several cell types, including human cord blood–derived mast cells, in which coaggregation with IgE-bound FcεRI led to the inhibition of IgE-induced β-hexosaminidase, tryptase, and IL-4 release, as well as a reduction in stem cell factor–mediated survival.[148] In addition, a bispecific anti-KIT/anti-CD300a antibody abolishes KIT-mediated cord blood–derived mast cell differentiation, survival, and IgE-dependent activation, as well as inhibiting mediator release in the malignant human MC line (HMC-1), where KIT is constitutively activated.[148] The CD300a murine orthologue Lmir-1 was also shown to be an inhibitory receptor in murine bone marrow–derived MCs, and the bispecific anti-IgE/anti-CD300a antibody was demonstrated to abrogate allergic peritonitis, passive cutaneous anaphylaxis, and acute asthma models in mice.[152] Another bispecific antibody fragment linking CD300a to CCR3 (which is specific for human MCs and eosinophils) was shown to affect eosinophil signaling and function *in vivo*, reducing the levels of proinflammatory mediators in bronchoalveolar lavage fluid and MC mediator release. It also reversed lung inflammation in a murine model of chronic

established asthma.[161] CD300a-deficient mice showed improved bacterial clearance in the peritoneal cavity and longer survival, which supports a role for CD300a in regulating MC-mediated inflammatory responses to microbial infections.[162]

Human Bs also express CD300a in the peripheral blood of both healthy and allergic subjects. The basal expression of CD300a from patients with birch pollen allergy is significantly lower than that in healthy control subjects.[150] Bs preincubated with anti-human CD300a/c mAbs displayed reduced IgE-mediated CD63 expression, indicating decreased activation.[150] Moreover, CD300a was shown to be rapidly upregulated after IgE-dependent triggering, indicating that Bs might express intracellular pools of this receptor, as was found in eosinophils,[163] and cross-linking this receptor suppressed anaphylactic degranulation in these cells.[150]

It was recently described that phosphatidylethanolamine and phosphatidylserine act as ligands for CD300a on dead cells,[164] which is interesting for its potential role in the removal of apoptotic cells[162] and might be highly relevant in the resolution phase of allergic inflammation.

It is clear that the inhibitory receptor CD300a, as expressed by MCs/Bs and eosinophils, might display therapeutic antiallergic potential, particularly when targeted through bispecific antibodies to the cells of interest.

IgG receptors

It has long been known that MCs/Bs not only express IgE but also IgG receptors, which consist of both excitatory and inhibitory receptor types. In mice allergen-IgG immune complexes cause systemic anaphylaxis and are dependent on Bs activation, as well as the release of platelet-activating factor from these cells.[165] However, in human subjects Bs cannot be activated through IgG receptors[166,167] unlike their MC counterparts, which have been shown to express FcγRI, which is induced by IFN-γ.[168] Cassard et al[154] recently demonstrated that the differential responses of mouse and human Bs to IgG-mediated triggering is because of the more robust responses of FcγRIIIA on mouse Bs than FcγRIIA, which is expressed on human Bs.

A human IgG-IgE Fc fusion protein (GE2), which co–cross-linked FcεRI with FcγRII receptors, inhibited histamine release from human Bs and lung tissue fragments, as well as reducing tissue reactivity to allergen stimulation in several *in vivo* models.[169-171] Recently, several studies have been carried out to enhance FcγRIIB affinity by designing fusion proteins that inhibit activation in a more specific and efficient way, regardless of the degree of activation. One recent study showed that coengagement of FcεRI with FcγRIIB, using a dual-targeting tandem IgE–IgG Fc domain biologic with 100-fold enhanced affinity compared with native IgG_1 Fc, resulted in marked suppression of MC degranulation.[155] Another fusion protein (Fcγ-Der f2) was shown to prevent and treat allergic inflammation in a murine model of dust mite–induced asthma, suggesting that chimeric human Fcγ allergen proteins can be used as an immunotherapy tool.[172]

Siglec-8

Siglec-8 can undergo alternative splicing to yield a "short form" and a "long form" containing 2 tyrosine cytoplasmic motifs.[173,174] In various human blood samples Siglec-8 was shown to be expressed at normal levels on Bs from patients with chronic eosinophilic and chronic myelogenous leukemia, on normal murine bone marrow MCs, and on MCs from patients with indolent systemic mastocytosis.[175] Siglec-8 is expressed by several MC lines, such as LAD2, LUVA, and HMC1.2.[175,176] In human MCs generated from $CD34^+$ precursors, Siglec-8 engagement did not induce apoptosis[177] compared with its apoptotic function on eosinophils.[178,179] However, preincubation with Siglec-8 mAb significantly inhibited FcεRI-dependent histamine and PGD_2 release from purified MCs and the FcεRI-dependent Ca^{2+} flux and release of β-hexosaminidase of MCs. It remains to be seen whether the synthetic Siglec-8 ligand polymeric 6′-sulfated sialyl Lewis X, as reported by Hudson et al,[180] would be more effective at causing MC/B apoptosis than Siglec-8 mAb. Siglec-8–mediated inhibition of MC degranulation and its apoptotic effects on eosinophils should be considered in concert when developing new therapies for MC- and eosinophil-related disorders, such as asthma (the Siglec-8 apoptotic function on human eosinophils was recently broadly reviewed by Farid et al).[181]

Siglec-F, which is the orthologue for Siglec-8 in mice, is expressed on a wider range of cells than Siglec-8,[182-184] although not on mouse MCs, and its function on these cells is not clear. Stimulation with IL-4 or IL-13 caused an increase in Siglec-F-Fc binding to airway epithelium *in vivo* and *in vitro*.[185,186] Engagement of Siglec-8 with antibodies or glycan ligands used as a cell-directed therapy can specifically inhibit or deplete MCs, eosinophils, and Bs and provide specific targets for treatment in MC-related diseases.

CBs

Two G protein–coupled CBs, CB1 and CB2, have been discovered thus far, which are targeted by 2 endogenous ligands and many more natural and synthetic exogenous compounds that can bind and activate them in either a specific or nonspecific manner. Endocannabinoids are being used already as therapeutic targets in the treatment of anxiety, obesity, movement disorders, and glaucoma,[187] and growing evidence supports their role in health and diseases of the immune system as well.

CB2 was shown to be expressed on cells of the immune system 2 decades ago, and recent studies support an important regulatory role of both CB2 and CB1 regarding allergy and MC-driven diseases, although the latter is found predominantly on cells from the central nervous system.[188] CB1 is expressed constitutively on T lymphocytes, which can be upregulated by cannabinoid stimulation through IL-4 and is involved in promoting a T_H2 phenotype.[189,190]

Regarding specific studies involving MCs and allergy, CB1 was shown to be expressed on human mucosal MCs (from serum-free nasal polyp organ culture model)[191] and on the connective tissue sheath MCs of human hair follicles.[192] In the latter it was demonstrated that blocking this receptor increased both MC degranulation and cell numbers without affecting MC proliferation *in situ*.[192] CB1 and CB2 were shown to be coexpressed and function through different pathways in the MC line RBL2H3.[193]

In rats there are controversial data. One group found that degranulation of resident MCs induced by substance P was fully abrogated by the endocannabinoid agonists anandamide and palmitoylethanolamide in the ear pinna.[194] Peritoneal MCs were shown to express both CB2 mRNA and protein,[195] although other groups were not able to confirm these observations.[160]

In addition, a selective CB2 agonist was shown to reduce MC-dependent edema in response to compound 48/80 in the mouse ear pinnae, and cannabidiol was shown to inhibit collagen-induced arthritis in mice.[196]

In guinea pigs the endogenous ligand 2-arachidonoylglycerol was shown to significantly reduce the release of histamine from MCs, an effect that was then reversed by a selective CB2 antagonist but not by an antagonist for CB1.[197]

To date, most of the data obtained in human studies indicate an inhibitory effect of endocannabinoids on MC function both directly through CB2 and indirectly through CB1. However, research in the field of allergy and endocannabinoids is still evolving, and along with some controversial animal studies, it is clear that further investigations are needed to reveal the underlying mechanisms of CB involvement in the treatment of allergic conditions.

ACTIVATING RECEPTORS AS TARGETS FOR NOVEL THERAPIES

FcεRI is the quintessential activating receptor expressed on MCs/Bs, and it plays a crucial role in the initiation of allergic reactions and chronic allergic inflammation, such as in asthmatic patients, by launching the rapid release of preformed and *de novo*–synthesized mediators. Therefore targeting this receptor provides an effective way for treating allergy and allergic inflammation. However, inhibition of other activating surface receptors is another way to target the proallergic and anti-inflammatory functions of MCs/Bs in the treatment of allergic diseases. Here we introduce activating receptors for which promising results have been shown both *in vitro* and *in vivo* for regulating MCs/Bs in allergy-driven conditions.

CD48 is a CD2-like molecule expressed on the surfaces of hematopoietic cells, including MCs/Bs (reviewed by Elishmereni and Levi-Schaffer[198]). This 40-kDa glycosyl-phosphatidyl inositol–anchored protein also has a soluble form that is generated by cleavage on cell activation. Stimulated CD48 associates to the kinase LCK and leads to tyrosine phosphorylation.[198]

The thymic stromal lymphopoietin receptor (TSLPR) is involved in promoting T_H2-type immune responses, such as the release of proallergic and inflammatory cytokines from MCs (reviewed by Migalovich-Sheikhet et al[4]), and supporting T_H2 cytokine responses of murine Bs during helminth infection.[199]

CD48

CD48, which is expressed on human MCs, was shown to bind to both gram-negative and gram-positive bacteria, leading to the release of prestored mediators and proinflammatory cytokines, including TNF-α.[200-204] The physical interaction of CD48 expressed on MCs with the human high-affinity ligand 2B4 on eosinophils plays an important role in allergic inflammation by facilitating the formation of an allergic effector unit between the 2 cells.[205] CD48-2B4 binding induces the degranulation of MCs and increases eosinophil survival and activation.[205] Interestingly, Bs and eosinophils both express 2B4, but it is unknown whether the functions of Bs are affected by CD48-2B4. CD48 is overexpressed in murine asthma models, where it serves as a signature gene in this condition.[206] Treatment with a neutralizing CD48-specific antibody was shown to markedly inhibit lung inflammation in these models.[207]

TSLPR

Thymic stromal lymphopoietin (TSLP), the ligand for TSLPR, is an IL-7–like cytokine that was shown to be expressed on a variety of hematopoietic cell lineages, including MCs/Bs, B cells, T cells, eosinophils, and dendritic cells.[208-211] TSLP plays a significant role in the initiation of T_H2 responses.[212] It is highly expressed at the interfaces of the body and the environment and can directly activate human MCs.[208] TSLPR has a low affinity to TSLP, but together with IL-7Ra, it triggers signaling.[213] TSLPR and IL-7Ra chain expressions were demonstrated on MC progenitors and different cell lines.[208,214,215]

There is an increased expression of TSLP in the inflamed tissues of patients with allergic rhinitis, atopic dermatitis, and asthma,[212,216] in whom MCs play an important role in TSLP production.[215] MC activation by TSLP reportedly increased the production of chemokines and cytokines by MCs but did not affect MC survival or proliferation.[217] Therefore TSLPR might be a promising candidate for antiallergic intervention. Indeed, Zhang et al[218] recently reported that soluble TSLPR immunoglobulin prevents airway inflammation by modulating dendritic cell function, and therefore this might be a viable strategy for treating asthma.

FcεRI

Activation of FcεRI on MCs/Bs by allergens results in the explosive release of mediators that are preformed in cytoplasmic granules. This is rapidly followed by the synthesis and release of newly synthesized mediators from cellular lipid components and, after the activation of specific genes, various cytokines, chemokines, and growth factors. Increasing evidence also shows an important role for FcεRI in tissue responses associated with chronic allergic inflammation and asthma.[219] Hence interfering with the activity of this receptor has been a prime goal for many years in the treatment of allergies.

FcεRI is a tetrameric structure composed of an IgE-binding α subunit and a single 4-transmembrane–containing β chain, as well as a disulfide-linked dimer of γ chains.[220] Both β and γ subunits are implicated in signal transduction.[221] The interaction of IgE with its receptor has been characterized extensively, and the tridimensional structure of this interaction was solved at the turn of this century.[222] The IgE monomer binds to FcεRI with 1:1 stoichiometry. The interaction is characterized by a slow dissociation rate ($k_{off} < 10^{-5}\ s^{-1}$), accounting, to a large extent, for the high affinity of the interaction.[223] As a consequence, any treatment interfering with IgE binding will not be effective immediately but requires considerable time, as has been observed in a rat model.[224]

Although under development,[225] thus far, no low-molecular-weight compound exists that can interfere with IgE binding. Likewise, inhibitors of signal transduction, although effective, do not show a high degree of specificity (see above). The only specific inhibitor in clinical use is the humanized mAb omalizumab (Xolair), which blocks the interaction of IgE with FcεRI by targeting IgE at a site that overlaps with receptor binding and thus by itself does not have any activating effect itself. This antibody has been approved for the treatment of moderate and severe asthma with proven efficacy and safety.[226] The major effect of treatment is the reduction of plasma IgE levels, as well as FcεRI expressions on MCs/Bs. Other effects, such as downregulation of IgE class-switching in B cells, might also contribute to its

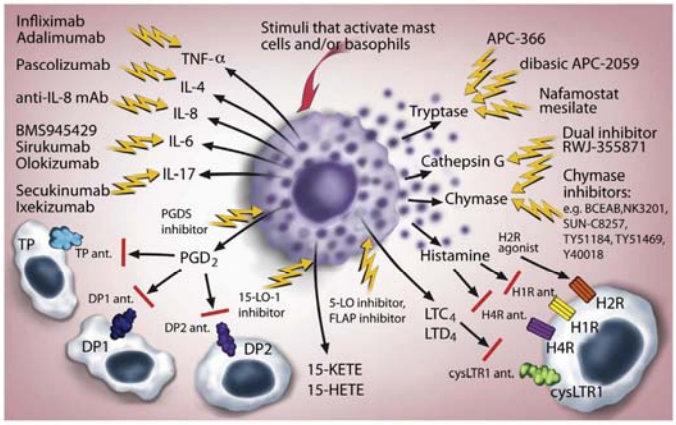

FIG 1. Soluble mediators of MCs, Bs, or both as targets for novel therapy. The effects of mediators stored in the secretory granules or produced *de novo* on cell activation can be prevented by drugs targeting tryptase, chymase, and/or cathepsin G by drugs targeting 5-LO, FLAP, 15-LO-1 or prostaglandin D synthase *(PGDS)*; by mAbs targeting proinflammatory cytokines; or by specific receptor antagonists. *TP*, Thromboxane receptor.

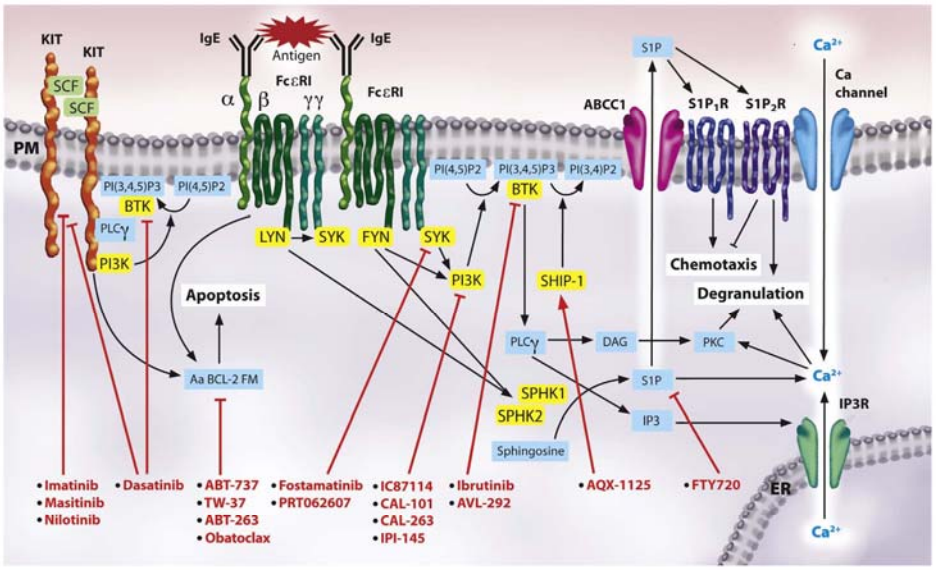

FIG 2. Intracellular signaling pathways of MCs, Bs, or both as targets for novel therapy. Antigen-aggregated IgE-FcεRI complexes or stem cell factor (SCF)–activated KIT initiate signaling pathways leading to degranulation, chemotaxis, and/or apoptosis depending on the signaling pathway triggered. Some of the proteins and other effectors executing these processes (in *yellow* and *blue boxes*) can be inhibited or potentiated by various drugs (in *red*), as described in the text. *Aa BCL-2 FM*, Antiapoptotic BCL-2 family members; *ER*, endoplasmic reticulum; *IP3*, inositol triphosphate; *IP3R*, inositol triphosphate receptor; *PKC*, protein kinase C; *PLC*, phospholipase C; *PM*, plasma membrane.

efficacy.[227] A recent phase 3 clinical trial has been completed, showing efficacy in patients with moderate-to-severe chronic idiopathic urticaria.[228] It has also been shown to be beneficial in food allergies,[229] atopic dermatitis,[230] and persistent allergic rhinitis,[231] as well as in some patients with idiopathic anaphylaxis and MC disorders.[232] However, the high treatment costs limit its

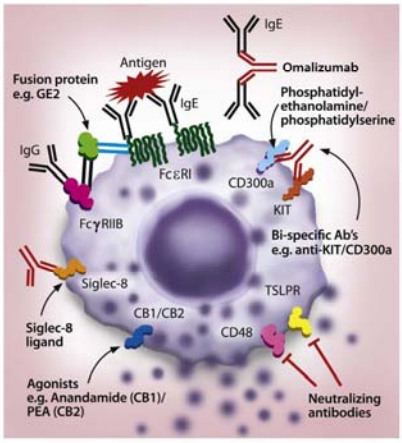

FIG 3. Novel surface receptors that alter IgE-dependent mediator release in MCs, Bs, or both. Stimulation of inhibitory receptors, such as CB1, CD300a, FcγRIIB, and Siglec-8, or blockade of surface activating receptors, such as CD48 and TSLPR, could potentially serve as targets for future allergy therapy. *PEA*, Palmitoylethanolamide.

use.[219] Much of the future will depend on the successful development of small molecular compounds that could further reduce treatment costs at a similar efficacy.

CONCLUSIONS

MCs/Bs generate a highly diverse number of mediators that perform crucial roles in the induction of symptoms and the pathogenesis of many diseases, primarily allergic and other inflammatory conditions. Indeed, it is increasingly apparent that MCs/Bs are capable of generating far more mediator types than previously appreciated. In addition to traditional antihistamines and LTC_4 blockers, there has been significant progress in the design of new candidate drugs that target MC/B mediators to a varying extent and specificity (Fig 1 and see Table E1 in this article's Online Repository at www.jacionline.org). These include inhibitors of serine proteinases, H4-antihistamines, FLAP inhibitors, inhibitors of 15-LO-1 and PGD synthase, and PGD_2 receptor antagonists. Furthermore, new biological agents directed against cytokines released by MCs/Bs might significantly reduce their ability to support inflammatory responses, as well as underlying T_H2 immunity.

Numerous inhibitors have been developed against individual components of signaling pathways that are involved in the activation and degranulation of MCs/Bs (Fig 2 and see Table E2 in this article's Online Repository at www.jacionline.org). These inhibitors are very useful in the treatment of various diseases, including allergy and asthma, and their usefulness could be further increased when used in combination with other drugs, gene-targeting techniques, or both. However, enzymes involved in the activation of MCs/Bs are not exclusively expressed in these cells, and therefore local rather than systemic applications could be preferable in many cases. Importantly, MCs/Bs are involved not only in undesirable hypersensitivity reactions but also in innate and acquired immunity; this should be taken into account when drugs that limit their functions are used for therapeutic purposes. It can be anticipated that the best therapeutic results will be obtained with multicomponent drugs that inhibit certain proinflammatory pathways and at the same time enhance the activity of enzymes involved in the termination of signaling pathways.

MCs/Bs express FcεRI, which is the traditional receptor responsible for the release of most of the proinflammatory mediators from these cells and is the prime target in therapeutics (Fig 3 and see Table E3 in this article's Online Repository at www.jacionline.org). However, there is growing evidence that MCs/Bs also express a variety of surface receptors that can either potentiate or limit the effects of FcεRI through several mechanisms (Fig 3). Surface-activating receptors, such as CD48 and TSLPR, and inhibitory receptors, such as CD300a, FcγRIIb, Siglec-8, and the CBs, provide promising possibilities in therapeutics. The direct or indirect blockade of FcεRI-mediated signaling might help prevent allergic reactions from developing and is a promising approach for treating allergies and other MC/B-driven diseases.

Finally, MCs interact with several cell types, including eosinophils, fibroblasts, airway smooth muscle cells, and neuronal cells. Under certain conditions, these interactions lead to increased MC survival, proliferation, activation, and secretion of proinflammatory mediators.[233,234] For example, interactions between human lung MCs and human airway smooth muscle cells and lung fibroblasts are mediated, in part, through cell adhesion molecule 1.[235-237] Recent studies in mice showed that the increased expression of cell adhesion molecule 1 causes enhanced nerve-MC interactions in a hapten-induced atopic dermatitis model.[238] MCs also express various receptors for chemoattractants that direct their migration into target tissues.[239] Thus cell adhesion molecules and chemoattractant receptors are potential therapeutic targets in diseases caused by aberrant localization of MCs in target tissues, their interactions with other cell types, or both.

REFERENCES

1. Harvima IT, Nilsson G. Mast cells as regulators of skin inflammation and immunity. Acta Derm Venereol 2011;91:644-50.
2. Falcone FH, Knol EF, Gibbs BF. The role of basophils in the pathogenesis of allergic disease. Clin Exp Allergy 2011;41:939-47.
3. Karra L, Berent-Maoz B, Ben-Zimra M, Levi-Schaffer F. Are we ready to downregulate mast cells? Curr Opin Immunol 2009;21:708-14.
4. Migalovich-Sheikhet H, Friedman S, Mankuta D, Levi-Schaffer F. Novel identified receptors on mast cells. Front Immunol 2012;3:238.
5. Bounab Y, Getahun A, Cambier JC, Daeron M. Phosphatase regulation of immunoreceptor signaling in T cells, B cells and mast cells. Curr Opin Immunol 2013; 25:313-20.
6. Pullen NA, Falanga YT, Morales JK, Ryan JJ. The Fyn-STAT5 pathway: a new frontier in IgE- and IgG-mediated mast cell signaling. Front Immunol 2012;3: 117.
7. Jogie-Brahim S, Min HK, Fukuoka Y, Xia HZ, Schwartz LB. Expression of α-tryptase and β-tryptase by human basophils. J Allergy Clin Immunol 2004; 113:1086-92.
8. Caughey GH. Mast cell tryptases and chymases in inflammation and host defense. Immunol Rev 2007;217:141-54.
9. Rice KD, Tanaka RD, Katz BA, Numerof RP, Moore WR. Inhibitors of tryptase for the treatment of mast cell-mediated diseases. Curr Pharm Des 1998;4:381-96.
10. He A, Shi GP. Mast cell chymase and tryptase as targets for cardiovascular and metabolic diseases. Curr Pharm Des 2013;19:1114-25.
11. Krishna MT, Chauhan A, Little L, Sampson K, Hawksworth R, Mant T, et al. Inhibition of mast cell tryptase by inhaled APC 366 attenuates allergen-induced late-phase airway obstruction in asthma. J Allergy Clin Immunol 2001; 107:1039-45.
12. Tremaine WJ, Brzezinski A, Katz JA, Wolf DC, Fleming TJ, Mordenti J, et al. Treatment of mildly to moderately active ulcerative colitis with a tryptase

inhibitor (APC 2059): an open-label pilot study. Aliment Pharmacol Ther 2002; 16:407-13.
13. Mori S, Itoh Y, Shinohata R, Sendo T, Oishi R, Nishibori M. Nafamostat mesilate is an extremely potent inhibitor of human tryptase. J Pharmacol Sci 2003;92: 420-3.
14. Hallgren J, Estrada S, Karlson U, Alving K, Pejler G. Heparin antagonists are potent inhibitors of mast cell tryptase. Biochemistry 2001;40:7342-9.
15. Schechter NM, Sprows JL, Schoenberger OL, Lazarus GS, Cooperman BS, Rubin H. Reaction of human skin chymotrypsin-like proteinase chymase with plasma proteinase inhibitors. J Biol Chem 1989;264:21308-15.
16. Huttunen M, Harvima IT. Mast cell tryptase and chymase in chronic leg ulcers: chymase is potentially destructive to epithelium and is controlled by proteinase inhibitors. Br J Dermatol 2005;152:1149-60.
17. D'Orléans-Juste P, Houde M, Rae GA, Bkaily G, Carrier E, Simard E. Endothelin-1 (1-31): from chymase-dependent synthesis to cardiovascular pathologies. Vascul Pharmacol 2008;49:51-62.
18. Yahiro E, Miura S, Imaizumi S, Uehara Y, Saku K. Chymase inhibitors. Curr Pharm Des 2013;19:3065-71.
19. Maryanoff BE, de Garavilla L, Greco MN, Haertlein BJ, Wells GI, Andrade-Gordon P, et al. Dual inhibition of cathepsin G and chymase is effective in animal models of pulmonary inflammation. Am J Respir Crit Care Med 2010;181: 247-53.
20. Di Girolamo N, Wakefield D. *In vitro* and *in vivo* expression of interstitial collagenase/MMP-1 by human mast cells. Dev Immunol 2000;7:131-42.
21. Di Girolamo N, Indoh I, Jackson N, Wakefield D, McNeil HP, Yan W, et al. Human mast cell-derived gelatinase B (matrix metalloproteinase-9) is regulated by inflammatory cytokines: role in cell migration. J Immunol 2006;177:2638-50.
22. Shi Z-G, Li J-P, Shi L-L, Li X. An updated patent therapeutic agents targeting MMPs. Recent Pat Anticancer Drug Discov 2012;7:74-101.
23. Saarinen J, Kalkkinen N, Welgus HG, Kovanen PT. Activation of human interstitial procollagenases through direct cleavage of the Leu^{83}-Thr^{84} bond by mast cell chymase. J Biol Chem 1994;269:18134-40.
24. Fang KC, Raymond WW, Blount JL, Caughey GH. Dog mast cell α-chymase activates progelatinase B by cleaving the Phe^{88}-Gln^{89} and Phe^{91}-Glu^{92} bonds of the catalytic domain. J Biol Chem 1997;272:25628-35.
25. Gruber BL, Marchese MJ, Suzuki K, Schwartz LB, Okada Y, Nagase H, et al. Synovial procollagenase activation by human mast cell tryptase dependence upon matrix metalloproteinase 3 activation. J Clin Invest 1989;84:1657-62.
26. Gibbs BF, Levi-Schaffer F. H4 receptors in mast cells and basophils: a new therapeutic target for allergy? Front Biosci 2012;17:430-7.
27. Ohsawa Y, Hirasawa N. The antagonism of histamine H1 and H4 receptors ameliorates chronic allergic dermatitis via anti-pruritic and anti-inflammatory effects in NC/Nga mice. Allergy 2012;67:1014-22.
28. Levi-Schaffer F, Eliashar R. Mast cell stabilizing properties of antihistamines. J Invest Dermatol 2009;129:2549-51.
29. Weller K, Maurer M. Desloratadine inhibits human skin mast cell activation and histamine release. J Invest Dermatol 2009;129:2723-6.
30. Krause K, Spohr A, Zuberbier T, Church MK, Maurer M. Up-dosing with bilastine results in improved effectiveness in cold contact urticaria. Allergy 2013;68: 921-8.
31. Masini E, Blandina P, Brunelleschi S, Mannaioni PF. Evidence for H2-receptor-mediated inhibition of histamine release from isolated rat mast cells. Agents Actions 1982;12:85-8.
32. Kazimierczak W, Szczepanik K, Bańkowska K. A modulation of the anaphylactic basophil histamine release by selective H2 histamine agonists. Agents Actions 1981;11:96-8.
33. Summers R, Sigler R, Shelhamer JH, Kaliner M. Effects of infused histamine on asthmatic and normal subjects: comparison of skin test responses. J Allergy Clin Immunol 1981;67:436-64.
34. Peters SP, Kagey-Sobotka A, MacGlashan DW Jr, Siegel MI, Lichtenstein LM. The modulation of human basophil histamine release by products of the 5-lipoxygenase pathway. J Immunol 1982;129:797-803.
35. Novak N, Mete N, Bussmann C, Maintz L, Bieber T, Akdis M, et al. Early suppression of basophil activation during allergen-specific immunotherapy by histamine receptor 2. J Allergy Clin Immunol 2012;130:1153-8.e2.
36. Kleine-Tebbe J, Schramm J, Bolz M, Lipp R, Schunack W, Kunkel G. Influence of histamine H3-antagonists on human leukocytes. Agents Actions 1990;30: 137-9.
37. Tedeschi A, Lorini M, Arquati M, Miadonna A. Regulation of histamine release from human basophil leucocytes: role of H1, H2 and H3 receptors. Allergy 1991; 46:626-31.
38. Lippert U, Artuc M, Grutzkau A, Babina M, Guhl S, Haase I, et al. Human skin mast cells express H2 and H4, but not H3 receptors. J Invest Dermatol 2004;123: 116-23.
39. Hofstra CL, Desai PJ, Thurmond RL, Fung-Leung WP. Histamine H4 receptor mediates chemotaxis and calcium mobilization of mast cells. J Pharmacol Exp Ther 2003;305:1212-21.
40. Thurmond RL, Desai PJ, Dunford PJ, Fung-Leung WP, Hofstra CL, Jiang W, et al. A potent and selective histamine H4 receptor antagonist with anti-inflammatory properties. J Pharmacol Exp Ther 2004;309:404-13.
41. Shiraishi Y, Jia Y, Domenico J, Joetham A, Karasuyama H, Takeda K, et al. Sequential engagement of FcεRI on mast cells and basophil histamine H(4) receptor and FcεRI in allergic rhinitis. J Immunol 2013;190:539-48.
42. Gutzmer R, Gschwandtner M, Rossbach K, Mommert S, Werfel T, Kietzmann M, et al. Pathogenetic and therapeutic implications of the histamine H4 receptor in inflammatory skin diseases and pruritus. Front Biosci (Schol Ed) 2011;3:985-94.
43. Kamo A, Negi O, Tengara S, Kamata Y, Noguchi A, Ogawa H, et al. Histamine H_4 receptor antagonists ineffective against itch and skin inflammation in atopic dermatitis mouse model. J Invest Dermatol 2014;134:546-8.
44. Salcedo C, Pontes C, Merlos M. Is the H4 receptor a new drug target for allergies and asthma? Front Biosci (Elite Ed) 2013;5:178-87.
45. Montuschi P, Peters-Golden ML. Leukotriene modifiers for asthma treatment. Clin Exp Allergy 2010;40:1732-41.
46. Laidlaw TM, Boyce JA. Cysteinyl leukotriene receptors, old and new: implications for asthma. Clin Exp Allergy 2012;42:1313-20.
47. Kubavat AH, Khippal N, Tak S, Rijhwani P, Bhargava S, Patel T, et al. A randomized, comparative, multicentric clinical trial to assess the efficacy and safety of zileuton extended-release tablets with montelukast sodium tablets in patients suffering from chronic persistent asthma. Am J Ther 2013;20:154-62.
48. Kent SE, Boyce M, Diamant Z, Singh D, O'Connor BJ, Saggu PS, et al. The 5-lipoxygenase-activating protein inhibitor, GSK2190915, attenuates the early and late responses to inhaled allergen in mild asthma. Clin Exp Allergy 2013; 43:177-86.
49. Gullikson M, Brunnström Å, Johannesson M, Backman L, Nilsson G, Harvima I, et al. Expression of 15-lipoxygenase type-1 in human mast cells. Biochim Biophys Acta 2007;1771:1156-65.
50. Jeon SG, Moon H-G, Kim Y-S, Choi J-P, Shin T-S, Hong S-W, et al. 15-Lipoxygenase metabolites play an important role in the development of a T-helper type 1 allergic inflammation induced by double-stranded RNA. Clin Exp Allergy 2009;39:908-17.
51. Rai G, Kenyon V, Jadhav A, Schultz L, Armstrong M, Jameson JB, et al. Discovery of potent and selective inhibitors of human reticulocyte 15-lipoxygenase-1. J Med Chem 2010;53:7392-404.
52. Dahlén S-E, Kumlin M. Monitoring mast cell activation by prostaglandin D2 *in vivo*. Thorax 2004;59:453-5.
53. Schuligoi R, Sturm E, Luschnig P, Konya V, Philipose S, Sedej M, et al. CRTH2 and D-type prostanoid receptor antagonists as novel therapeutic agents for inflammatory diseases. Pharmacology 2010;85:372-82.
54. Joo M, Sadikot RT. PGD synthase and PGD2 in immune response. Mediators Inflamm 2012;2012:503128.
55. Ugajin T, Satoh T, Kanamori T, Aritake K, Urade Y, Yokozeki H. FcεRI, but not FcγR, signals induce prostaglandin D2 and E2 production from basophils. Am J Pathol 2011;179:775-82.
56. Davì G, Santilli F, Vazzana N. Thromboxane receptors antagonists and/or synthase inhibitors. Handb Exp Pharmacol 2012;210:261-86.
57. Horak F, Zieglmayer R, Lemell P, Collins LP, Hunter MG, Steiner J, et al. The CRTH2 antagonist OC000459 reduces nasal and ocular symptoms in allergic subjects exposed to grass pollen, a randomized, placebo-controlled, double-blind trial. Allergy 2012;67:1572-9.
58. Barnes N, Pavord I, Chuchalin A, Bell J, Hunter M, Lewis T, et al. A randomized, double-blind, placebo-controlled study of the CRTH2 antagonist OC000459 in moderate persistent asthma. Clin Exp Allergy 2011;42:38-48.
59. Straumann A, Hoesli S, Ch Bussmann, Stuck M, Perkins M, Collins LP, et al. Anti-eosinophil activity and clinical efficacy of the CRTH2 antagonist OC000459 in eosinophilic esophagitis. Allergy 2013;68:375-85.
60. Busse WW, Wenzel SE, Meltzer EO, Kerwin EM, Liu MC, Zhang N, et al. Safety and efficacy of the prostaglandin D_2 receptor antagonist AMG 853 in asthmatic patients. J Allergy Clin Immunol 2013;131:339-45.
61. Philip G, van Adelsberg J, Loeys T, Liu N, Wong P, Lai E, et al. Clinical studies of the DP1 antagonist laropiprant in asthma and allergic rhinitis. J Allergy Clin Immunol 2009;124:942-8.
62. Nabe T, Kuriyama Y, Mizutani N, Shibayama S, Hiromoto A, Fujii M, et al. Inhibition of hematopoietic prostaglandin D synthase improves allergic nasal blockage in guinea pigs. Prostaglandins Other Lipid Med 2011;95:27-34.
63. Kajiwara D, Aoyagi H, Shigeno K, Togawa M, Tanaka K, Inagaki N, et al. Role of hematopoietic prostaglandin D synthase in biphasic nasal obstruction in guinea pig model of experimental allergic rhinitis. Eur J Pharmacol 2011; 667:389-95.

64. Schneider E, Thieblemont N, De Moraes ML, Dy M. Basophils: new players in the cytokine network. Eur Cytokine Netw 2010;21:142-53.
65. Ackermann L, Harvima IT. Mast cells of psoriatic and atopic dermatitis skin are positive for TNF-α and their degranulation is associated with expression of ICAM-1 in the epidermis. Arch Dermatol Res 1998;290:353-9.
66. Falkencrone S, Poulsen LK, Bindslev-Jensen C, Woetmann A, Odum N, Poulsen BC, et al. IgE-mediated basophil tumour necrosis factor alpha induces matrix metalloproteinase-9 from monocytes. Allergy 2013;68:614-20.
67. Suttle MM, Nilsson G, Snellman E, Harvima IT. Experimentally induced psoriatic lesion associates with interleukin (IL)-6 in mast cells and appearance of dermal cells expressing IL-33 and IL-6 receptor. Clin Exp Immunol 2012;169: 311-9.
68. Smolen JS, Schoels MM, Nishimoto N, Breedveld FC, Burmester GR, Dougados M, et al. Consensus statement on blocking the effects of interleukin-6 and in particular by interleukin-6 receptor inhibition in rheumatoid arthritis and other inflammatory conditions. Ann Rheum Dis 2013;72:482-92.
69. Lin AM, Rubin CJ, Khandpur R, Wang JY, Riblett M, Yalavarthi S, et al. Mast cells and neutrophils release IL-17 through extracellular trap formation in psoriasis. J Immunol 2011;187:490-500.
70. Kenna TJ, Brown MA. The role of IL-17-secreting mast cells in inflammatory joint disease. Nat Rev Rheumatol 2013;9:375-9.
71. Patel DD, Lee DM, Kolbinger F, Antoni C. Effect of IL-17A blockade with secukinumab in autoimmune diseases. Ann Rheum Dis 2013;72:ii116-23.
72. Fischer M, Harvima IT, Carvalho RFS, Möller C, Naukkarinen A, Enblad G, et al. Mast cell CD30 ligand is up-regulated in cutaneous inflammations and mediates degranulation-independent chemokine secretion. J Clin Invest 2006;116:2748-56.
73. Skov L, Beurskens FJ, Zachariae COC, Reitamo S, Teeling J, Satijn D, et al. IL-8 as antibody therapeutic target in inflammatory diseases: reduction of clinical activity in palmoplantar pustulosis. J Immunol 2008;181:669-79.
74. Tabrizi W, Wang B, Lu H, Huang S, Bell G, Schwab G, et al. Population pharmacokinetic evaluation of a fully human IgG monoclonal antibody in patients with inflammatory diseases. Inflamm Allergy Drug Targets 2010;9:229-37.
75. Schroeder JT. Basophils: emerging roles in the pathogenesis of allergic disease. Immunol Rev 2011;242:144-60.
76. Messingham KN, Pietras TA, Fairley JA. Role of IgE in bullous pemphigoid: a review and rationale for IgE directed therapies. G Ital Dermatol Venereol 2012; 147:251-7.
77. Hart TK, Blackburn MN, Brigham-Burke M, Dede K, Al-Mahdi N, Zia-Amirhosseini P, et al. Preclinical efficacy and safety of pascolizumab (SB 240683): a humanized anti-interleukin-4 antibody with therapeutic potential in asthma. Clin Exp Immunol 2002;130:93-100.
78. Karasuyama H, Obata K, Wada T, Tsujimura Y, Mukai K. Newly appreciated roles for basophils in allergy and protective immunity. Allergy 2011;66:1133-41.
79. Crivellato E, Travan L, Ribatti D. Mast cells and basophils: a potential link in promoting angiogenesis during allergic inflammation. Int Arch Allergy Immunol 2009;151:89-97.
80. Sumbayev VV, Nicholas SA, Streatfield CL, Gibbs BF. Involvement of hypoxia-inducible factor-1 HiF(1α) in IgE-mediated primary human basophil responses. Eur J Immunol 2009;39:3511-9.
81. Sumbayev VV, Yasinska I, Oniku AE, Streatfield CL, Gibbs BF. Involvement of hypoxia-inducible factor-1 in the inflammatory responses of human LAD2 mast cells and basophils. PLoS One 2012;7:e34259.
82. Gulliksson M, Carvalho RFS, Ullerås E, Nilsson G. Mast cell survival and mediator secretion in response to hypoxia. PLoS One 2010;5:e12360.
83. Lusková P, Dráber P. Modulation of the Fce receptor I signaling by tyrosine kinase inhibitors: search for therapeutic targets of inflammatory and allergy diseases. Curr Pharm Des 2004;10:1727-37.
84. Riccaboni M, Bianchi I, Petrillo P. Spleen tyrosine kinases: biology, therapeutic targets and drugs. Drug Discov Today 2010;15:517-30.
85. Braselmann S, Taylor V, Zhao H, Wang S, Sylvain C, Baluom M, et al. R406, an orally available spleen tyrosine kinase inhibitor blocks fc receptor signaling and reduces immune complex-mediated inflammation. J Pharmacol Exp Ther 2006; 319:998-1008.
86. Weinblatt ME, Kavanaugh A, Genovese MC, Jones DA, Musser TK, Grossbard EB, et al. Effects of fostamatinib (R788), an oral spleen tyrosine kinase inhibitor, on health-related quality of life in patients with active rheumatoid arthritis: analyses of patient-reported outcomes from a randomized, double-blind, placebo-controlled trial. J Rheumatol 2013;40:369-78.
87. Simmons DL. Targeting kinases: a new approach to treating inflammatory rheumatic diseases. Curr Opin Pharmacol 2013;13:426-34.
88. Guyer BJ, Shimamoto SR, Bradhurst AL, Grossbard EB, Dreskin SC, Nelson HS. Mast cell inhibitor R112 is well tolerated and affects prostaglandin D2 but not other mediators, symptoms, or nasal volumes in a nasal challenge model of allergic rhinitis. Allergy Asthma Proc 2006;27:208-13.
89. Masuda ES, Schmitz J. Syk inhibitors as treatment for allergic rhinitis. Pulm Pharmacol Ther 2008;21:461-7.
90. Foster JG, Blunt MD, Carter E, Ward SG. Inhibition of PI3K signaling spurs new therapeutic opportunities in inflammatory/autoimmune diseases and hematological malignancies. Pharmacol Rev 2012;64:1027-54.
91. Blunt MD, Ward SG. Pharmacological targeting of phosphoinositide lipid kinases and phosphatases in the immune system: success, disappointment, and new opportunities. Front Immunol 2012;3:226.
92. Randis TM, Puri KD, Zhou H, Diacovo TG. Role of PI3Kδ and PI3Kγ in inflammatory arthritis and tissue localization of neutrophils. Eur J Immunol 2008;38: 1215-24.
93. Lee KS, Lee HK, Hayflick JS, Lee YC, Puri KD. Inhibition of phosphoinositide 3-kinase δ attenuates allergic airway inflammation and hyperresponsiveness in murine asthma model. FASEB J 2006;20:455-65.
94. So L, Fruman DA. PI3K signalling in B- and T-lymphocytes: new developments and therapeutic advances. Biochem J 2012;442:465-81.
95. Blunt MD, Ward SG. Pharmacological targeting of phosphoinositide lipid kinases and phosphatases in the immune system: success, disappointment, and new opportunities. Front Immunol 2013;3:1-15.
96. Blunt MD, Ward SG. Targeting PI3K isoforms and SHIP in the immune system: new therapeutics for inflammation and leukemia. Curr Opin Pharmacol 2012;12: 444-51.
97. Norman P. Selective PI3Kδ inhibitors, a review of the patent literature. Expert Opin Ther Pat 2011;21:1773-90.
98. Kalesnikoff J, Baur N, Leitges M, Hughes MR, Damen JE, Huber M, et al. SHIP negatively regulates IgE + antigen-induced IL-6 production in mast cells by inhibiting NF-κB activity. J Immunol 2002;168:4737-46.
99. Oh SY, Zheng T, Bailey ML, Barber DL, Schroeder JT, Kim YK, et al. Src homology 2 domain-containing inositol 5-phosphatase 1 deficiency leads to a spontaneous allergic inflammation in the murine lung. J Allergy Clin Immunol 2007; 119:123-31.
100. Haddon DJ, Antignano F, Hughes MR, Blanchet MR, Zbytnuik L, Krystal G, et al. SHIP1 is a repressor of mast cell hyperplasia, cytokine production, and allergic inflammation in vivo. J Immunol 2009;183:228-36.
101. Stenton GR, Mackenzie LF, Tam P, Cross JL, Harwig C, Raymond J, et al. Characterization of AQX-1125, a small molecule SHIP1 activator: Part 1. Effects on inflammatory cell activation and chemotaxis in vitro and pharmacokinetic characterization in vivo. Br J Pharmacol 2013;168:1506-18.
102. Stenton GR, Mackenzie LF, Tam P, Cross JL, Harwig C, Raymond J, et al. Characterization of AQX-1125, a small molecule SHIP1 activator: Part 2. Efficacy studies in allergic and pulmonary inflammation models in vivo. Br J Pharmacol 2013;168:1519-29.
103. Ellmeier W, Abramova A, Schebesta A. Tec family kinases: regulation of FceRI-mediated mast-cell activation. FEBS J 2011;278:1990-2000.
104. Honigberg LA, Smith AM, Sirisawad M, Verner E, Loury D, Chang B, et al. The Bruton tyrosine kinase inhibitor PCI-32765 blocks B-cell activation and is efficacious in models of autoimmune disease and B-cell malignancy. Proc Natl Acad Sci U S A 2010;107:13075-80.
105. Soucek L, Buggy JJ, Kortlever R, Adimoolam S, Monclus HA, Allende MT, et al. Modeling pharmacological inhibition of mast cell degranulation as a therapy for insulinoma. Neoplasia 2011;13:1093-100.
106. MacGlashan D Jr, Honigberg LA, Smith A, Buggy J, Schroeder JT. Inhibition of IgE-mediated secretion from human basophils with a highly selective Bruton's tyrosine kinase, Btk, inhibitor. Int Immunopharmacol 2011;11: 475-9.
107. Chang BY, Huang MM, Francesco M, Chen J, Sokolove J, Magadala P, et al. The Bruton tyrosine kinase inhibitor PCI-32765 ameliorates autoimmune arthritis by inhibition of multiple effector cells. Arthritis Res Ther 2011;13:R115.
108. Evans EK, Tester R, Aslanian S, Karp R, Sheets M, Labenski MT, et al. Inhibition of Btk with CC-292 provides early pharmacodynamic assessment of activity in mice and humans. J Pharmacol Exp Ther 2013;346:219-28.
109. D'Cruz OJ, Uckun FM. Novel Bruton's tyrosine kinase inhibitors currently in development. Onco Targets Ther 2013;6:161-76.
110. Ustun C, DeRemer DL, Akin C. Tyrosine kinase inhibitors in the treatment of systemic mastocytosis. Leuk Res 2011;35:1143-52.
111. Verstovsek S, Akin C, Manshouri T, Quintas-Cardama A, Huynh L, Manley P, et al. Effects of AMN107, a novel aminopyrimidine tyrosine kinase inhibitor, on human mast cells bearing wild-type or mutated codon 816 c-kit. Leuk Res 2006;30:1365-70.
112. Vega-Ruiz A, Cortes JE, Sever M, Manshouri T, Quintas-Cardama A, Luthra R, et al. Phase II study of imatinib mesylate as therapy for patients with systemic mastocytosis. Leuk Res 2009;33:1481-4.
113. Eklund KK, Joensuu H. Treatment of rheumatoid arthritis with imatinib mesylate: clinical improvement in three refractory cases. Ann Med 2003;35:362-7.

114. Juurikivi A, Sandler C, Lindstedt KA, Kovanen PT, Juutilainen T, Leskinen MJ, et al. Inhibition of c-kit tyrosine kinase by imatinib mesylate induces apoptosis in mast cells in rheumatoid synovia: a potential approach to the treatment of arthritis. Ann Rheum Dis 2005;64:1126-31.
115. Tristano AG. Tyrosine kinases as targets in rheumatoid arthritis. Int Immunopharmacol 2009;9:1-9.
116. El-Agamy DS. Anti-allergic effects of nilotinib on mast cell-mediated anaphylaxis like reactions. Eur J Pharmacol 2012;680:115-21.
117. Kneidinger M, Schmidt U, Rix U, Gleixner KV, Vales A, Baumgartner C, et al. The effects of dasatinib on IgE receptor-dependent activation and histamine release in human basophils. Blood 2008;111:3097-107.
118. Paul C, Sans B, Suarez F, Casassus P, Barete S, Lantermier F, et al. Masitinib for the treatment of systemic and cutaneous mastocytosis with handicap: a phase 2a study. Am J Hematol 2010;85:921-5.
119. Humbert M, de Blay F, Garcia G, Prud'homme A, Leroyer C, Magnan A, et al. Masitinib, a c-kit/PDGF receptor tyrosine kinase inhibitor, improves disease control in severe corticosteroid-dependent asthmatics. Allergy 2009;64:1194-201.
120. Gotlib J, DeAngelo DJ, George TI, Corless CL, Linder A, Langford C, et al. KIT inhibitor midostaurin exhibits a high rate of clinically meaningful and durable responses in advanced systemic mastocytosis: report of a fully accrued phase II trial. Blood 2010;116:Abstract 316.
121. Jolly PS, Bektas M, Olivera A, Gonzalez-Espinosa C, Proia RL, Rivera J, et al. Transactivation of sphingosine-1-phosphate receptors by FcεRI triggering is required for normal mast cell degranulation and chemotaxis. J Exp Med 2004; 199:959-70.
122. Ammit AJ, Hastie AT, Edsall LC, Hoffman RK, Amrani Y, Krymskaya VP, et al. Sphingosine 1-phosphate modulates human airway smooth muscle cell functions that promote inflammation and airway remodeling in asthma. FASEB J 2001;15: 1212-4.
123. Oskeritzian CA, Alvarez SE, Hait NC, Price MM, Milstien S, Spiegel S. Distinct roles of sphingosine kinases 1 and 2 in human mast-cell functions. Blood 2008; 111:4193-200.
124. Ryan JJ, Spiegel S. The role of sphingosine-1-phosphate and its receptors in asthma. Drug News Perspect 2008;21:89-96.
125. Hogenauer K, Billich A, Pally C, Streiff M, Wagner T, Welzenbach K, et al. Phosphorylation by sphingosine kinase 2 is essential for in vivo potency of FTY720 analogues. ChemMedChem 2008;3:1027-9.
126. Takabe K, Paugh SW, Milstien S, Spiegel S. "Inside-out" signaling of sphingosine-1-phosphate: therapeutic targets. Pharmacol Rev 2008;60:181-95.
127. Brinkmann V, Billich A, Baumruker T, Heining P, Schmouder R, Francis G, et al. Fingolimod (FTY720): discovery and development of an oral drug to treat multiple sclerosis. Nat Rev Drug Discov 2010;9:883-97.
128. Vig M, Dehaven WI, Bird GS, Billingsley JM, Wang H, Rao PE, et al. Defective mast cell effector functions in mice lacking the CRACM1 pore subunit of store-operated calcium release-activated calcium channels. Nat Immunol 2008;9:89-96.
129. Baba Y, Nishida K, Fujii Y, Hirano T, Hikida M, Kurosaki T. Essential function for the calcium sensor STIM1 in mast cell activation and anaphylactic responses. Nat Immunol 2008;9:81-8.
130. Putney JW Jr. Pharmacology of capacitative calcium entry. Mol Interv 2001;1: 84-94.
131. Ng SW, Di CJ, Singaravelu K, Parekh AB. Sustained activation of the tyrosine kinase Syk by antigen in mast cells requires local Ca^{2+} influx through Ca^{2+} release-activated Ca^{2+} channels. J Biol Chem 2008;283:31348-55.
132. Parekh AB, Putney JW Jr. Store-operated calcium channels. Physiol Rev 2005;85: 757-810.
133. Di CJ, Nelson C, Bates G, Parekh AB. Targeting Ca^{2+} release-activated Ca^{2+} channel channels and leukotriene receptors provides a novel combination strategy for treating nasal polyposis. J Allergy Clin Immunol 2009;124:1014-21.
134. Takezawa R, Cheng H, Beck A, Ishikawa J, Launay P, Kubota H, et al. A pyrazole derivative potently inhibits lymphocyte Ca^{2+} influx and cytokine production by facilitating transient receptor potential melastatin 4 channel activity. Mol Pharmacol 2006;69:1413-20.
135. He LP, Hewavitharana T, Soboloff J, Spassova MA, Gill DL. A functional link between store-operated and TRPC channels revealed by the 3,5-bis(trifluoromethyl)pyrazole derivative, BTP2. J Biol Chem 2005;280: 10997-1006.
136. Yoshino T, Ishikawa J, Ohga K, Morokata T, Takezawa R, Morio H, et al. YM-58483, a selective CRAC channel inhibitor, prevents antigen-induced airway eosinophilia and late phase asthmatic responses via Th2 cytokine inhibition in animal models. Eur J Pharmacol 2007;560:225-33.
137. Wulff H, Castle NA. Therapeutic potential of KCa3.1 blockers: recent advances and promising trends. Expert Rev Clin Pharmacol 2010;3:385-96.
138. Ekoff M, Nilsson G. Mast cell apoptosis and survival. Adv Exp Med Biol 2011; 716:47-60.
139. Willis SN, Fletcher JI, Kaufmann T, van Delft MF, Chen L, Czabotar PE, et al. Apoptosis initiated when BH3 ligands engage multiple Bcl-2 homologs, not Bax or Bak. Science 2007;315:856-9.
140. Xiang Z, Moller C, Nilsson G. IgE-receptor activation induces survival and Bfl-1 expression in human mast cells but not basophils. Allergy 2006;61:1040-6.
141. Ekoff M, Lyberg K, Krajewska M, Arvidsson M, Rak S, Reed JC, et al. Anti-apoptotic BFL-1 is the major effector in activation-induced human mast cell survival. PLoS One 2012;7:e39117.
142. Oltersdorf T, Elmore SW, Shoemaker AR, Armstrong RC, Augeri DJ, Belli BA, et al. An inhibitor of Bcl-2 family proteins induces regression of solid tumours. Nature 2005;435:677-81.
143. Mohammad RM, Goustin AS, Aboukameel A, Chen B, Banerjee S, Wang G, et al. Preclinical studies of TW-37, a new nonpeptidic small-molecule inhibitor of Bcl-2, in diffuse large cell lymphoma xenograft model reveal drug action on both Bcl-2 and Mcl-1. Clin Cancer Res 2007;13:2226-35.
144. Tse C, Shoemaker AR, Adickes J, Anderson MG, Chen J, Jin S, et al. ABT-263: a potent and orally bioavailable Bcl-2 family inhibitor. Cancer Res 2008;68:3421-8.
145. Rudin CM, Hann CL, Garon EB, Ribeiro de OM, Bonomi PD, Camidge DR, et al. Phase II study of single-agent navitoclax (ABT-263) and biomarker correlates in patients with relapsed small cell lung cancer. Clin Cancer Res 2012;18:3163-9.
146. Karlberg M, Ekoff M, Huang DC, Mustonen P, Harvima IT, Nilsson G. The BH3-mimetic ABT-737 induces mast cell apoptosis in vitro and in vivo: potential for therapeutics. J Immunol 2010;185:2555-62.
147. Peter B, Cerny-Reiterer S, Hadzijusufovic E, Schuch K, Stefanzl G, Eisenwort G, et al. The pan-Bcl-2 blocker obatoclax promotes the expression of Puma, Noxa, and Bim mRNA and induces apoptosis in neoplastic mast cells. J Leukoc Biol 2014;95:95-104.
148. Bachelet I, Munitz A, Moretta A, Moretta L, Levi-Schaffer F. The inhibitory receptor IRp60 (CD300a) is expressed and functional on human mast cells. J Immunol 2005;175:7989-95.
149. Munitz A, Bachelet I, Eliashar R, Moretta A, Moretta L, Levi-Schaffer F. The inhibitory receptor IRp60 (CD300a) suppresses the effects of IL-5, GM-CSF, and eotaxin on human peripheral blood eosinophils. Blood 2006;107:1996-2003.
150. Sabato V, Verweij MM, Bridts CH, Levi-Schaffer F, Gibbs BF, De Clerck LS, et al. CD300a is expressed on human basophils and seems to inhibit IgE/FcεRI-dependent anaphylactic degranulation. Cytometry B Clin Cytom 2012;82:132-8.
151. Gibbs BF, Sabato V, Bridts CH, Ebo DG, Ben Zimra M, Levi Schaffer F. Expressions and inhibitory functions of CD300a receptors on purified human basophils. Exp Dermatol 2012;21:884-6.
152. Bachelet I, Munitz A, Levi-Schaffer F. Abrogation of allergic reactions by a bispecific antibody fragment linking IgE to CD300a. J Allergy Clin Immunol 2006; 117:1314-20.
153. Zhao W, Kepley CL, Morel PA, Okumoto LM, Fukuoka Y, Schwartz LB. Fc gamma RIIa, not Fc gamma RIIb, is constitutively and functionally expressed on skin-derived human mast cells. J Immunol 2006;177:694-701.
154. Cassard L, Jönsson F, Arnaud S, Daëron M. Fcγ receptors inhibit mouse and human basophil activation. J Immunol 2012;189:2995-3006.
155. Cemerski S, Chu SY, Moore GL, Muchhal US, Desjarlais JR, Szymkowski DE. Suppression of mast cell degranulation through a dual-targeting tandem IgE-IgG Fc domain biologic engineered to bind with high affinity to FcγRIIb. Immunol Lett 2012;143:34-43.
156. Cady CT, Powell MS, Harbeck RJ, Giclas PC, Murphy JR, Katial RK, et al. IgG antibodies produced during subcutaneous allergen immunotherapy mediate inhibition of basophil activation via a mechanism involving both FcγRIIA and FcγRIIB. Immunol Lett 2010;130:57-65.
157. Floyd H, Ni J, Cornish AL, Zeng Z, Liu D, Carter KC, et al. Siglec-8. A novel eosinophil-specific member of the immunoglobulin superfamily. J Biol Chem 2000;275:861-6.
158. Kikly KK, Bochner BS, Freeman SD, Tan KB, Gallagher KT, D'alessio KJ, et al. Identification of SAF-2, a novel siglec expressed on eosinophils, mast cells, and basophils. J Allergy Clin Immunol 2000;105:1093-100.
159. Kiwamoto T, Kawasaki N, Paulson JC, Bochner BS. Siglec-8 as a drugable target to treat eosinophil and mast cell-associated conditions. Pharmacol Ther 2012;135: 327-36.
160. Pini A, Mannaioni G, Pellegrini-Giampietro D, Passani MB, Mastroianni R, Bani D, et al. The role of cannabinoids in inflammatory modulation of allergic respiratory disorders, inflammatory pain and ischemic stroke. Curr Drug Targets 2012; 13:984-93.
161. Munitz A, Bachelet I, Levi-Schaffer F. Reversal of airway inflammation and remodeling in asthma by a bispecific antibody fragment linking CCR3 to CD300a. J Allergy Clin Immunol 2006;118:1082-9.
162. Nakahashi-Oda C, Tahara-Hanaoka S, Shoji M, Okoshi Y, Nakano-Yokomizo T, Ohkohchi N, et al. Apoptotic cells suppress mast cell inflammatory responses via the CD300a immunoreceptor. J Exp Med 2012;209:1493-503.

163. Nissim Ben Efraim AH, Karra L, Ben-Zimra M, Levi-Schaffer F. The inhibitory receptor CD300a is up-regulated by hypoxia and GM-CSF in human peripheral blood eosinophils. Allergy 2013;68:397-401.
164. Simhadri VR, Andersen JF, Calvo E, Choi SC, Coligan JE, Borrego F. Human CD300a binds to phosphatidylethanolamine and phosphatidylserine, and modulates the phagocytosis of dead cells. Blood 2012;119:2799-809.
165. Tsujimura Y, Obata K, Mukai K, Shindou H, Yoshida M, Nishikado H, et al. Basophils play a pivotal role in immunoglobulin-G-mediated but not immunoglobulin-E-mediated systemic anaphylaxis. Immunity 2008;28:581-9.
166. Kepley CL, Cambier JC, Morel PA, Lujan D, Ortega E, Wilson BS, et al. Negative regulation of FceRI signaling by FcγRII costimulation in human blood basophils. J Allergy Clin Immunol 2000;106:337-48.
167. Bruhns P, Frémont S, Daëron M. Regulation of allergy by Fc receptors. Curr Opin Immunol 2005;17:662-9.
168. Okayama Y, Kirshenbaum AS, Metcalfe DD. Expression of a functional high-affinity IgG receptor, FcγRI, on human mast cells: upregulation by IFN-γ. J Immunol 2000;164:4332-9.
169. Zhu D, Kepley CL, Zhang M, Zhang K, Saxon A. A novel human immunoglobulin Fcγ-Fcε bifunctional fusion protein inhibits FcεRI-mediated degranulation. Nat Med 2002;8:518-21.
170. Zhu D, Kepley CL, Zhang K, Terada T, Yamada T, Saxon A. A chimeric human-cat fusion protein blocks cat-induced allergy. Nat Med 2005;11:446-9.
171. Zhang K, Kepley CL, Terada T, Zhu D, Perez H, Saxon A. Inhibition of allergen-specific IgE reactivity by a human Ig Fcγ-Fcε bifunctional fusion protein. J Allergy Clin Immunol 2004;114:321-7.
172. Lin LH, Zheng P, Yuen JW, Wang J, Zhou J, Kong CQ, et al. Prevention and treatment of allergic inflammation by an Fcγ-Der f2 fusion protein in a murine model of dust mite-induced asthma. Immunol Res 2012;52:276-83.
173. Foussias G, Yousef GM, Diamandis EP. Molecular characterization of a Siglec8 variant containing cytoplasmic tyrosine-based motifs, and mapping of the Siglec8 gene. Biochem Biophys Res Commun 2000;278:775-81.
174. Aizawa H, Plitt J, Bochner BS. Human eosinophils express two Siglec-8 splice variants. J Allergy Clin Immunol 2002;109:176.
175. Hudson SA, Herrmann H, Du J, Cox P, Haddad el-B, Butler B, et al. Developmental, malignancy-related, and cross-species analysis of eosinophil, mast cell, and basophil siglec-8 expression. J Clin Immunol 2011;31:1045-53.
176. Yokoi H, Myers A, Matsumoto K, Crocker PR, Saito H, Bochner BS. Alteration and acquisition of Siglecs during in vitro maturation of CD34+ progenitors into human mast cells. Allergy 2006;61:769-76.
177. Yokoi H, Choi OH, Hubbard W, Lee HS, Canning BJ, Lee HH, et al. Inhibition of FceRI-dependent mediator release and calcium flux from human mast cells by sialic acid-binding immunoglobulin-like lectin 8 engagement. J Allergy Clin Immunol 2008;121:499-505.e1.
178. Nutku-Bilir E, Hudson SA, Bochner BS. Interleukin-5 priming of human eosinophils alters siglec-8 mediated apoptosis pathways. Am J Respir Cell Mol Biol 2008;38:121-4.
179. Na HJ, Hudson SA, Bochner BS. IL-33 enhances Siglec-8 mediated apoptosis of human eosinophils. Cytokine 2012;57:169-74.
180. Hudson SA, Bovin NV, Schnaar RL, Crocker PR, Bochner BS. Eosinophil-selective binding and proapoptotic effect in vitro of a synthetic Siglec-8 ligand, polymeric 6'-sulfated sialyl Lewis x. J Pharmacol Exp Ther 2009;330:608-12.
181. Farid SSh, Mirshafiey A, Razavi A. Siglec-8 and Siglec-F, the new therapeutic targets in asthma. Immunopharmacol Immunotoxicol 2012;34:721-6.
182. Stevens WW, Kim TS, Pujanauski LM, Hao X, Braciale TJ. Detection and quantitation of eosinophils in the murine respiratory tract by flow cytometry. J Immunol Methods 2007;327:63-74.
183. Tateno H, Li H, Schur MJ, Bovin N, Crocker PR, Wakarchuk WW, et al. Distinct endocytic mechanisms of CD22 (Siglec-2) and Siglec-F reflect roles in cell signaling and innate immunity. Mol Cell Biol 2007;27:3699-710.
184. Zhang M, Angata T, Cho JY, Miller M, Broide DH, Varki A. Defining the in vivo function of Siglec-F, a CD33-related Siglec expressed on mouse eosinophils. Blood 2007;109:4280-7.
185. Cho JY, Song DJ, Pham A, Rosenthal P, Miller M, Dayan S, et al. Chronic OVA allergen challenged Siglec-F deficient mice have increased mucus, remodeling, and epithelial Siglec-F ligands which are up-regulated by IL-4 and IL-13. Respir Res 2010;11:154.
186. Kiwamoto T, Ishii Y, Morishima Y, Yoh K, Kikuchi N, Haraguchi N, et al. Blockade of cysteinyl leukotriene-1 receptors suppresses airway remodelling in mice overexpressing GATA-3. Clin Exp Allergy 2011;41:116-28.
187. Merighi S, Simioni C, Gessi S, Varani K, Borea PA. Binding thermodynamics at the human cannabinoid CB1 and CB2 receptors. Biochem Pharmacol 2010;79:471-7.
188. Pacher P, Mechoulam R. Is lipid signaling through cannabinoid 2 receptors part of a protective system? Prog Lipid Res 2011;50:193-211.
189. Börner C, Höllt V, Sebald W, Kraus J. Transcriptional regulation of the cannabinoid receptor type 1 gene in T cells by cannabinoids. J Leukoc Biol 2007;81:336-43.
190. Börner C, Bedini A, Höllt V, Kraus J. Analysis of promoter regions regulating basal and interleukin-4-inducible expression of the human CB1 receptor gene in T lymphocytes. Mol Pharmacol 2008;73:1013-9.
191. Sugawara K, Zákány N, Hundt T, Emelianov V, Tsuruta D, Schäfer C, et al. Cannabinoid receptor 1 controls human mucosal-type mast cell degranulation and maturation in situ. J Allergy Clin Immunol 2013;132:182-93.
192. Sugawara K, Bíró T, Tsuruta D, Tóth BI, Kromminga A, Zákány N, et al. Endocannabinoids limit excessive mast cell maturation and activation in human skin. J Allergy Clin Immunol 2012;129:726-38.e8.
193. Samson MT, Small-Howard A, Shimoda LM, Koblan-Huberson M, Stokes AJ, Turner H. Differential roles of CB1 and CB2 cannabinoid receptors in mast cells. J Immunol 2003;170:4953-62.
194. Aloe L, Leon A, Levi-Montalcini R. A proposed autacoid mechanism controlling mastocyte behaviour. Agents Actions 1993;39 Spec No:C145-7.
195. Lau AH, Chow SS. Effects of cannabinoid receptor agonists on immunologically induced histamine release from rat peritoneal mast cells. Eur J Pharmacol 2003;464:229-35.
196. Hanus L, Breuer A, Tchilibon S, Shiloah S, Goldenberg D, Horowitz M, et al. HU-308: a specific agonist for CB(2), a peripheral cannabinoid receptor. Proc Natl Acad Sci U S A 1999;96:14228-33.
197. Facci L, Dal Toso R, Romanello S, Buriani A, Skaper SD, Leon A. Mast cells express a peripheral cannabinoid receptor with differential sensitivity to anandamide and palmitoylethanolamide. Proc Natl Acad Sci U S A 1995;92:3376-80.
198. Elishmereni M, Levi-Schaffer F. CD48: a co-stimulatory receptor of immunity. Int J Biochem Cell Biol 2011;43:25-8.
199. Giacomin PR, Siracusa MC, Walsh KP, Grencis RK, Kubo M, Comeau MR, et al. Thymic stromal lymphopoietin-dependent basophils promote Th2 cytokine responses following intestinal helminth infection. J Immunol 2012;189:4371-8.
200. Malaviya R, Gao Z, Thankavel K, van der Merwe PA, Abraham SN. The mast cell tumor necrosis factor alpha response to FimH-expressing Escherichia coli is mediated by the glycosylphosphatidylinositol-anchored molecule CD48. Proc Natl Acad Sci U S A 1999;96:8110-5.
201. Malaviya R, Abraham SN. Mast cell modulation of immune responses to bacteria. Immunol Rev 2001;179:16-24.
202. Proft T, Baker EN. Pili in gram-negative and gram-positive bacteria—structure, assembly and their role in disease. Cell Mol Life Sci 2009;66:613-35.
203. Muñoz S, Hernández-Pando R, Abraham SN, Enciso JA. Mast cell activation by Mycobacterium tuberculosis: mediator release and role of CD48. J Immunol 2003;170:5590-6.
204. Rocha-de-Souza CM, Berent-Maoz B, Mankuta D, Moses AE, Levi-Schaffer F. Human mast cell activation by *Staphylococcus aureus*: interleukin-8 and tumor necrosis factor alpha release and the role of Toll-like receptor 2 and CD48 molecules. Infect Immun 2008;76:4489-97.
205. Elishmereni M, Alenius HT, Bradding P, Mizrahi S, Shikotra A, Minai-Fleminger Y, et al. Physical interactions between mast cells and eosinophils: a novel mechanism enhancing eosinophil survival in vitro. Allergy 2011;66:376-85.
206. Zimmermann N, King NE, Laporte J, Yang M, Mishra A, Pope SM, et al. Dissection of experimental asthma with DNA microarray analysis identifies arginase in asthma pathogenesis. J Clin Invest 2003;111:1863-74.
207. Munitz A, Bachelet I, Finkelman FD, Rothenberg ME, Levi-Schaffer F. CD48 is critically involved in allergic eosinophilic airway inflammation. Am J Respir Crit Care Med 2007;175:911-8.
208. Allakhverdi Z, Comeau MR, Jessup HK, Yoon BR, Brewer A, Chartier S, et al. Thymic stromal lymphopoietin is released by human epithelial cells in response to microbes, trauma, or inflammation and potently activates mast cells. J Exp Med 2007;204:253-8.
209. Astrakhan A, Omori M, Nguyen T, Becker-Herman S, Iseki M, Aye T, et al. Local increase in thymic stromal lymphopoietin induces systemic alterations in B cell development. Nat Immunol 2007;8:522-31.
210. Liu YJ, Soumelis V, Watanabe N, Ito T, Wang YH, Malefyt Rde W, et al. TSLP: an epithelial cell cytokine that regulates T cell differentiation by conditioning dendritic cell maturation. Annu Rev Immunol 2007;25:193-219.
211. Siracusa MC, Saenz SA, Hill DA, Kim BS, Headley MB, Doering TA, et al. TSLP promotes interleukin-3-independent basophil haematopoiesis and type 2 inflammation. Nature 2011;477:229-33.
212. Ziegler SF, Artis D. Sensing the outside world: TSLP regulates barrier immunity. Nat Immunol 2010;11:289-93.
213. Park LS, Martin U, Garka K, Gliniak B, Di Santo JP, Muller W, et al. Cloning of the murine thymic stromal lymphopoietin (TSLP) receptor: Formation of a functional heteromeric complex requires interleukin 7 receptor. J Exp Med 2000;192:659-70.

214. Comeau MR, Ziegler SF. The influence of TSLP on the allergic response. Mucosal Immunol 2010;3:138-47.
215. Shikotra A, Choy DF, Ohri CM, Doran E, Butler C, Hargadon B, et al. Increased expression of immunoreactive thymic stromal lymphopoietin in patients with severe asthma. J Allergy Clin Immunol 2012;129:104-11, e1-9.
216. Le TA, Takai T, Vu AT, Kinoshita H, Chen X, Ikeda S, et al. Flagellin induces the expression of thymic stromal lymphopoietin in human keratinocytes via toll-like receptor 5. Int Arch Allergy Immunol 2011;155:31-7.
217. Kaur D, Doe C, Woodman L, Wan WY, Sutcliffe A, Hollins F, et al. Mast cell-airway smooth muscle crosstalk: the role of thymic stromal lymphopoietin. Chest 2012;142:76-85.
218. Zhang F, Huang G, Hu B, Song Y, Shi Y. A soluble thymic stromal lymphopoietin (TSLP) antagonist, TSLPR-immunoglobulin, reduces the severity of allergic disease by regulating pulmonary dendritic cells. Clin Exp Immunol 2011;164:256-64.
219. Galli SJ, Tsai M. IgE and mast cells in allergic disease. Nat Med 2012;18:693-704.
220. Blank U, Ra C, Miller L, White K, Metzger H, Kinet JP. Complete structure and expression in transfected cells of high affinity IgE receptor. Nature 1989;337:187-9.
221. Blank U, Rivera J. The ins and outs of IgE-dependent mast-cell exocytosis. Trends Immunol 2004;25:266-73.
222. Garman SC, Wurzburg BA, Tarchevskaya SS, Kinet JP, Jardetzky TS. Structure of the Fc fragment of human IgE bound to its high-affinity receptor FcεRIα. Nature 2000;406:259-66.
223. Kulczycki A Jr, Isersky C, Metzger H. The interaction of IgE with rat basophilic leukemia cells. I. Evidence for specific binding of IgE. J Exp Med 1974;139:600-16.
224. Spiegelberg HL, Canning KM, Scheetz M, Koppel G, Chiller JM. Effect of myeloma IgE injections on passive and active cutaneous anaphylaxis in rats. J Immunol 1986;136:131-5.
225. Smith LD, Leatherbarrow RJ, Spivey AC. Development of small molecules to target the IgE: FcεRI protein-protein interaction in allergies. Future Med Chem 2013;5:1423-35.
226. Corren J, Casale TB, Lanier B, Buhl R, Holgate S, Jimenez P. Safety and tolerability of omalizumab. Clin Exp Allergy 2009;39:788-97.
227. Chang TW, Shiung YY. Anti-IgE as a mast cell-stabilizing therapeutic agent. J Allergy Clin Immunol 2006;117:1203-12.
228. Maurer M, Rosén K, Hsieh HJ, Saini S, Grattan C, Gimenéz-Arnau A, et al. Omalizumab for the treatment of chronic idiopathic or spontaneous urticaria. N Engl J Med 2013;368:924-35.
229. Rafi A, Do LT, Katz R, Sheinkopf LE, Simons CW, Klaustermeyer W. Effects of omalizumab in patients with food allergy. Allergy Asthma Proc 2010;31:76-83.
230. Sheinkopf LE, Rafi AW, Do LT, Katz RM, Klaustermeyer WB. Efficacy of omalizumab in the treatment of atopic dermatitis: a pilot study. Allergy Asthma Proc 2008;29:530-7.
231. Holgate ST, Djukanović R, Casale T, Bousquet J. Anti-immunoglobulin E treatment with omalizumab in allergic diseases: an update on anti-inflammatory activity and clinical efficacy. Clin Exp Allergy 2005;35:408-16.
232. Lieberman JA, Chehade M. Use of omalizumab in the treatment of food allergy and anaphylaxis. Curr Allergy Asthma Rep 2013;13:78-84.
233. Piliponsky AM, Gleich GJ, Nagler A, Bar I, Levi-Schaffer F. Non-IgE-dependent activation of human lung- and cord blood-derived mast cells is induced by eosinophil major basic protein and modulated by the membrane form of stem cell factor. Blood 2003;101:1898-904.
234. Hollins F, Kaur D, Yang W, Cruse G, Saunders R, Sutcliffe A, et al. Human airway smooth muscle promotes human lung mast cell survival, proliferation, and constitutive activation: cooperative roles for CADM1, stem cell factor, and IL-6. J Immunol 2008;181:2772-80.
235. Yang W, Kaur D, Okayama Y, Ito A, Wardlaw AJ, Brightling CE, et al. Human lung mast cells adhere to human airway smooth muscle, in part, via tumor suppressor in lung cancer-1. J Immunol 2006;176:1238-43.
236. Moiseeva EP, Leyland ML, Bradding P. CADM1 isoforms differentially regulate human mast cell survival and homotypic adhesion. Cell Mol Life Sci 2012;69:2751-64.
237. Moiseeva EP, Roach KM, Leyland ML, Bradding P. CADM1 is a key receptor mediating human mast cell adhesion to human lung fibroblasts and airway smooth muscle cells. PLoS One 2013;8:e61579.
238. Hagiyama M, Inoue T, Furuno T, Iino T, Itami S, Nakanishi M, et al. Increased expression of cell adhesion molecule 1 by mast cells as a cause of enhanced nerve-mast cell interaction in a hapten-induced mouse model of atopic dermatitis. Br J Dermatol 2013;168:771-8.
239. Halova I, Draberova L, Draber P. Mast cell chemotaxis—chemoattractants and signaling pathways. Front Immunol 2012;3:119.

Table E1. Soluble mediators of mast cells and basophils as targets for therapy

Target cell	Target molecule	Candidate drug/action mechanism	Stage of development	Reference
MC	Tryptase	APC-366, enzyme inhibitor APC-2059, enzyme inhibitor Nafamostat mesilate, enzyme inhibitor (non-specific)	Randomized, double-blinded, placebo-controlled, crossover study Open-label phase 2 pilot study In clinical use (largely in Asia) for, e.g., DIC and pancreatitis	E1 E2 E3
MC	Chymase Cathepsin G	Numerous synthetic compounds, e.g., dual inhibitor RWJ-355871	Preclinical testing: animal models, *in vitro* models	E4-E6
MC and Basophil	Histamine	H4R antagonists: JNJ7777120, JNJ28307474 ZPL-3893787 UR-63325	Preclinical testing: animal models, *in vitro* models Phase 1 trials with healthy volunteers completed Phase 2 clinical trial in allergic rhinitis completed	E7,E8 www.ziarcopharma.com/h4.html E9 http://clinicaltrials.gov/
MC and Basophil	LTC_4	cysLTR1 antagonists: zafirlukast, pranlukast, montelukast	In clinical use for asthma	
MC and Basophil	5-LO	5-LO inhibitors: Zileuton	In clinical use for asthma (UK, USA)	
MC and Basophil	FLAP	FLAP inhibitors: MK-886, MK-0591, veliflapon	Clinical trials in asthma in the mid 1990s (products not brought to market)	E10

		GSK-2190915	Phase 2 clinical trials in asthma completed	E10,E11 http://clinicaltrials.gov/
MC	15-LO-1	15-LO inhibitors: PD146176	Preclinical testing: animal models	E12,E13
MC (and basophil)	PGD_2	PD2 receptor antagonists: S-555739	Phase 2a and 2b clinical trials in allergic rhinitis completed	http://clinicaltrials.gov/
		OC000459	Phase 2 clinical trials in asthma, rhinoconjunctivitis and eosinophilic esophagitis completed	E14-E16 http://clinicaltrials.gov/
		Dual DP1-DP2 antagonist: AMG 853	Phase 2 clinical trial in asthma completed	E17
		DP1 antagonist: Laropiprant	Phase 2 clinical trial in asthma and allergic rhinitis completed	E18
MC (and basophil)	hematopoietic PGD synthase	TAS-204, TFC-007	Preclinical testing: guinea pig model of allergic rhinitis	E19,E20
MC and basophil	TNF-α	monoclonal antibodies: Infliximab, Adalimumab, TNF-receptor: etanercept	In clinical use for a variety of chronic inflammatory diseases of the skin, joint and bowel	
MC and basophil	IL-6	monoclonal antibodies: BMS945429	Phase 2b clinical trial in psoriatic arthritis ongoing	E21 http://clinicaltrials.gov/
		Sirukumab	Phase 1 or 2 trials in rheumatoid arthritis, lupus nephritis or lupus erythematosus completed	
		Olokizumab	Phase 2 clinical trials in rheumatoid arthritis completed	

MC and basophil	IL-6 receptor	monoclonal antibodies: tocilizumab Sarilumab	Numerous phase 3 clinical trials completed Phase 2 clinical trials in rheumatoid arthritis and spondylitis completed	E21 http://clinicaltrials.gov/
MC	IL-17A	Monoclonal antibodies: Secukinumab Ixekizumab RG4934, NI-1401, SCH900117	Phase 3 trials in psoriasis completed Phase 2 trial in rheumatoid arthritis completed Phase 1 trials	E22 http://clinicaltrials.gov/ E22
MC	IL-17A receptor	Monoclonal antibody: Brodalumab	Phase 3 trials in psoriasis and phase 2 trial in asthma ongoing	E22 http://clinicaltrials.gov/
MC and basophil	IL-8	Monoclonal antibodies: HuMab 10F8 ABX-IL8	Open-label multicenter study in palmoplantar pustulosis Pharmacokinetic study in psoriasis and rheumatoid arthritis; phase 2 trial in chronic bronchitis completed	E23 E24 http://clinicaltrials.gov/
Basophil (and MC)	IL-4	Pascolizumab	Phase 2 trial in asthma completed	E25 http://clinicaltrials.gov/

Abbreviations: MC = mast cell; LTC_4 = leukotriene C_4; 5-LO = 5-lipoxygenase; FLAP= five-lipoxygenase-activating protein; 15-LO-1 = 15-lipoxygenase-1; PGD synthase = prostaglandin D synthase; TNF = tumor necrosis factor; IL = interleukin

Table E2. Intracellular signalling and survival proteins of mast cells and basophils as targets for therapy

Target cell	Target molecule	Candidate drug/action mechanism	Stage of development	Reference
MC and basophil	SYK	Fostamatinib, inhibits SYK	Phase 3 clinical trials in rheumatoid arthritis were discontinued	E26, E27
		PRT062607, inhibits SYK with high selectivity	Reduced inflammation in preclinical *in vivo* models of rheumatoid arthritis/phase 2 clinical trials in rheumatoid arthritis were withdrawn	E26, E28
		R343, inhibits SYK	Phase 2 clinical trial in asthma failed	E29
		R112, inhibits SYK	Phase 2 clinical trial in allergic rhinitis failed	E30
MC	PI3K	IC87114, inhibits the δ isoform of PI3K	Preclinical testing: murine asthma model	E31
		CAL-101, inhibits the δ isoform of PI3K	Completed phase 1 clinical trials to treat allergic rhinitis	E32
		CAL-263, inhibits the δ isoform of PI3K	Completed phase 1 clinical trials to treat allergic rhinitis	E33
		IPI-145, inhibits the δ and γ isoforms of PI3K	In phase 2 study to treat allergic asthma and rheumatoid arthritis	E34,E35
MC	SHIP-1	AXQ-1125, increases catalytic activity of human SHIP-1	Completed phase 2a clinical studies to treat mild and moderate asthma	E34-E36
MC and basophil	BTK	Ibrutinib, inhibits BTK	In cancer related clinical trials/potential for arthritis treatment, inhibits activation of human basophils	E37,E38
		AVL-292, inhibits BTK	Completed phase 1a clinical studies	E39

MC	KIT, PDGFR, BCR/ABL	Imatinib, inhibits KIT	FDA approved for treatment of systemic mastocytosis/treatment of rheumatoid arthritis	E40-E42
	KIT, PDGFR, BCR/ABL	Nilotinib, inhibits KIT	Phase 2 trials to treat systemic mastocytosis/anti-allergic effect on MC-mediated anaphylaxis reactions	E40,E43
	KIT, PDGFR, VEGFR2, FLT3, PKCα	Midostaurin, inhibits KIT, insensitive to D816V mutation	Phase 2 trials to treat systemic mastocytosis	E44
MC and basophil	KIT, BTK, BCR/ABL, PDGFR, SRC, Ephrins	Dasatinib, inhibits KIT and other tyrosine kinases, including BTK	Phase 2 trials to treat systemic mastocytosis/in sensitized individuals blocks histamine release	E40,E45
MC	KIT, PDGFR, LYN/FYN	Masitinib, inhibits KIT, targets also LYN and FYN	Phase 2 trials to treat systemic or cutaneous mastocytosis and asthma	E40,E46, E47, E48
MC	S1P receptors	FTY720, antagonist for S1P receptors	Approved for treatment of multiple sclerosis/in animal models highly effective in reducing the severity of autoimmune diseases	E49,E50
MC	$K_{Ca}3.1$	ICA-17043, inhibits $K_{Ca}3.1$ channel	Phase 2 clinical trials in asthma failed	E51
MC	CRAC channels	BTP2, inhibits CRAC, TRPC3 and TRPC5 channels, facilitates TRPM4	Inhibitory effect in allergy asthma models in rats and guinea pigs	E52
MC	BCL-2 family members	ABT-737, mimicking BH3 domain, BCL-2 antagonist	In cancer related clinical trials, in mice abolishment of MC in peritoneum, *ex vivo* in human skin biopsies increased MC apoptosis	E53

		Obatoclax, mimicking BH3 domain, BCL-2 antagonist	Growth arrest in primary human neoplastic MC and in various MC lines, synergistic effects on MC when combined with other drugs	E54

Abbreviations: MC = mast cell; SYK = spleen tyrosine kinase; PI3K = phosphatidylinositol 3-kinase; SHIP-1 = Src homology 2 (SH2) domain-containing inositol 5' phosphatase 1; KIT = a MC surface receptor with tyrosine kinase activity; BTK = Bruton´s tyrosine kinase; S1P = Sphingosine-1-phosphate; BCL-2 = B-cell lymphoma 2; BH3 = BCL-2 homology 3; PDGFR = platelet-derived growth factor receptor.

Table E3. Cell surface molecules of mast cells and basophils as targets for therapy.

Target cell	Target molecule	Candidate drug/action mechanism	Stage of development	Reference
MC and basophil	CD300a		Preclinical testing: only animal models	E55-E57, E58-E60
MC and basophil	FcγRIIB		Preclinical testing: only animal models	E61-E64
Basophil	Siglec-8		Preclinical testing: only animal models	E65,E66
MC	CB1 / CB2	Agonists such as AEA and PEA	Preclinical testing: only animal models	E67-E72
MC and basophil	CD48		Preclinical testing: only animal models	E73,E74
MC	TSLPR	TSLPR-immunoglobulin	Preclinical testing: only animal models	E75
MC and basophil	FcεRI	Omalizumab	In clinical use for asthma	E76

Abbreviations: MC = mast cell; CB = cannabinoid receptor; AEA = anandamide; PEA = palmitoylethanolamide; TSLPR = thymic stromal lymphopoietin receptor

References

E1. Krishna MT, Chauhan A, Little L, Sampson K, Hawksworth R, Mant T, et al. Inhibition of mast cell tryptase by inhaled APC 366 attenuates allergen-induced late-phase airway obstruction in asthma. J Allergy Clin Immunol 2001;107:1039-45.

E2. Tremaine WJ, Brzezinski A, Katz JA, Wolf DC, Fleming TJ, Mordenti J, et al. Treatment of mildly to moderately active ulcerative colitis with a tryptase inhibitor (APC 2059): an open-label pilot study. Aliment Pharmacol Ther 2002;16:407-13.

E3. Mori S, Itoh Y, Shinohata R, Sendo T, Oishi R, Nishibori M. Nafamostat mesilate is an extremely potent inhibitor of human tryptase. J Pharmacol Sci 2003;92:420-23.

E4. D'Orléans-Juste P, Houde M, Rae GA, Bkaily G, Carrier E, Simard E. Endothelin-1 (1-31): from chymase-dependent synthesis to cardiovascular pathologies. Vascul Pharmacol 2008;49:51-62.

E5. Yahiro E, Miura S, Imaizumi S, Uehara Y, Saku K. Chymase inhibitors. Curr Pharm Des 2013;19:3065-71.

E6. Maryanoff BE, de Garavilla L, Greco MN, Haertlein BJ, Wells GI, Andrade-Gordon P, et al. Dual inhibition of cathepsin G and chymase is effective in animal models of pulmonary inflammation. Am J Respir Crit Care Med 2010;181:247-53.

E7. Thurmond RL, Desai PJ, Dunford PJ, Fung-Leung WP, Hofstra CL, Jiang W, et al. A potent and selective histamine H4 receptor antagonist with anti-inflammatory properties. J Pharmacol Exp Ther 2004;309:404-13.

E8. Kamo A, Negi O, Tengara S, Kamata Y, Noguchi A, Ogawa H, et al. Histamine H4 receptor antagonists ineffective against itch and skin inflammation in atopic dermatitis mouse model. J Invest Dermatol 2013; Aug 20 (e-pub ahead of print).

E9. Salcedo C, Pontes C, Merlos M. Is the H4 receptor a new drug target for allergies and asthma? Front Biosci (Elite Ed) 2013;1;5:178-87.

E10. Montuschi P, Peters-Golden ML. Leukotriene modifiers for asthma treatment. Clin Exp Allergy 2010;40:1732-41.

E11. Kent SE, Boyce M, Diamant Z, Singh D, O'Connor BJ, Saggu PS, et al. The 5-lipoxygenase-activating protein inhibitor, GSK2190915, attenuates the early and late responses to inhaled allergen in mild asthma. Clin Exp Allergy 2013;43:177-86.

E12. Jeon SG, Moon H-G, Kim Y-S, Choi J-P, Shin T-S, Hong S-W, et al. 15-Lipoxygenase metabolites play an important role in the development of a T-helper type 1 allergic inflammation induced by double-stranded RNA. Clin Exp Allergy 2009;39:908-17.

E13. Rai G, Kenyon V, Jadhav A, Schultz L, Armstrong M, Jameson JB, et al. Discovery of potent and selective inhibitors of human reticulocyte 15-lipoxygenase-1. J Med Chem 2010;53:7392-404.

E14. Horak F, Zieglmayer R, Lemell P, Collins LP, Hunter MG, Steiner J, et al. The CRTH2 antagonist OC000459 reduces nasal and ocular symptoms in allergic subjects exposed to grass pollen, a randomized, placebo-controlled, double-blind trial. Allergy 2012;67:1572-9.

E15. Barnes N, Pavord I, Chuchalin A, Bell J, Hunter M, Lewis T, et al. A randomized, double-blind, placebo-controlled study of the CRTH2 antagonist OC000459 in moderate persistent asthma. Clin Exp Allergy 2011;42:38-48.

E16. Straumann A, Hoesli S, Bussmann Ch, Stuck M, Perkins M, Collins LP, et al. Anti-eosinophil activity and clinical efficacy of the CRTH2 antagonist OC000459 in eosinophilic esophagitis. Allergy 2013;68:375-85.

E17. Busse WW, Wenzel SE, Meltzer EO, Kerwin EM, Liu MC, Zhang N, et al. Safety and efficacy of the prostaglandin D2 receptor antagonist AMG 853 in asthmatic patients. J Allergy Clin Immunol 2013;131:339-45.

E18. Philip G, van Adelsberg J, Loeys T, Liu N, Wong P, Lai E, et al. Clinical studies of the DP1 antagonist laropiprant in asthma and allergic rhinitis. J Allergy Clin Immunol 2009;124:942-8.

E19. Nabe T, Kuriyama Y, Mizutani N, Shibayama S, Hiromoto A, Fujii M, et al. Inhibition of hematopoietic prostaglandin D synthase improves allergic nasal blockage in guinea pigs. Prostaglandins Other Lipid Med 2011;95:27-34.

E20. Kajiwara D, Aoyagi H, Shigeno K, Togawa M, Tanaka K, Inagaki N, et al. Role of hematopoietic prostaglandin D synthase in biphasic nasal obstruction in guinea pig model of experimental allergic rhinitis. Eur J Pharmacol 2011;667:389-95.

E21. Smolen JS, Schoels MM, Nishimoto N, Breedveld FC, Burmester GR, Dougados M, et al. Consensus statement on blocking the effects of interleukin-6 and in particular by interleukin-6 receptor inhibition in rheumatoid arthritis and other inflammatory conditions. Ann Rheum Dis 2013;72:482-92.

E22. Patel DD, Lee DM, Kolbinger F, Antoni C. Effect of IL-17A blockade with secukinumab in autoimmune diseases. Ann Rheum Dis 2013;72:ii116-ii123.

E23. Skov L, Beurskens FJ, Zachariae COC, Reitamo S, Teeling J, Satijn D, et al. IL-8 as antibody therapeutic target in inflammatory diseases: reduction of clinical activity in palmoplantar pustulosis. J Immunol 2008;181:669-79.

E24. Tabrizi W, Wang B, Lu H, Huang S, Bell G, Schwab G, et al. Population pharmacokinetic evaluation of a fully human IgG monoclonal antibody in patients with inflammatory diseases. Inflamm Allergy Drug Targets 2010;9:229-37

E25. Hart TK, Blackburn MN, Brigham-Burke M, Dede K, Al-Mahdi N, Zia-Amirhosseini P, Cook RM. Preclinical efficacy and safety of pascolizumab (SB 240683): a humanized anti-interleukin-4 antibody with therapeutic potential in asthma. Clin Exp Immunol 2002;130:93-100.

E26. Simmons DL. Targeting kinases: a new approach to treating inflammatory rheumatic diseases. Curr Opin Pharmacol 2013;13:426-34.

E27. http://www.astrazeneca.com/Media/Press-releases/Article/20130504-astrazeneca-announces-topline-results-from-phase-iii-o

E28.http://www.biocentury.com/weekinreview/clinicalstatus/2012-11-12/prt062607-development-discontinued-301234

E29. http://ir.rigel.com/phoenix.zhtml?c=120936&p=irol-newsArticle&ID=1849671&highlight=

E30. http://www.rigel.com/rigel/pr_1133385395

E31. Lee KS, Lee HK, Hayflick JS, Lee YC, Puri KD. Inhibition of phosphoinositide 3-kinase δ attenuates allergic airway inflammation and hyperresponsiveness in murine asthma model. FASEB J 2006;20:455-65.

E32. Blunt MD, Ward SG. Pharmacological targeting of phosphoinositide lipid kinases and phosphatases in the immune system: success, disappointment, and new opportunities. Front Immunol 2013;3:1-15.

E33. Blunt MD, Ward SG. Targeting PI3K isoforms and SHIP in the immune system: new therapeutics for inflammation and leukemia. Curr Opin Pharmacol 2012;12:444-51.

E34. Norman P. Selective PI3Kδ inhibitors, a review of the patent literature. Expert Opin Ther Pat 2011;21:1773-90.

E35. Stenton GR, Mackenzie LF, Tam P, Cross JL, Harwig C, Raymond J, et al. Characterization of AQX-1125, a small molecule SHIP1 activator: Part 1. Effects on inflammatory cell activation and chemotaxis in vitro and pharmacokinetic characterization in vivo. Br J Pharmacol 2013;168:1506-18.

E36. Stenton GR, Mackenzie LF, Tam P, Cross JL, Harwig C, Raymond J, et al. Characterization of AQX-1125, a small molecule SHIP1 activator: Part 2. Efficacy studies in allergic and pulmonary inflammation models in vivo. Br J Pharmacol 2013;168:1519-29.

E37. MacGlashan D, Jr., Honigberg LA, Smith A, Buggy J, Schroeder JT. Inhibition of IgE-mediated secretion from human basophils with a highly selective Bruton's tyrosine kinase, Btk, inhibitor. Int Immunopharmacol 2011;11:475-9.

E38. Chang BY, Huang MM, Francesco M, Chen J, Sokolove J, Magadala P, et al. The Bruton tyrosine kinase inhibitor PCI-32765 ameliorates autoimmune arthritis by inhibition of multiple effector cells. Arthritis Res Ther 2011;13:R115.

E39. D'Cruz OJ, Uckun FM. Novel Bruton's tyrosine kinase inhibitors currently in development. Onco Targets Ther 2013;6:161-76.

E40. Ustun C, DeRemer DL, Akin C. Tyrosine kinase inhibitors in the treatment of systemic mastocytosis. Leuk Res 2011;35:1143-52.

E41. Eklund KK, Joensuu H. Treatment of rheumatoid arthritis with imatinib mesylate: clinical improvement in three refractory cases. Ann Med 2003;35:362-7.

E42. Juurikivi A, Sandler C, Lindstedt KA, Kovanen PT, Juutilainen T, Leskinen MJ, et al. Inhibition of c-kit tyrosine kinase by imatinib mesylate induces apoptosis in mast cells in rheumatoid synovia: a potential approach to the treatment of arthritis. Ann Rheum Dis 2005;64:1126-31.

E43. El-Agamy DS. Anti-allergic effects of nilotinib on mast cell-mediated anaphylaxis like reactions. Eur J Pharmacol 2012;680:115-21.

E44. 117. Gotlib J, DeAngelo DJ, George TI, Corless CL, Linder A, Langford C, et al. KIT inhibitor midostaurin exhibits a high rate of clinically meaningful and durable responses in advanced systemic mastocytosis: report of a fully accrued phase II trial. Blood 2010;116:Abstract 316.

E45. Kneidinger M, Schmidt U, Rix U, Gleixner KV, Vales A, Baumgartner C, et al. The effects of dasatinib on IgE receptor-dependent activation and histamine release in human basophils. Blood 2008;111:3097-107.

E46. Vega-Ruiz A, Cortes JE, Sever M, Manshouri T, Quintas-Cardama A, Luthra R, et al. Phase II study of imatinib mesylate as therapy for patients with systemic mastocytosis. Leuk Res 2009;33:1481-4.

E47. Paul C, Sans B, Suarez F, Casassus P, Barete S, Lanternier F, et al. Masitinib for the treatment of systemic and cutaneous mastocytosis with handicap: a phase 2a study. Am J Hematol 2010;85:921-5.

E48. Humbert M, de Blay F, Garcia G, Prud'homme A, Leroyer C, Magnan A, et al. Masitinib, a c-kit/PDGF receptor tyrosine kinase inhibitor, improves disease control in severe corticosteroid-dependent asthmatics. Allergy 2009;64:1194-201.

E49. Takabe K, Paugh SW, Milstien S, Spiegel S. "Inside-out" signaling of sphingosine-1-phosphate: therapeutic targets. Pharmacol Rev 2008;60:181-95.

E50. Brinkmann V, Billich A, Baumruker T, Heining P, Schmouder R, Francis G, et al. Fingolimod (FTY720): discovery and development of an oral drug to treat multiple sclerosis. Nat Rev Drug Discov 2010;9:883-97.

E51. Wulff H, Castle NA. Therapeutic potential of KCa3.1 blockers: recent advances and promising trends. Expert Rev Clin Pharmacol 2010;3:385-96.

E52. Yoshino T, Ishikawa J, Ohga K, Morokata T, Takezawa R, Morio H, et al. YM-58483, a selective CRAC channel inhibitor, prevents antigen-induced airway eosinophilia and late phase asthmatic responses via Th2 cytokine inhibition in animal models. Eur J Pharmacol 2007;560:225-33.

E53. Karlberg M, Ekoff M, Huang DC, Mustonen P, Harvima IT, Nilsson G. The BH3-mimetic ABT-737 induces mast cell apoptosis in vitro and in vivo: potential for therapeutics. J Immunol 2010;185:2555-62.

E54. Peter B, Cerny-Reiterer S, Hadzijusufovic E, Schuch K, Stefanzl G, Eisenwort G, et al. 2013. The pan-Bcl-2 blocker obatoclax promotes the expression of Puma, Noxa, and Bim mRNA and induces apoptosis in neoplastic mast cells. J Leukoc Biol 2013; Sep 19 (E-pub ahead of print). doi:jlb.1112609 [pii];10.1189/jlb.1112609 [doi].

E55. Bachelet I, Munitz A, Moretta A, Moretta L, Levi-Schaffer F. The inhibitory receptor IRp60 (CD300a) is expressed and functional on human mast cells. J Immunol 2005;175:7989-95.

E56. Sabato V, Verweij MM, Bridts CH, Levi-Schaffer F, Gibbs BF, De Clerck LS, et al. CD300a is expressed on human basophils and seems to inhibit IgE/FcepsilonRI-dependent anaphylactic degranulation. Cytometry B Clin Cytom 2012;82:132-8.

E57. Bachelet I, Munitz A, Levi-Schaffer F. Abrogation of allergic reactions by a bispecific antibody fragment linking IgE to CD300a. J Allergy Clin Immunol 2006;117:1314-20.

E58. Munitz, A, Bachelet I, Levi-Schaffer F. Reversal of airway inflammation and remodeling in asthma by a bispecific antibody fragment linking CCR3 to CD300a. J Allergy Clin Immunol 2006;118:1082-9.

E59. Nakahashi-Oda C, Tahara-Hanaoka S, Shoji M, Okoshi Y, Nakano-Yokomizo T, Ohkohchi N, et al. Apoptotic cells suppress mast cell inflammatory responses via the CD300a immunoreceptor. J Exp Med 2012;209:1493-503.

E60. Nissim Ben Efraim AH, Karra L, Ben-Zimra M, Levi-Schaffer F. The inhibitory receptor CD300a is up-regulated by hypoxia and GM-CSF in human peripheral blood eosinophils. Allergy 2013;68:397-401.

E61. Cassard L, Jönsson F, Arnaud S, Daëron M. Fcγ receptors inhibit mouse and human basophil activation. J Immunol 2012;189:2995-3006.

E62. Cemerski S, Chu SY, Moore GL, Muchhal US, Desjarlais JR, Szymkowski DE. Suppression of mast cell degranulation through a dual-targeting tandem IgE-IgG Fc domain biologic engineered to bind with high affinity to FcγRIIb. Immunol Lett 2012;143:34-43.

E63. Zhang K, Kepley CL, Terada T, Zhu D, Perez H, Saxon A. Inhibition of allergen-specific IgE reactivity by a human Ig Fcgamma-Fcepsilon bifunctional fusion protein. J Allergy Clin Immunol 2004;114:321-7.

E64. Lin LH, Zheng P, Yuen JW, Wang J, Zhou J, Kong CQ, et al. Prevention and treatment of allergic inflammation by an Fcγ-Der f2 fusion protein in a murine model of dust mite-induced asthma. Immunol Res 2012;52:276-83.

E65. Zhang M, Angata T, Cho JY, Miller M, Broide DH, Varki A. Defining the in vivo function of Siglec-F, a CD33-related Siglec expressed on mouse eosinophils. Blood 2007;109:4280-7.

E66. Cho JY, Song DJ, Pham A, Rosenthal P, Miller M, Dayan S, et al. Chronic OVA allergen challenged Siglec-F deficient mice have increased mucus, remodeling, and epithelial Siglec-F ligands which are up-regulated by IL-4 and IL-13. Respir Res 2010;11:154.

E67. Sugawara K, Bíró T, Tsuruta D, Tóth BI, Kromminga A, Zákány N, et al. Endocannabinoids limit excessive mast cell maturation and activation in human skin. J Allergy Clin Immunol 2012;129:726-38.e8.

E68. Samson MT, Small-Howard A, Shimoda LM, Koblan-Huberson M, Stokes AJ, Turner H. Differential roles of CB1 and CB2 cannabinoid receptors in mast cells. J Immunol 2003;170:4953-62.

E69. Aloe L, Leon A, Levi-Montalcini R. A proposed autacoid mechanism controlling mastocyte behaviour. Agents Actions 1993;39 Spec No:C145-7.

E70. Lau AH, Chow SS. Effects of cannabinoid receptor agonists on immunologically induced histamine release from rat peritoneal mast cells. Eur J Pharmacol 2003;464:229-35.

E71. Hanus L, Breuer A, Tchilibon S, Shiloah S, Goldenberg D, Horowitz M, et al. HU-308: a specific agonist for CB(2), a peripheral cannabinoid receptor. Proc Natl Acad Sci USA 1999;96:14228-33.

E72. Facci L, Dal Toso R, Romanello S, Buriani A, Skaper SD, Leon A. Mast cells express a peripheral cannabinoid receptor with differential sensitivity to anandamide and palmitoylethanolamide. Proc Natl Acad Sci USA 1995;92:3376-80.

E73. Zimmermann N, King NE, Laporte J, Yang M, Mishra A, Pope SM, et al. Dissection of experimental asthma with DNA microarray analysis identifies arginase in asthma pathogenesis. J Clin Invest 2003;111:1863-74.

E74. Munitz A, Bachelet I, Finkelman FD, Rothenberg ME, Levi-Schaffer F. CD48 is critically involved in allergic eosinophilic airway inflammation. Am J Respir Crit Care Med 2007;175:911-8.

E75. Zhang F, Huang G, Hu B, Song Y, Shi Y. A soluble thymic stromal lymphopoietin (TSLP) antagonist, TSLPR-immunoglobulin, reduces the severity of allergic disease by regulating pulmonary dendritic cells. Clin Exp Immunol 2011;164:256-64.

E76. Corren J, Casale TB, Lanier B, Buhl R, Holgate S, Jimenez P. Safety and tolerability of omalizumab. Clin Exp Allergy 2009;39:788-97.

DISCUSSION

Mast cells are known as key effector cells in allergic disorders, asthma and other IgE-associated disorders. FcεRI has been studied intensely and even though its structure is well known for several decades, some of the signaling mechanisms of FcεRI-mediated signaling pathway are still not fully understood. There are still molecules whose exact function, activation and involvement in the pathway remains unclear and deeper understanding could have a therapeutic significance. To fully understand the activation machinery and to know exactly which molecules and in what manner they are involved might benefit in the search for new strategies of targeting and regulating mast cell activation in IgE-associated acquired immune responses.

The role of transmembrane adaptor protein NTAL in mast cell signaling after FcεRI engagement still raises questions because of conflicting reports being published about its function. When NTAL was first described [65], it was suggested that it is similar to another structurally related adaptor protein LAT and instead of activation of T cells it functions in activation of B cells. However LAT expression is not exclusive only to T cells and NTAL expression to B cells, and mast cells were found to express both adaptors.

NTAL-deficient mice do not show a notable phenotypic alteration, mice are born viable and healthy and no defect in the development of bone marrow or splenic B cells is observed. Two groups, one in Prague [66] and another one in Durham, NC [69] simultaneously described properties of mast cells isolated from NTAL knock-out mice. These mast cells did not show any developmental abnormalities, expressed normal levels of FcεRI and KIT, and their numbers in the peritoneum did not differ from wild-type mice. Interestingly, mice lacking NTAL developed enhanced anaphylactic reaction. The consequence of genetic deletion of NTAL in mast cells resulted in increased mast cell degranulation and calcium mobilization after FcεRI activation. Also phosphorylation of LAT and ERK was increased and production of several cytokines was enhanced. In contrast to these findings Tkaczyk et al. [70] described opposite results when examining human mast cells with reduced NTAL expression using siRNA. In another study, the authors used the lentiviral transduction system to stably knock down NTAL expression in human mast cells. They found that NTAL is required for optimal antigen-induced and SCF-potentiated degranulation in human mast cells [57]. Reduced expression of NTAL by siRNA in rat basophilic leukemia cells also inhibited calcium mobilization and secretory response [105] led to conclusion that NTAL could have both positive and negative regulatory roles in FcεRI signaling.

In contrast to NTAL-deficient mice, LAT knock-out mice are resistant to IgE-mediated passive systemic anaphylaxis. Whereas LAT deficiency completely blocks T cell development [106], it has no effect on mast cell development in mice and BMMC isolated from these mice grow and develop normally. After FcεRI engagement LAT-deficient BMMCs showed normal FcεRI and SYK phosphorylation but dramatic decrease in phosphorylation of SLP-76 and PLCγ, molecules that bind to LAT. LAT-deficient BMMCs exhibited profound defects in degranulation, calcium mobilization and of MAPK activation [63]. Interestingly, loss of both NTAL and LAT caused even stronger inhibitory effect on FcεRI-mediated degranulation than loss of LAT alone. This suggested that NTAL could also have a positive regulatory role in FcεRI signaling, manifested only in the absence of LAT [66, 69].

The above mentioned discrepancies in NTAL-deficient cells could reflect different methodological approaches used for NTAL down-regulation; the generation of NTAL knock-out in mice and the RNA silencing techniques used for NTAL knock-down in human and rat mast cells. Or it could be due to developmental alterations in knock-out mice as described in other systems where absence of a given gene is compensated for by enhanced transcriptional activity of other genes [107-109].

To rigorously examine the regulatory role of NTAL in murine mast cells and to test possible contribution of compensatory mechanisms in genetic deletion of NTAL in mice, we prepared BMMCs with NTAL knock-out or knock-down and the corresponding controls and investigated for the first time the properties of mouse BMMCs with silenced NTAL expression and compared them with BMMCs from mice with NTAL knock-out. The results obtained in both type of NTAL-deficient cells were highly similar in most assays and support the concept that NTAL is mostly a negative regulator of FcεRI signaling, independently of possible compensatory developmental alterations.

FcεRI-mediated degranulation was increased to the same extent in both NTAL-deficient cells and compared to control cells showed the highest increase in degranulation at suboptimal concentrations of antigen. At optimal and supraoptimal antigen concentrations the differences were less pronounced. Interestingly, activation through KIT was not potentiated by the absence of NTAL, even though NTAL is tyrosine phosphorylated in KIT-activated mast cells [57, 70]. The simultaneous activation through KIT enhances degranulation of antigen-activated mast cells, and even more so of NTAL-deficient cells.

The Ca^{2+} response of antigen-activated BMMCs with NTAL knock-down was significantly higher when compared to its corresponding control cells, but lower when compared to NTAL knock-out cells. And again, no significant difference in Ca^{2+} response between NTAL-deficient

cells and controls was observed after KIT triggering, even though KIT activation accelerated Ca^{2+} response in antigen-activated control cells, and the enhancement was again stronger in NTAL-deficient cells.

The FcεRI phosphorylation in antigen activated mast cells is followed by phosphorylation of numerous molecules, including ERK and LAT [110, 111]. Theoretically, the enhanced tyrosine phosphorylation of LAT and some other substrates in NTAL knock-out cells could possibly reflect a better accessibility of kinases to LAT in the absence of competition between NTAL and LAT as substrates [66] and thus this mechanism could be subjected to compensatory developmental alterations. We therefore compared antigen activated wild type BMMCs with NTAL knock-down and knock-out cells and observed enhanced tyrosine phosphorylation of ERK and LAT in NTAL-deficient cells. These data support the hypothesis that competition between NTAL and LAT as kinase substrates could attenuate the response in WT cells through decreased tyrosine phosphorylation of LAT, followed by decreased binding and activation of phospholipase Cγ1 and subsequent events [60, 66, 112] and that developmental compensation mechanisms are unlikely to be responsible for enhanced phosphorylation of the targets.

In FcεRI-activated mast cells, NTAL was shown to be important to obtain full-value spreading on fibronectin [113]. In cells with NTAL knock-down antigen-mediated spreading was significantly decreased in the same manner as in NTAL knock-out cells, but was similarly unaffected after SCF triggering. Parallel activation with both antigen and SCF also reduced the spreading of both types of NTAL-deficient cells. These data suggest that positive regulatory role of NTAL on antigen-mediated spreading is not the result of developmental compensatory events. Rather, spreading could be related to transient actin depolymerization which was observed in antigen-activated wild type cells and even more in NTAL-deficient cells, but not in SCF-activated control or NTAL-deficient cells.

We also tested the chemotactic response of NTAL-deficient cells in comparison to control cells and observed comparable migration towards antigen in both types of NTAL-deficient cells. Their migration was significantly higher than the migration of control cells. Recent study on NTAL knock-out BMMCs reported that the level of active RhoA in resting cells is at least twice as high as in wild type cells [113]. Although active RhoA transiently decreased after FcεRI triggering, more in NTAL knock-out cells than in wild type cells, it is likely that differences in regulation of RhoA activity in NTAL-deficient cells and WT cells are responsible for the enhanced NTAL-regulated chemotaxis. RhoA was already shown to regulate chemotaxis in other cell types, such as lymphocytes [114], neutrophils [115], dendritic cells [116], and macrophages [117].

FcεRI-induced activation of BMMCs is accompanied by rapid F-actin depolymerization [118]. Antigen mediated activation of NTAL-deficient cells showed increased F-actin depolymerization when compared to control cells. And again, the decrease in F-actin content was enhanced even more after simultaneous triggering with both antigen and SCF. We also observed that SCF activation induced clear increase in F-actin formation, rather than actin depolymerization, and no difference between NTAL-deficient cells and control cells was noticed. F-actin depolymerization precedes degranulation [118, 119] and the observed decrease in amount of F-actin could account for the observed higher degranulation in NTAL-deficient cells than in control cells after simultaneous activation with the combination of antigen and SCF.

These data, together with those from the previously published studies on NTAL-deficient mice and BMMCs derived from these mice [66, 69], support the concept that NTAL functions as a negative regulator of FcεRI-mediated signaling in mouse mast cells. Where as in human and rat mast cells NTAL seems to have a positive regulatory role in mast cell signaling [57, 70, 105]. The observed differences could have several causes. And thus, NTAL could play different roles in mast cells of different species origin. Human mast cells differ from mouse mast cells in production of several cytokines, expression of types of immunoglobulin receptor, and in the ability of different stimuli to cause degranulation and release of mediators [120]. It has to be taken in consideration that rat basophilic leukemia cells are an immortalized cell line of tumor origin and this could be responsible for the observed properties of NTAL. Furthermore, when total tyrosine phosphorylated proteins were compared between this cell line and freshly isolated peritoneal and pleural rat mast cells, dramatic differences were observed. Importantly, mouse and human mast cells were obtained after differentiation under different cell culture conditions, which could modify their responsiveness. Mouse BMMCs were obtained by culturing bone marrow precursors in the presence of IL-3 and SCF (this study; [66]) or IL-3 alone [69], whereas human mast cells were derived from CD34+ pluripotent peripheral blood progenitors cultured in the presence of human SCF, IL-6 and IL-3 [57, 70]. Previous study showed that differentiation of mast cells from their precursors in the presence of various cytokines could result in different responsiveness of the cells to various activators [121]. Finally, one cannot exclude the possibility that silencing vectors used for generation of NTAL knock-down in human and/or RBL-2H3 mast cells exhibited off-target effects, which modified responsiveness of the cells to FcεRI triggering.

In our study we focused on elimination of possible off-target effects on several levels. In the beginning we tested a set of five shRNA hairpins and selected two that exhibited the strongest

silencing potential. These were used in most of the experiments and similar results were obtained for both of them. In parallel negative control of silencing procedure was prepared by transducing wild type cells with empty lentiviral vector bearing no shRNA sequence. No decrease in NTAL expression was observed in cells infected with empty vector. Flow cytometry analysis of both type of the transduced cells showed similar levels of expressed FcεRI and KIT compared to those in wild type cells and knock-out cells. Additionally, to exclude off-target effect of the hairpins on mast cell degranulation, we also transduced NTAL knock-out cells with the shRNA hairpins and observed no alterations in degranulation. Wild type cells transduced with empty vector did not show any significant alterations from wild type cells in the performed assays thus excluding the lentiviral approach to modulate the signaling in activated mast cells. Results obtained later from comparison of expression profiles of activated wild type cells and wild type cells transduced with empty vector also supported this notion.

Comparing to the other studies utilizing the RNA interference approach where the NTAL expression was suppressed from about 70%; in our study we were able to obtain very strong permanent knock-down of NTAL. The protein expression was diminished from over 90%, in some cases reached even up to 98%, thus the remaining small amount of NTAL left in the mast cells could likely not significantly influence our data.

To gain a better understanding of the role of NTAL in FcεRI mediated signaling and to find out of the genes regulated through NTAL-dependent pathways, we further examined the gene expression profiles of resting and antigen-activated BMMCs with NTAL knock-out or knock-down and the corresponding controls. The detailed analysis of these profiles surprisingly revealed mainly those genes that were not related to known immunoreceptor signaling pathways in mast cells. Interestingly, NTAL-dependent changes in the expression revealed a number of genes related to metabolism and biosynthetic processes, and a subgroup of these genes was involved in lipid metabolism, including synthesis of cholesterol. The exact mechanisms and pathways through which NTAL causes changes in transcription of these genes remain to be determined.

An unexpected finding was the relatively small overlap between the genes differentially regulated in NTAL knock-out cells and NTAL knock-down cells obtained by intersection of two gene lists based of comparisons of NTAL knock-out cells versus wild type cells and NTAL knock-down cells versus their control cells. The degree of the overlap was independent of antigen-mediated activation. Some of the overlapping genes showed differential expression in resting as well as activated cells. Even when applying weaker selection criteria regarding fold change and FDR to generate the gene list, the number of genes in the intersection increased

only slightly. The limited overlap could be due to methodological differences in production of NTAL-deficient cells. However, as mentioned before, comparison of the activated wild type cells and cells used as control of infection did not show differences in expression of genes. Though some differences were obtained in comparison of resting cells, it can be concluded that in activated mast cells lentiviral infection itself and puromycin selection do not affect the expression of genes.

The most dramatic changes in gene expression were observed between the antigen-activated and resting cells, no matter if NTAL was present or diminished, suggesting that activation of mast cells itself is a very robust process leading to a wide range of changes in gene regulation.

Based on the results of transcriptional analysis, we decided to focus on several molecules that were differentially regulated in both types of NTAL-deficient cells. The first choice was dual specificity phosphatase 5 (DUSP5) that was up-regulated in the absence of NTAL in resting cells. DUSP5 negatively regulates MAPK pathway by inactivating ERK1 in the nucleus and because of the altered ERK phosphorylation in the absence of NTAL, it was an interesting molecule to investigate closer. Even though real-time PCR confirmed its up-regulation on mRNA level, immunoblotting using DUSP5 specific antibody to show difference in protein level expression failed mainly due to poor performance of the only commercially available antibody.

Second focus was targeted on APPL2 (adaptor protein, phosphotyrosine interaction, PH domain and leucine zipper containing 2) because of its possible involvement in signal transduction pathways and overexpression in NTAL-deficient cells. The assessed amount of mRNA level was reproducibly higher in cells lacking NTAL; however the protein level assessed by immunoblotting and flow cytometry did not reveal any differences in expression between NTAL-deficient and control cells.

Last but not least, the attention was directed to the identified group of genes involved in lipid metabolism, including synthesis of cholesterol and the involvement of cholesterol regulation in chemotaxis towards antigen. Although decreased transcription of several genes involved in cholesterol synthesis was confirmed by real-time PCR, no significant difference in total amount of cellular cholesterol was detected between wild type cells and NTAL-deficient cells. The pretreatment of BMMCs with methyl-β-cyclodextrin had different effect on NTAL knock-out and wild type cells. In NTAL knock-out cells it caused significant inhibition of chemotaxis at all tested concentrations, whereas in wild type cells methyl-β-cyclodextrin either slightly, but reproducibly increased chemotaxis at a low concentration or had no significant effect at higher concentrations. Methyl-β-cyclodextrin is known to remove cholesterol from cells [122, 123]

and thus the enhanced chemotaxis in NTAL-deficient cells could possibly be regulated in part by plasma membrane cholesterol distribution. Molecular mechanism of the cholesterol-dependent regulations of chemotaxis is poorly understood, but could be related to differences in synthesis and/or distribution of cholesterol into plasma membrane sheets. Molecular mechanisms of the cross-talk between NTAL and cholesterol remain to be determined.

Mast cells also possess another transmembrane adaptor protein PAG that after tyrosine phosphorylation serves as an anchor for CSK, an inhibitor of Src family kinases [72]. A negative regulatory role of PAG in T cell signaling was confirmed in experiments with PAG knock-downs [124], but not with PAG knock-downs [125, 126], suggesting that developmental compensatory mechanisms are involved. Overexpression of PAG inhibited FcεRI-mediated degranulation in rat basophilic leukemia (RBL) cells [74].

We prepared BMMCs derived from PAG knock-out and wild type mice and to minimize the possible effects of compensatory developmental alterations in PAG knock-out cells, we also prepared BMMCs with PAG knock-down and corresponding control cells. Several lines of evidence indicated that PAG has positive as well as negative regulatory roles in FcεRI- and/or KIT-mediated signaling in mice.

We examined the role of PAG in cells activated through FcεRI and showed that PAG-deficient BMMCs exhibit impaired antigen-induced degranulation, extracellular calcium uptake, tyrosine phosphorylation of several key signaling proteins, production of several cytokines and chemokines, and chemotaxis. Activation of PAG-deficient mast cells via the receptor KIT lead to enhanced degranulation and tyrosine phosphorylation of the receptor itself. The combined data indicate that PAG functions as a positive or negative regulator of mast cell signaling depending on the receptor triggered and the particular signaling pathway involved. We suggested that through the interaction with CSK, PAG serves as a negative regulator of Src family kinases, which are involved in both positive and negative regulatory events in mast cell activation.

We also decided to examine the expression profiles of BMMCs prepared from PAG knock-out and wild type cells and looked at the differentially expressed genes after antigen or SCF activation. The analysis of these expression profiles revealed very different list of up-/down-regulated genes when compared to the analysis of NTAL-deficient and control cells. There was no large group of genes involved in metabolism and biosynthetic processes. Instead the list contained genes involved in signal transduction, protein phosphorylation, and cell adhesion. And again, principal component analysis (PCA) showed that the most robust process was the antigen activation followed by SCF activation and not the deletion of PAG (Figure 5A). The

differences between knock-out and wild type cells were more restrained after SCF activation which supports our data showing more differences in signaling in cells after activation through FcεRI than KIT (Figure 5B).

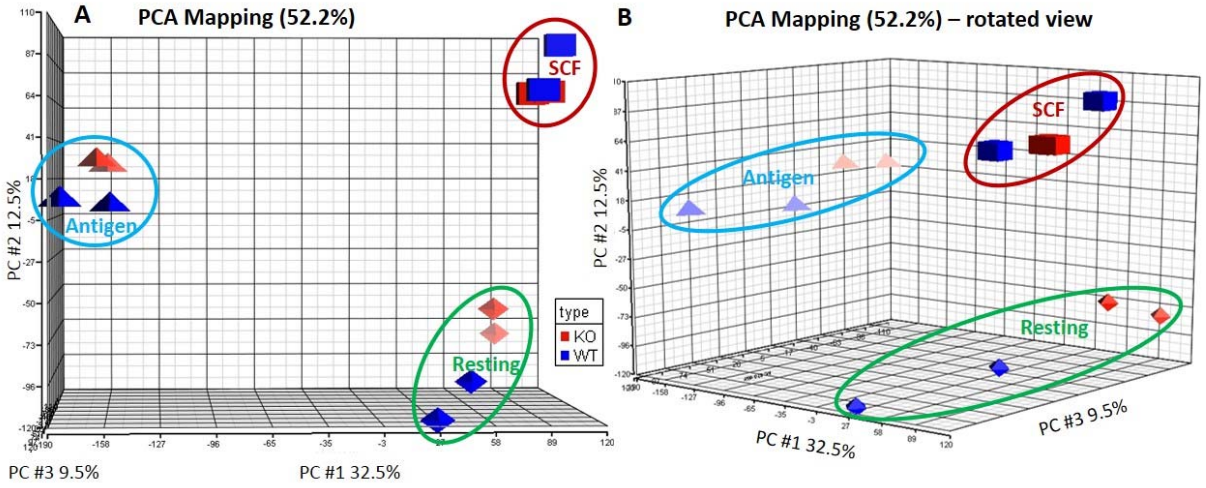

Figure 5. Principal component analysis of the microarrays. Each colored circle represents different treatment of cells: antigen activation (blue), SCF activation (red), and resting (green). The BMMCs isolated from wild type mice are pictured in blue shapes and from knock-out in red shapes. The arrays cluster according to the treatment groups showing separation along (principal component) PC #1 (antigen) and PC #2 (SCF). The percentage values indicate the proportion of total variance described by each PC; PC #1 (X-axis), PC #2 (Y-axis), and PC #3 (Z-axis).

We created three gene lists by comparison of knock-out cells versus wild type cells for all three conditions of cell treatment: antigen, SCF, and none. These gene lists show a large overlap of 18 genes meaning that most of the differentially regulated genes are already up- or down-regulated even in the resting state of cells when PAG is deleted. The overlap of the gene lists is presented in Figure 6. Several of these genes function in signal transduction and protein phosphorylation. Importantly, functions of some of the genes have not been described yet. When searching for more information of these genes in BIOGPS, the expression profiles uploaded in the database show high expression of some of these genes in murine mast cells. The expression of the genes was also verified by real-time PCR and most of the obtained results were in accordance with the microarray data analysis. These genes will be a subject of further investigation.

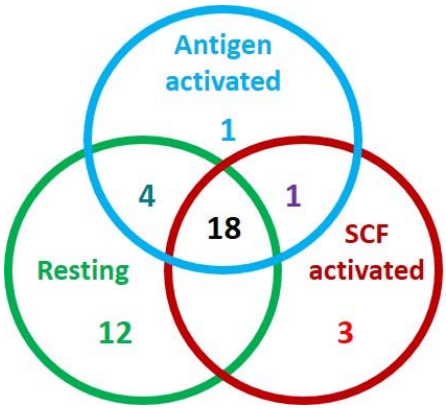

Figure 6. Venn diagram of gene list comparison
The Venn diagram illustrates the numbers of genes that are significantly differentially up- or down-regulated (fold change >1.8; FDR <0.1) when PAG wild type and knock-out profiles are compared. Each colored circle represents different treatment of the cells: antigen activation (blue), SCF activation (red), and resting (green). 18 genes showed overlap among all 3 types of treatment

Comparison of the gene lists obtained in both transcriptional studies, in which NTAL- and PAG-deficient cells were used, showed no overlap. This suggests that different genes are regulated by these adaptors. Based on our results we conclude that in mouse mast cells PAG and NTAL play different regulatory roles in transcription and thus regulate different pathways. Our data also show that NTAL may be involved in regulation of some metabolic or biosynthetic processes while PAG mostly in immunomodulatory pathways.

When looking at mast cells from a different angle, focusing on their role in innate and acquired immunity, it is likely that other functions of the transmembrane adaptor proteins will be revealed. First findings in this direction have been published recently by Rivera's group [52]. They investigated how FcεRI discriminates high- from low-affinity stimulation and modulates the response. The receptor phosphorylation was similar after exposure of the cells to the high- or low-affinity stimuli, but the size of FcεRI clusters, their mobility and distribution was decreased after low-affinity stimuli. Interestingly, after low-affinity stimuli, FcεRI associated with the Src family kinase FGR and the activation signals were shifted to NTAL instead of LAT. The events included enhanced phosphorylation of NTAL and its colocalization with FcεRI, but reduced phosphorylation of LAT and PLCγ. This resulted in decreased LAT-dependent calcium signaling important for mast cell degranulation and, on the other hand, enhanced NTAL-dependent production of chemokines. Consistent with these findings was also the decrease in passive cutaneous anaphylaxis in mice after low-affinity stimuli. This study shows, for the first time, that triggering of the FcεRI and probably other immunoreceptors, by stimuli of different strength results in engagement of different signaling pathways. In this process transmembrane adaptor proteins could play a key role.

CONCLUSIONS

1. Using a wide array of assays, we found that murine BMMCs with silenced expression of NTAL share similar properties with those prepared from NTAL knock-out mice. Our results thus support the notion that in murine mast cells NTAL is predominantly a negative regulator of FcεRI signaling and that compensatory developmental alteration do not contribute to this phenotype.
   1.1. Mast cells with NTAL knock-down were prepared by lentiviral delivery of vectors bearing NTAL specific shRNAs into wild type cells and corresponding controls were transduced with empty vectors. Immunoblotting with NTAL-specific monoclonal antibody confirmed very strong inhibition of NTAL expression on protein level. Thus these cells were suitable for further experiments.
   1.2. For functional comparison of mast cells with NTAL knock-out or knock-down we examined several parameters characteristic for FcεRI signaling including antigen-mediated degranulation, calcium mobilization, and tyrosine phosphorylation of LAT and ERK. The results obtained with the NTAL knock-down mast cells were very similar to those of NTAL knock-out cells confirming the negative regulatory role of NTAL in these events. In both cells types, combination of antigen and SCF even enhanced degranulation and calcium mobilization.
   1.3. Using both types of NTAL-deficient cells we confirmed that full mast cells spreading is dependent on NTAL, and that F-actin depolymerization and chemotaxis are increased in cells lacking NTAL. In case of F-actin depolymerization, this effect was again even more pronounced when simultaneously activated by both antigen and SCF.
   1.4. To better understand the role of NTAL in mast cells, we isolated RNAs from nonactivated and antigen-activated NTAL-deficient mast cells and the corresponding controls and examined gene expression profiles.
   1.5. The obtained gene expression analysis interestingly revealed NTAL-dependent changes in the expression of a number of genes related to metabolism and biosynthetic processes but only a small group of genes that were similarly regulated in both types of NTAL-deficient cell either resting or antigen-activated. Among those identified genes were also few genes related to cholesterol metabolism.
   1.6. The data obtained from the microarray approach were verified by real-time PCR and confirmed the differential expression of most of the selected genes in accordance with the microarray data analysis.

1.7. Further analysis showed that some of the genes could be involved in regulation of cholesterol-dependent events in chemotaxis towards antigen. Chemotaxis of cholesterol depleted cells lead us to hypothesis that enhanced chemotaxis in NTAL-deficient cells can be regulated in part by plasma membrane cholesterol distribution.

2. Using mast cells isolated from PAG knock-out mice we investigated the regulation of mast cell signaling by PAG adaptor. We showed that PAG functions as both a positive and negative regulator of mast cell signaling, depending on the signaling pathway involved. We proposed that through interaction with CSK, PAG serves as a negative regulator of Src kinases involved in both positive and negative regulatory events in mast cell activation. We also obtained gene expression profiles from nonactivated and antigen-activated PAG knock out and wild type cells and the gene expression analysis revealed genes that can be involved in immunological signaling.

3. To improve the performance of real-time PCR routinely used in our laboratory and to cut the costs, we optimized PCR master mixes. In our search we compared performance of various dyes in buffers of different salt composition and additives. Using a unique fidelity assay we demonstrated that the observed differences were not due to changes introduced by induction of mutation frequencies of Taq DNA polymerase in PCR mixes. We found excellent amplification of DNA fragments from whole blood and/or GC-rich templates in PCR master mix supplemented with 1 M 1,2-propanediol and 0.2 M trehalose. This master mix was suitable for our real-time PCR experiments and when compared to several commercially available real-time PCR master mixes it proved to be more efficient.

4. To summarize the recent progress that has been made in developing new drugs to treat illnesses where mast cells play key roles, we focused on recently developed inhibitors directed against key intracellular enzymes involved in mast cell signal transduction. Based on literature data, and the fact that mast cells share most of the signaling pathways with other cell types, we propose that the best therapeutic results would be obtained with multicomponent drugs that inhibit certain proinflammatory pathways and at the same time enhance the activity of enzymes involved in the termination of signaling pathways.

REFERENCES

1. Beaven MA. Our perception of the mast cell from Paul Ehrlich to now. *Eur J Immunol* 2009; **39**: 11-25.

2. Ribatti D, Crivellato E. Mast cell ontogeny: An historical overview. *Immunol Lett* 2014; **159**: 11-4.

3. Paton WD. Compound 48/80: a potent histamine liberator. *J Pharmacol Chemother* 1951; **6**: 499-508.

4. Galli SJ, Kalesnikoff J, Grimbaldeston MA et al. Mast cells as "tunable" effector and immunoregulatory cells: Recent advances. *Annu Rev Immunol* 2005; **23**: 749-86.

5. Gilfillan AM, Beaven MA. Regulation of mast cell responses in health and disease. *Crit Rev Immunol* 2011; **31**: 475-529.

6. Kitamura Y, Shimada M, Hatanaka K, Miyano Y. Development of mast cells from grafted bone marrow cells in irradiated mice. *Nature* 1977; **268**: 442-3.

7. Dahlin JS, Hallgren J. Mast cell progenitors: Origin, development and migration to tissues. *Mol Immunol* 2014; [Epub ahead of print]

8. Kirshenbaum AS, Kessler SW, Goff JP, Metcalfe DD. Demonstration of the origin of human mast cells from CD34+ bone marrow progenitor cells. *J Immunol* 1991; **146**: 1410-5.

9. Arinobu Y, Iwasaki H, Gurish MF et al. Developmental checkpoints of the basophil/mast cell lineages in adult murine hematopoiesis. *Proc Natl Acad Sci U S A* 2005; **102**: 18105-10.

10. Qi X, Hong J, Chaves L et al. Antagonistic Regulation by the Transcription Factors C/EBPα and MITF Specifies Basophil and Mast Cell Fates. *Immunity* 2013; **39**: 97-110.

11. Stevens RL, Adachi R. Protease–proteoglycan complexes of mouse and human mast cells and importance of their β-tryptase–heparin complexes in inflammation and innate immunity. *Immunol Rev* 2007; **217**: 155-67.

12. Puxeddu I, Piliponsky AM, Bachelet I, Levi-Schaffer F. Mast cells in allergy and beyond. *Int J Biochem Cell Biol* 2003; **35**: 1601-7.

13. Sredni B, Friedman MM, Bland CE, Metcalfe DD. Ultrastructural, biochemical, and functional characteristics of histamine-containing cells cloned from mouse bone marrow: tentative identification as mucosal mast cells. *J Immunol* 1983; **131**: 915-22.

14. Marshall JS. Mast-cell responses to pathogens. *Nat Rev Immunol* 2004; **4**: 787-99.

15. Prussin C, Metcalfe DD. 4. IgE, mast cells, basophils, and eosinophils. *J Allergy Clin Immunol* 2003; **111**: S486-94.

16. Gordon JR, Galli SJ. Mast cells as a source of both preformed and immunologically inducible TNF-α/cachectin. *Nature* 1990; **346**: 274-6.

17. Halova I, Draberova L, Draber P. Mast cell chemotaxis - chemoattractants and signaling pathways. *Front Immunol* 2012; **3**: 119.

18. Galli SJ, Maurer M, Lantz CS. Mast cells as sentinels of innate immunity. *Curr Opin Immunol* 1999; **11**: 53-9.

19. Carroll-Portillo A, Surviladze Z, Cambi A et al. Mast cell synapses and exosomes: membrane contacts for information exchange. *Front Immunol* 2012; **3**: 46.

20. Jawdat DM, Albert EJ, Rowden G et al. IgE-mediated mast cell activation induces Langerhans cell migration in vivo. *J Immunol* 2004; **173**: 5275-82.

21. Tedla N, Wang HW, McNeil HP et al. Regulation of T lymphocyte trafficking into lymph nodes during an immune response by the chemokines macrophage inflammatory protein (MIP)-1α and MIP-1β. *J Immunol* 1998; **161**: 5663-72.

22. Heib V, Becker M, Warger T et al. Mast cells are crucial for early inflammation, migration of Langerhans cells, and CTL responses following topical application of TLR7 ligand in mice. *Blood* 2007; **110**: 946-53.

23. Malaviya R, Abraham SN. Role of mast cell leukotrienes in neutrophil recruitment and bacterial clearance in infectious peritonitis. *J Leukoc Biol* 2000; **67**: 841-6.

24. Nakae S, Suto H, Iikura M et al. Mast cells enhance T cell activation: importance of mast cell costimulatory molecules and secreted TNF. *J Immunol* 2006; **176**: 2238-48.

25. Blank U, Ra C, Miller L et al. Complete structure and expression in transfected cells of high affinity IgE receptor. *Nature* 1989; **337**: 187-9

.

26. Kinet JP. The high-affinity IgE receptor FcεRI: from physiology to pathology. *Annu Rev Immunol* 1999; **17**: 931-72.

27. Garman SC, Wurzburg BA, Tarchevskaya SS et al. Structure of the Fc fragment of human IgE bound to its high-affinity receptor FcεRIα. *Nature* 2000; **406**: 259-66.

28. Lin S, Cicala C Fau - Scharenberg AM, Scharenberg Am Fau - Kinet JP, Kinet JP. The FcεRIβ subunit functions as an amplifier of FcεRIγ-mediated cell activation signals. *Cell* 1996; **85**: 985-95.

29. Cambier JC. Antigen and Fc receptor signaling. The awesome power of the immunoreceptor tyrosine-based activation motif (ITAM). *J Immunol* 1995; **155**: 3281-5.

30. Siraganian RP, de Castro RO, Barbu EA, Zhang J. Mast cell signaling: the role of protein tyrosine kinase Syk, its activation and screening methods for new pathway participants. *FEBS Lett* 2010; **584**: 4933-40.

31. Parravicini V, Gadina M, Kovarova M et al. Fyn kinase initiates complementary signals required for IgE-dependent mast cell degranulation. *Nat Immunol* 2002; **3**: 741-8.

32. Kraft S, Kinet J-P. New developments in FcεRI function and inhibition. *Nat Rev Immunol* 2007; **7**: 365-78.

33. Nishizumi H, Horikawa K, Mlinaric-Rascan I, Yamamoto T. Impaired tyrosine phosphorylation and Ca2+ mobilization, but not degranulation, in lyn-deficient bone marrow-derived mast cells. *J Exp Med* 1998;**187**:1343-8.

34. Alvarez-Errico D, Lessmann E, Rivera J. Adapters in the organization of mast cell signaling. *Immunol Rev* 2009; **232**: 195-217.

35. Siraganian RP. Mast cell signal transduction from the high-affinity IgE receptor. *Curr Opin Immunol* 2003; **15**: 639-46.

36. Siraganian RP, Zhang J, Suzuki K, Sada K. Protein tyrosine kinase Syk in mast cell signaling. *Mol Immunol* 2002; **38**: 1229-33.

37. Zhang SL, Yu Y, Roos J et al. STIM1 is a Ca2+ sensor that activates CRAC channels and migrates from the Ca2+ store to the plasma membrane. *Nature* 2005; **437**: 902-5.

38. Ozawa K, Szallasi Z, Kazanietz MG et al. Ca(2+)-dependent and Ca(2+)-independent isozymes of protein kinase C mediate exocytosis in antigen-stimulated rat basophilic RBL-2H3 cells. Reconstitution of secretory responses with Ca2+ and purified isozymes in washed permeabilized cells. *J Biol Chem* 1993; **268**: 1749-56.

39. Gilfillan AM, Rivera J. The tyrosine kinase network regulating mast cell activation. *Immunol Rev* 2009; **228**: 149-69.

40. Ma HT, Beaven MA. Regulation of Ca2+ signaling with particular focus on mast cells. *Crit Rev Immunol* 2009; **29**: 155-86.

41. Spiegel S, Milstien S. Sphingosine-1-phosphate: an enigmatic signalling lipid. *Nat Rev Mol Cell Biol* 2003; **4**: 397-407.

42. Jolly PS, Bektas MF, Olivera A et al. Transactivation of sphingosine-1-phosphate receptors by FcεRI triggering is required for normal mast cell degranulation and chemotaxis. *J Exp Med* 2004; **199**: 959-70.

43. Oskeritzian CA, Alvarez SE, Hait NC et al. Distinct roles of sphingosine kinases 1 and 2 in human mast-cell functions. *Blood* 2008; **111**: 4193-200.

44. Urtz N, Olivera A, Bofill-Cardona E et al. Early activation of sphingosine kinase in mast cells and recruitment toFcεRI are mediated by its interaction with Lyn kinase. *Mol Cell Biol* 2004; **24**: 8765-77.

45. Hait NC, Oskeritzian CA, Paugh SW et al. Sphingosine kinases, sphingosine 1-phosphate, apoptosis and diseases. *Biochim Biophys Acta* 2006; **1758**: 2016-26.

46. Rivera J, Gilfillan AM. Molecular regulation of mast cell activation. *J Allergy Clin Immunol* 2006; **117**: 1214-25.

47. Furumoto Y, Brooks S, Olivera A et al. Cutting edge: Lentiviral short hairpin RNA silencing of PTEN in human mast cells reveals constitutive signals that promote cytokine secretion and cell survival. *J Immunol* 2006; **176**: 5167-71.

48. Odom S, Gomez G, Kovarova M et al. Negative regulation of immunoglobulin E-dependent allergic responses by Lyn kinase. *J Exp Med* 2004; **199**: 1491-502.

49. Okayama Y, Matsuda AF, Kashiwakura JI et al. Highly expressed cytoplasmic FcεRIβ in human mast cells functions as a negative regulator of the FcRγ-mediated cell activation signal. *Clin Exp Allergy* 2014;**44**:238-49.

50. Kepley CL, Taghavi S, Mackay G et al. Co-aggregation of FcγRII with FcepsilonRI on human mast cells inhibits antigen-induced secretion and involves SHIP-Grb2-Dok complexes. *J Biol Chem* 2004; **279**: 35139-49.

51. Scharenberg AM, El-Hillal O, Fruman DA et al. Phosphatidylinositol-3,4,5-trisphosphate (PtdIns-3,4,5-P3)/Tec kinase-dependent calcium signaling pathway: a target for SHIP-mediated inhibitory signals. *EMBO J* 1998; **17**: 1961-72.

52. Suzuki R, Leach S, Liu W et al. Molecular editing of cellular responses by the high-affinity receptor for IgE. *Science* 2014; **343**: 1021-5.

53. Gilfillan AM, Tkaczyk C. Integrated signalling pathways for mast-cell activation. *Nat Rev Immunol* 2006; **6**: 218-30.

54. Vosseller K, Stella G, Yee NS, Besmer P. c-Kit receptor signaling through its phosphatidylinositide-3'-kinase-binding site and protein kinase C: Role in mast cell enhancement of degranulation, adhesion, and membrane ruffling. *Mol Biol Cell* 1997; **8**: 909-22.

55. Linnekin D. Early signaling pathways activated by c-Kit in hematopoietic cells. *Int J Biochem Cell Biol* 1999; **31**: 1053-74.

56. Roskoski R, Jr. Signaling by Kit protein-tyrosine kinase--the stem cell factor receptor. *Biochem Biophys Res Commun* 2005; **337**: 1-13.

57. Iwaki S, Spicka J, Tkaczyk C et al. Kit- and FcεRI-induced differential phosphorylation of the transmembrane adaptor molecule NTAL/LAB/LAT2 allows flexibility in its scaffolding function in mast cells. *Cell Signal* 2008; **20**: 195-205.

58. Ali K, Bilancio A, Thomas M et al. Essential role for the p110 δ phosphoinositide 3-kinase in the allergic response. *Nature* 2004; **431**: 1007-11.

59. Iwaki S, Tkaczyk C, Satterthwaite AB et al. Btk plays a crucial role in the amplification of FcεRI-mediated mast cell activation by kit. *J Biol Chem* 2005; **280**: 40261-70.

60. Draber P, Halova I, Levi-Schaffer F, Draberova L. Transmembrane adaptor proteins in the high-affinity IgE receptor signaling. *Front Immunol* 2011; **2**: 95.

61. Horejsi V. Transmembrane adaptor proteins in membrane microdomains: important regulators of immunoreceptor signaling. *Immunol Lett* 2004; **92**: 43-9.

62. Sieh M, Batzer A, Schlessinger J, Weiss A. GRB2 and phospholipase C-γ1 associate with a 36- to 38-kilodalton phosphotyrosine protein after T-cell receptor stimulation. *Mol Cell Biol* 1994; **14**: 4435-42.

63. Saitoh S, Arudchandran R, Manetz TS et al. LAT is essential for FcεRI-mediated mast cell activation. *Immunity* 2000; **12**: 525-35.

64. Saitoh S, Odom S, Gomez G et al. The four distal tyrosines are required for LAT-dependent signaling in FcεRI-mediated mast cell activation. *J Exp Med* 2003; **198**: 831-43.

65. Brdicka T, Imrich M, Angelisova P et al. Non-T cell activation linker (NTAL): a transmembrane adaptor protein involved in immunoreceptor signaling. *J Exp Med* 2002; **196**: 1617-26.

66. Volna P, Lebduska P, Draberova L et al. Negative regulation of mast cell signaling and function by the adaptor LAB/NTAL. *J Exp Med* 2004; **200**: 1001-13.

67. Koonpaew S, Janssen E, Zhu M, Zhang W. The importance of three membrane-distal tyrosines in the adaptor protein NTAL/LAB. *J Biol Chem* 2004; **279**: 11229-35.

68. Janssen E, Zhu M, Zhang W et al. LAB: A new membrane-associated adaptor molecule in B cell activation. *Nat Immunol* 2003; **4**: 117-23.

69. Zhu M, Liu Y, Koonpaew S et al. Positive and negative regulation of FcεRI-mediated signaling by the adaptor protein LAB/NTAL. *J Exp Med* 2004; **200**: 991-1000.

70. Tkaczyk C, Horejsi V, Iwaki S et al. NTAL phosphorylation is a pivotal link between the signaling cascades leading to human mast cell degranulation following kit activation and FcεRI aggregation. *Blood* 2004; **104**: 207-14.

71. Polakovicova I, Draberova L, Simicek M, Draber P. Multiple Regulatory Roles of the Mouse Transmembrane Adaptor Protein NTAL in Gene Transcription and Mast Cell Physiology. *PLoS ONE* 2014; **9**: e105539.

72. Brdicka T, Pavilstova D, Leo A et al. Phosphoprotein associated with glycosphingolipid-enriched microdomains (PAG), a novel ubiquitously expressed transmembrane adaptor protein, binds the protein tyrosine kinase Csk and is involved in regulation of T cell activation. *J Exp Med* 2000; **191**: 1591-604.

73. Kawabuchi M, Satomi Y, Takao T et al. Transmembrane phosphoprotein Cbp regulates the activities of Src-family tyrosine kinases. *Nature* 2000; **404**: 999-1003.

74. Ohtake H, Ichikawa N, Okada M, Yamashita T. Cutting Edge: Transmembrane phosphoprotein Csk-binding protein/phosphoprotein associated with glycosphingolipid-enriched microdomains as a negative feedback regulator of mast cell signaling through the FcεRI. *J Immunol* 2002;**168**:2087-90.

.

75. Zhu M, Janssen E, Leung K, Zhang W. Molecular cloning of a novel gene encoding a membrane-associated adaptor protein (LAX) in lymphocyte signaling. *J Biol Chem* 2002; **277**: 46151-8.

76. Zhu M, Granillo O, Wen R et al. Negative regulation of lymphocyte activation by the adaptor protein LAX. *J Immunol* 2005; **174**: 5612-9.

77. Zhu M, Rhee I, Liu Y, Zhang W. Negative regulation of Fc epsilonRI-mediated signaling and mast cell function by the adaptor protein LAX. *J Biol Chem* 2006; **281**: 18408-13.

78. Liu Y, Zhang WG. Identification of a new transmembrane adaptor protein that constitutively binds Grb2 in B cells. *J Leukocyte Biol* 2008; **84**: 842-51.

79. Harvima IT, Levi-Schaffer F, Draber P et al. Molecular targets on mast cells and basophils for novel therapies. *J Allergy Clin Immunol* 2014; **134**: 530-44.

80. Ohsawa Y, Hirasawa N. The antagonism of histamine H1 and H4 receptors ameliorates chronic allergic dermatitis via anti-pruritic and anti-inflammatory effects in NC/Nga mice. *Allergy* 2012; **67**: 1014-22.

81. Laidlaw TM, Boyce JA. Cysteinyl leukotriene receptors, old and new; implications for asthma. *Clin Exp Allergy* 2012; **42**: 1313-20.

82. Montuschi P, Peters-Golden ML. Leukotriene modifiers for asthma treatment. *Clin Exp Allergy* 2010; **40**: 1732-41.

83. Kent SE, Boyce M, Diamant Z et al. The 5-lipoxygenase-activating protein inhibitor, GSK2190915, attenuates the early and late responses to inhaled allergen in mild asthma. *Clin Exp Allergy* 2013; **43**: 177-86.

84. Ackermann L, Harvima IT. Mast cells of psoriatic and atopic dermatitis skin are positive for TNF-alpha and their degranulation is associated with expression of ICAM-1 in the epidermis. *Arch Dermatol Research* 1998; **290**: 353-9.

85. Kenna TJ, Brown MA. The role of IL-17-secreting mast cells in inflammatory joint disease. *Nat Rev Rheumatol* 2013; **9**: 375-9.

86. Weinblatt ME, Kavanaugh A, Genovese MC et al. Effects of fostamatinib (R788), an oral spleen tyrosine kinase inhibitor, on health-related quality of life in patients with active rheumatoid arthritis: analyses of patient-reported outcomes from a randomized, double-blind, placebo-controlled trial. *J Rheumatol* 2013; **40**: 369-78.

87. Blunt MD, Ward SG. Pharmacological targeting of phosphoinositide lipid kinases and phosphatases in the immune system: success, disappointment, and new opportunities. *Front Immunol* 2012; **3**: 226.

88. Lee KS, Lee HK, Hayflick JS et al. Inhibition of phosphoinositide 3-kinase δ attenuates allergic airway inflammation and hyperresponsiveness in murine asthma model. *FASEB J* 2006; **20**: 455-65.

89. Randis TM, Puri KD, Zhou H, Diacovo TG. Role of PI3Kδ and PI3Kγ in inflammatory arthritis and tissue localization of neutrophils. *Eur J Immunol* 2008; **38**: 1215-24.

90. Winkler DG, Faia KL, DiNitto JP et al. PI3K-δ and PI3K-γ inhibition by IPI-145 abrogates immune responses and suppresses activity in autoimmune and inflammatory disease models. *Chem Biol* 2013; **20**: 1364-74.

91. Honigberg LA, Smith AM, Sirisawad M et al. The Bruton tyrosine kinase inhibitor PCI-32765 blocks B-cell activation and is efficacious in models of autoimmune disease and B-cell malignancy. *Proc Natl Acad Sci U S A* 2010; **107**: 13075-80.

92. Pan Z, Scheerens H, Li SJ et al. Discovery of selective irreversible inhibitors for Bruton's tyrosine kinase. *ChemMedChem* 2007; **2**: 58-61.

93. Evans EK, Tester R, Aslanian S et al. Inhibition of Btk with CC-292 provides early pharmacodynamic assessment of activity in mice and humans. *J Pharmacol Exp Ther* 2013; **346**: 219-28.

94. Leaker BR, Barnes PJ, O'Connor BJ et al. The effects of the novel SHIP1 activator AQX-1125 on allergen-induced responses in mild-to-moderate asthma. *Clin Exp Allergy* 2014; **44**: 1146-53.

95. Ustun C, DeRemer DL, Akin C. Tyrosine kinase inhibitors in the treatment of systemic mastocytosis. *Leuk Res* 2011; **35**: 1143-52.

96. Bachelet I, Munitz A, Levi-Schaffer F. Abrogation of allergic reactions by a bispecific antibody fragment linking IgE to CD300a. *J Allergy Clin Immunol* 2006; **117**: 1314-20.

97. Sabato V, Verweij MM, Bridts CH, et al. CD300a is expressed on human basophils and seems to inhibit IgE/FcRI-dependent anaphylactic degranulation. *Cytometry B Clin Cytom* 2012;**82**:132-8.

98. Kikly KK, Bochner BS, Freeman SD et al. Identification of SAF-2, a novel siglec expressed on eosinophils, mast cells, and basophils. *J Allergy Clin Immunol* 2000; **105**: 1093-100.

99. Kiwamoto T, Kawasaki N, Paulson JC, Bochner BS. Siglec-8 as a drugable target to treat eosinophil and mast cell-associated conditions. *Pharmacol Ther* 2012; **135**: 327-36.

100. Cemerski S, Chu SY, Moore GL et al. Suppression of mast cell degranulation through a dual-targeting tandem IgE-IgG Fc domain biologic engineered to bind with high affinity to FcγRIIb. *Immunol Lett* 2012; **143**: 34-43.

101. Lin LH, Zheng P, Yuen JW et al. Prevention and treatment of allergic inflammation by an Fcgamma-Der f2 fusion protein in a murine model of dust mite-induced asthma. *Immunol Res* 2012; **52**: 276-83.

102. Zhang K, Kepley CL, Terada T et al. Inhibition of allergen-specific IgE reactivity by a human Ig Fcγ-Fcε bifunctional fusion protein. *J Allergy Clin Immunol* 2004; **114**: 321-7.

103. Corren J, Casale TB, Lanier B et al. Safety and tolerability of omalizumab. *Clin Exp Allergy* 2009; **39**: 788-97.

104. Horakova H, Polakovicova I, Shaik G et al. 1,2-propanediol-trehalose mixture as a potent quantitative real-time PCR enhancer. *BMC Biotechnology* 2011; **11**: 41.

105. Draberova L, Shaik GM, Volna P et al. Regulation of Ca2+ signaling in mast cells by tyrosine-phosphorylated and unphosphorylated non-T cell activation linker. *J Immunol* 2007; **179**: 5169-80.

106. Zhang W, Sommers CL, Burshtyn DN et al. Essential role of LAT in T cell development. *Immunity* 1999; **10**: 323-32.

107. Fernandes AR, Easton AC, De Souza Silva MA et al. Lentiviral-mediated gene delivery reveals distinct roles of nucleus accumbens dopamine D2 and D3 receptors in novelty- and light-induced locomotor activity. *Eur J Neurosci* 2012; **35**: 1344-53.

108. Reaume AG, de Sousa PA, Kulkarni S et al. Cardiac malformation in neonatal mice lacking connexin43. *Science* 1995; **267**: 1831-4.

109. Thyagarajan T, Totey S, Danton MJ, Kulkarni AB. Genetically altered mouse models: the good, the bad, and the ugly. *Crit Rev Oral Biol Med* 2003; **14**: 154-74.

110. Paz PE, Wang S, Clarke H et al. Mapping the Zap-70 phosphorylation sites on LAT (linker for activation of T cells) required for recruitment and activation of signalling proteins in T cells. *Biochem J* 2001; **356**: 461-71.

111. Zhu M, Janssen E, Zhang W. Minimal requirement of tyrosine residues of linker for activation of T cells in TCR signaling and thymocyte development. *J Immunol* 2003; **170**: 325-33.

112. Orr SJ, McVicar DW. LAB/NTAL/Lat2: a force to be reckoned with in all leukocytes? *J Leukoc Biol.* 2011;**89**:11-9.

113. Tumova M, Koffer A, Simicek M et al. The transmembrane adaptor protein NTAL signals to mast cell cytoskeleton via the small GTPase Rho. *Eur J Immunol* 2010; **40**: 3235-45.

114. Ishizaki H, Togawa A, Tanaka-Okamoto M et al. Defective chemokine-directed lymphocyte migration and development in the absence of Rho guanosine diphosphate-dissociation inhibitors alpha and beta. *J Immunol* 2006; **177**: 8512-21.

115. Lecut C, Frederix K, Johnson DM et al. P2X1 ion channels promote neutrophil chemotaxis through Rho kinase activation. *J Immunol* 2009; **183**: 2801-9.

116. Wang Z, Kumamoto Y, Wang P et al. Regulation of immature dendritic cell migration by RhoA guanine nucleotide exchange factor Arhgef5. *J Biol Chem* 2009; **284**: 28599-606.

117. Fan H, Hall P, Santos LL et al. Macrophage migration inhibitory factor and CD74 regulate macrophage chemotactic responses via MAPK and Rho GTPase. *J Immunol* 2011; **186**: 4915-24.

118. Frigeri L, Apgar JR. The role of actin microfilaments in the down-regulation of the degranulation response in RBL-2H3 mast cells. *J Immunol* 1999; **162**: 2243-50.

119. Tolarova H, Draberova L, Heneberg P, Draber P. Involvement of filamentous actin in setting the threshold for degranulation in mast cells. *Eur J Immunol* 2004; **34**: 1627-36.

120. Finkelman FD. Anaphylaxis: lessons from mouse models. *J Allergy Clin Immunol* 2007; **120**: 506-15.

121. Nocka KH, Levine BA, Ko JL et al. Increased growth promoting but not mast cell degranulation potential of a covalent dimer of c-Kit ligand. *Blood.* 1997;**90**:3874-83.

122. Kilsdonk EP, Yancey PG, Stoudt GW et al. Cellular cholesterol efflux mediated by cyclodextrins. *J Biol Chem* 1995; **270**: 17250-6.

123. Yancey PG, Rodrigueza WV, Kilsdonk EP et al. Cellular cholesterol efflux mediated by cyclodextrins. Demonstration Of kinetic pools and mechanism of efflux. *J Biol Chem* 1996; **271**: 16026-34.

124. Smida M, Cammann C, Gurbiel S et al. PAG/Cbp suppression reveals a contribution of CTLA-4 to setting the activation threshold in T cells. *Cell Commun Signal* 2013; **11**: 28.

125. Dobenecker MW, Schmedt C, Okada M, Tarakhovsky A. The ubiquitously expressed Csk adaptor protein Cbp is dispensable for embryogenesis and T-cell development and function. *Mol Cell Biol* 2005; **25**: 10533-42.

126. Xu S, Huo J, Tan JE, Lam KP. Cbp deficiency alters Csk localization in lipid rafts but does not affect T-cell development. *Mol Cell Biol* 2005; **25**: 8486-95.